An electrophysiological investigation of established and novel animal models of epileptogenesis

By

Zachariah Smith

B.A., University of Colorado Boulder

M.A., University of Colorado Boulder

A thesis submitted to the

Faculty of the Graduate School of the

University of Colorado in partial fulfillment

of the requirement for the degree of

Doctor of Philosophy

Department of Psychology and Neuroscience

2019

This thesis entitled:

An electrophysiological investigation of established and novel animal models of epileptogenesis

Written by Zachariah Smith has been approved by the

Department of Psychology and Neuroscience

_____

Dr. Daniel Barth

_____

Dr. Chris Lowry

_____

Dr. Michael Saddoris

_____

Dr. Ryan Bachtell

_____

Dr. Robert Spencer

_____

Dr. Lewis Harvey

Date:_____

The final copy of this thesis has been examined by the signatories, and we find that both the content and the form meet acceptable presentation standards of scholarly work in the above mentioned discipline

Abstract

Smith, Zachariah (Ph.D., Psychology and Neuroscience)

An electrophysiological investigation of established and novel animal models of epileptogenesis

Thesis directed by Professor Daniel S. Barth

Temporal lobe epilepsy, defined by the increased propensity to display spontaneous seizures originating in the temporal lobe, is a pervasive condition presenting in nearly 1% of the global population. Epilepsy is also significantly comorbid with several affective and neurological disorders, including autism spectrum disorder (ASD). Despite significant inroads in the understanding of epilepsy throughout the past few decades, the underlying processes contributing to the slow development of epilepsy, known as epileptogenesis, are largely unknown. Utilizing 24/7 video EEG, these studies aimed to explore electrophysiological and behavioral changes within animals during the development of epilepsy.

First, these experiments focused on a well-established animal model using pilocarpine-induced *status-epilepticus* to trigger epileptogenesis. Within this model, these studies charted electrophysiological biomarkers of epileptogenesis that serve predictive value in determining the time-course and risk for spontaneous seizures. Development of an active biomarker was able to chart the long-term changes in hippocampal auditory evoked potentials indicative of epilepsy risk. Continuous monitoring of animals within this model was then used to solidify quantitative characteristics of seizure subtypes and epilepsy progression that should serve as a definitive framework for future epilepsy studies. These findings indicated that seizures associated with mild behavioral impairments in animals, reflective of partial seizures in the human population, present with similar electrographic and temporal characteristics as more severe convulsive seizures. Additionally, this work demarcated between spectral characteristic indicative of bona-fide seizures and alternative electrographic events that may be benign. Together, both studies within the pilocarpine model demonstrated the progressive nature of epileptogenesis.

Finally, the relational aspects of epileptogenesis in conjunction with co-occurring ASD was assessed using a novel stress-terbutaline animal model of ASD and epilepsy comorbidity by targeting stress-induced inflammation with repeated immunizations of a heat-killed immunomodulatory microbe *Mycobacterium vaccae.* Results from this final experiment demonstrated a divergence of ASD-like behavior from the development of spontaneous seizures, identifying common pathological mediator, but delineating between mechanisms of comorbidity expression. The amelioration of ASD-like behavior, despite progressive epileptogenesis, suggests that these comorbid disorders may be more separate than initially thought.

Dedication

This work is dedicated to my parents, Vincent and Georgina Smith, for their unwavering love and encouragement. Their infectious perseverance has always been a source of inspiration, and their guidance an integral component in making this possible.

Acknowledgements

First, the indispensable guidance and patience of my principal investigator and friend Daniel S. Barth. None of this work would be possible without your mentoring. I owe a special thanks to past and present members of the Bart Lab: Rebecca Kubiak, Sean Tatum, Jeremy Taylor, Taylor Crist, Allie Bernier, Florencia Bercum, Heidi Grabenstatter, Alex Benison, and Krista Rodgers for their help and foundational discoveries guiding this research.

The studies presented in this dissertation required the work of multiple laboratories and I owe them all a debt of gratitude. Collaborations with the Francois Meyer, Ed Dudek, and Christopher Lowry make up a significant portion of this dissertation and would not have been possible without them. Direct help from Matt Arnold, Kelsey Loupy, Jared Heinze, Rachel Daut, and Heather D'Angello were especially helpful during these studies.

Thank you to my committee members: Christopher Lowry, Michael Saddoris, Ryan Bachtell, Robert Spencer, and Lewis Harvey for taking the time to read through my dissertation.

I would like to acknowledge Gary Erickson for inventing the CLIF bar, a significant portion of my caloric intake during graduate school. Without the CLIF bar, I would have starved. I am sure that helping graduate students eat while running experiments and writing their dissertation is exactly what you had in mind the day you added chocolate chips and sugar to a bowl of old oatmeal and decided to sell it.

I would like to thank my family and friends for supporting me and being there every step of the way. I don't think I would have made it without you.

Contents

Figures

Tables

Chapter 1:

Introduction

Seizures vs Epilepsy

Epilepsy can be thought of as a set of heterogeneous disorders that share a singular common characteristic, the spontaneous seizure. Because of this, there is a general desire to conflate the term seizure with epilepsy. However, seizures and epilepsy have fundamentally different properties that need to be addressed to understand existing issues surrounding the field. The term seizure derives from Greek meaning *to take hold* and is broadly defined within epilepsy as "a **transient** occurrence of signs and/or symptoms due to **abnormal** excessive or synchronous neuronal activity in the brain" (Fisher et al., 2005). This activity can begin at a specific brain region (the seizures focus) and remain "focal" (also known as partial) or can arise in most/all brain regions at the same time and be "generalized". Focal onset seizures can also spread to other brain regions and eventually involve most of the brain (also known as complex-partial). Seizure activity can be accompanied by varying behavioral outcomes, ranging from slight alterations in awareness, to nonconvulsive interruptions in behavior (referred to here as nonconvulsive), to a complete loss of consciousness and severe convulsions (convulsive/tonic-clonic seizures). These characteristics in seizure onset and behavioral components make up the current operational classification scheme introduced by the International League Against Epilepsy in 2017 to outline universal definitions of seizure subtypes (Fisher et al., 2017). This gives rise to several interrelated disorders defined as epilepsy, each identified by seizure onset zones and seizure subtypes.

However, experiencing a seizure does not result in an epilepsy diagnosis. 1 in 10 people will have at least one seizure throughout their lifetime, while conservative estimates put epilepsy at a lifetime prevalence of 7.6 per 1000 people (Fiest et al., 2017). This disconnect in incidence can be best explained by the definition of epilepsy, in which seizures must continue to happen due to an existing pathological feature. So, while several events may induce an acute seizure, epilepsy is a disease of spontaneous recurrent seizures (SRS). The most common form of epilepsy is known as temporal lobe epilepsy (TLE), defined by seizures originating from a focal

onset within the temporal lobe and accounting for nearly 60% of all epilepsy cases (Engel, 2001). While some forms of epilepsy are spontaneously regressive (mainly childhood epilepsies), temporal lobe epilepsy is a chronic disorder with episodic manifestations and no cure (Haut, Bigal, & Lipton, 2006). Additionally, TLE is considered a progressive disorder that worsens over time (Coan & Cendes, 2013). For clinical diagnosis, a person must have at least two unprovoked seizures to be considered epileptic, where it is hypothesized that permanent underlying processes have occurred, fundamentally alter the identity of a brain away from "normal" and towards "epileptic". This process by which a brain becomes capable of producing spontaneous seizures is thought to consist of incremental changes that promote hyperexcitability in epileptogenic circuits and is known as epileptogenesis (Pitkänen, Lukasiuk, Dudek, & Staley, 2015). While this process is poorly understood, identifying the mechanisms of epileptogenesis could be instrumental for preventing the progressive nature of TLE.

Within most forms of temporal lobe epilepsy, epileptogenesis begins with a precipitating insult such as a traumatic brain injury (TBI), an infection, or a cerebral vascular accident such as a stroke (Agrawal, Timothy, Pandit, & Manju, 2006). Despite the potential to and relative frequency by which these insults result in immediate acute seizures, clinically there is a period between the insult and the development of spontaneous seizures known as "the latent period". The latent period has been classically described as "a silent period of strange ripening" (Penfield, 1961; Potter, 1978) in which it is thought that unknown epileptogenic processes set in motion by the initial injury result in the slow and eventual emergence of epilepsy. The duration of this period is highly variable among individuals, ranging from a few months to greater than 10 years in which little or no signs of epileptic abnormalities may exist (Pitkanen & Sutula, 2002). In addition, epilepsy-associated insults are not diagnostically reliable. Precipitating insults are not guaranteed to cause epilepsy, even when they result in acute seizures (Serafini et al., 2015), and the severity of epileptogenic insults is not predictive of the duration of the latent period (Ding, Gupta, & Diaz-Arrastia, 2016). There is currently no way to predict if or when an insult will result in epilepsy.

Spontaneous seizures, indicative of a chronic epileptic state, are the singular definitive outcome measure of progressive TLE. However, the idea of a pre-epileptic latent period is an attractive concept, as it could represent a therapeutic window of opportunity to prevent spontaneous seizures before a brain becomes “epileptic”. The development of a non-seizure continuous variable within epileptogenesis, or a biomarker predictive of seizure risk, would have tremendous value within the field.

Despite the popular association of flashing-light-induced convulsive seizures with epilepsy, most seizures in people with epilepsy (PWE) do not appear to be directly triggered by external factors (Irmen, Wehner, & Lemieux, 2015). Previously described as partial or complex-partial, focal-onset seizures involving one or more brain regions within the temporal lobe, and presenting with mild behavioral impairments, represent the majority of seizures experienced by PWE (Cascino, 1992; Roffman & Stern, 2006). While this lack of severe convulsive activity may seem innocuous, this adds to the already inherent diagnostic and treatment issues surrounding epilepsy. Partial seizures have the highest rate of recurrence, with untreated patients at a 94% risk of having a second seizure within 36 months of their first clinically identified partial seizure (Hart, Sander, Shorvon, & Johnson, 1990). Epilepsy severity and seizure frequency is also highly variable on a per individual basis, with yearly seizure rates ranging from 1 to over 100 (Moran et al., 2004). As of now, self-reported seizures represent the major criteria for identifying epilepsy and treatment efficacy. The correct identification of an epileptic seizure can be greatly improved by eyewitness accounts (Kammerman & Wasserman, 2001). However, because seizures are transient, can be rare, or exist without overt behavioral manifestations, the reliability of self-report is highly questionable.

EEG

Physicians must rely on a combination of clinical and electroencephalogram (EEG) data for the chance of an accurate diagnosis (Kammerman & Wasserman, 2001). Non-seizure epileptiform EEG abnormalities occurring *between-seizures* (*inter-ictal*) known as interictal spikes

(referred to as epileptiform spikes or ES throughout this thesis) can facilitate diagnosis, but are not present in all patients (Velioğlu, Ozmenoğlu, & Komsuoğlu, 1997). Additionally, 40% of patients with epilepsy will have a at least one normal inter-ictal EEG session during diagnosis (Binnie & Prior, 1994). Even when epileptiform abnormalities are present, EEG recordings can lead to false negatives, necessitating repeated outpatient procedures (Burkholder et al., 2016; Salinsky, Kanter, & Dasheiff, 1987). Additionally, several technical and optimization issues limit the effectiveness of EEG in epilepsy diagnosis (Panayiotopoulos, 2005). 24/7 ambulatory EEG recording can be used to more accurately identify abnormalities but is currently not a cost-effective strategy for diagnosis and is rarely used (Nickels, 2016). 24/7 video EEG is limited to certain indications, such as differential diagnosis, presurgical evaluation, and medication adjustments (Shih et al., 2018). In a comparison between video EEG-identified seizures and self-report, patients failed to identify 55% of their own seizures (Hoppe, Poepel, & Elger, 2007). In situations where seizures present with few behavioral manifestations, or a patient lives alone, 24/7 EEG may be the only method for identifying seizures at all. However, once a diagnosis of epilepsy has been achieved patients undergo a series of drug treatments aimed at mitigating the presentation of spontaneous seizures.

Epilepsy treatments

Since the invention and adoption of first generation anti-epileptic drugs (AEDs) like phenytoin (Putnam & Merritt, 1937), seizures have been treated with several different frontline pharmacological options that directly dampen the excitability of the central nervous system (CNS). In general, these treatments are designed to stop seizures by preventing acute shifts in the balance of network excitation and inhibition (E/I). Enhancing GABAergic inhibition is a popular target for conventional anti-convulsants and are used during acute severe seizure episodes (Greenfield, 2013). Alternatively, second generation AEDs targeting fast-acting sodium channels, such as carbamazepine, are used as frontline treatments to reduce excitability. However, 1 out of 3 PWE have conditions that do not respond to conventional treatments (Kwan, Schachter, &

Brodie, 2011), or that transition into a drug-resistant (refractory) state over time (French, 2007). Only half of PWE will respond effectively to a single AED (St. Louis, Rosenfeld, & Bramley, 2009). While strategies aimed at increasing extracellular GABA, mimicking GABA, or potentiating GABA currents are effective anticonvulsants, they are largely ineffective at treating refractory epilepsy and can result in paradoxical increases in seizure activity (French, 2005; Genton, 2000; Liu et al., 2006; Sazgar & Bourgeois, 2005). Additionally, several issues surround commonly used AEDs such as the upregulation of cytochrome p450, drug interactions, affective side-effects, and the creation of toxic byproducts during metabolism (Al Khalili & Murphy, 2019). While newer AEDs created within the past two decades are better tolerated and less toxic, they generally target the same mechanisms as previous drugs (Kellinghaus, 2009). Because of this, the development of new third-generation frontline epileptic drugs has made little to no impact on the treatment for refractory patients (Löscher, 2005; Viteva, 2014).

The singular pharmacological intervention approved by the FDA within the past twenty years to target an alternative process other than fast-acting sodium channels or enhancing GABAergic inhibition is levetiracetam (Keppra) (Jain, 2000). This drug is believed to act by inhibiting presynaptic calcium induced vesicle release due to its high affinity for SV2A (Matagne, Margineanu, Kenda, Michel, & Klitgaard, 2008) to slow action potential firing (Deshpande & DeLorenzo, 2014). Additionally, some animal work has suggested that there is a potential for anti-epileptogenic effects of this drug in addition to the anti-seizure effects (Kikuyama et al., 2017). While operating under a new mechanism (and still being on patent), this drug has been pushed as a safer alternative to second generation AEDs like carbamazepine (no longer on patent). However, this drug has no increase in efficacy over previous AEDs, and clinical trials have failed to demonstrate an anti-epileptogenic effect outweighing serious affective side effects (Trinka & Brigo, 2014). Recently, there has been a push back to widespread administration of this drug due to concerns over these side effects, specifically the enhancement of suicidality and the

development of what is being referred to as “Keppra rage” (Molokwu, Ezeala-Adikaibe, & Onwuekwe, 2015).

Despite a large population with a major unmet medical need for treatment, investment in newer AEDs has slowed significantly (Wilcox et al., 2013). A major roadblock toward the development of newer AEDs, identified within the field, is the loss of support and momentum for drug design from pharmaceutical companies. From a rational, business perspective, there is no reason to fund the development of a drug without some chance of a return on investment. Out of the 40 third generation AEDs developed within preclinical models, only two made it to market. Both drugs are derivatives of carbamazepine and offer no increase in efficacy for seizure treatment over established AEDs. Additionally, there have been no phase 3 trials and only 2 phase 2 trials for anti-epileptogenesis solutions in the past 15 years (Klein, 2017). Drug development towards epileptogenesis has generally been regarded as a failure (Ventola, 2014).

There are three prevailing thoughts as to why drug development has made little progress. Foremost, is that AEDs directly target neuronal firing, treating the symptomology of epilepsy but not the underlying epileptogenic processes (D. Schmidt, 2012). Epilepsy-promoting factors, such as neuroinflammation may be beneficial as an anti-epileptogenic strategy (Vezzani, 2015). However, there are currently no biomarkers for epileptogenesis, and self-reported seizures remain the singular outcome measure for treatment efficacy. Measuring anti-epileptogenesis can only be assessed by the lack of seizure development. A marker for epileptogenesis that could be charted would aide in understanding the processes behind epileptogenesis to target epilepsy as well as seizures. Second, animal models of epileptogenesis may not accurately reflect the human condition (Kandratavicius et al., 2014). Current models demonstrate rapid convulsive seizures, which are readily identifiable without 24/7 video EEG. Limited studies have addressed nonconvulsive partial seizures within animal models. Because partial seizures are more common in humans, often refractory, and have not been routinely observed in current animal models it is possible that treatments designed within these models will not adequately translate for partial

seizures within humans. Therefore, etiologically relevant animal models should be explored that present similar seizures and progression as human TLE. Third, treatments ignore disorders that co-occur with epilepsy. Several affective and neurodevelopmental disorders present with spontaneous seizures. However, epilepsy is not well understood within the framework of comorbidities and environmental risk factors. Additionally, environmental risk factors associated with these disorders are shared, suggesting common underlying pathophysiological mechanisms that could be a potential treatment target. Several funding organizations have adjusted research priorities worldwide to match the needs associated with current treatment limitations (Baulac et al., 2015; Kwan et al., 2015; Lowenstein, 2011).

Animal models of epilepsy and seizures

Understanding epileptogenesis with the intent to treat the underlying epileptic processes contributing to epilepsy requires the use of animal models. Experimental induction of a seizure is a relatively straightforward process both in-vivo and in-vitro. This can be done via acute shifts in the balance of excitation and inhibition with pharmacological blockade of GABAergic inhibition via centrally acting antagonists (Pentylenetetrazol; PTZ; (Dichter & Ayala, 1987) or an enhancement of glutamate dependent excitatory signaling via NMDA targeted agonists. Additionally, seizures can be induced via electrical stimulation paradigms aimed at testing seizure thresholds and resistance to the development of acute seizures (Löscher, 2011). While these experimental models have tremendous value for rapid screening of anti-seizure/anti-convulsive compounds, their translational validity towards understanding epileptogenesis is limited, as most of these acute manipulations fail to produce animals that have spontaneous seizures.

Producing temporal lobe epilepsy, without the use of genetic models, is experimentally challenging. Experimenters must create the underlying pathology that causes epilepsy by inducing a state in which the brain is capable of having seizures spontaneously. Because the mechanisms behind epileptogenesis are still unknown, experimenters are reliant on precipitating brain insults or risk-factor manipulations that have been proposed to be causative factors for

epileptogenesis. However, the challenges that exist with 24/7 ambulatory EEG in human populations are much less severe in animal populations, who can be readily implanted with permanent recording devices. With the recent advancements in storage capabilities, large scale 24/7 Video EEG can be performed to accurately address electrographic and behavioral features that span the entire duration of epileptogenesis in rat models (Bin et al., 2017).

Chemoconvulsant animal models of epilepsy have been the gold standard for the study of spontaneous seizures since their development in the late 80s and early 90s. Through systemic injection or direct application of kainic acid (potent kainate receptor agonist) or pilocarpine (M3 muscarinic receptor agonist), researchers induce a period of extended seizure insult known as *status-epilepticus* (SE). This can be controlled via the administration of anti-convulsant drugs like diazepam that limit SE duration to temporally confined periods to replicate an initial insult. Spontaneous seizures then begin to emerge in these animals over the course of weeks. Several pathological features within chemoconvulsant models accurately reflect human TLE, such as the latent period, the development of hippocampal sclerosis, mossy fiber sprouting, and the emergence of drug resistance (Kandratavicius et al., 2014). Refinement of techniques used in this procedure have resulted in high rate of success for spontaneous seizure induction and animal survival (Curia, Longo, Biagini, Jones, & Avoli, 2008). From an experimental perspective, this rate of success is necessary for high throughput research, especially when combined with long-term 24/7 video/EEG monitoring to accurately identify electrographic seizures. However, pilocarpine treatment also causes widespread neuronal damage outside regions typically associated with temporal lobe epilepsy in humans (Scholl, Dudek, & Ekstrand, 2013). Additionally, prolonged status-epilepticus is a rare cause of epilepsy within the human population (Falco-Walter & Bleck, 2016) and epileptogenesis can be extremely rapid within this model, creating severe epilepsy associated with convulsive activity, limiting its direct translatability.

Etiologically relevant models of epilepsy Issues surrounding the fundamental definition of seizures

In the past 15 years, significant focus within the epilepsy field has been targeted towards creating clinically relevant models of post-traumatic epilepsy (PTE) using precipitating insults that reflect the human condition. With etiological relevance comes significant hurdles. PTE occurs in a small percentage of people following an injury and may take years to develop. Successful animal models of PTE demonstrate complex partial seizures in roughly 10% of all animals following latent periods greater than a year (Kharatishvili, Nissinen, McIntosh, & Pitkänen, 2006). Additionally, if animal models demonstrate a low rate of seizures, with the mild behavioral impairments reflective of partial seizures in humans, then 24/7 video EEG is required to identify epilepsy. These factors are challenging, requiring a large population of animals, significant funding, and years of demanding EEG monitoring.

D'ambrosio and colleagues demonstrated, utilizing a single episode of fluid percussion injury (LFPi), that animals rapidly develop 7-14 Hz rhythmic discharges that increase in propensity and duration over the life of the rat (D'Ambrosio et al., 2004). These electrographic epileptiform events (EEEs) were occasionally of focal origin and accompanied by behavioral arrest, consistent with non-convulsive seizures regularly seen in temporal lobe epilepsy (D'Ambrosio et al., 2005). Additionally, EEEs resembled spike-wave-discharges (SWDs) seen in childhood "absence" epilepsy and genetic animal models of generalized absence seizures (Brigo et al., 2018). These qualities of this electrographic activity allowed them to be considered as ictal activity, fundamentally altering the definition of partial seizures within animal models of post-traumatic epilepsy (D'Ambrosio et al., 2009). With the relative frequency of events and rapidity of expression following injury, LFP-induced traumatic brain injury heralded in a new era of post-traumatic epilepsy research. Researchers were now unrestrained from the traditional time demands of models of epilepsy designed to reflect extended latent periods and able to reproducibly create electrographic nonconvulsive seizures in almost all animals. Thus, with the rapid adoption of EEEs and the implementation of LFPi, researchers could potentially target electrographic activity immediately after injury as a marker for epileptogenesis and a reliable outcome measure for

therapeutic intervention, with the hope of considerable improvement in treatment outcomes for post-traumatic epilepsy.

Despite promise, issues began to emerge generating considerable discussion within the field on the accuracy of this approach to studying PTE (D'Ambrosio & Miller, 2010; Dudek & Bertram, 2010). First and foremost is the disconnect between electrographic characteristics in clinically measured focal onset seizures within the human population and features of EEEs observed in animals. These events manifested rapidly, were quantitatively shorter, and lacked qualitative electrographic properties of seizures observed in patients with TLE. Secondly, the discovery and abundance of EEEs within control animals raised the question as to whether these events are pathological in nature. Several studies from our lab have suggested that EEEs are age-related activity and highly prevalent in control animals (Rodgers, Dudek, & Barth, 2015). These "seizures" can be interrupted with external click stimulation and animals can be trained decrease the duration of these bouts voluntarily (Taylor et al., 2017). Additionally, EEE's are prevalent in several genetic rat lines including wild-caught animals (Taylor et al., 2019). However, the inclusion of these events as partial seizures continues, in part due to the lack of definitive guidelines for electrographic identification of nonconvulsive seizures reflecting human partial seizures.

The identification of EEE's as the initial signs of progressive TLE has been accepted as a fact within the field without adequate analysis. Limited studies have been completed verifying the presence convulsive activity within etiologically relevant animal models of epilepsy (Kharatishvili, Nissinen, McIntosh, et al., 2006) and no studies have identified a relationship between EEEs and the progressive development of complex-partial or convulsive seizures. Additionally, very few studies have identified and described nonconvulsive seizures within chemoconvulsant animal models of epilepsy (Williams et al., 2009). This is of great concern with respect to treatment, as drugs targeting SWDs or partial seizures are bidirectionally contraindicated. Carbamazepine aggravates childhood absence epilepsy (Liu et al., 2006), and ethosuximide has the potential to

enhance tonic-clonic convulsive seizures (Perucca, Gram, Avanzini, & Dulac, 1998). Accurate identification of seizure subtypes within animal models needs to be addressed to understand epileptogenesis and explore the relationship between nonconvulsive and convulsive seizures.

Inflammation and epilepsy

Specific interest in the contributing role of inflammation in epileptogenesis (Pitkänen, 2010; Rana & Musto, 2018), and the potential for inflammation targeting anti-epileptogenesis strategies (Vezzani, 2015) has been garnered within the past decade. The risk for epilepsy is significantly elevated in conjunction with diseases reflective of chronic inflammatory conditions such as multiple sclerosis (Calabrese et al., 2008), type 1 diabetes (Chou et al., 2016), celiac disease (Orrin Devinsky, Schein, & Najjar, 2013), systemic lupus erythematous (SLE) (Tsai, Lin, Lin, Sung, & Lue, 2014), and rheumatoid arthritis (Ong, Kohane, Cai, Gorman, & Mandl, 2014). TLE is promoted by inflammatory insults such as infections (Vezzani et al., 2015) and traumatic brain injury (Webster et al., 2017). Additionally, a bidirectional relationship between seizures and inflammatory cytokines exists. Inflammatory cytokines can be both released during a seizure and contribute to changes in excitability leading to seizures (Rodgers et al., 2009). Additionally, non-inflammatory modulation of glial cells within the CNS is enough to drive the development of spontaneous seizures (Zhao et al., 2018). Epilepsy promoting insults also drive the expression of inflammatory mediators for several days and weeks following an insult and have been thought to contribute to the long-term changes in excitability contributing to epileptogenesis. All of these together have made neuroinflammation and attractive novel disease modifying target for epileptogenesis (Dey, Kang, Qiu, Du, & Jiang, 2016).

Excitation inhibition imbalance and comorbidity

Because seizures can arise due to excessive synchronous neuronal activity, epilepsy is often thought of as an imbalance between excitation and inhibition (E/I imbalance) within the brain (Bromfield, Cavazos, & Sirven, 2006). Whether it is too much excitation, or too little inhibition, something is wrong chronically that allows spontaneous seizures to emerge. However, epilepsy

diagnostics do not always exist in a vacuum. Epilepsy shares significant comorbidities with neurodevelopmental and affective disorders (autism spectrum disorders, anxiety, depression, etc). E/I imbalance is a proposed integral defective element responsible for both epilepsy and the observed comorbidities (Bozzi, Provenzano, & Casarosa, 2018; Fritschy, 2008; Uzunova, Pallanti, & Hollander, 2016; Velíšková, Silverman, Benson, & Lenck-Santini, 2018; Yizhar et al., 2011). In this sense, studying the mechanistic links between epilepsy and its shared disorders is a critical endeavor toward treatment and general understanding about neurological disorders and function. However, it is unknown whether behavioral comorbidities and epileptogenesis are bidirectionally causative.

One of the most pervasive comorbid disorder within epilepsy is autism spectrum disorders (ASD). ASD are a group of disorders identified by two core behaviors; deficits social communication and restricted, repetitive behaviors or interests (American Psychiatric Association, 2013). Additionally, ASD is often associated with symptoms such as GI distress (Chaidez, Hansen, & Hertz-Picciotto, 2014), immune abnormalities (Edmiston, Ashwood, & Van de Water, 2017), anxiety (White, Oswald, Ollendick, & Scahill, 2009), and improper stress regulation (Mazefsky et al., 2013). The cooccurrence with epilepsy, reflected by the increased propensity to develop spontaneous seizures among people with ASD is as high as 30% (Besag, 2017; Gillberg & Billstedt, 2000), with epileptiform abnormalities present in up to 70% of people with ASD (Ghacibeh & Fields, 2015). Some reports have shown that epileptic phenotypes increase the risk for the development of ASD, suggesting that seizures themselves can act as a driving force behind the development of ASD like symptoms (Sundelin et al., 2016). E/I imbalance has often been used as mechanistic framework for the shared underlying etiology of ASD and epilepsy (Bozzi et al., 2018; Buckley & Holmes, 2016; Frye et al., 2016). This concept is further supported by genetic knockout models of developmental disorders that present with ASD-like features and spontaneous seizures, such as Tuberous Sclerosis Complex (TSC1; Bateup, Takasaki, Saulnier, Denefrio, & Sabatini, 2011), Fragile X Syndrome (FRMP; Dölen & Bear, 2008), and focal cortical

dysplasia (CNTNAP2; Peñagarikano et al., 2011) that display synaptic dysfunctions indicative of an E/I imbalance. However, these common pathological mechanisms exist between epilepsy and ASD remain theoretical (Gao & Penzes, 2015), and have not been adequately applied to non-genetic forms of epilepsy co-occurring with ASD. While both disorders are likely the result of several interacting genetic and environmental factors, inflammatory processes are thought to be an integral mediator in the development of ASD and the development of spontaneous seizures. Therefore, exploring these factors within an animal model may help elucidate common underlying mechanisms.

Stress-terbutaline

Terbutaline is among a class of beta-mimetic drugs that are commonly utilized as tocolytic agents for the prevention of preterm labor. Acting as a β_2 adrenergic receptor agonist, terbutaline prevents birth canal muscle contractions as an emergency stopgap for labor prevention. Tocolytic agents like terbutaline are commonly used within the first 48 hours to prevent pre-term labor, followed with antenatal corticosteroids like dexamethasone to stimulate the lung development for fetus survivability (Haas, Benjamin, Sawyer, & Quinney, 2014). Receptor desensitization to β_2 adrenergic mimetics is relatively rapid, limiting its effectiveness to 48-72 hours (Berg, Andersson, & Rydén, 1985). However, support of chronic terbutaline administration for the maintenance of tocolysis exists due to the low rate of maternal side effects outweighing the proposed benefits for maintained tocolysis (Elliott & Morrison, 2013). Because of this, off-label or prolonged use of terbutaline and dexamethasone is a common practice to prevent pre-term labor (Gaudet et al., 2012).

However, terbutaline freely crosses the placenta and acts on the fetus (Ingemarsson et al., 1981), where this receptor desensitization does not occur, sensitizing the developing brain to future norepinephrine signaling (Slotkin, Tate, Cousins, & Seidler, 2001). Prenatal overexposure to β_2 adrenergic receptor agonists or genetic polymorphisms in the β_2 adrenergic receptor lead to an increase risk for autism (Connors et al., 2005). Exposure to terbutaline for greater than 48

hours during the third trimester is associated with a fourfold increase in the risk for developing ASD (Croen et al., 2011). This association also remains when controlling for medication indications such as asthma (Gidaya et al., 2016). Recently, In- vitro studies have demonstrated that terbutaline and stress-associated corticosteroids are synergistically neurotoxic during development (Slotkin, Skavicus, & Seidler, 2018).

Recently, our lab developed the first non-genetic rat model of ASD/Epilepsy by implementing a two-hit stress + terbutaline procedure during development (Bercum et al., 2015). This combination resulted in ASD-like behavioral features, spontaneous seizures and markers of neuroinflammation. Because both prenatal stress and terbutaline early in development have been previously shown to result in a dysregulation of CNS inflammatory responses necessary for the development, we hypothesized that neuroinflammation during developmental critical periods was a major contributing factor toward ASD/epilepsy comorbidity. Targeting stress-terbutaline induced inflammation may guide our understanding of environmental factors contributing to ASD/Epilepsy comorbidity. Work from the lab of Christopher Lowry utilizing a heat-killed microbe *Mycobacterium vaccae* had demonstrated that repeated immunizations prior to the exposure to chronic stress prevented stress-induced inflammation via the initiation of a peripheral anti-inflammatory phenotype (Reber et al., 2016). Subsequent work also demonstrated the induction of a CNS mediated anti-inflammatory and stress-protective immunophenotype (Frank et al., 2018). Therefore, by combining a stress-terbutaline procedure with repeated immunization of heat-killed *M. vaccae* it would be possible to explore the effects of a novel anti-inflammatory intervention in ASD and epilepsy.

Dissertation focus

This dissertation encompasses work using two distinct animal models of acquired epilepsy, each with its own advantages and disadvantages. The first section involves work using pilocarpine-induced *status epilepticus* model of acquired epilepsy. For the past few decades, this manipulation has represented the gold standard for the study of spontaneous seizures and the

development of anti-seizure compounds. With a wealth of research using this pilocarpine, tackling basic problems that plague the epilepsy field, like the fundamental definition of a spontaneous seizure, needs to start at a well-established model to avoid the risk of being dismissed as a model specific phenomenon**.** Experiments outlined within this dissertation will use a combination of 24/7 video EEG in pilocarpine rats to chart epileptogenesis, identify predictive biomarkers indicative of seizure risk, and characterize electrographic characteristics of nonconvulsive and convulsive seizures.

The second section focuses on a novel model of epilepsy developed by our lab that uses a combination of etiologically relevant teratogens (maternal stress + terbutaline) to produce a comorbid model of autism spectrum disorder and epilepsy. While this manipulation is still in its infancy, this is currently the only established paradigm that allows for the study of the underlying mechanisms that can contribute to both disorders at the same time, without the use of genetic manipulations. This puts this research at a unique advantage for exploring the potential links between the expression of ASD and the development of SRS. A focus during this section is the use of a novel anti-inflammatory immunization procedure using heat-killed *M. vaccae* to explore the relationship between ASD-like behavior and epileptogenesis.

Epileptogenesis within the pilocarpine-induced *status epilepticus* model

Chapter 2:

Archetypal Early and Late Excitability Changes During Epileptogenesis Revealed by Sensory Evoked and Spontaneous Field Potentials in Rat Hippocampus

Abstract

Acquired epilepsy is characterized by a precipitating insult followed by a latent period of varying duration before the appearance of spontaneous recurrent seizures. The latent period is assumed to be a time when epileptogenesis, or the physiological changes leading to chronic epilepsy, occurs, and therefore provides an opportunity for intervention. Yet, to explore these physiological changes, there is a need for sensitive biomarkers that can monitor the transition to disease.

We actively probed the excitability of hippocampus during the latent period following *status epilepticus* in a lithium/pilocarpine model of acquired epilepsy, by using auditory evoked field potentials recorded continuously for weeks. We found that the hippocampal auditory evoked potential (hAEP) underwent archetypal changes in waveform morphology during epileptogenesis; changes that were sufficiently stereotyped between rats to use machine learning to classify distinct pathological stages in any animal. An "early" and "proleptic" stage were identified during the latent period. The early stage occurred immediately after injury in all rats regardless of whether they went on to develop epilepsy. In non-epileptic rats, the hAEP recovered to baseline morphology, suggesting a reversibility that may indicate a time window for intervention. Rats that developed epilepsy displayed an epileptic hAEP waveform many days in advance of the first seizure with accompanying presence of epileptiform spikes.

These data suggest that by actively probing hippocampal responsiveness with sensory stimulation, the hAEP may serve as a useful biomarker for epileptogenesis, particularly for early phases of the latent period post-injury, when passive EEG measures have been unrevealing.

INTRODUCTION

Acquired epilepsy is characterized by the development of spontaneous recurring seizures (SRS) following a precipitating insult, including febrile seizure (French et al., 1993), status epilepticus (SE; (Lowenstein, 2006)), traumatic brain injury (Pitkänen & Immonen, 2014), and hypoxic ischemic encephalitis (HIE; Kadam, White, Staley, & Dudek, 2010). Initial brain trauma is

followed by a highly variable latent period that can last from weeks to years prior to the development of SRS (Pitkanen & Sutula, 2002). While this period of apparent quiescence is defined by the lack of convulsive seizures, it is thought to involve progressive neuropathological changes leading to cellular hyper-excitability and eventually epilepsy. The progression of physiological changes during the latent period remains largely unknown. Developing biomarkers to identify these changes could help assess disease risk and elucidate the time course of pathological changes leading to epilepsy, aiding in preventative drug development.

In the search for biomarkers reflecting epileptogenesis, a promising focus has been on molecular probes and non-invasive imaging techniques to track whole system and cellular responses associated with epileptic disease evolution (Engel et al., 2013). However, with the capacity for high temporal resolution, and long-term continuous monitoring, electrophysiological measurements remain the focus of many epileptogenesis studies. The presence of epileptiform spikes (ES) (Staley, Hellier, & Dudek, 2005; Staley & Dudek, 2006; Staley, White, & Dudek, 2011), systematic changes in ES morphology (Chauvière et al., 2012), increases in ES frequency (White et al., 2010), associated pathological high-frequency oscillations (pHFO) (Bragin, Wilson, Almajano, Mody, & Engel, 2004; Salami et al., 2014), as well as the appearance of non-convulsive "microseizures" in the EEG restricted to single cortical columns (Stead et al., 2010), have been implicated as possible indicators of epileptogenesis. Yet, these passive measures rely on spontaneous discharge that may lack sensitivity to subtle changes in excitability, particularly during the critical early "silent" period following injury, when the EEG appears normal.

The objective of the present study was to develop a means by which we could actively and continuously probe hippocampal cortex for excitability changes during the entire time-course of epileptogenesis. To this end, we took advantage of the fact that a sensory responsive zone of the rat dorsal hippocampus receives auditory input (Agster & Burwell, 2009), evoking stereotyped responses in both field potential and unit recording (Brankack & Buzsaki, 1986). We used chronically recorded hippocampal auditory evoked potentials (hAEP) as an active and continuous

probe of excitability changes in the lithium pilocarpine model of post-SE acquired epilepsy (Curia, Longo, Biagini, Jones, & Avoli, 2008). hAEP were examined with machine-learning methods to determine if this biomarker could identify distinct stages of epileptogenesis during the latent period and if archetypal changes in hAEP waveform morphology might have universal predictive value for the development of SRS in this model.

MATERIALS AND METHODS

Adult, male, Sprague-Dawley rats (Harlan Laboratories, Madison, WI; 250-300g) were housed in temperature (23 ± 3 °C) and light (12:12 light: dark) controlled rooms with *ad libitum* access to food and water. All procedures were performed in accordance with University of Colorado Institutional Animal Care and Use Committee guidelines for the humane use of laboratory rats in biological research.

Chronic video/EEG and hAEP recording

Aseptic surgical procedures were used for all chronic preparations. Under isoflurane (Abbott Laboratories) anesthesia (2.5%), rats were implanted with a Teflon-coated hippocampal wire electrode (AP, -3.8, ML, 1.1, DV 3.8), a ground screw (AP, -1, ML, 1), and a reference screw over the occipital bone. Buprenorphine (0.1mg/kg, subcutaneously) was administered immediately after the surgical procedure and again every 12 hr for a 72 hr period. Following a 2-week recovery period, animals were tethered to an electrode harness (Plastics One, 363) and slip-ring commutator (Plastics One, SL6C) permitting free movement for 24/7 video/EEG monitoring throughout the duration of the experiment. Spontaneous EEG signals were amplified and then digitized at 500 Hz. Chambers for chronic recording were fitted with top-mounted speakers to provide auditory click stimulation evoking hAEP. Hippocampal responses to 120 monopolar square-wave clicks (0.1 ms duration, 2 sec ISI, 45dB SPL) were amplified (10,000x; band-pass cut-off = -6 dB at .001 to 3000 Hz; roll-off = 5 dB/octave), digitized (10 kHz), averaged and stored. hAEPs were collected at the end of each 30-minute block of spooled video/EEG data 24/7 for the entire experiment. Spontaneous time-locked EEG (500 Hz) and video (30 FPS) were

stored for subsequent seizure detection. Chronic hAEPs were recorded from 3 groups: animals that received lithium-pilocarpine (n=16), animals that received all drug injections in the li-pilo model (lithium, scopolamine, paraldehyde and saline) where pilocarpine was substituted with the vehicle saline (n=2), and animals that only had chronic electrodes implanted with no injections (n=5).

Lithium Pilocarpine (li-pilo) model of TLE

After full recovery from chronic electrode implantation (2 weeks) and at least one additional week of chronic recording of baseline video/EEG and hAEP, we administered an IP injection of Lithium chloride (3mEq/kg, 1ml/kg, Sigma, St. Louis, MO). Twenty hours later, an IP injection of scopolamine (1 mg/kg, 1 ml/kg, Sigma, St. Louis, MO) was given to ameliorate any peripheral muscarinic effects of pilocarpine. Twenty minutes after scopolamine administration a single injection of pilocarpine hydrochloride (50 mg/kg i.p., 1 ml/kg, Sigma) was administered to induce status epilepticus (SE). The beginning of SE was determined by the emergence of bilateral forelimb clonus and rearing, leading to continuous generalized convulsive seizure activity consistent with previous studies using the pilocarpine model (Curia et al. 2008; Brandt et al. 2015). After 1 hour of status epilepticus, the animals were administered an IM dose of paraldehyde (0.3mg/kg, Sigma, St. Louis, MO) to terminate convulsions. A second dose of paraldehyde was given 8-10 hours later and 5 ml of saline co-administered (SC) with both doses. Paraldehyde has been shown to rapidly terminate pilocarpine induced status epilepticus both behaviorally and electrographically, which quickly becomes intractable to standalone anti-convulsants such as Diazepam (Morrisett et al 1987; Goodkin et al. 2003). In concordance with previous studies, we found that paraldehyde improved long term survival rates (Kubová et al 2005) while maintaining high success rates for SRS development (Curia et al. 2008) and a subset of animals failing to develop SRS. Animals were kept on post-surgical nutritional gel (Diet Gel, Clearh2o, Portland, OR) and their water was replaced with an electrolyte sports drink for 72 hours. Vehicle-drug

animals received all drug injections except pilocarpine, which was replaced with a 0.9% saline vehicle injection.

Epileptiform spike detection

We used supervised pattern recognition to detect ES. For each rat, 20-30 ES were visually identified, temporally aligned according to the negative peak of the spike and averaged to create a template (± 200 msec window surrounding the peak). The spike template was then shifted point by point through the same data from which the spikes were visually identified and the covariance between data and template were computed as a function of time. The covariance time-series was visually thresholded to separate noise from correct detections. The time-shifted covariance between the spike template and 5 hr baseline data (before pilocarpine administration) was computed and the threshold applied to examine false detections. False detections from the baseline were averaged to create a non-spike template. All subsequent detections compared the covariance between the data and both the spike and non-spike templates. While the two template approach improved correct detections, many spikes were still falsely detected in the baseline. To reduce false detections further, we added a second level of analysis relying on a Support Vector Machine (SVM) for pattern recognition (Orrù, Pettersson-Yeo, Marquand, Sartori, & Mechelli, 2012). For each rat individually, the SVM kernel was trained to discriminate the 20-30 initially identified spikes from approximately 1000 miss-identified spikes in the baseline. The combination of templates and SVM were then used to detect ES for all subsequent data for a given rat.

Seizure detection

Visual detection of seizures was done using custom software. EEG for a given rat was displayed in 30 min blocks on high-resolution monitors. Electroencephalographic seizures were differentiated from background noise by the appearance of large-amplitude (at least three times baseline), high frequency (minimum of 5 Hz) activity, with progression of the spike frequency that lasted for a minimum of 30 seconds. Behavioral video data was used to determine seizure

intensity on the Racine scale (Racine, 1972) and to confirm EEG seizure activity versus potential animal generated noise such as eating and grooming.

Evoked potential analysis

For training a machine-learning algorithm that could decode the condition of an animal from the hAEP, the responses were initially segmented into four experimental conditions consisting of “Baseline” (all responses before SE), “SE” (72 hr immediately following termination of SE), “Acute” (remaining hAEP prior to the first SRS), and “Chronic” (responses following the first SRS; **Fig. 2.1B**). Data analysis was performed using in-house MATLAB software. Recordings corrupted by artifacts were removed automatically using robust statistical analysis: hAEPs that differed significantly from the median waveform (computed separately for the four conditions over a time window of several hours) were discarded. Daytime hAEPs, which were least contaminated by movement artifact, were selected for further analysis. For each animal, the hAEPs were normalized in such a way that the total energy of the average baseline response (measured over several days) for that animal was one.

Feature extraction: In order to reveal the morphological changes between the hAEPs associated with the different experimental conditions and to extract a parsimonious set of salient features for the analysis of the hAEPs, we decomposed each response with a discrete stationary wavelet transform (Jaffard, 2001). We used the Cohen-Daubechies-Feauveau biorthogonal 9-7 because it has linear phase and did not introduce frequency-dependent artifactual delays (Bradley & Wilson, 2004). The stationary wavelet decomposition output two tables of coefficients: the wavelet (or detail) coefficients that encoded the changes in the shape of the hAEP at different scales (frequencies), and the approximation (or average) coefficients that provided a smooth sketch of the trend of the response captured at different scales (frequencies). Each wavelet coefficient at a given time and scale quantified the rate of change of the derivative (local curvature) of the hAEP, being large and positive when the signal has a hairpin shaped trough, and large and positive around a sharp peak. When the response was a low degree polynomial (linear, quadratic, etc.),

the wavelet coefficient was very small. Conversely, each approximation coefficient quantified the value of the "average" computed at the corresponding time instant and scale. Among the 10 scales and 3000 time samples of the wavelet decomposition, we only retained the time intervals and the scales that most significantly separated (after controlling for false discovery rate (Benjamini & Hochberg, 1995)) the hAEPs taken from the four experimental conditions, across all the animals. The most useful approximation coefficients corresponded to the time-frequency regions: [70,120] ms × [10,20] Hz and [100,150] ms ×[5,10] Hz; while the most useful wavelet coefficients were found in the region: [0,100] ms × [5,10] Hz (see **Fig. 2.1**). We therefore kept two sets of 1000 (wavelet and approximation) coefficients for each hAEP recording. Finally, for each hAEP measured at time t_i, we concatenated the wavelet and approximation coefficients within a 3 hr time window centered at t_i. This first step of the analysis resulted therefore in a window, $w(t_i)$, of 6×2000 coefficients that uniquely characterized the short-time dynamics associated with the changes in the shape of the hAEP recorded at time t_i.

Dimension reduction: We conjectured that the information captured by the high-dimensional (12,000 dimensions = 6 recordings × 2000 coefficients) temporal array of coefficients, $w(t_i)$, could in fact be explained by a much smaller number of independent variables. We sought therefore a parsimonious representation of each time window $w(t_i)$ that would reveal the consistency of the shape of the various hAEPs within a given condition, while removing the variability between animals. Standard linear methods (such as Principal Component Analysis) proved unsuccessful, whereas a nonlinear method based on spectral embedding (Bengio, Delalleau, Le Roux, & Paiement, 2006; Cunningham & Byron, 2014) correctly identified well-defined clusters associated with the four experimental conditions. Briefly, we defined a similarity matrix K that quantified how any two time window of coefficients $w(t_i)$ and $w(t_j)$, extracted from the same or from different conditions, and from the same or from a different animal, at the respective times t_i and t_j co-vary, according to

$$K_{i,j} = \exp\left(-\left\|w(t_i) - w(t_j)\right\|^2/\sigma^2\right),$$

where the scaling constant σ was chosen to be a multiple of the median distance between the time window of coefficients. $K_{i,j}$ quantified the similarity between hAEPs: large values corresponded to windows $w(t_i)$ and $w(t_j)$ extracted from the same condition; small values corresponded to windows extracted from different conditions. The first three eigenvectors, ψ_1, ψ_2, ψ_3, corresponding to the three largest eigenvalues of the matrix K were computed and were used to define the spectral embedding as follows (Bengio et al., 2006). For each time window of coefficients $w(t_i)$, the entry t_i of the eigenvectors, $\psi_1(t_i)$, $\psi_2(t_i), \psi_3(t_i)$, provided the first, second, and third reduced "*spectral coordinates*" of $w(t_i)$. These spectral coordinates are unitless, encoding the relative position of each time window $w(t_i)$ with respect to the other time windows. It can be shown that if the original data were composed of several distinct clusters of data points, then the spectral coordinates would optimally separate the clusters (Bengio et al., 2006).

Parameterization of the four conditions: For each hAEP, measured at time t_i, we computed the spectral coordinates $\psi_1(t_i), \psi_2(t_i), \psi_3(t_i)$, of the corresponding time window $w(t_i)$. We observed that the training hAEPs for the same condition c = condition, were organized around a smooth low dimensional structure (see **Fig. 2.2**). We therefore modeled all the hAEPs associated with a given condition c using a mixture of probabilistic principal components (Tipping & Bishop, 1999). The mixture model resulted in a remarkably low dimensional parameterization of each condition because it was able to describe with a small number of components the geometric structure created by the statistical distribution of the spectral coordinates of the time windows associated with the corresponding condition. It also provided a simple mechanism to estimate the posterior probability, $P(\pi_c | w(t_i))$, that the mixture model π_c, which modeled condition c, would generate the time window $w(t_i)$ corresponding to the hAEP measured at time t_i.

Classification of epileptogenic states: In order to confirm the ability of the hAEPs to reliably predict the condition or "epileptogenic state" of a given rat, we developed a machine learning approach

to decode the condition of a rat as a function of the hAEP. We used a hidden Markov Model to capture the dynamics of the hidden brain states associated with the progression of epileptogenesis (Wong, Gardner, Krieger, & Litt, 2007) as well as the resulting changes in the shape of the hAEP triggered by this hidden condition. The state space of the hidden Markov chain was composed of the four experimental conditions. The observed data of the hidden Markov Model was given by the posterior probability $P(\pi_c|\, w(t_i))$ that the hAEP, and its associated time window, $w(t_i)$, originated during condition c. The discrete time processes associated with the hidden Markov model were sampled at the same rate as the hAEPs (every 30 minutes). The probability transition matrix that encoded the transitions from one state to another (e.g., SE → Acute) was estimated from the training data. We also used the training data to learn the probability that a given state generates a given posterior probability $P(\pi_c|\, w(t_i))$. The trained hidden Markov model was then used in a "reverse mode" (Cappé, Moulines, & Rydén, 2005) to decode the most likely sequence of hidden conditions that could trigger a temporal sequence of hAEPs. We evaluated our approach using a 'leave one animal out' cross-validation: the algorithm was trained on 11 rats and evaluated with one animal that was not part of the training data. For any hAEP recording, the decoding algorithm returned the condition of an animal, as measured by the probability of being in one of the four states. These probabilities were computed at each time a hAEP was measured (every 30 minutes).

Histology

At the termination of all experiments, animals were deeply anesthetized, perfused with 2.5% paraformaldehyde and Nissl stained to verify electrode placement.

Statistics

All descriptive statistics are reported as Mean±SEM (standard error of the mean). Differences between means were evaluated with unpaired two-tailed t-tests. Linear correlations between variables were evaluated with two-tailed Pearson product-moment correlations. Threshold for significance was set to $p \leq .05$.

RESULTS

Status epilepticus (SE)

Figure 2.1 displays a typical temporal pattern of status epilepticus (SE) and recovery seizures in the lithium/pilocarpine model. SE reliably began within 15 minutes of pilocarpine injection and consisted of continuous high-frequency spiking (**Fig. 2.1B and Fig. 2.1C;** dashed line) accompanied by tonic-clonic seizures (Racine scale 4-5; (Racine, 1972). Injection of anticonvulsant after one hour rapidly reduced behavioral convulsions and fully suppressed SE, as determined electrographically, within several hours (total SE duration 3.8±0.8 hr). In all rats, the anticonvulsant effect was transient (9.8±1.1 hr), resulting in a recovery of seizure activity (**Fig. 2.1B**; "1st recovery") lasting for a period of 10.6±1.0 hr. The 1st recovery differed from SE in that the seizures were discontinuous (20-40 sec duration each; **Fig. 2.1;** "seizure") and interspersed with epileptiform spikes (**Fig. 2.1D; "**ES"). A second injection also had transient anticonvulsant effects, permitting a 2nd recovery of seizures lasting for a period of 14.5±7.1 hr before entering a "silent" period **(Fig. 2.1B and E**) where no seizures or ES were observed.

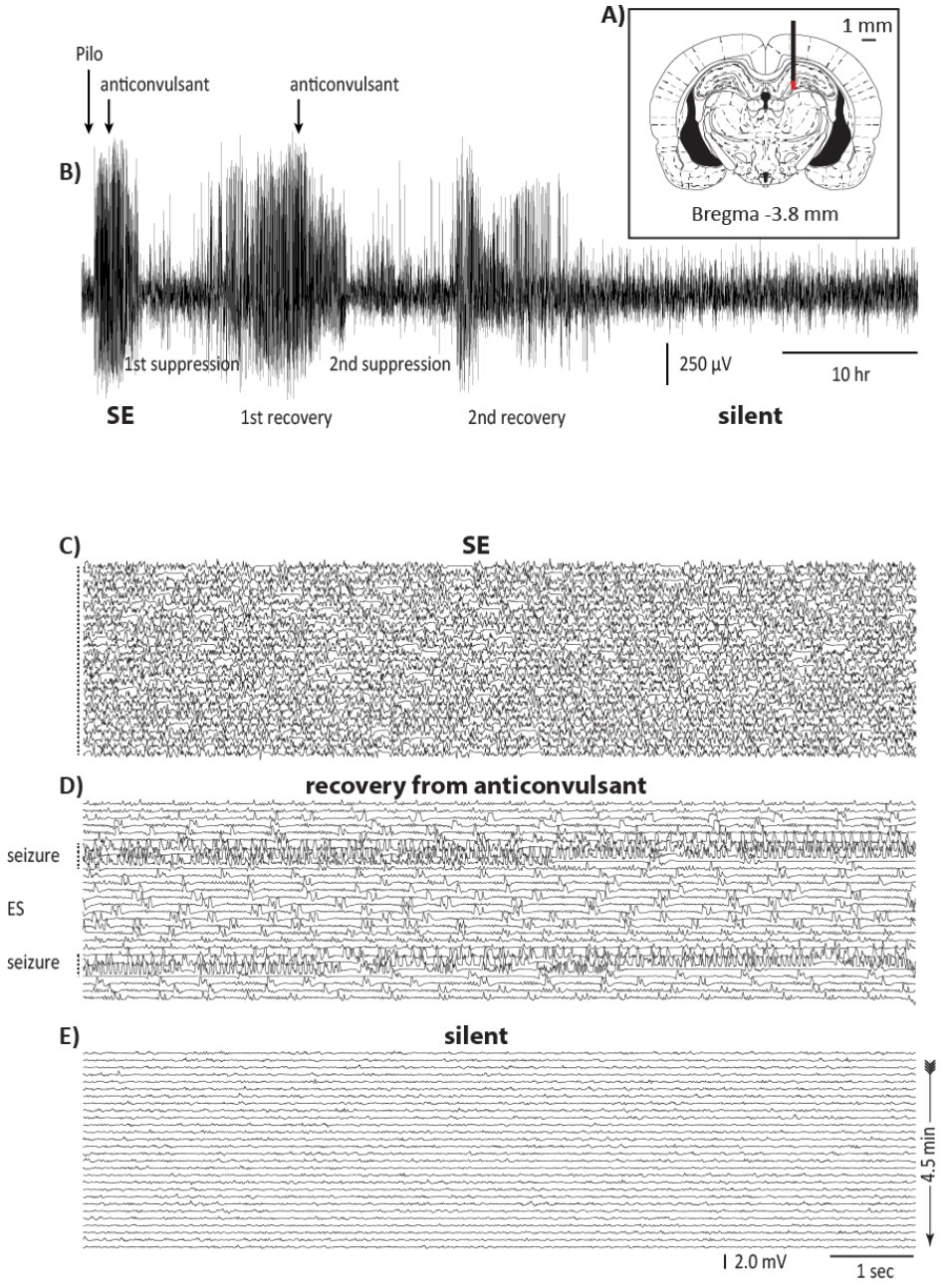

Figure 2.1 Electrographic characteristics of SE and recovery seizures. **(A)** Location of the recording electrode in auditory responsive zone of rat dorsal hippocampus. **(B)** Time compressed representation of approximately 2 days recording following pilocarpine injection. Injection of anticonvulsant after one hour SE resulted in seizure suppression (1st suppression) followed by a recovery of ictal activity (1st recovery). All rats received an additional dose of anticonvulsant, resulting in another suppression/recovery cycle (2nd suppression/recovery) before onset the silent period. **(C)** SE was characterized by continuous spiking, shown here as a raster plot of a 4.5 minute sample (10 sec/trace). **(D)** Recovery seizures were distinguished from SE by brief (30-40 sec) seizures separated by periods of interictal ES. **(E)** The subsequent silent period was devoid of seizures or ES.

Epileptiform spikes (ES)

As can be seen in Figure 2.2A, showing the progression of ES counts averaged across rats (n=12), the seizure and spike free "silent" period lasted for an average of 4.7±0.4 days before the onset of detectable ES (6.4±0.4 days post-pilo). ES onset occurred well in advance (5.8±2.4 days) of the first spontaneous recurrent seizure (SRS; **Fig. 2.2C**), during what we have termed the "pre-ictal" period (**Fig. 2.2B**); the time between ES onset and the first SRS. The average latent period (**Fig. 2.2A**; silent plus pre-ictal periods) was 10.4±2.7 days. ES onset not only consistently presaged the first SRS, their latencies (post-pilo) were correlated ($r(12) = 0.71$, $p=.048$), suggesting a linked timing of excitability changes progressing into epilepsy. SE duration was negatively correlated with the latencies of both the first SRS ($r(12) = -0.79$, $p=.002$) as well as ES onset ($r(12) = -0.62$, $p=.03$). Longer SE reliably shortened the post-pilocarpine latencies of SRS and ES onset, but this was limited to SE; the durations of the 1st and 2nd bouts of recovery seizures as well total duration of insult had no significant influence. While the onset of ES was predictive of SRS, in contrast to other reports (Chauvière et al., 2012), we did not find any systematic changes in ES waveform morphology during epileptogenesis or following the first SRS. ES averaged across animals at different stages of epileptogenesis during the pre-ictal period and beyond, showed a consistent positive spike followed by a slow negative wave (**Fig. 2.2A**).

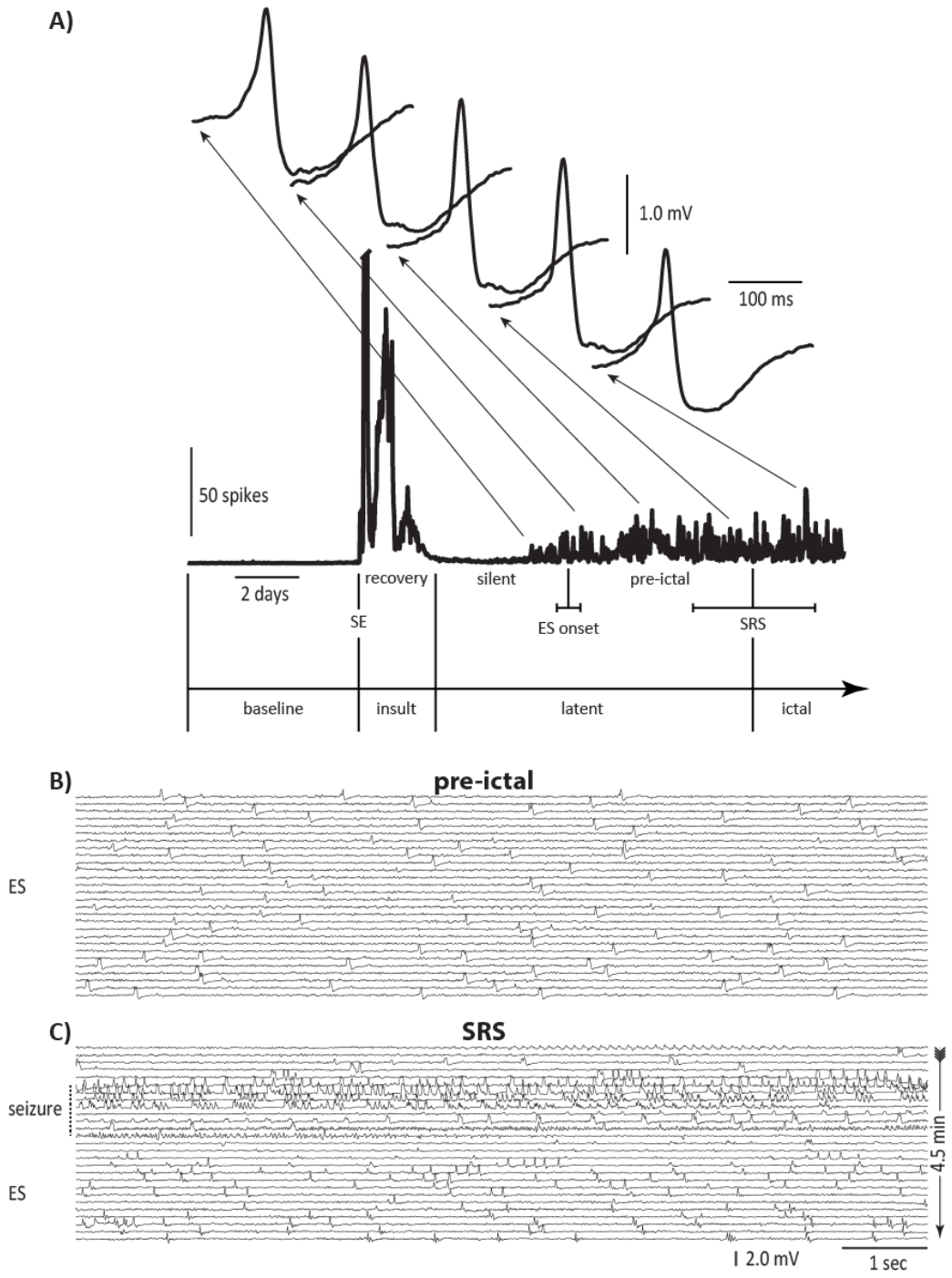

Figure 2.2 Pattern of ES preceding the first SRS. **(A)** ES counts averaged across all SRS rats revealed peaks during SE and the subsequent recovery seizure periods ("insult"). ES were notably absent for several days following the silent period ("silent") before increasing in number over the week preceding the first SRS ("pre-ictal"). ES averaged across rats indicated a consistent positive spike and negative slow-wave throughout the entire pre-ictal and ictal periods. **(B)** ES during the pre-ictal period were similar in frequency and morphology to those following the first SRS **(C)**.

Results described so far were for 12/16 rats that developed SRS. The remaining four of our rats failed to develop SRS even after several months of continuous recording. Figure 2.3A shows a plot of ES counts averaged across these 4 “non-SRS” rats. The temporal pattern and magnitude of ES counts during SE and subsequent recovery seizures (**Fig. 2.3A**) appeared similar to that of the SRS rats (**Fig. 2.2A**). Qualitatively, the appearance of SE (**Fig. 3B**) and recovery seizures (**Fig. 2.3C**) was also similar to the SRS rats (**Figs. 2.1C and D**, respectively). The response to pilocarpine insult in the non-SRS rats could not be statistically distinguished from that of the SRS rats on any measured parameter (**Fig. 2.3D**). This included the duration of SE and the durations of the 1st and 2nd suppression/recovery periods following SE as well as the total insult duration (from pilocarpine injection to the end of the 2nd recovery period). The total number of recovery seizures in the non-SRS rats (53±18.5) were also indistinguishable from the SRS rats (52.4±15.3). The only distinguishing feature in the non-SRS rats was a near absence of ES following the insult (**Fig. 2.3A**), suggesting that the presence ES during the pre-ictal period predicts subsequent SRS.

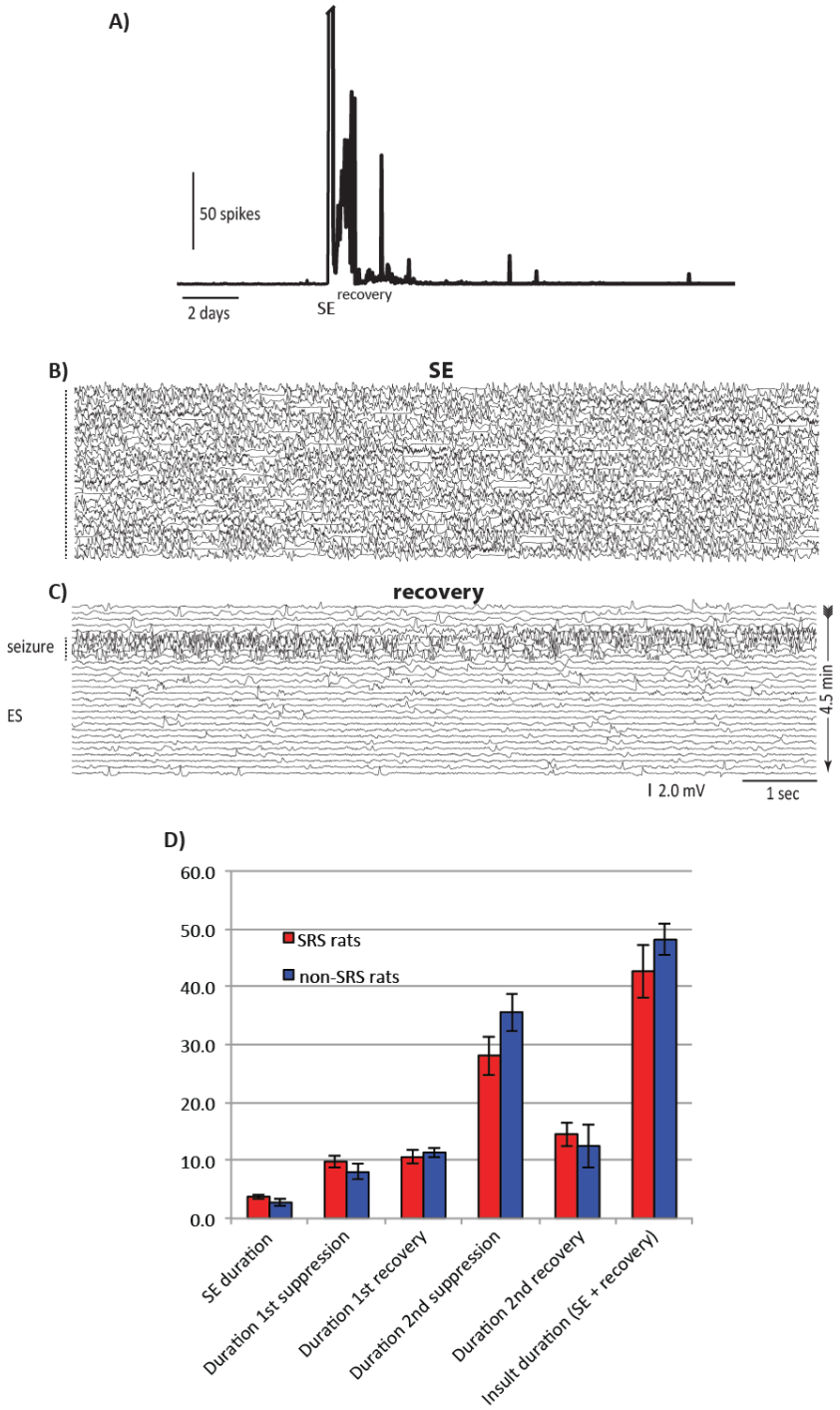

Figure 2.3 Electrographic characteristics of rats that failed to develop epilepsy. **(A)** As in rats that developed SRS, all non-SRS rats revealed peaks in ES averaged across animals, corresponding to SE and the two recovery seizure periods. However, none of the non-SRS produced subsequent ES. **(B)** SE in these animals appeared similar to the SRS rats. **(C)** Recovery seizures also appeared similar to the SRS rats, with intervening ES of similar frequency and morphology. **(D)** All parameters of the initial insult (SE and recovery seizures) were not distinguishable between the SRS and non-SRS rats.

Hippocampal auditory evoked potential (hAEP) changes during epileptogenesis

Figure 2.4A (dark trace) depicts a characteristic hAEP recorded from a single rat during the baseline period prior to SE. Similar baseline hAEPs recorded for the other 11 SRS rats are superimposed in the background (**Fig. 2.4A**; light grey traces). The hAEP consisted of a sharp negative wave followed by a slower positive wave (termed “N1” and “P1”). The N1 and P1 are represented as blue and red peaks in the isopotential map to the right, reflecting sequentially obtained hAEPs (2/hr) during the 31-day recording period in this animal. During SE and the subsequent recovery seizure period (**Fig. 2.4B**; “insult”), the hippocampus was unresponsive to sensory stimulation and the hAEP was markedly attenuated. The hAEP regained amplitude during the latent period (**Fig. 2.4C**), however, even at the earliest reappearance, it was apparent that the morphology had been changed from baseline. The durations of the N1 and P1 components (light red traces) were longer and the slopes less than the baseline hAEP. These morphological changes continued throughout the latent period, taking on an ictal waveform (**Fig. 2.4D**) prior to the first SRS and remaining stable throughout the ictal period.

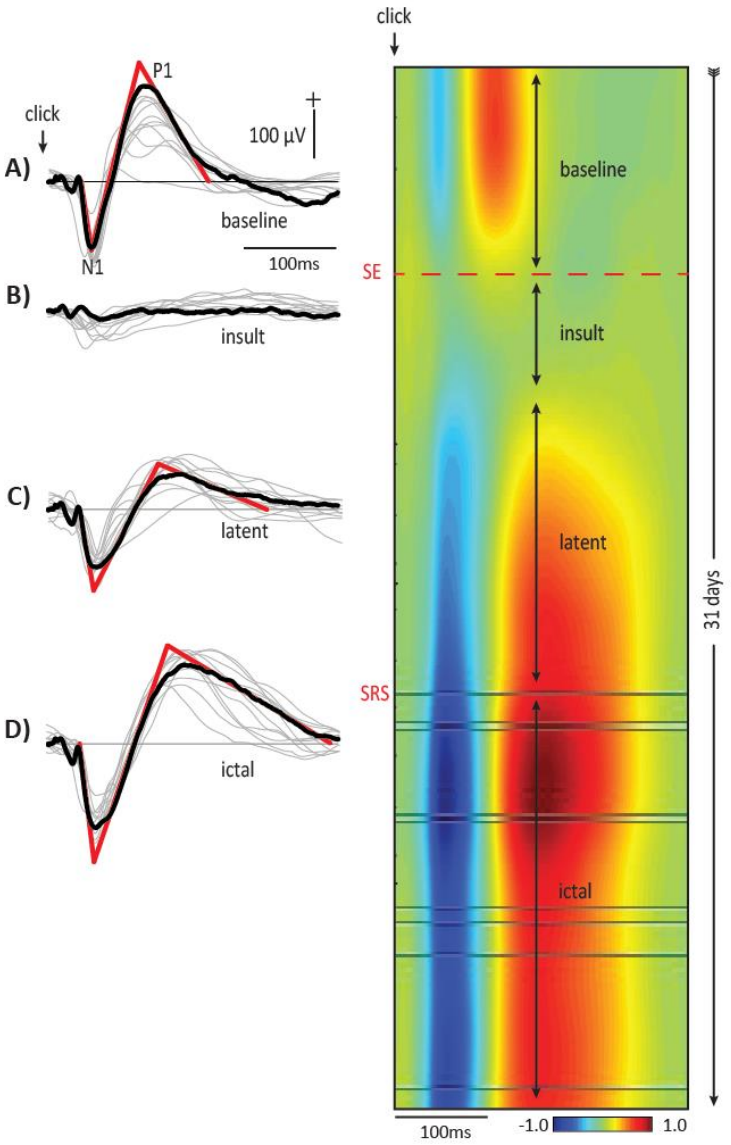

Figure 2.4 Example of stereotypical changes in hAEP morphology during epileptogenesis. **(A)** During the baseline prior to SE, the hAEP consisted of a sharp negative wave (N1) followed by a slower positive wave (P1). The slope and amplitude of these components are highlighted by red lines. hAEPs from the other SRS rats are superimposed in the background (light grey traces). The N1/P1 are plotted as blue and red regions of the normalized isopotential map to the right. This map represents post-stimulus latency on the X-axis with successive hAEPs recorded every 30 minutes over days on the Y-axis. SE and subsequent spontaneous recurrent seizures (SRS) are indicated as horizontal lines. **(B)** The hAEP was suppressed for several days during the insult. **(C)** Immediately after suppression, when the hAEP could again be recorded, the morphology was characteristically changed to a broader and delayed N1/P1 complex. **(D)** Leading into and following the first SRS, the hAEP stabilized to an ictal morphology.

Wavelet feature extraction of hAEPs

Morphological changes in the hAEP during the latent and ictal periods compared to baseline appeared similar across animals, suggesting that they might be sufficiently stereotyped to classify stages of hippocampal excitability changes during epileptogenesis, even during the silent period when spontaneous ES were absent. Figure 2.5 demonstrates the use of wavelet analysis to extract features of the hAEP for subsequent machine learning/classification. Figures 2.5A and 2.5B show a subset of the detail and approximation coefficients (scales 3 to 10) of the average hAEP computed over the four experimental conditions for the rat shown in Figure 2.4. An intuitive interpretation of the detail vs. approximation coefficients is that they respectively capture the local variability (high-pass filtered output) and local trend (low-pass filtered output) that is present in the hAEP at a given temporal scale (frequency). The median detail and approximation coefficients, computed over all the SRS animals, were compared to determine the post-stimulus latency and scales of the most significant differences ($p \leq 0.05$) between conditions. The white rectangles delineate the time intervals and ranges of scales that were found to be most useful for discriminating between conditions. Only these coefficients were retained for subsequent classification.

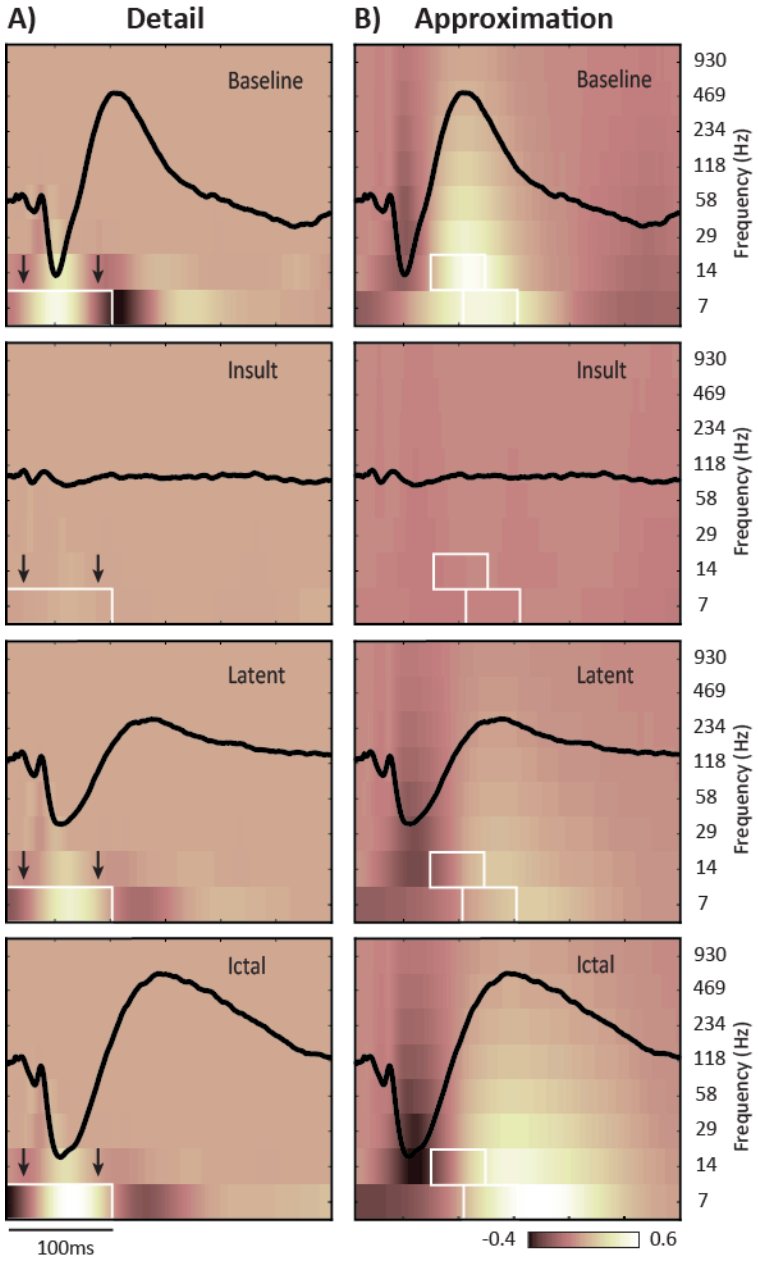

Figure 2.5 Extraction of hAEP features using wavelet analysis. The same averaged hAEP traces depicted in Figure 2.4 are superimposed on associated maps depicting the detail **(A)** and approximation **(B)** coefficients, plotted separately for each experimental condition. Superimposed white boxes highlight the subset of coefficients that best discriminated experimental conditions across animals. The coefficients were used as features for subsequent machine learning/classification.

Classification of hAEPs

To evaluate the performance of the machine learning algorithm on the SRS rats, we used a “leave one animal out” cross validation scheme where hAEPs for a target rat were removed from the training data and the algorithm was optimized using only the hAEPs of the remaining animals for the 4 conditions. The classifier was then applied to the target rat and the decoding algorithm computed probabilities (**Fig. 2.6A;** “p”) that the animal was in one of the four conditions as a function of experimental days. The time course of classification probabilities, or weights, for the rat described in Figures 2.4 and 2.5 is depicted in Figure 2.6A, and at expanded time scale in Figure 2.6B. The time course of ES (light grey) and presence of seizures (solid black) are also plotted in figure 2.6A for comparison to the time course of classification. hAEPs during the 5-day baseline were accurately classified as Baseline (**Fig. 2.6 A&B**; blue), whereas weights for the other conditions remained at zero during this period. Following SE, hAEPs were classified as Insult (cyan) for a brief period before shifting to a classification of Latent (green) for a period of several days. For the final condition, even though training hAEPs were drawn exclusively from the Ictal time period (following the first SRS in the other rats), actual classification indicated the hAEP morphology had changed to Ictal (red) approximately 14 days *before* the first SRS in this rat. Ictal classification of the hAEP also corresponded to the onset of ES (**Fig. 2.6**; grey trace; arrow). After the first SRS, subsequent hAEPs were stably classified as Ictal throughout the remaining recording during which a total of 15 seizures were logged for this animal.

Early and proleptic stages of hAEP classification

By aligning the time series of classification weights to the moment of SE occurrence in each rat, it was possible to average across rats to visualize central tendencies in the time-course of hAEP changes during the latent period (**Fig. 2.6C**). Averaged weights indicated two distinct stages of hAEP progression. The first stage we term “early”, with a post-SE onset defined as the point Insult weights declined and were exceeded by Latent weights suggesting the animals were undergoing physiological changes contributing to epileptogenesis. Similarly, onset of the

“proleptic” stage of the hAEP was defined as the point after SE when and Ictal weights surpassed the Latent weight, a predictive point at which the animal had not yet developed SRSs, but the hAEP morphology could reliably predict the eventual onset of SRS. . hAEPs averaged across all SRS rats during the Baseline and Ictal classifications are plotted to the right of Figure 2.6C (upper blue and lower red traces, respectively), showing the stereotyped broadening and slowing of the N1 and P1 during the “proleptic” hAEP stage compared to baseline.

Averaged ES counts for the SRS rats are re-plotted in the background of Figure 2.6C (light grey) for comparison to the “early” and “proleptic” hAEP periods. Similar to both ES onset and SRS latency noted earlier, the onset of the “proleptic” hAEP stage post-SE was negatively correlated with SE duration ($r(12) = -0.63$, $p = .031$); longer SE duration resulted in decreased latencies of the “proleptic” hAEP stage as well as ES and SRS. Latencies of the “proleptic” AEP stage were also positively correlated with ES onset ($r(12) = 0.94$, $p < .001$) and SRS ($r(12) = 0.66$, $p = .05$). Post-SE onsets of the proleptic stage (6.2±1.2 days) and ES (6.4±0.4 days) did not significantly differ ($p=0.45$). In contrast, the onset latency of the “early” hAEP stage (3.1±0.3 days) was not only significantly earlier than either the “proleptic” hAEP stage or ES ($p = .006$; $p = .019$; respectively), but was uncorrelated with either of these measures ($r(12) = .07$, $p = 0.83$; $r(12) = .05$, $p = 0.87$; respectively), as well as SE duration and SRS latency ($r(12) = 0.12$, $p = 0.71$; $r(12) = 0.17$, $p = 0.6$; respectively).

Figure 2.6D shows averaged classification weights of hAEPs for the non-SRS rats. Similar to the SRS rats, hAEP morphology changes following SE were immediate and persistent, resulting in classification as Insult (suppressed hAEP) for multiples days followed by several days of Latent classification, indicating the beginning of a transitional stage. However, in contrast to SRS rats, these animals displayed a complete recovery of hAEP morphology and a return to Baseline classification at a time when SRS rats typically entered the “proleptic” hAEP stage. hAEPs averaged across all non-SRS rats during the early Baseline and late recovery Baseline classifications (**Fig. 2.6D**; upper and lower traces, respectively), are nearly identical.

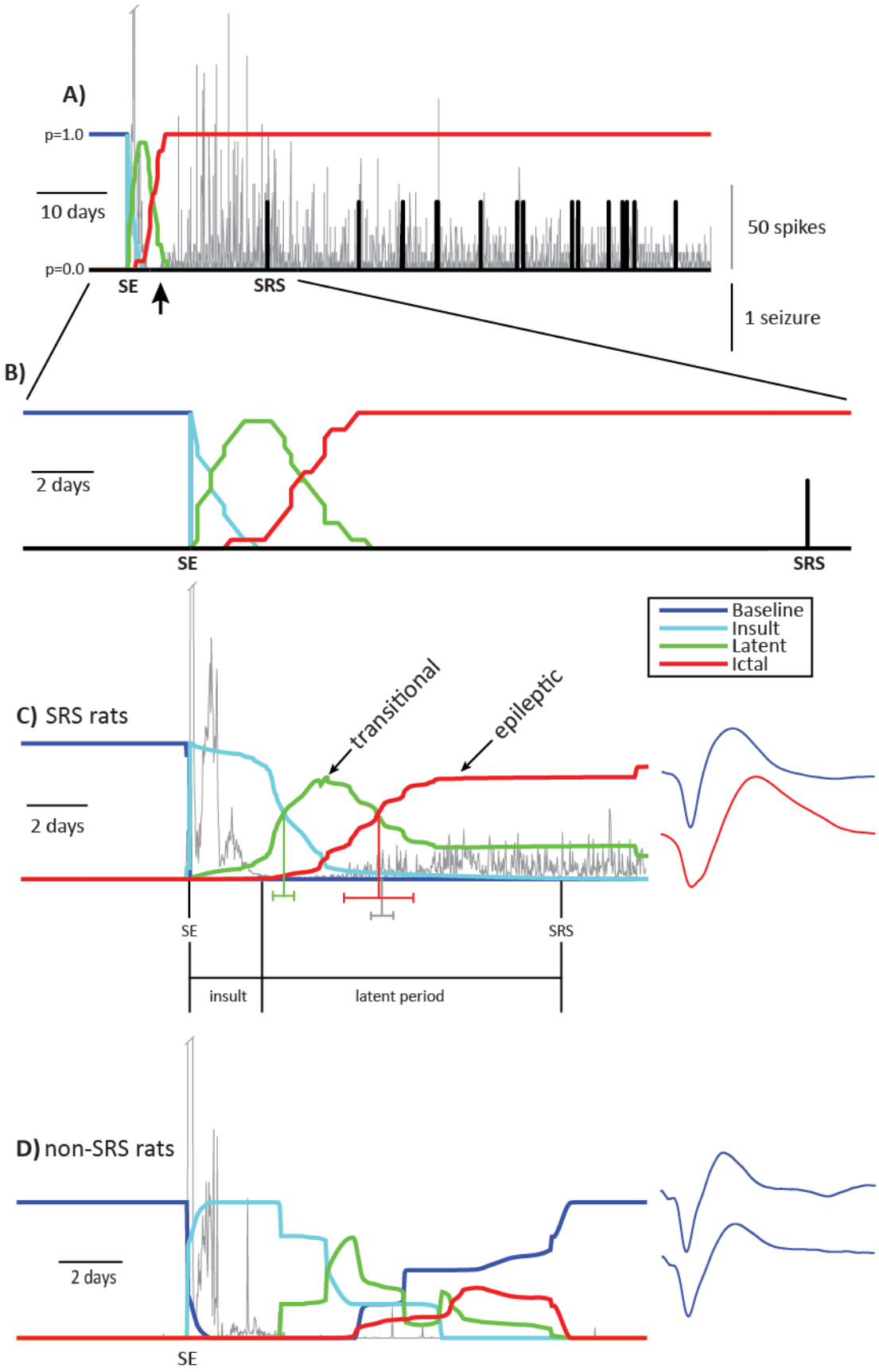
A)
p=1.0
10 days
p=0.0
SE
SRS
50 spikes
1 seizure
B)
2 days
SE
SRS
Baseline
Insult
Latent
Ictal
C) SRS rats
transitional
epileptic
2 days
SE
SRS
insult
latent period
D) non-SRS rats
2 days
SE

Figure 2.6 hAEP classification probabilities during epileptogenesis. **(A; expanded view in B)** Machine classification of hAEPs for the same animal as depicted in Figures 2.4 and 2.5. ES counts for this rat are superimposed in the background (light grey) for temporal comparison. In the "leave one out" scheme, the classifier was trained on hAEPs from all other rats and then tested on the this rat. Prior to SE, the hAEPs were accurately classified as Baseline (p=1.0; blue trace). During SE and recovery seizures, hAEPs were briefly classified as Insult (cyan) before switching to Latent (green) and ultimately to Ictal (red) classification, many days in advance of the first SRS. Ictal classification of the hAEP was concurrent with the appearance of ES. **(C)** Classification weights were averaged across all SRS rats by aligning the weights to the time of pilocarpine injection in each animal. Averaged ES counts from Figure 2.2A are superimposed in the background. Two stages of epileptogenesis can be identified. The "transitional" stage peaks during the silent period. The "epileptic" stage grows along with the appearance of ES and continues up to and beyond the first SRS. hAEPs averaged across all SRS rats during the Baseline and Ictal classifications are plotted to the right (upper blue and lower red traces, respectively). **(D)** Classification weights for the non-SRS rats were similar to the SRS rats during the Baseline, Insult and Latent periods. However, in contrast to the SRS animals, the beginning Ictal classification gives way to a return to Baseline. hAEPs averaged across all non-SRS rats during the early Baseline and late recovery Baseline classifications are plotted to the right (upper and lower traces, respectively).

Summary of Results

The key results from these experiments are: (1) Lithium/pilocarpine administration (plus paraldehyde) produced a total insult persisting for nearly two days that consisted of SE followed by two groups of subsequent recovery seizures separated by anticonvulsant suppression. (2) This insult was followed by a silent period, absent of ES, and a pre-ictal period where ES appeared days before the first SRS. (3) Machine classification, based on the waveform morphology of hAEP, indicated a stereotypical change from baseline indicative of epileptogenesis. First, an early stage of epileptogenesis where temporal components of the hAEP were delayed and broadened but ES are absent, followed secondly by further morphological changes in the evoked response (i.e., the proleptic hAEP classification) coinciding with the appearance of ES, signaling the eventual development of spontaneous seizures. (4) Post-SE latencies of the "proleptic" hAEP stage, ES onset, and the first SRS were correlated with each other and negatively correlated with SE duration, indicating that more prolonged SE resulted in an overall acceleration of epileptogenesis. (5) Post-SE latency of the "early" hAEP stage was not correlated with any parameter of the insult. (6) Whereas the "early" hAEP stage of epileptogenesis occurred whether or not rats went on to develop epilepsy, both the "proleptic" hAEP stage and ES only occurred in epileptic rats and were predictive of epilepsy days in advance of the first SRS; non-epileptic rats did not produce ES and showed a return of hAEP morphology to pre-insult baseline despite being indistinguishable in all parameters of the initial insult.

DISCUSSION

SE and recovery seizures comprise the total insult

Accurately characterizing the temporal progression of epileptogenesis during the latent period, and relating this progression to the severity of insult, requires accurate characterization of the insult itself. To decrease variation in SE length and improve comparability between studies, as well as to decrease mortality, SE is typically terminated after 1-2 hr with anticonvulsant drugs (Löscher & Brandt, 2010). However, most anticonvulsant drugs are rapidly eliminated by rats

(Löscher, 2007), resulting in SE recurrence that might be overlooked without continuous EEG recording (Löscher & Brandt, 2010; Reddy & Kuruba, 2013). All rats demonstrated two bouts of SE recurrence, timed to injections of paraldehyde that were separated by approximately 12 hr. We termed these "recovery seizures" because they were discontinuous (numerous discrete seizures) as opposed to the continuous electrographic and behavioral convulsions characterizing SE. However, they were clearly a continuation of the SE process, separated only by transient anticonvulsant induced suppression. While it has been proposed that early occurring seizures may represent the first unprovoked seizures in the SE model (i.e. the first SRS; Jung et al., 2007), our data suggest that they are actually part of the initial insult, similar to insult-associated symptomatic ("early") seizures (Brandt, Töllner, Klee, Bröer, & Löscher, 2015; Rattka, Brandt, Bankstahl, Bröer, & Löscher, 2011; Sirven, 2009). As proposed by others (Brandt et al., 2015; Curia et al., 2008; Mazzuferi, Kumar, Rospo, & Kaminski, 2012; Rattka et al., 2011), we therefore regard recovery seizures as part of the total insult but distinct from SE.

The transitional stage of hAEPs is immediate and reversible

Following general suppression of hippocampal responsiveness after insult, hAEP amplitude recovered during the silent period, but with a morphology grossly altered from baseline. This prototypical shift in sensory responsiveness reflects *immediate* changes in hippocampal excitability not identified in previous epileptogenesis studies relying on passive measures of EEG (i.e. ES or associated pHFO). The altered hAEP appears days before the development of ES. A number of pathological events related to epileptogenesis may occur during the silent period that could contribute to hippocampal excitability changes, capable of producing alterations in the hippocampal sensory response. These include synaptic reorganization, reactive gliosis, mossy fiber sprouting, cell proliferation and various channelopathies (Dalby & Mody, 2001; Jung et al., 2007; Pitkanen & Sutula, 2002). However, the present results put two constraints on possible mechanisms. First, they must occur rapidly, within days of insult, since hAEP changes are present at the earliest recovery from post-SE suppression. Second and most important, potentially

epileptogenic processes during the early hAEP stage must be largely reversible. This last constraint is based on the observation that our non-SRS rats, while indistinguishable in all parameters of initial insult when compared to SRS-rats and presenting identically altered hAEP morphology during the early hAEP stage, display a complete recovery of the hAEP. Instead of evolving to the proleptic stage with accompanying ES, the hAEP returns to pre-insult baseline and remains that way for months of continuous recording. The reversibility observed here suggests that antecedent epileptogenic processes during the "early" hAEP stage are plastic and less indicative of long-term anatomical/circuit alterations than they are reflective of more dynamic events such as rapid inflammatory processes altering microglial morphology (Dissing-Olesen et al., 2014), astrocytic uncoupling (Bedner et al., 2015) or impaired ionic buffering and disturbed gliotransmission (Steinhäuser, Grunnet, & Carmignoto, 2016). Spontaneous recovery of the hAEP in non-SRS rats also suggests that the plastic early phase may represent an opportune window for disease modification in this model, with the hAEP serving as an objective measure of success.

The epileptic stage of hAEPs and appearance of ES predict epilepsy

In contrast to non-SRS rats, SRS-rats undergo further hAEP changes and simultaneously develop ES. The close correlation between onset of the hAEP proleptic stage and ES onset suggests that they reflect a common process. Progressive increases in hippocampal excitability indexed by the hAEP may also serve to trigger ES. While stereotyped morphological changes in the hAEP occurred days in advance of the first SRS, we were not able to detect any changes in ES wave shape prior to or following SRS. This was surprising in light of recent evidence to the contrary (Chauvière et al., 2012). These researchers have described "Type 1" spikes (characterized by a spike followed by a slow wave) that decrease in number, amplitude, and duration prior to the development of spontaneous seizures, and "Type 2" spikes (characterized by a spike without a slow wave) appearing transiently prior to the first seizure. ES in the present study were similar to Type 1. It is possible that a bias arose due to selective training of the SVM

model using the most common spikes. However, visual examination of ECoG records just prior to the first SRS in all rats also revealed only Type 1 spikes. Our lack of morphological change may therefore be more reflective of electrode placement and region specificity. Salami et al. (Salami et al., 2014) demonstrated structure specific alterations in spike morphology in the entorhinal cortex and CA3 region inconsistent with changes shown in the CA1 by (Chauvière et al., 2012). In contrast, dentate granule cells are relatively resistant to damage during the time course of epileptogenesis, as demonstrated by temporal analysis of network properties and progressive hippocampal cell loss in animal models of acquired epilepsy (Buckmaster & Dudek, 1997a; Heinemann et al., 1992; Lothman, Stringer, & Bertram, 1992). This may explain the consistency in spike morphology we observed in dentate granule cell layer both preceding and following the first SRS. While we found no changes in ES morphology representative of the progressive nature of epileptogenesis, we did find that ES activity consistently arose days prior to the development of SRS in rats that developed epilepsy and was absent in non-SRS rats. This finding concurs with previous studies (White et al., 2010; Salami et al., 2014; Lévesque et al., 2015) suggesting that, regardless of spike morphology, ES incidence during the latent period, combined with epileptic hAEP morphology, may provide a highly reliable indicator of epilepsy risk.

SE duration predicts the onset latencies of the epileptic stage, ES, and SRS

We found that the duration of SE alone was negatively correlated with onset latencies of the proleptic hAEP stage and ES, as well as the first SRS, suggesting a powerful influence of initial injury on the rate of epileptogenesis. This finding is in agreement with other studies of the pilocarpine model, indicating a direct influence of SE duration on the latency to the first SRS (Biagini et al., 2006; Klitgaard, Matagne, Vanneste-Goemaere, & Margineanu, 2002; Lemos & Cavalheiro, 1995). However, reported correlations have been both positive and negative, possibly due to differences in the definition of SE duration (Brandt et al., 2015). These studies monitored SE duration behaviorally but not electrographically. We confined our definition of SE to the period of continuous convulsive EEG spiking, extending from pilocarpine injection to the first suppression

with anticonvulsant. Thus, SE duration was distinguished from the subsequent repetitive recovery seizure periods, which did not correlate significantly with onsets of the epileptic stage, ES or the first SRS. Our findings are consistent with recent work using the pilocarpine model, where total insult was confined to just SE without subsequent recovery seizures by using a cocktail of diazepam, pentobarbital and scopolamine (Brandt et al., 2015). With this preparation it was possible to highlight the direct influence of SE alone on epileptogenesis, with durations greater than one hour required for subsequent SRS and marked increases in hippocampal neurodegeneration, reflecting the key influence of early injury parameters. Paradoxically, while we found that SE duration inversely influenced the span of the latent period, we did not detect any feature of injury, including SE, that differed between SRS and non-SRS rats. This outcome places additional importance on discovering potentially reversible processes of epileptogenesis during the early phase of the hAEP.

The hAEP as a biomarker for epileptogenesis

Epileptogenesis is a multifactorial and continuous process, remaining poorly understood due in part to the lack of definitive biomarkers (Engel et al., 2013). However, despite the high degree of phenotypic variance in epilepsy development within our experimental animals, consistent evocable electrophysiological changes occurred during the latent period that signaled the onset of epilepsy. These changes occurred in conjunction with increases in ES with animals later developing SRS. While it is unlikely that any single biomarker will be perfect, we have demonstrated the ability to actively measure epileptogenesis with near real-time feedback, tracking changes in localized hyperexcitability indicative of epilepsy risk. hAEP and ES analysis should be used in conjunction with emerging epileptic biomarkers such as the analysis of pHFO's in future studies. The 24/7 field potential analysis alone presents an electrographic window into the epileptogenic "silent period", providing insight into the time-sensitive pathological network alterations that differentiate an epileptic brain from a normal one. With the clear pre-seizure

delineation between animals that will or will not develop SRS, this tool could be further used as a real-time measure for therapeutic windows of opportunity in the development of future AEDs.

Chapter 3:

Progression of Convulsive and Nonconvulsive Seizures During Epileptogenesis After Pilocarpine-Induced Status Epilepticus

Abstract

Although convulsive seizures occurring during pilocarpine-induced epileptogenesis have received considerable attention, nonconvulsive seizures have not been closely examined, even though they may reflect the earliest signs of epileptogenesis and potentially guide research on antiepileptogenic interventions. The definition of nonconvulsive seizures based on brain electrical activity alone has been controversial. Here, we define and quantify electrographic properties of convulsive and nonconvulsive seizures in the context of the acquired epileptogenesis that occurs after pilocarpine-induced status epilepticus (SE). Lithium pilocarpine was used to induce the prolonged repetitive seizures characteristic of SE; when SE was terminated with paraldehyde, seizures returned during the 2-day period after pilocarpine treatment. A distinct latent period ranging from several days to >2 weeks was then measured with continuous, long-term video-EEG. Nonconvulsive seizures dominated the onset of epileptogenesis and consistently preceded the first convulsive seizures but were still present later. Convulsive and nonconvulsive seizures had similar durations. Postictal depression (background suppression of the EEG) lasted for >100 s after both convulsive and nonconvulsive seizures. Principal component analysis was used to quantify the spectral evolution of electrical activity that characterized both types of spontaneous recurrent seizures. These studies demonstrate that spontaneous nonconvulsive seizures have similar electrographic properties to convulsive seizures and confirm that nonconvulsive seizures link the latent period and the onset of convulsive seizures during post-SE epileptogenesis in an animal model. Nonconvulsive seizures may also reflect the earliest signs of epileptogenesis in human acquired epilepsy when intervention could be most effective.

Abbreviations. AED, antiepileptic drug; EEE, epileptiform electrographic events; FPI, fluid percussion injury; MID, mid-ictal depression; PCA, principal components analysis; PID, post-ictal depression; PTE, post-traumatic epilepsy; SE, status epilepticus; SRS, spontaneous recurrent seizures; SVM, support vector machine; SWD, spike-wave-discharge; sSWD, slow spike-wave-discharge.

Introduction

In humans with acquired (i.e., injury-induced, non-genetic) epilepsy, nonconvulsive seizures may represent the earliest and most abundant epileptiform events. These seizures, however, often go unidentified – and thus unreported – due to the relative absence of clear behavioral symptoms (e.g., convulsions). While posing as an impediment to accurate diagnosis, nonconvulsive seizures also present problems for treatment, since unreported seizures could confound issues such as the assessment of drug efficacy. Epileptogenesis, the transformation from normal to epileptic neural circuits, is thought to begin during a *latent period*, which is the time between brain injury and development of convulsive, spontaneous, recurrent seizures (SRSs). Early identification of nonconvulsive epileptic seizures may therefore be critical for developing clinically effective treatments, and the primary clinical tool is the electroencephalogram (EEG). However, the identification, and even definition, of nonconvulsive seizures using EEG in various animal models of acquired epilepsy remains controversial (D'Ambrosio & Miller, 2010; Dudek & Bertram, 2010; Rodgers et al., 2015).

Brief, oscillatory, electrographic events have been proposed to be nonconvulsive seizures in rat models of acquired epilepsy based on fluid percussion injury (D'Ambrosio et al., 2004), neonatal hypoxia (Rakhade et al., 2011) and hyperthermia-induced convulsions (Dubé et al., 2006). In each case, these putative nonconvulsive seizures consisted of rhythmic spike-wave discharges (SWDs) in the neocortex or hippocampus. SWDs are stereotyped electrographic bursts associated with nonconvulsive behavior (i.e., "behavioral arrest") that are reportedly recorded after injury and therefore proposed to be analogous to human focal post-traumatic seizures (D'Ambrosio et al., 2009). Studies are now underway with these models to use nonconvulsive SWDs as outcome measures for exploration of mechanisms underlying epileptogenesis, as well for developing antiepileptic drugs (AEDs) and/or anti-epileptogenic compounds (e.g., Eastman et al., 2015). However, SWDs do not reliably reflect post-traumatic nonconvulsive seizures, since they are also observed in control animals without injury (Kelly et

al., 2006; Kelly, 2004; Kelly, Miller, Lepsveridze, Kharlamov, & Mchedlishvili, 2015; Pearce et al., 2014; Rodgers et al., 2015). SWD bursts have been reported in a variety of otherwise healthy outbred and inbred rat strains and become more prevalent with age (Rodgers et al., 2015; Taylor et al., 2017). It is therefore possible that potential AEDs targeting these nonconvulsive events could be ineffective, if not contraindicated, if this brain activity can also be normal for uninjured laboratory rats.

Most research on acquired epileptogenesis has been with animal models that are based on status epilepticus (SE; characterized by hours of continuous seizure discharge), acutely induced through pilocarpine, kainate, or electrical stimulation. In SE models, the initial seizure-induced injury is typically followed by days or weeks of behavioral quiescence before convulsive SRSs appear. It is during this latent period that epileptogenesis may begin. Indeed, early studies of electrical stimulation-triggered SE (Bertram & Cornett, 1994) and subsequently of kainate-induced SE (Williams et al., 2009) have reported nonconvulsive seizures occurring during the latent period (defined as the time until the first clinical seizure), which may represent the first signs of epileptogenesis otherwise undetected without continuous EEG recording. Long-term EEG recordings after perinatal hypoxia-ischemia (Kadam et al., 2010) have also demonstrated that the development of SRSs is progressive, with initial occurrence of nonconvulsive seizures. A common finding in these studies is that the nonconvulsive seizures do not resemble SWDs, but instead, subjectively appear electrographically more similar to subsequent convulsive SRSs. However, except for seizure duration, objective measures do not exist to compare and contrast potential epileptiform events.

In the present experiments, we used long-term video-EEG recording in a pilocarpine-induced SE model of acquired epilepsy to examine progressive changes in the SRSs during epileptogenesis. Specifically, our objectives were to leverage signal analysis methods to identify, define, quantify and contrast electrographic features of nonconvulsive and convulsive seizures, to discriminate these ictal features from non-epileptic events, and finally to determine the temporal

evolution of nonconvulsive/convulsive seizure components that may be beneficial for future studies aimed at finding better treatments for pharmacoresistant epilepsy.

Materials and Methods

Ethical Approval

Twenty viral-free, adult male, Sprague-Dawley rats (Harlan Laboratories, Madison, WI; 250-300g) were housed in temperature (23 ± 3 °C) and light (12:12 light: dark) controlled rooms with *ad libitum* access to food and water. All procedures were performed in accordance with University of Colorado Institutional Animal Care and Use Committee guidelines for the humane use of laboratory rats in biological research.

Continuous video EEG recording

All animals were implanted using aseptic surgical techniques and sterilized recording implants. Animals were anesthetized using isoflurane (Abbott laboratories; 3.5% induction, 2-2.5% maintenance), followed by the implantation of Teflon-coated hippocampal wire electrodes with an exposed tip (AP, -3.8; ML, 1.1-1.5; DV, 3.5-3.8) driven stereotaxically into the dorsal dentate gyrus and verified by the presence of high-frequency granule-cell activity and hippocampal auditory evoked-potential responses. Three stainless-steel screw electrodes (Plastics One part #E363) were implanted up to the surface of the cortex as ground (occipital bone), reference (AP, +4.5; ML, 2.0), and somatosensory (AP, -2.0; ML, - 2.0) screws. To reduce the loss of head caps, self-tapping stainless-steel screws (Small Parts, B000FN89DM) were implanted bilaterally into the surface of the skull without making contact with the cortical surface. Wire bundles were affixed to a head-stage (Plastics One, MS363) using dental acrylic. Buprenorphine (0.1 mg/kg, I.M.) was administered immediately after the surgical procedure and again every 12 h for a 72-h period. Animals were given antibiotic in their water (HITECH Pharma) for 1 week following surgery to prevent infection. Following a 2-week recovery, animals were tethered to an electrode harness (Plastics One, 363) and slip-ring commutator (Plastics One, SL6C) permitting free movement for continuous video-EEG monitoring throughout the duration of

the experiment. EEG was amplified (X10,000), filtered (1-250 Hz), digitized at 500 Hz to minimize file size, time-locked to video (30 FPS), and saved in 30-min blocks for subsequent analysis.

Lithium-pilocarpine model of temporal lobe epilepsy (TLE)

Following full recovery from surgery, baseline EEG was measured from animals for 1 week before chemoconvulsant administration to verify signal efficacy. The day before pilocarpine treatment, we delivered an IP injection of lithium chloride (3 mEq/kg, 1 ml/kg, Sigma, St. Louis, MO). Twenty hours later, an IP injection of the peripherally acting anti-cholinergic drug methyl-scopolamine (1 mg/kg, 1 ml/kg, Sigma, St. Louis, MO) was given to ameliorate peripheral muscarinic effects of pilocarpine. Twenty minutes after scopolamine administration, a single injection of pilocarpine hydrochloride (50 mg/kg i.p., 1 ml/kg, Sigma) was administered to induce SE. The beginning of SE was determined by the emergence of bilateral forelimb clonus and rearing, leading to continuous generalized convulsive seizure activity consistent with previous studies using the pilocarpine model (Brandt, Töllner, Klee, Bröer, & Löscher, 2015; Curia et al., 2008). After 1 h of SE, the animals were administered an IM dose of paraldehyde (0.3 mg/kg, Sigma, St. Louis, MO) to terminate convulsions. A second dose of paraldehyde was given 24 h later and 5 ml of saline co-administered (SC) with both doses. We found that paraldehyde was much more effective than diazepam for increasing post-SE survival and terminating electrographic SE activity by maintaining a 90% survival rate (18/20 rats) (Morrisett et al. 1987, Kubova et al. 2005). Animals were kept on post-surgical nutritional gel (Diet Gel, ClearH2O, Portland, OR) and their water was replaced with an electrolyte sports drink (Gatorade) for 72 h. Video-EEG was continuously monitored throughout SE and subsequently for 3-4 mo. We have found that this method of aseptic electrode implantation, postsurgical care, SE induction, SE termination, and post-SE care maximized animal survivability and long-term recording efficacy by reducing the risk of infections and head-cap loss. However, this was not fully prevented, 7/18 rats eventually lost their head stage before the 98-day time point (black arrows **Fig. 3.3**). Data for

these animals was analyzed up to the time of head-stage loss (i.e., animals were not re-implanted).

Manual EEG analysis

High-resolution monitors were used to display 30-min blocks of EEG divided into 10-s segments in raster-plot format. Both cortical and hippocampal channels could be observed simultaneously with on-demand time-locked video. Observers (ZZS and AMB) were trained to identify epileptiform EEG activity, monitor the behavioral correlates while ignoring obvious noise from normal behaviors (chewing, head scratching, etc.), and identify possible ictal patterns for further analysis. Electroencephalographic seizures were differentiated from background noise by the appearance of large-amplitude, high-frequency (minimum 5 Hz) activity, with an evolution of EEG spike frequency lasting at least 5 s. However, to prevent missed seizures, all suspected seizure discharges with no minimum time limit were observed with concurrent video. Seizure flags were time-locked to the EEG and scored via the Racine scale (Racine, 1972) through video observation. Animals demonstrating electrical seizure activity, with a behavioral Racine scale of 2 or below (head bobbing, staring, lack of forelimb clonus) were identified as having a nonconvulsive seizure, while animals demonstrating a behavioral Racine scale of 3 or above (forelimb clonus, rearing, rearing and falling) were identified as having a convulsive seizure. Video monitoring was performed during the entire seizure as well as 40 s before and after an event. To prevent possible misidentifications, all seizures were behaviorally scored twice for Racine verification by independent observers. Seizures were quantified for 98 d following SE to standardize cross-animal signal viability.

Automated seizure detection and feature analysis

Following complete manual identification of seizures, we developed a seizure detection algorithm based on power spectral analysis of the EEG signature. For each individual animal, we isolated epochs of ictal activity for at least 10 seizures totaling over 250 s for use in seizure identification. We then isolated periods of non-ictal activity and noise for comparison. Using the

power spectral density of the two groups, we trained an individually tailored support vector machine (SVM) (Orrù et al., 2012) for supervised seizure detection. All seizure candidates within an animal were isolated and then checked for false positives. Seizure candidates determined to be noise were deleted and not used in subsequent analysis. Seizure candidates were compared to manual identification to verify behavioral Racine score. Candidates that were identified via SVM but missed by initial manual identification were behaviorally scored.

To completely isolate seizure events and observe the patterns before, during, and after a seizure episode, the onset of each seizure was visually marked, and the time-period from 100 s before to 350 s after the onset was isolated. For seizure event analysis, the initial 80-s period leading into the detected seizure was used as the pre-ictal baseline, where the standard deviation was computed for identification of signal change once the seizure had begun. Successive 1-s segments of EEG were analyzed for each isolated 450-s segment. Signal changes at 1.5 standard deviations (SDs) above or below the baseline signal were identified as “spiking” or “depression” respectively. All isolated seizure events were also manually observed with custom software allowing for the identified deviations to be overlaid onto the EEG, color coded, and verified. Deviation values were chosen only after visual examination verified the accuracy of using 1.5 SD to identify differences in EEG. Finally, during visual examination of each seizure, the occurrence of spiking and depression were used to guide digital marking of the period of ictus, mid-ictal depression (MID), and post-ictal depression (PID). Ictus (i.e., seizure) was defined as the period from spiking onset to offset, whether or not this period was interdigitated with periods of MID. PID was defined as the period of depression following ictus (see below).

Supervised pattern recognition of non-ictal events

Following manual identification of suspected ictal-like events during initial EEG analysis, we used the same supervised pattern recognition previously described (Rodgers et al., 2015) to isolate and quantify cortical activity in order to identify temporal patterns of epileptiform non-ictal events. Two event types were studied: SWDs (7-9 Hz) and “slow SWDs” (sSWDs; 3-5

Hz); the latter were prominent in the first week post-SE. For SWDs, data were analyzed in 1 s segments, across 48 h time epochs per rat, at post-SE intervals of 1, 2, 3, 4, and 5 mo. (approximately 3, 4, 5, 6, and 7 months of age). Approximately 20 segments containing SWDs were visually selected for analysis. For identified sSWDs, data were analyzed in the same manner, but at post-SE intervals of 3, 7, 10, 30, and 60 d. One-second segments selected for sSWDs were biased towards 3 d post SE due to the ease of identification during this time. Approximately 150 single-second segments of SWDs or sSWDs were selected for template production. The amplitude, frequency, and morphology of the 1 s waveforms were captured through autocovariance functions. These were then used in conjunction with autocovariance functions for 1 s segments of noise (approximately 5,000) to train the SVM to automatically discriminate between noise and identified segments throughout 48 h of data at each time point. In this way, SVM was individually tailored for each animal using the animal's own 1-s segments of data. All detected data were visually examined during each time point for every animal to identify and remove artifacts prior to quantification. Behavioral monitoring was performed using time-locked video during manual EEG analysis.

Epileptiform Spike (ES) Detection

We also used supervised pattern recognition to detect ESs. For each rat, 20-30 ESs were visually identified, temporally aligned according to the negative peak of the spike, and averaged to create a template (± 150 ms window surrounding the peak). The spike template was then shifted point by point through the same data from which the spikes were visually identified and the covariance between data and template were computed as a function of time. The covariance time-series was visually thresholded to separate noise from correct detections. The time-shifted covariance between the spike template and 5 hr baseline data (before pilocarpine administration) was computed and the threshold applied to examine false detections. False detections from the baseline were averaged to create a non-spike template. All subsequent detections compared the covariance between the data and both the spike and non-spike

templates. While the two-template approach improved correct detections, many spikes were still falsely detected in the baseline. To reduce false detections further, we added a second level of analysis relying on a Support Vector Machine (SVM) for pattern recognition (Orrù et al., 2012). For each rat individually, the SVM kernel was trained to discriminate the 20-30 initially identified spikes from approximately 1000 miss-identified spikes in the baseline. The combination of templates and SVM were then used to detect ESs for all subsequent data for a given rat.

Spectral power stability analysis

The power spectral density of isolated seizures, SWD and sSWD events was computed to observe the relative contribution of specific frequencies to the overall signal. Animal-specific spectral density was charted as a function of time, with the frequency contribution to 1-s segments of isolated seizures plotted contiguously for all seizures of the animal as a spectrogram. To observe the variability in signal composition, principal components analysis (PCA) was performed on the spectrogram for each animal (for an intuitive explanation of PCA used with field potential analysis, see (Barth, Di, & Baumgartner, 1989). PCA, a multivariate statistical procedure, was used in the present study to determine whether the variance of the spectrogram (system variance) could be explained by the linear combination of a small number of fundamental spectra (principal components). The analysis began by defining the spectrogram in a signal space of N spectra (N reflecting the number of 1-s segments across which the original spectrogram was computed). The spectrogram was therefore completely represented as 250 points (frequency coefficients) in an N-dimensional signal space. The task of PCA was to determine if the same data points could be represented in a subspace using fewer dimensions than the original signal space. The principal components were those linear combinations of the original spectra which explained successively a maximum of the system variance and were orthogonal to each other. In geometrical terms, this means that the coordinate axes of the original signal space were rigidly rotated so that the first principal component was aligned in the direction of the maximum variation of the data points, the second principal component was aligned in the direction of the maximum residual variance and

orthogonal to the first and so forth. The coefficients of the linear combinations are called component-loadings and correspond geometrically to the direction cosines of the principal components. From N original spectra, N principal components could be achieved. However, usually a significantly smaller number of principal components sufficed to adequately represent the data. Thus, the original signal space could be well represented in space of much lower dimension (common factor space) with the principal components as coordinate axes. The values of the principal components calculated for each 1-s segment of the spectrogram are called component-scores. Thus, the original spectrogram can be reconstructed by multiplying the loadings with the scores of only the significant principal components and adding them linearly.

If only a single spectrum was capable of fitting the entire spectrogram, only the 1st principal component would be required to explain all of the variance. In this case, subtracting a model of the spectrogram, based on the 1st principal component, from the original spectrogram would yield zero residual variance. The percent of residual variance with only the 1st principal model was therefore used as an index of spectral variability across all seizures (or SWD, sSWD events) for a given animal and was also computed separately for convulsive and non-convulsive seizures to determine if behavioral seizure score had any contribution to frequency variability.

Statistics

Results are expressed as mean ± SEM, with the exception of the post-SE onset latencies of initial spontaneous convulsive seizures. Because these onsets were highly variable, with extreme values in several rats, they were reported as the median ± MAD (median absolute deviation). MAD is a robust statistic, more resilient to outliers than the standard deviation. A two-way analysis of variance (ANOVA) was performed with latency post-SE (2-20 vs 21-98 d) and convulsive intensity (nonconvulsive vs convulsive) as the independent factors. Distributions for nonconvulsive and convulsive seizure rates deviated significantly from normal (Shapiro-Wilk test). Therefore, a non-parametric Mann-Whitney test was used for subsequent planned comparisons. A one-way ANOVA was used to examine age-related differences in SWD event counts and

durations. Fisher's LSD was used to conduct planned pairwise comparisons to follow-up significant overall ANOVAs. A one-way MANOVA with seizure intensity as the independent variable was performed to summarize findings and account for any potential interaction of recorded variables (ictus, MID, PID, and % power in the residuals) in the hippocampus. In conjunction, a two-way MANOVA was performed with the addition of location (cortex-hippocampus) as a second independent variable. Data were analyzed using SPSS® Statistics software and, in all cases, statistical significance was set at $p < 0.05$.

Results

Properties of pilocarpine-induced status epilepticus and operational definition of duration

SE typically commenced within 15 min of pilocarpine injection and consisted of an initial, prolonged period of continuous spiking in the hippocampal electrode with convulsions (**Fig. 3.1A & B**; SE). All initial analysis was confined to the hippocampal lead, and subsequently compared to the cortex. At 1 h post-pilocarpine, anticonvulsant injection resulted in a suppression of SE for several hours, yet the seizures invariably returned and appeared as alternating periods of high- and low-frequency spiking (**Fig. 3.1C**) with associated convulsions. The second anticonvulsant injection produced a second cycle of seizure suppression followed by a return of seizure activity that lasted for hours before SE finally resolved. This pattern of seizure suppression with returning convulsive SE following the two injections of anticonvulsants was typical, as can be seen in the seizure counts across all animals (**Fig. 3.1D**; arrows). We therefore regarded the entire 2-d duration as the period of ongoing injury and referred to it simply as SE. All subsequent analysis was limited to >2 d after the pilocarpine injection to avoid including seizures that appeared directly associated with the acute SE as part of the resultant epilepsy. The SE was followed by a behaviorally silent period free of convulsive seizures, with the first convulsive seizures occurring at a median of 9.2±4.6 M.A.D. (median absolute deviation) days following the end of SE (11.2±4.6 M.A.D. days post-pilocarpine). However, as shown in Figure 3.1E on a longer timescale, the post-SE latency to the first seizure ranged from 4 to 55 days.

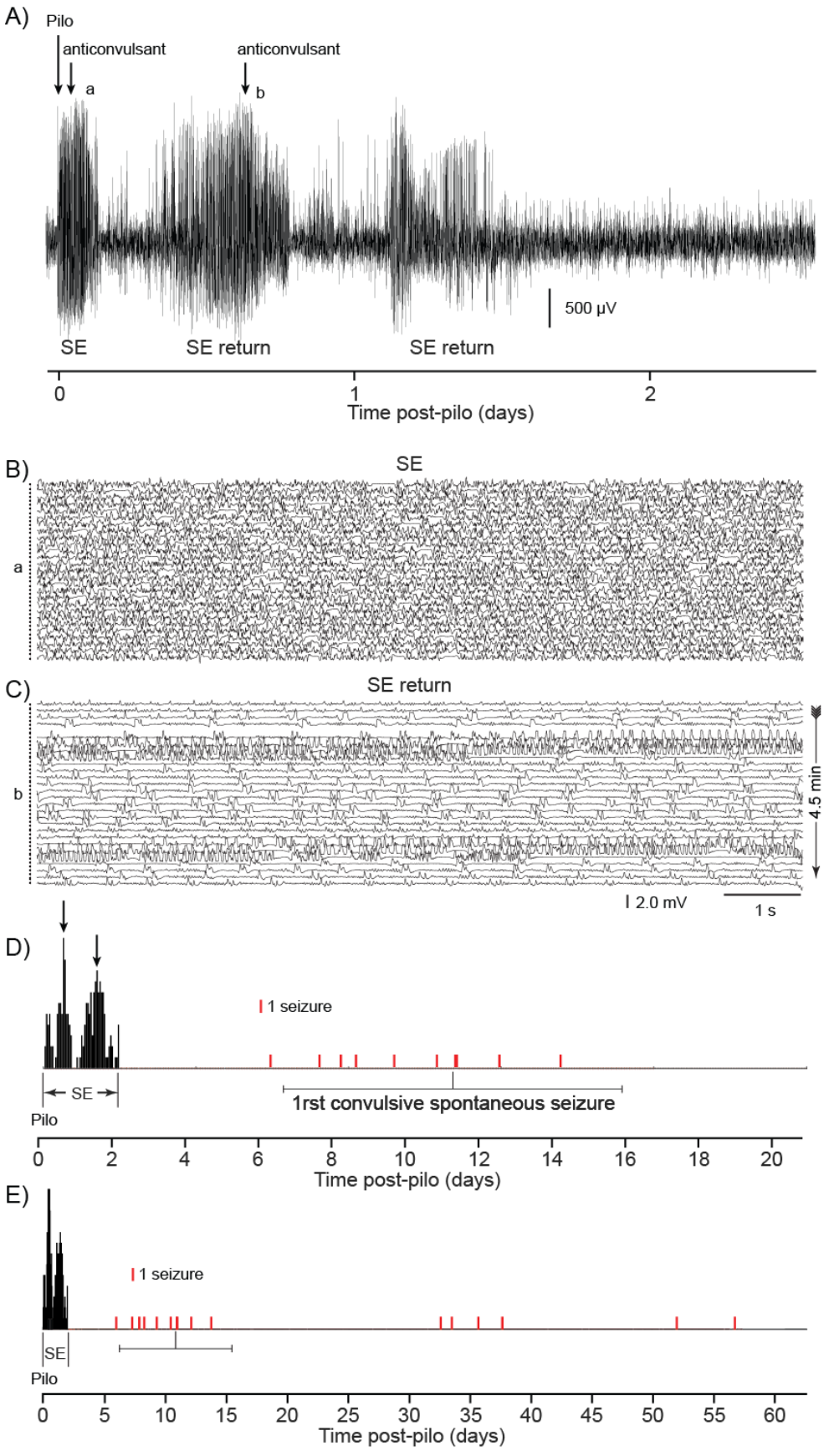
A)
Pilo
anticonvulsant
a
anticonvulsant
b
500 µV
SE
SE return
SE return
0
1
2
Time post-pilo (days)
B)
SE
a
C)
SE return
b
4.5 min
2.0 mV
1 s
D)
1 seizure
SE
1rst convulsive spontaneous seizure
Pilo
0
2
4
6
8
10
12
14
16
18
20
Time post-pilo (days)
E)
1 seizure
SE
Pilo
0
5
10
15
20
25
30
35
40
45
50
55
60
Time post-pilo (days)

Figure 3.1. Properties of pilocarpine-induced SE. **(A)** Spike counts show the initial period of continuous spiking characteristic of pilocarpine-induced SE, which was terminated after 1 h by an injection of anticonvulsant. SE returned the next day and was again terminated by a second anticonvulsant injection. A third return to SE was typical before cessation. **(B)** Raster plot of 4.5 min EEG (10 s/trace) during initial SE with continuous convulsive spiking (marked “a” in **A** and **B**). **(C)** SE return was characterized by convulsive bursts of spikes with lower frequency spikes interposed (marked “b” in **A** and **C**). **(D)** Seizure counts averaged across all rats. The initial period of continuous spiking, plus the two periods of subsequent spiking, were together considered the total period of SE. The median post-SE latency to the first convulsive seizure (red marks) was 9.2±(4.6; median absolute deviation) days. **(E)** Same as **D** but at a more compressed time scale to show first convulsive seizures at the longer post-SE latencies for all rats.

Supervised pattern recognition for seizure detection

All chronic video-EEG data for a given rat were first examined visually to identify both convulsive (Racine 3-5) and nonconvulsive (Racine 1-2) seizures. Figure 3.2 depicts an example of overlapping power spectra for convulsive seizures in one rat, taken from 200 10-s samples of ictal (red) and non-ictal EEG (black; selected at random intervals between seizures). As seen in this example, both ictal and non-ictal spectra displayed substantial power in lower frequencies (1-20 Hz) in all rats. However, there were disproportionate increases in higher frequency power (>20 Hz; **Fig. 3.2 A&B**; arrow) during seizures, which facilitated the training of the SVM for automated seizure detection in a manner that was tailored to each animal. Following seizure detection, "candidate" seizures were visually examined and edited for accuracy. Of the total number of seizures detected across rats, approximately 5-10% were false positives (visually determined by ZZS, blinded to rat or sequence of events), and deleted. Ninety-seven percent of visually identified seizures were confirmed with SVM. SVM also detected an additional 5% of seizures that were missed by visual examination. In all, 1055 convulsive (80.5%) and 255 nonconvulsive (19.5%) seizures across 18 rats were used for the subsequent analyses.

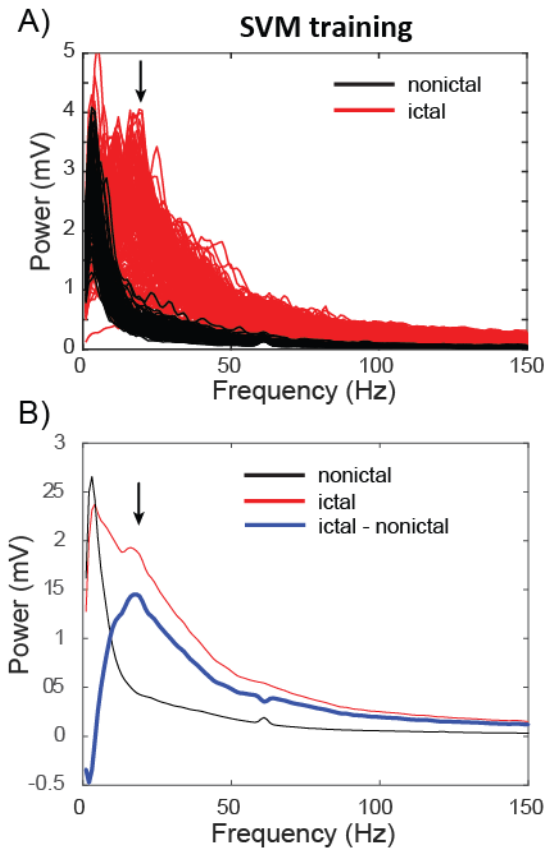

Figure 3.2. Ictal and non-ictal power spectra for one rat. **(A)** Superimposed power spectra of visually identified ictal (red) and non-ictal (black) EEG were used to individually train an SVM to perform supervised pattern recognition of seizures in each rat. The ictal EEG consistently displayed increased power in higher frequencies (>20 Hz; arrow). **(B)** Averaged power spectra for the same rat. The difference between ictal and non-ictal (blue trace) highlights increased power during ictus in the higher frequency bands.

Post-SE progression of nonconvulsive and convulsive seizures

Figure 3.3 displays seizure counts for SE (black), for post-SE nonconvulsive (blue), and convulsive (red) seizures in each of the 18 rats denoted by individual animal ID (right, ID; h40-h1). In Figures 3.3 and 3.4, when nonconvulsive and convulsive seizures occurred in the same time frame, the bars were plotted in a stacked format rather than superimposed. The total number of seizures varied widely between rats, ranging from 0 to 117 (mean = 5.13±2.5) for nonconvulsive and 0 to 292 (mean = 20.2±7.3) for convulsive events. In several rats with frequent seizures (e.g., **Fig. 3.3**; h40 – z5), clusters (denoted by "#") were observed, where several seizures occurred over a short period of time, separated by much longer inter-cluster intervals. During the early period of epileptogenesis (2-20 d post-SE), when nonconvulsive seizures predominated, clusters were not apparent. Also during the subsequent 20 d, when the frequency of convulsive seizures increased, the inter-seizure intervals still appeared to be largely random. It was not until >40 d after pilocarpine-induced SE that convulsive seizure clusters emerged, although clustering was not confined to convulsive seizures; nonconvulsive seizures also formed clusters that overlapped with clusters of convulsive seizures (**Fig. 3.3**; ID; h40-z1).

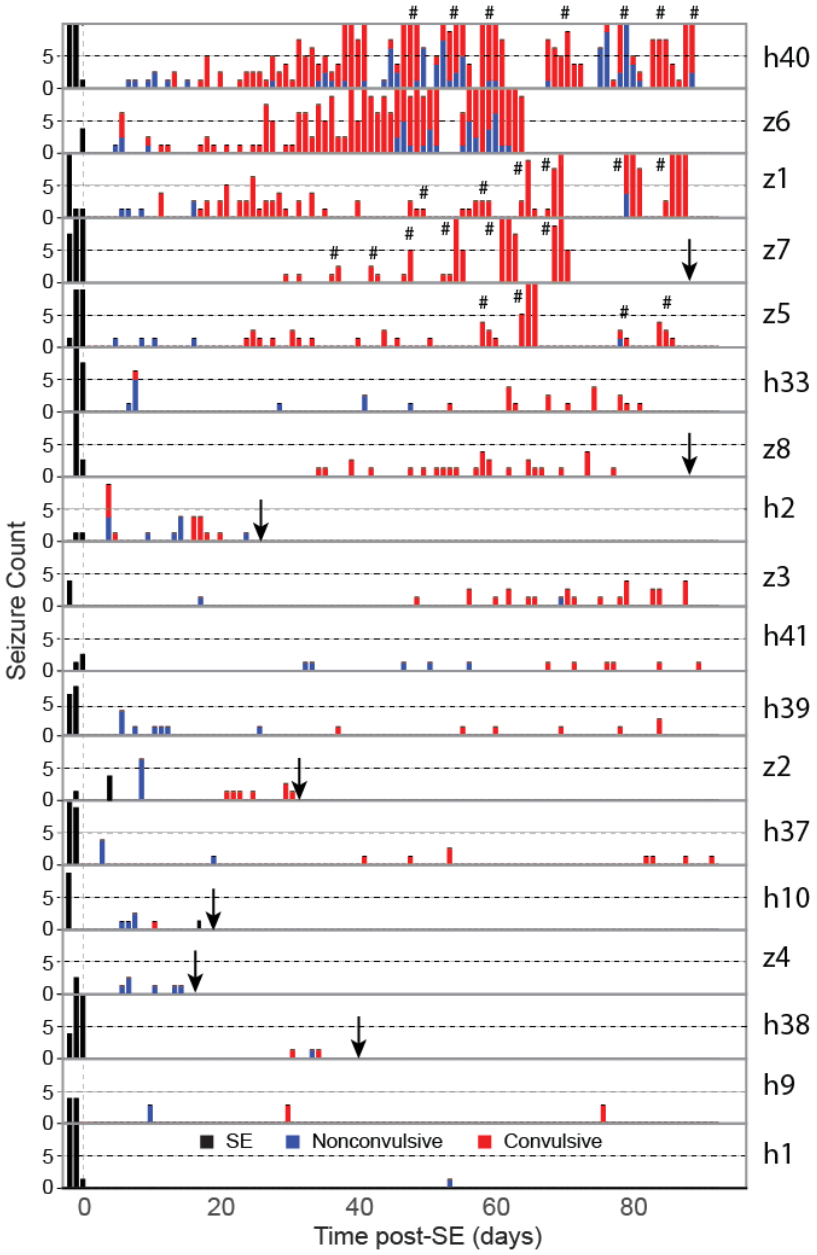

Figure 3.3. Time-course of the development of seizures post-SE for individual rats. The code for each animal is shown along the left margin, and the downward arrows for some animals indicates when the recording was terminated e.g., lost headset; too much noise). Counts for nonconvulsive (blue) and convulsive seizures (red) varied widely between animals. Epileptiform Spikes (ES; gray) counts are shown as a time-locked histogram for each animal.

The cumulative (across all 18 rats) timeline of nonconvulsive and convulsive seizures (**Fig. 3.4A1**) suggested two distinct post-SE periods. Epileptogenesis began in a slow continuous manner between Day 2 and Day 20 (post-SE) with predominantly nonconvulsive seizures, followed between Day 21 and Day 98 (post-SE) by a *mixture* of nonconvulsive and convulsive seizures. The median post-SE latency of the first nonconvulsive seizure was 4.7 d, compared to 9.2 d for convulsive seizures, but the large variability of these estimates (M.A.D. of 9.6 and 6.5 d, respectively) obscured any significant difference between the latencies. However, no nonconvulsive seizure occurred in less than 2.3 d, and no convulsive seizure less than 4.6 d, following the end of SE, establishing absolute minimums on the duration of the seizure-free latent period. Two-way ANOVA indicated a significant interaction between the post-pilocarpine period (2-20 versus 21-98 d) and convulsive intensity (nonconvulsive versus convulsive; $F(1,68)=4.7$, $p=.033$). However, Shapiro-Wilk tests indicated significant deviations from normal distributions for nonconvulsive (2-20 d; $p=0.009$; 21-98 d; $p=0.000$) and convulsive (2-20 d; $p=0.000$; 21-98 d; $p=0.000$) seizures. Therefore, planned comparisons were performed using a non-parametric Mann-Whitney test for two independent samples. The rate of nonconvulsive seizures (0.21± 0.04/d) was significantly higher than convulsive seizures (0.07± 0.03/d) at 2-20 d post-SE (**Fig. 3.4B1**; $p=0.05$). Subsequently (21-98 d post-SE), nonconvulsive seizure rates (0.15± 0.09/d) did not significantly change, indicating that nonconvulsive seizures are not just a feature of early epileptogenesis, but a consistent presence throughout epilepsy. Convulsive seizure rates substantially increased during epileptogenesis (0.74± 0.31/d), exceeding both their earlier rate ($p=0.005$) and the later nonconvulsive rates ($p=0.008$).

Because 7 rats (**Fig. 3.3**, ID; z7, z8, h2, z2, h10, z4 and h38) were not recorded for a full 98 days post-SE, the analysis was repeated for the 11 rats that were recorded for 98 days (**Fig 3.4 A2&B2**). Results for these rats were similar to analysis of the entire group, with two-way ANOVA indicating a significant interaction between the post-pilocarpine period and convulsive intensity ($F(1,43)=4.2$, $p=.047$). The rate of nonconvulsive seizures (0.20± 0.06/d) was higher than

convulsive seizures (0.07± 0.04/d) at 2-20 d post-SE, but did not reach significance with the smaller N (**Fig. 3.4B**; p=0.34). Subsequently (21-98 d post-SE), nonconvulsive seizure rates (0.24± 0.15/d) did not significantly change, whereas convulsive seizure rates substantially increased (1.05± 0.48/d), exceeding both their earlier rate (p=0.028) and the later nonconvulsive rates (p=0.012).

Figure 3.3 also contains the timeline for epileptiform spike (ES) progression throughout the lifetime of each rat (**Fig 3.3**; gray histogram). ESs were detected in 14 out of 18 rats but were undetectable in 4 rats (**Fig 3.3**; ID# z3, z4, z8, h9). Complete visual examination of the data indicated that ESs were absent from these animals outside of ictal events. In animals with detectable ES, spikes emerged on average 3.21 d ± 0.1 after the injury period, and 8.2 d ± 1.1 prior to the first spontaneous seizure. In all animals where ESs were detected (14/18), spiking emerged prior to the first seizure. In 11 out of 18 animals, ESs were clearly present days prior to the first spontaneous seizure (10.5d ± 1.3), while 3 out of 18 animals displayed an emergence of detected ESs less than 24 hr before the first seizure (**Fig 3.3**; ID; z1, h2, h37). Dividing the seizure free portion of epileptogenesis into two time periods revealed a significant correlation, with the "silent" period being the duration of time between the injury and the presence of ESs and the "pre-ictal" period after ES have emerged but prior to the development of nonconvulsive spontaneous seizures. There was a significant positive relationship between the duration of the "silent" period and the duration of the "pre-ictal" period, $r(12) = 0.64$, $p = 0.006$. However, there was no correlation between the duration of the "silent" period and the delay to the emergence of convulsive seizures $r(12) = 0.08$, $p=0.33$. No consistent significant discernable pattern of spike frequency changes across the lifetime of the rat and progression of epileptogenesis appeared evident in animals with detectable ESs. Some animals had peak spiking activity prior to their first seizure (**Fig 3.3**; ID; z7), while others appear to have seizure induced increases in ESs (**Fig 3.3**; ID; h40). Additionally, some animals had higher rates of ES early during epileptogenesis (**Fig 3.3**; ID; z5) while others had rapidly increasing ES rates (**Fig 3.3**; ID; h33).

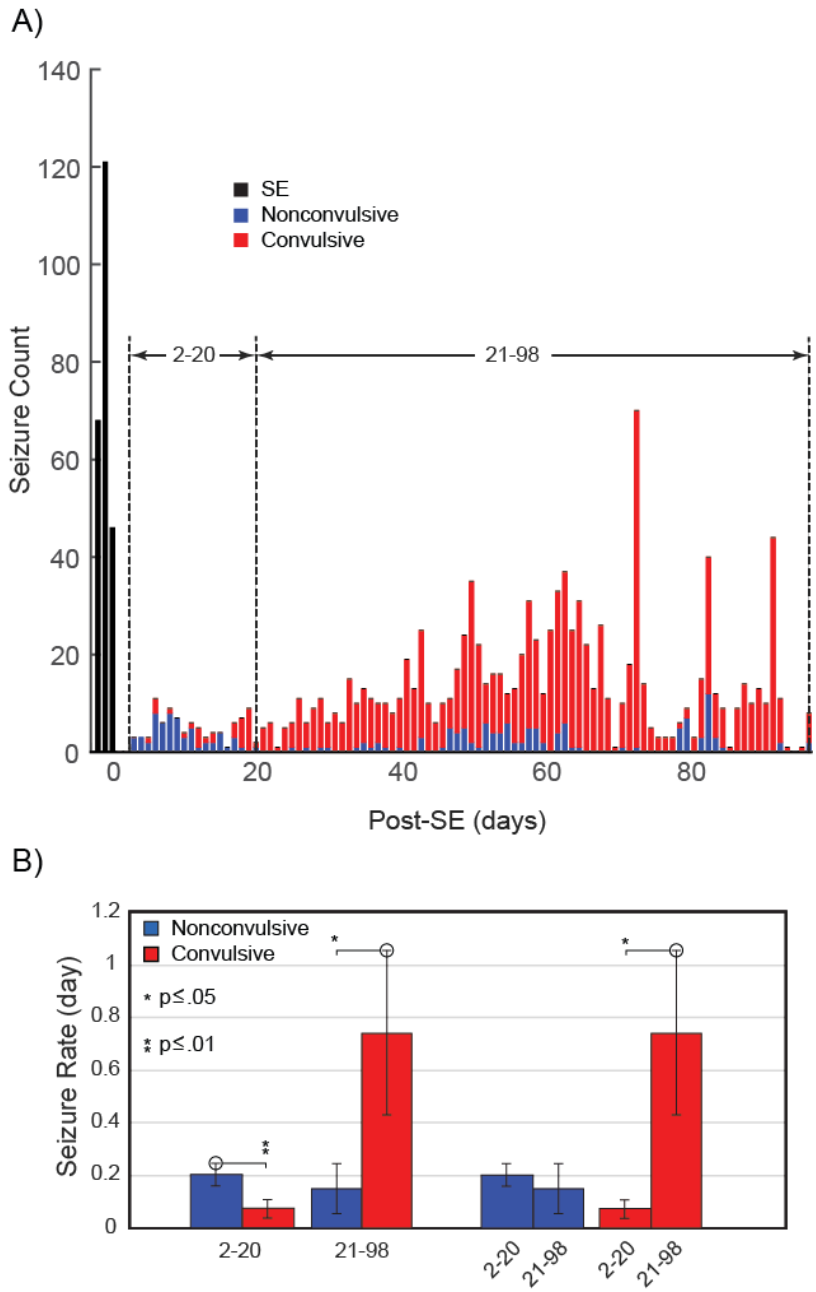

Figure 3.4. Time-course of the development of seizures post-SE. **(A1)** Analysis for all 18 rats indicated that nonconvulsive seizures (blue) were more prevalent than convulsive seizures (red) during the early period (2-20 d post-SE). During the later period (21-98 d), there was a mixture of convulsive and nonconvulsive seizures. **(B1)** Mean seizure counts for all rats for the 2-20 and 21-98 d periods post-SE. **(A2 and B2)** Same as **A1** and **B1** but only including seizures from the 11 rats completing all 98 says of recording post-SE.

Ictal spiking and mid- and post-ictal depression

Figure 3.5A depicts a convulsive (stage 5) seizure. Seizures typically consisted of distinct epochs of EEG spiking (where EEG amplitude was greater than baseline during the interictal period) and depression (where the EEG amplitude appeared below baseline). To estimate seizure durations, we first computed the standard deviation over successive 1-s segments of EEG (**Fig. 3.5A**; yellow). The standard deviation averaged across 80 s of pre-ictal baseline (**Fig. 3.5A**; black) was used as a reference. Epochs of EEG spiking (**Fig. 3.5A**; red) and depression (**Fig. 3.5A**; green) were indicated when the signal was 1.5 standard deviations above or below baseline, respectively. These computed epochs were then examined visually to determine *three durations* for analysis. (1) An *ictus*, or seizure, was defined as the period from the onset of EEG spiking to its termination. The ictus was often interrupted by brief episodes of depression; (2) these periods were defined as *mid-ictal depression (MID)*. (3) *Post-ictal depression (PID)* was defined as all depression that occurred after the termination of the ictus. In this example, the actual seizure - or ictus - lasted for approximately 120 s, it was interrupted by a 40-s period of MID, and PID lasted for approximately 120 s (**Fig. 3.5B**).

We did not find significant differences in any duration parameter between nonconvulsive (**Fig. 3.5C**; blue) and convulsive (**Fig. 3.5C**; red) seizures. Two-way ANOVA indicated the main effect of seizure intensity (nonconvulsive vs convulsive) was not significant ($F(1,50)=0.002$, $p=0.96$), and there was no significant interaction between intensity and duration (ictus, MID, PID; $F(1,50)=0.3$, $p=0.58$). However, there was a significant main effect of duration ($F(1,50)=12.279$, $p=0.001$). Thus, no differences between nonconvulsive and convulsive seizures were detected; however, for both seizure types, the durations for PID were nearly twice as long (121±17.5 and 130±14.3 s, respectively) as those for ictus (61±6.0 and 68.5±10.1 s, respectively; $p<0.001$) and 10 times as long as MID (10.3±2.9 and 12.1±2.7 s, respectively; $p<0.001$). Ictus during both nonconvulsive and convulsive seizures was also significantly longer than MID ($p<0.001$).

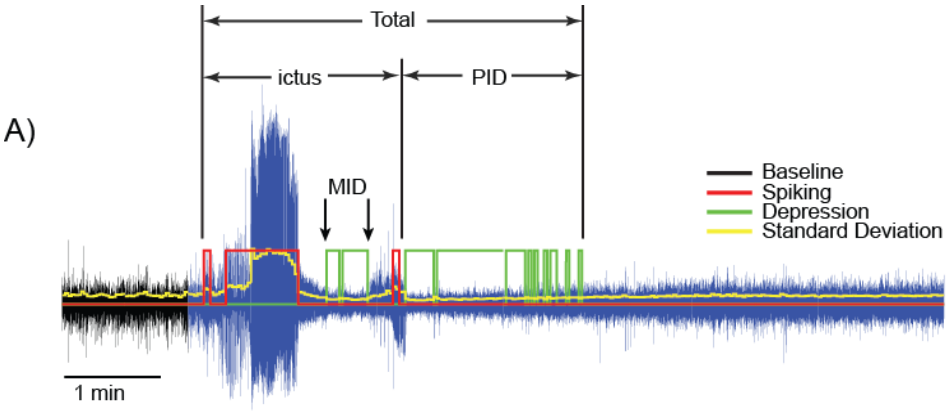
A)
Total
ictus
PID
MID
Baseline
Spiking
Depression
Standard Deviation
1 min

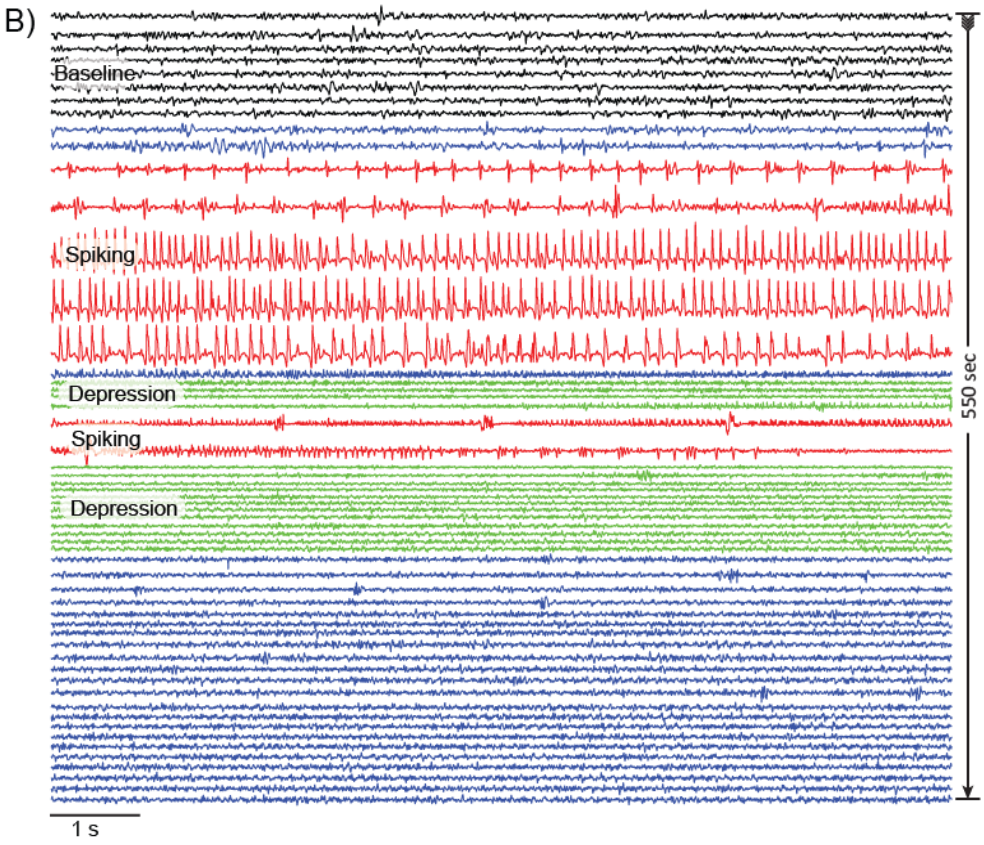
B)
Baseline
Spiking
Depression
Spiking
Depression
550 sec
1 s

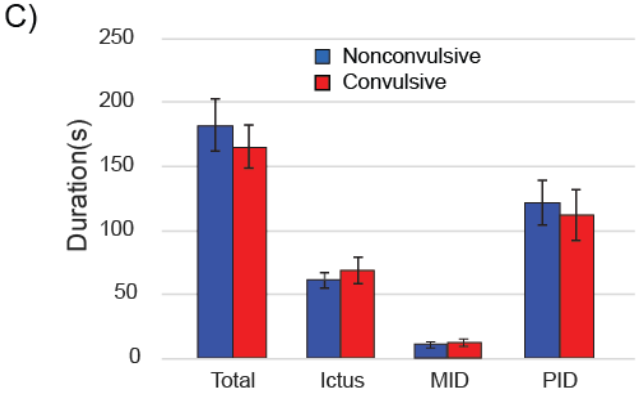
C)
Nonconvulsive
Convulsive
Duration(s)
250
200
150
100
50
0
Total
Ictus
MID
PID

Figure 3.5. Durations of ictal spiking and depression. **(A)** A pre-ictal period (black; 80 s) was used to compute a baseline standard deviation (SD; yellow line). When the subsequent EEG changed 1.5 SD above or below baseline, periods of spiking (red) and depression (green) were identified, respectively. Depression mid-seizure was termed mid-ictal depression (MID). Ictus was defined as the total period of spiking, inclusive of MID when it occurred. Post-ictal depression (PID) was defined as the total period of depression following ictus. **(B)** Raster plot of the EEG depicted in **(A)**. **(C)** The durations of ictus, MID, PID and the total seizure duration ("Total") did not significantly differ between nonconvulsive (blue) and convulsive (red) seizures.

Power spectra and spectral variability

Figure 3.6 shows power spectra averaged across all rats for convulsive (A) and nonconvulsive (B) seizures. During convulsive seizures, EEG power during spiking (i.e., ictus) and depression was significantly higher and lower (respectively; $p<0.001$) than baseline with a disproportionate increase during ictal spiking in higher frequency power (>20 Hz; **Fig. 3.6A**; arrow), a feature that facilitated automated seizure detection. However, spectra for baseline, spiking, and depression were nearly identical between convulsive (**Fig. 3.6B**; dashed traces) and nonconvulsive (**Fig. 3.6B**; solid traces) seizures ($p= 0.78$, 0.94 and 0.99, respectively).

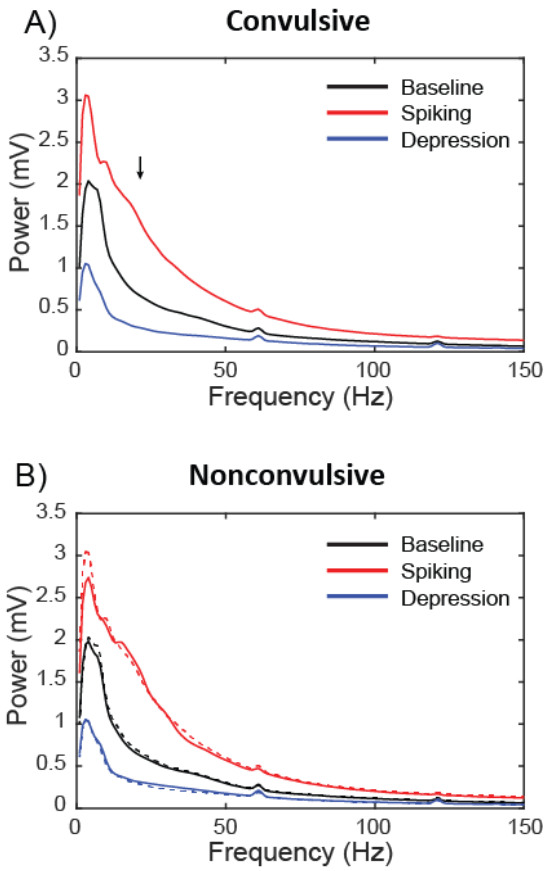

Figure 3.6. Power spectra averaged across rats, for all convulsive **(A)** and nonconvulsive **(B)** seizures. Ictal spiking showed increased power compared to baseline and depression, particularly in frequencies >20 Hz (arrow). The observation that the power spectra are virtually further supports the hypothesis that the convulsive and nonconvulsive seizures are nearly identical in their electrical properties.

The stability of power spectra when averaged across rats was unexpected given considerable frequency variability within each seizure and between seizures in any particular rat. Figure 3.7A depicts the total period of spiking during a single seizure, with successive 1-s segments enlarged to show activity at approximately 18, 3, 28, 9 and 3 Hz (**Fig. 3.7A**; a-e, respectively). These samples appeared as peaks in the corresponding spectrogram (**Fig. 3.7B**; left plate), which showed the evolution of spiking frequency throughout the entire seizure. To quantify frequency variability, we used PCA to determine what percentage of power within the spectrogram could be modeled by a single spectrum (1st component "score") weighted according to latency within the seizure (1st component "loads"). By multiplying the component score (single best fitting spectrum) by the loads, we obtained a model spectrogram (**Fig. 3.7B**; center plate). In this example, the model best fit the first minute of the seizure (**Fig. 3.7B**; dashed oval) where the ictal spiking amplitude and thus spectral power was greatest. However, due to spectral variability that characterized the seizure, the model only accounted for 42% of the power of the original seizure. Figure 3.7B (right plate) shows a map of the residuals resulting from subtracting the model from the original spectrogram. Here, the effect of spectral variability can be visualized, comprising 58% of the total power. When all seizures for this rat were plotted contiguously in time as a single spectrogram (**Fig. 3.7C**), spectral variability was evident not only within seizures, but also across seizures, as reflected by 56% of the power in the residuals. Spectral variability, computed in this way for all rats, was high for both convulsive (41.7±5.6 %) and nonconvulsive (31.1±5.2 %) seizures (**Fig. 3.7D**). Similar to analysis of the overall power spectrum, however, this variability did not significantly differ with seizure severity (i.e., convulsive vs nonconvulsive) ($p=0.21$).

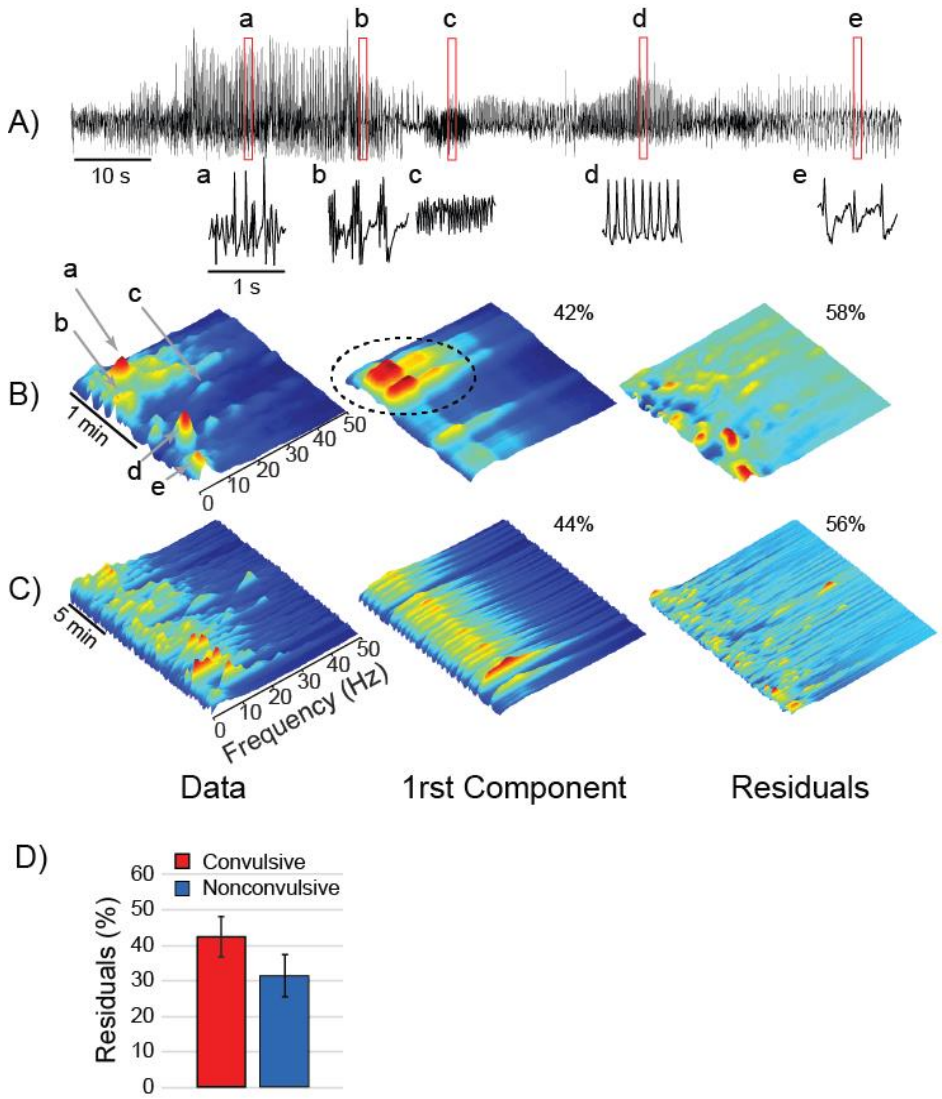

Figure 3.7. Quantification of spectral variability. **(A)** Time series of just the ictal period of a single seizure. One-second segments (a-e; red boxes) are enlarged to show highly variable fundamental frequencies throughout the seizure, at approximately 14, 3, 28, 12 and 3 Hz, respectively. **(B)** Spectrogram of the same ictal epoch (left plate; "Data") shows the variable spectral peaks identified in a-e. Center plate ("1st Component") is a model of the spectrogram using only the first principle component, accounting for the maximum power across the seizure with only a single spectrum. Right plate shows the residuals from subtracting the component model from the raw data, indicating a poor fit of the model using only a single spectrum because of frequency variability across the seizure. In this example, the model accounted for only 42% of the system variance, leaving 58% of the variance reflecting high "spectral variability". **(C)** Same as **(B)** but computed over all of the ictal periods for this rat. **(D)** Spectral variability (residuals) did not differ between convulsive and nonconvulsive seizures.

Comparison of seizures in the hippocampus and neocortex

To summarize the effects of seizure intensity recorded from the hippocampal electrode alone, we conducted a one-way MANOVA with intensity (nonconvulsive vs convulsive) as the independent variable and our measured durations (ictus, MID and PID) as well as spectral variability (percent power in the residuals) as dependent variables. As expected, there were no significant differences between nonconvulsive and convulsive seizures measured from our hippocampal electrode ($F(4,10)=0.64$, $p=0.643$).

Both nonconvulsive and convulsive seizures measured from the hippocampal electrode were accompanied by similar activity in the neocortical lead. Figure 3.8 depicts a convulsive seizure recorded simultaneously from the hippocampal (blue) and neocortical (red) electrodes. Seizure waveforms were plotted as absolute values to facilitate comparison of amplitudes. A total of 16 out of 18 rats had viable neocortical and hippocampal electrodes for comparison. All seizures, whether nonconvulsive or convulsive, that were recorded in the hippocampal electrode were also detected with the neocortical electrode. We were not able to detect a delay in onset between neocortical and hippocampal electrodes for any seizure. However, the rate of amplitude "build-up" in neocortex often appeared slower than the hippocampus (**Fig. 3.8** a & b, respectively). To compare seizures measured with the neocortical and hippocampal electrodes , we performed a two-way MANOVA with intensity (nonconvulsive vs convulsive) and location (neocortex vs hippocampus) as independent variables and half-amplitude delay as well as our other measures (ictus, MID and PID durations and spectral variability) as dependent variables. The interaction between location and intensity was not significant ($F(4,24)=0.64$, $p=0.58$), indicating no overall differences between nonconvulsive and convulsive seizures influenced by recording location. There was a significant main effect of location on the time to reach half-amplitude ($F(1,27)=8.1$, $p=0.008$), with neocortical seizure recordings delayed (11.04±1.25 s) compared to hippocampal recordings (6.53±0.77 s), but this was not affected by seizure intensity ($F(1,27)=1.8$, $p=0.19$). There was also an effect of seizure intensity on spectral variability ($F(1,27)=7.8$, $p=0.009$) with

nonconvulsive seizures showing smaller residuals (49.08±3.09 %) than convulsive seizures (59.22±1.72 %), but this only occurred in the neocortical electrode. Thus, while we were not able to distinguish nonconvulsive and convulsive seizures in the hippocampal electrode based on electrographic parameters alone, nonconvulsive seizures were less complex in the cortical electrode. It might be expected that seizure intensity would be reflected in relative spread to include neocortical structures. This however was not the case, at least for the single somatosensory recording location and filtering methods used here.

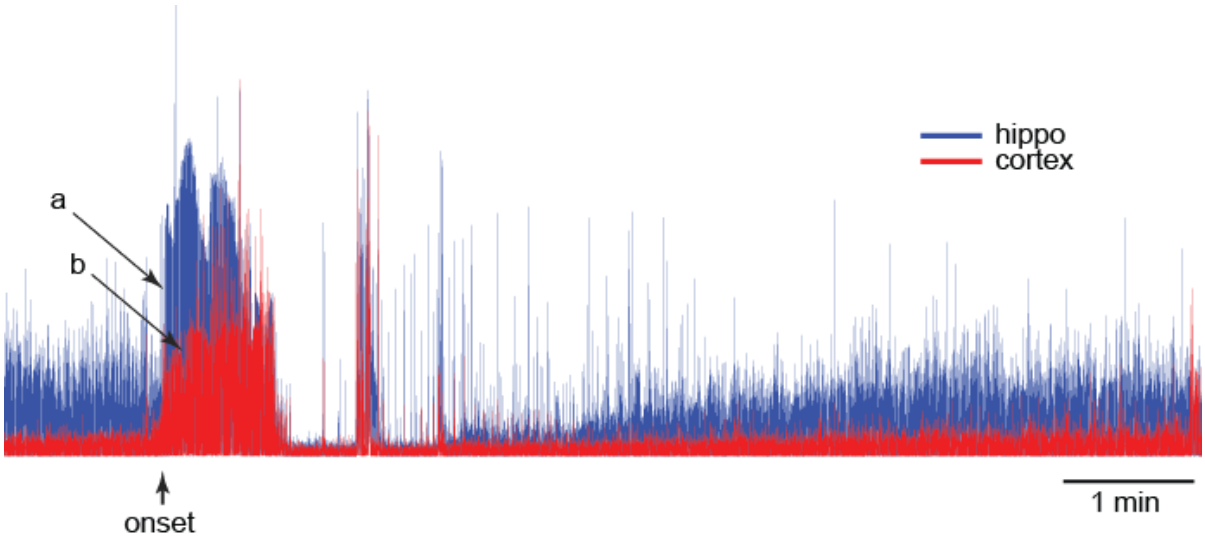

Figure 3.8. Comparison of seizures in the hippocampus and neocortex. A typical example of a Racine 5 convulsive seizure plotted as absolute values of seizure waveforms. The seizure was recorded simultaneously in the hippocampus (blue) and the neocortex (red). Seizure onset, termination, as well as periods of MID and PID appear identical in both locations. The rate of amplitude change following seizure onset appears faster in the hippocampus (a) than in the cortex (b).

Other nonconvulsive sequelae to SE: **Spike-wave-discharge**

We also observed two types of nonconvulsive seizure-like events following SE. The first were SWDs (**Fig. 3.9A**), identifiable in 11 of our 18 experimental rats and similar to our previous observations in untreated animals (Rodgers et al., 2015). When present, SWDs were typically of largest amplitude in the cortical electrode, although they could sometimes be detected in the hippocampal lead. Our analysis concentrated on the cortical signals. SWD bursts greater than 3-s duration were associated with behavioral freezing, similar to nonconvulsive seizures; however, they were distinguishable from seizures on several key parameters. SWD epochs began and ended suddenly with no sign of MID or PID during or after the event (**Fig. 3.9A**; arrows). The distinct spike-wave morphology of SWDs resulted in a signal that was quasi-periodic, having unique spectra with high values at a fixed fundamental frequency and at whole multiples (harmonics) of this fundamental frequency. While SWD amplitude waxed and waned within and across multiple events, this frequency signature remained stable with low variability. Stability is evident in Figure 3.9B, where 135 s of short (typically 1-5 s) SWD events in a single rat were plotted contiguously. The amplitude, frequency, and waveform morphology remained little changed from the beginning, middle, and end of the series (**Fig. 3.9B** a-c, respectively). In contrast to contiguous seizures depicted in Figure 3.7C, the spectrogram of contiguous SWD events revealed little frequency variability (**Fig. 3.9C**; left plate) and was dominated by the fundamental frequency (7-9 Hz) and the first harmonic (14-18 Hz) throughout. The mono-spectral model (1st principal component; **Fig. 3.9C**; center plate) reflected these two peaks and accounted for 89% of the original spectral power, leaving 11% of residual power due to frequency variability (**Fig. 3.9C**; right plate). Frequency variability was low across rats, with residuals representing 15.5±0.9% of the original spectral power.

In contrast to both convulsive and nonconvulsive seizures, with average ictal durations of approximately 1 min, the lengths of SWD events were typically 1-5 s (**Fig. 3.9D**) and the event counts did not increase with time post-SE. Compared to SWD events in normal untreated rats

(Rodgers et al., 2015), the SWDs following pilocarpine were typically short ‘larval’ events, even in older animals. One-way ANOVA of the total number of SWD events (**Fig. 3.9E**) and total time (**Fig. 3.9F**) showed no significant effects of age ($F(4,33)=1.42$, $p=0.25$ and $F(4,33)=1.24$, $p=0.32$, respectively), thus indicating no post-SE progression. Total SWD events and time, averaged across all age groups, was 77.5±0.9/d and 122.3±25.2 s, respectively, which was less than the 66±46.7/d and 146.6±115.6 s previously recorded for normal age-matched control rats (see **Fig. 6A&B** of Rodgers et al., 2015). Thus, SWD following SE did not appear to differ from normal controls except for a lack of age progression, suggesting that it was not produced by SE.

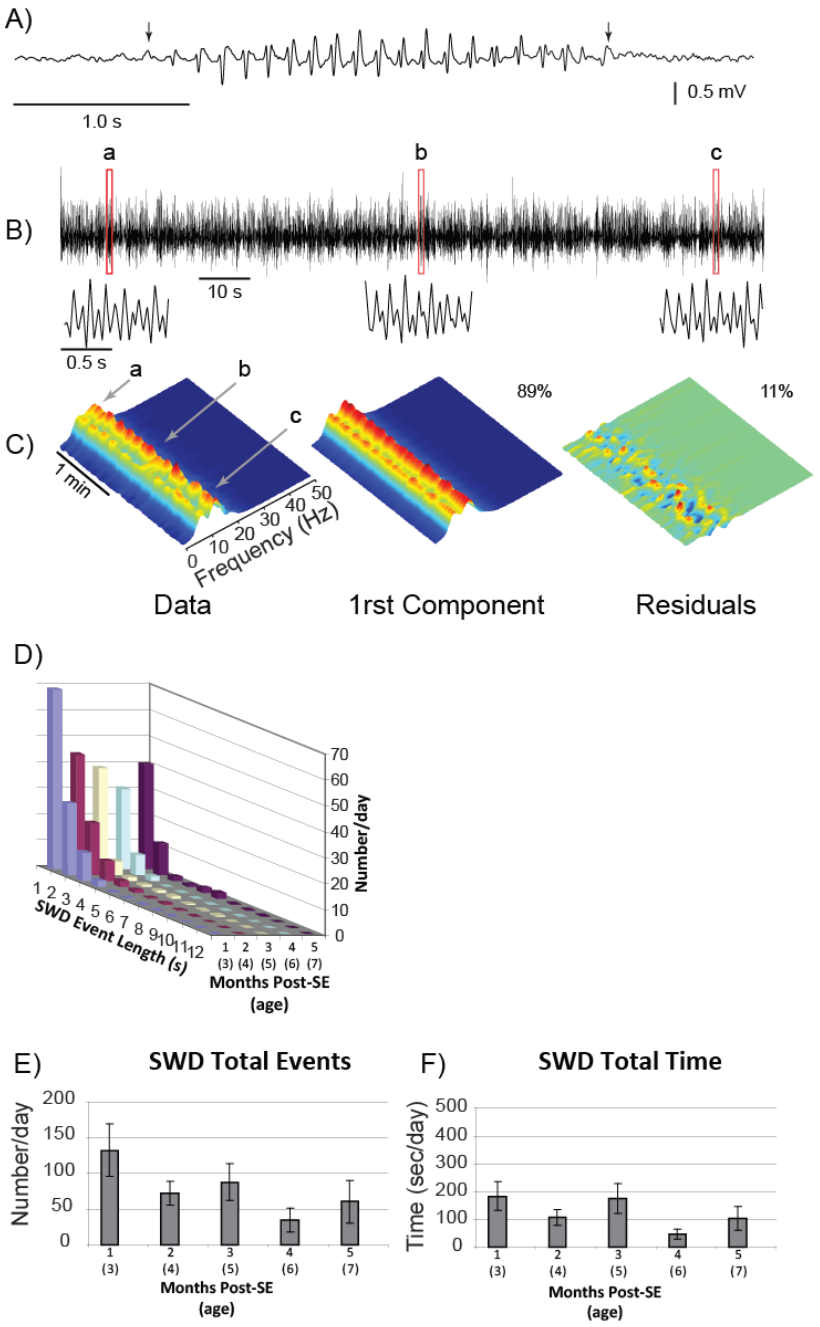

Figure 3.9. Quantification of spike-wave-discharge (SWD). **(A)** Typical 3 s epoch of SWDs with sudden onset and offset (arrows) and no MID or PID. **(B)** Contiguously plotted SWDs (135 s) show little change in morphology, frequency or amplitude at the start, middle and end of activity (a-c) for this rat. **(C)** Spectrogram for contiguous SWDs of **(B)** indicates a consistent and simple spectrum with peaks at the fundamental frequency (7-9 Hz) and the first harmonic (14-18 Hz). The first component accounted for 89% of the raw spectrogram and left only 11% in the residuals due to spectral variability. **(D)** SWD events were dominated by short (1-5 s) bursts with little change over 5 m post-SE. The lack of temporal progression is evident in both total event counts **(E)** and total time **(F)**.

Other nonconvulsive sequelae to SE: **Slow spike-wave-discharge**

We also regularly observed nonconvulsive seizure-like events following SE that appeared as "slow" spike-wave-discharge (sSWD; **Fig. 3.10**) only detected in the cortex and not hippocampus. A distinguishing feature of sSWDs was a consistently lower fundamental frequency (3-5 Hz) compared to SWD (7-9 Hz). This discharge pattern was evident in 14 animals (2 rats did not have viable cortical leads and 2 did not show sSWDs). The sSWDs had a morphology similar to normal SWDs and also displayed sudden onset and termination with no associated depression (**Fig. 3.10A**; arrows). Also like SWDs, sSWDs demonstrated a simple frequency spectrum characteristic of quasiperiodic signals with peaks at the fundamental frequency (3-5 Hz) and the first harmonic (6-10 Hz) that remained stable within and across successive bursts (**Fig. 3.10B**; left plate; 11 min contiguous bursts). Small frequency variability resulted in small residuals (17±1.1% of the original spectral power) with the principle component model (**Fig. 3.10B**; right plate). The post-SE period within which sSWDs were evident was quite short in all rats. The sSWDs were abundant during the 3rd day post-SE but nearly gone by day 7 (**Fig. 3.10C**). There was a significant main effect of latency (post-SE) on both sSWD rate (**Fig. 3.10E**; $F(4,30)=16.08$, $p=0.000$) and total time (**Fig. 3.10F**; $F(4,30)=11.97$, $p=0.000$). Post-hoc analysis indicated that for both measures, sSWDs during the 3rd day were significantly ($p\leq0.001$) greater than subsequent days, and no significant progression occurred after this time. During the 3rd day, sSWDs were remarkably frequent, averaging 1969±461 events/d and 3626±997 s/d. Unlike SWDs, which are frequent and common in untreated rats, we have not recorded sSWDs except those that occurred immediately following SE. Also unlike SWDs, during sSWDs, animals were active instead of immobile. Activity during sSWDs was highly variable (sipping water bottle, moving about the cage etc.) and appeared normal, not reflective of convulsive behavior. The sSWD waveforms were clearly distinct from motor artifact detected during other periods of similar activity.

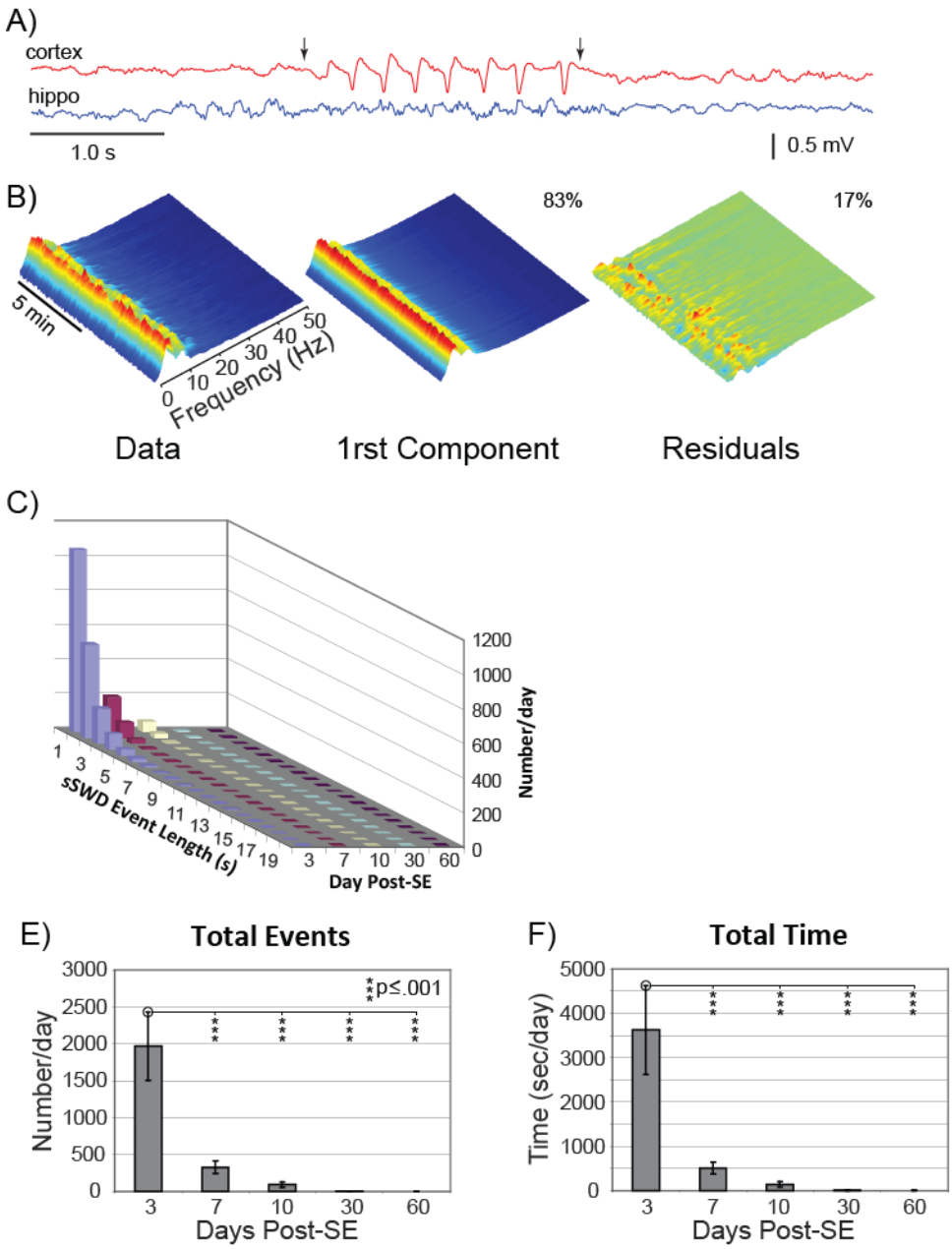

Figure 3.10. Quantification of slow spike-wave-discharge (sSWD). **(A)** sSWDs had a morphology similar to SWDs but about half (4 vs 8 Hz) the frequency. Similar to SWDs, epochs began and ended suddenly (arrows) with no MID or PID. sSWDs were only recorded in the cortex. **(B)** Spectrogram of contiguous sSWD epochs had a simple and stable spectral signature with peaks at 3-5 Hz and the first harmonic at 6-10 Hz. The mono-spectral model accounted for 83% of the original power, leaving only 18% in the residuals. **(C)** sSWDs were characterized by typical 1-8 s bursts, prominent only during the 3rd day post-SE. The total event count **(E)** and time **(F)** for sSWDs was greatest during day 3 and nearly gone by day 10.

Discussion

Long-term (98 d) continuous video-EEG recordings combined with specific, hypothesis-driven experiments and computer analyses have provided insights about the properties of nonconvulsive seizures compared to convulsive seizures in the pilocarpine model. Key results from these experiments are: (1) Pilocarpine-induced epilepsy involves both nonconvulsive and convulsive seizures. (2) Nonconvulsive seizures are one of the earliest signs of epileptogenesis in the weeks after SE, followed by a prolonged if not permanent period of *both* nonconvulsive and convulsive seizures. (3) Nonconvulsive and convulsive seizures have very similar identities according to our recording parameters, with similar frequency spectra, spectral variability, seizure durations, MID and PID, and similar tendencies to participate in seizure clusters. (4) Nonconvulsive and convulsive seizures are distinct from other electrographic events that are possible sequelae of SE in the form of SWDs and sSWDs, which do not appear to reflect epilepsy in this model.

The latent period and progressive epileptogenesis

With clinical PTE, TLE and other forms of acquired epilepsy, the durations of the seizure-free latent period range from weeks to >10 yr (Annegers, Hauser, Coan, & Rocca, 1998). Although with PTE it is clear when the TBI occurred, with other forms of acquired epilepsy the initial causative factors, and duration of the ensuing latent period, may be harder to identify. For short latent periods, identification of the first clinical seizure as epileptic requires that it be distinguished from “early” insult-related seizures (i.e., directly associated with the injury). The role of injury-induced “immediate” and “early” seizures has not yet been elucidated, but they may represent a risk factor for the later development of epilepsy (Frey, 2003). Clinically, “early” subacute seizures can occur for at least 1-2 weeks after virtually any brain insult, so it can be difficult to determine whether a particular seizure was an ”early”, injury-associated seizure or a “late” spontaneous, epileptic seizure (Annegers et al., 1998; Asikainen, Kaste, & Sarna, 1999). Some authors have

reported seizures immediately after SE in animal models (Mazzuferi, et al., 2012; Puttachary et al., 2015) challenging the idea of a classical latent period (Löscher, Hirsch, & Schmidt, 2015; Sloviter & Bumanglag, 2013). Using the kainate model, Williams and coworkers (Williams et al., 2009) proposed that epileptogenesis is a *continuous process* after brain injury, with the latent period as the longest inter-seizure interval (see **Fig. 3A** of (Williams et al., 2009). Our results were similar for most animals, showing latent period durations up to 25 days after the termination of acute SE-induced seizures, followed by an increase in seizure frequency and severity (**Fig 3.1D and E**; **Fig. 3.3**). Figure 3 shows examples where the longest inter-seizure interval was not the first interval after SE, raising the possibility that an *apparent* short latent period in these animals was instead due to a subacute seizure (i.e., non-spontaneous) at the end of SE (e.g., ID; h33 in **Fig. 3.3**); thus, if the first seizure in these cases was actually part of the SE (and not indicative of epileptogenesis), then the actual latent period could be much longer than otherwise measured, leading researchers to mistake subacute seizures for rapid epileptogenesis in this and other models. However, our data also show variability in latent period duration between animals, with some animals having short periods before the emergence of spontaneous nonconvulsive seizures that appeared distinct from SE. This supports the idea that spontaneous seizures in this model may not require extended secondary mechanisms to emerge and that a latent period is not a necessary requisite for epileptogenesis, even though most animals had a discernable latent period. Our data provide insights concerning the nature of the latent period in SE-based models, but when using models of rapid epileptogenesis that result in variable latent periods and seizure frequency, the interpretation of the latent period can be complicated both practically and conceptually (**Fig. 3.3**). Our results suggest that epileptogenesis is a continuous process that begins during injury, continues through the classical latent period and well into the development of spontaneous seizures, and is variable between animals. The clinical definition of the latent period in the human population is the time between an initial insult and the development of convulsive seizures (Walker, White, & Sander, 2002; Williams et al., 2009). This does not take

into account the nonconvulsive seizures that typically appear before convulsive seizures and represent the first electrographic evidence that epileptogenesis is under way. With several animals (**Fig. 3.3**) having multiple nonconvulsive seizures before the development of convulsive seizure activity, our data suggests that this definition is not a completely accurate representation of the latent period and should be adjusted to reflect the first spontaneous seizure that is not associated directly with the initial injury. Taken together, these results highlight the need to undertake continuous electrophysiological monitoring of seizures for *at least* several weeks (or more) to both address the problematic distinction between traditional "early" and "late" seizures and to accurately determine the progression of epileptogenesis in animal models and the human population.

Inter-ictal like spikes as a marker of epileptogenesis

ES activity is a common phenomenon in both epileptic patients and animal models of epilepsy. While this spiking is correlated to the long-term worsening of epilepsy over time in post-operative patients (Kelemen et al., 2006), the role of ES in epilepsy is not fully understood (Avoli, Biagini, & de Curtis, 2006; Avoli, de Curtis, & Köhling, 2013; Karoly et al., 2016; Staley et al., 2011). Using the kainate model, White and colleagues demonstrated that ES activity consistently preceded the first seizure and represented a diagnostic signature that could accurately predict the emergence of spontaneous seizures (White et al., 2010). Researchers have argued that ES activity prior to the first seizure (pre-ictal spiking) may reflect epilepsy-associated alterations in circuit activity that emerge during epileptogenesis, representing a predictive biomarker, or potential contributor, to the future development of seizures (Staley et al., 2011). For most animals in the present study, ES activity follows a similar pattern by emerging before the development of nonconvulsive seizures during the latent period. This pattern of ES manifestation before the first seizure, and the positive temporal relationship between the "silent" and the "pre-ictal" stages of the latent period provide credence to the concept that ESs reflect slowly developing circuit

changes leading to epilepsy. However, a smaller portion of animals do not follow this trend, suggesting that either ES were missed by our limited electrode placement (i.e. occurred elsewhere) or that they are not always a necessary phenotype for an epileptic brain in this model. Additionally, assuming few false ES detections, which is an advantage of the pattern recognition methods used here, there does not seem to be a clear relationship between the frequency of spiking and the severity of epileptogenesis to the extent that would be expected if ES were solely a reflection of the maturation of underlying epileptogenic circuitry that leads to the increased propensity for seizures.

Recent evidence suggests that shape features may provide a better predictive angle for the analysis of ESs (Huneau et al., 2013). Subtle changes in ES morphology, described as "Type 1" spikes (characterized by a spike followed by a slow wave) that decrease in number, amplitude, and duration prior to the development of spontaneous seizures, and "Type 2" spikes (characterized by a spike without a slow wave) appearing transiently prior to the first seizure may allow for predictive information to be extracted from the actual signature of ES (Chauvière et al., 2012). Utilizing the tools at our disposal, we were unable to differentiate between spike features that may be indicative of epilepsy as demonstrated in these studies. ESs in the present study were similar to Type 1. It is possible that a bias arose due to selective training of the SVM model using the most common spikes. However, visual examination of ECoG records just prior to the first SRS in all rats also revealed only Type 1 spikes. Our lack of morphological change may therefore be more reflective of electrode placement and region specificity. Salami et al. (Salami et al., 2014) demonstrated more structure-specific alterations in spike morphology in the entorhinal cortex and CA3 region than the changes shown in the CA1 by Chauvière and colleagues. Additionally, research involving seizure-induced changes in human patients have shown that ES morphology only shifts in a small subset of electrodes, or not at all, which may mean that spatial specificity is required to observe this phenomenon (Bower et al., 2017). Dentate granule cells are relatively resistant to damage during the time course of epileptogenesis, as

demonstrated by temporal analyses of network properties and progressive hippocampal cell loss in animal models of acquired epilepsy (Buckmaster & Dudek, 1997b; Heinemann et al., 1992; Lothman et al., 1992). This may explain the consistency in spike morphology we observed in dentate granule cell layer both preceding and following the first SRS. While we found no changes in ES morphology representative of the progressive nature of epileptogenesis, we did find that ES activity consistently arose days prior to the development of SRS in rats that developed epilepsy. This finding concurs with previous studies (Lévesque, Behr, & Avoli, 2015; Salami et al., 2014; White et al., 2010) suggesting that, regardless of spike morphology or spike frequency, ES incidence during the latent period provides, at the very least, a reliable indicator of epilepsy risk.

Nonconvulsive and convulsive seizures have similar electrographic properties: implications for the latent period and the time course of epileptogenesis

Clinically, simple- and complex-partial (nonconvulsive) seizures generally last from tens-of-seconds to minutes (Devinsky, 2008; Theodore et al., 1994; Theodore, Porter, & Penry, 1983) (see **Table 1**). Figure 3.11 contrasts durations of nonconvulsive seizures, convulsive seizures, seizure events following MID, and both types of SWD. Nonconvulsive and convulsive seizure durations are variable, but analogous, and rarely <20 s or >1 min, similar to patients with acquired epilepsy (Table 1). PID is difficult to measure, because the onset and termination of a lack of electrical activity is not readily discernible. However, automated methods performed here revealed that both convulsive and nonconvulsive seizures have similar PIDs, establishing the PID as a viable diagnostic criterion for seizures. Furthermore, nonconvulsive seizures are not characterized by being shorter than convulsive seizures, as has been suggested to be a key feature of nonconvulsive seizures using other models without convulsive seizures (D'Ambrosio et al., 2009; D'Ambrosio & Miller, 2010; compare with Dudek & Bertram, 2010); instead, the duration of the actual electrographic activity for nonconvulsive and convulsive seizures in this model (and PIDs) were indistinguishable. That both seizure types are identical in all measures of duration

suggests they are both equally part of the phenomenon of acquired epilepsy and that the latent period of epileptogenesis should actually be determined by measuring the time to the first *electrographic seizure*, whether convulsive or nonconvulsive.

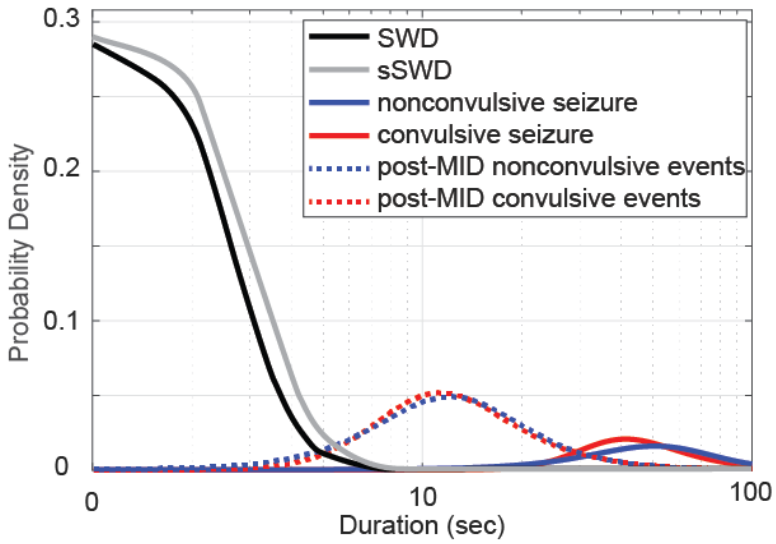

Figure 3.11. Probability density of event durations. Probability density functions (PDF) were computed in respect to duration to determine the likelihood that a randomly chosen event would occur within a specific time frame. PDFs reveal the temporal signature of all events while taking into account temporal variation. Both SWD (black) and sSWD (grey) events are almost always less than 3 seconds. Nonconvulsive (blue) and convulsive (red) seizures have wide, yet similar probability density functions, with seizure durations almost never less than 20 seconds and peaking in the 30-40 s range, with longer seizure durations highly probable. Ictal activity following mid-ictal depression for both nonconvulsive (blue, dashed) and convulsive (red, dashed) peaks around 10 seconds, but can have variable event durations.

Changes in the pattern of electrical activity during seizures

A classical feature of seizures associated with acquired epilepsy is an evolution in the pattern of ictal electrical activity during the seizure. Specifically, shifts in frequency and amplitude components have been described during early-ictal, focal, and generalized tonic-clonic seizure events in patients with epilepsy (Alarcon, 1996; Hamer et al., 2003). Decomposing the spectral characteristics using PCA, we used an objective and quantitative method to analyze this subjective observation. Based on this approach, nonconvulsive and convulsive seizures appear almost identical in their evolving *changes of electrographic activity* during seizures. This is in contrast to the SWDs and sSWDs observed in our study, which showed little spectral changes, potentially reflecting a feature uncharacteristic of acquired epilepsy. Using the recording methods here, within this model, nonconvulsive and convulsive seizures appear almost identical. The singular measurable difference between convulsive and nonconvulsive seizures in this study was a slight decrease in cortical electrode measured signal complexity during evolution of the seizure. However, further studies are warranted to explore the potential differences in spectral identity between nonconvulsive and convulsive seizures, as this study filtered out high-frequency population spike activity that could provide additional information on electrophysiological parameters of a seizure.

Mid-ictal depression (MID) and short seizures

Many researchers have noticed amplitude attenuation that can occur during or near the end of a seizure; however, to our knowledge, MID has not been directly addressed in the literature. MID is likely a reflection of the same phenomenon as PID, but MID also provides an explanation for the observation from Cook et al. (Cook et al., 2016) during long-term continuous electrographic recordings in patients with intractable epilepsy that the *shortest seizures were consistently preceded by short inter-seizure intervals.* Because MID can last 10's of seconds with subsequent

seizure activity persisting for ≥10 s, human observers and automated seizure detectors would score a seizure with prominent MID as two seizures, where the MID (i.e., appearing as an extremely short inter-seizure interval) and the apparent second seizure have a much shorter duration than the initial part of the seizure (see **Figs. 3.5 and 3.10**). Several reports have noted that simple- and complex-partial seizures can be as short as a few seconds (Table 1). We propose that these cases of brief seizures from human patients (1) are typically due to the reemergence of seizure activity following MID and not due to multiple independent events, which (2) can possibly explain observations of brief seizures in human acquired epilepsy (D'Ambrosio et al., 2009).

Table 1: Average Duration for Seizure Subtype

Table 1.	Reference	Mean or median	Range/standard deviation
Subconvulsive	(Jin et al., 2016)	mean = 47.18 s	range = 5-311 s
	(Zangaladze, Nei, Liporace, & Sperling, 2008)	mean = 47 s	S.D. = 37 s
	(D. Kim et al., 2011)	median = 47.0 s	range = 4-1,016 s
Simple partial	(Zangaladze et al., 2008)	mean = 50 s	S.D. = 34 s
	(O. Devinsky et al., 1989)	48 s	range = 2-205 s
	(D. Kim et al., 2011)	62.5 s	range = 5-777 sec
	(Theodore et al., 1994) (preceding GTCS)	mean = 40 sec	S.D. = 80.1 sec range = 8-19 sec
	(Jenssen, Gracely, & Sperling, 2006)	median = 28 sec	range of median per patient = 3-180 sec
Complex partial	(Zangaladze et al., 2008)	mean = 123 sec	S.D. = 75 sec
	(Afra, Jouny, & Bergey, 2008) neocortical/ mesial temporal	median = 78 sec	range = global 33-551 sec focal 16-341 sec
	(Jenssen et al., 2006)	median = 106 sec	range = global 66-319 sec focal 64-203 sec
	(D. Kim et al., 2011)	median = 78 sec	range of median per patient = 8-298 sec
	(Theodore et al., 1994)(pre-GTCS)	95.0 sec	range = 7-1,005 sec
		32 sec	S.D. = 43.1 sec range = 7-258 sec
Tonic-clonic (convulsive)	(Zangaladze et al., 2008)	mean = 126 sec	S.D. = 60 sec
	(Jenssen et al., 2006)	primary 66 secondary 130	59-75 sec 37-139 sec
	(D. Kim et al., 2011)	median = 110.0 sec	range = 28-483 sec
	(Theodore et al., 1994) (preceding GTCS)	tonic component = 9.2 sec clonic component = 3.9 sec	S.D. = 7.9 sec range = 2-18 sec S.D. = 2.4 sec range = 1-8 sec
Not specified	(Cook et al., 2016) extratemporal onset	70-87 sec	range of means per patient = 1.7-486 sec
	temporal onset (Williamson et al., 1998) (MTLE)		range of means per patient = 2.5-2,259 sec 15-1,036 sec

Spike-and-wave discharges (SWDs) have different electrographic properties than convulsive or nonconvulsive seizures.

In contrast to nonconvulsive and convulsive seizures following SE, SWDs have a distribution of durations ranging from a few seconds (common) to >10 s (rare), no PID (or MID), and little if no spectral evolution. Furthermore, the incidence and electrographic characteristics of SWDs appear unrelated to post-SE epileptogenesis in the pilocarpine model. While SWDs are distinct from either nonconvulsive or convulsive seizures, they closely resemble the epileptiform electrographic events (EEEs) described for the FPI model (D'Ambrosio et al., 2009; D'Ambrosio & Miller, 2010) as well as SWD-like events reported as nonconvulsive seizures in a model of febrile seizures based on hyperthermia (Dubé et al., 2006), and the neonatal hypoxia-induced seizure model (Rakhade et al., 2011). Our results call into question the epileptic nature of SWDs in other models, particularly in light of studies using FPI that report more traditional electrographic representations of seizures (Kharatishvili, Nissinen, Immonen, Grohn, & Pitkanen, 2006; Shultz et al., 2013), as described here following SE.

Slow SWDs

Despite several similarities, sSWDs and SWDs appear to be two distinct classes of cortical activity, with different frequency identity (3-5 Hz vs 7-14 Hz, respectively) and progression dynamics, and with substantial differences in event incidence (**Figs. 3.8E and 3.9E**). sSWDs may be similar to 5-Hz events described by Jung et al. (Jung et al., 2007) from Day 3 to Day 6 post pilocarpine. While these authors interpreted the events as "class 0" nonconvulsive seizures, only cortical recordings were performed in this study. We only found sSWDs in the cortex and not hippocampus. The acute temporal window (concentrated on the 3rd day post-SE), variable behavioral activity (typically normal behavior instead of behavioral arrest), and cortical focus of sSWD activity leads us to question its involvement in acquired TLE, but the rhythmic epileptiform

activity appears immediately following the cessation of SE-associated seizures leading into the latent period, raising the possibility that sSWD activity could have predictive value. Further research using SE models with extended latent periods or lack of SRS development would serve as a necessary control to determine the functional identity of post-SE sSWD activity.

Conclusion

The present results confirm that, for the pilocarpine-induced SE model, nonconvulsive seizures during epileptogenesis are an early sign of acquired epilepsy and represent the terminal part of the classical latent period (Bertram & Cornett, 1994; Williams et al., 2009). In addition, these events are a prominent feature throughout the life history of this and other animal models of acquired epilepsy. Nonconvulsive and convulsive seizures were indistinguishable by almost every measure used in this study, suggesting that nonconvulsive and convulsive seizures should be viewed as similarly "epileptic" in the pilocarpine model. While it has been noted that brief SWDs could also be early nonconvulsive seizures of PTE (D'Ambrosio et al., 2009; D'Ambrosio & Miller, 2010), similar events have been reported extensively in control animals (Kelly et al., 2006; Kelly, 2004; Kelly et al., 2015; Pearce et al., 2014; Rodgers et al., 2015), suggesting they are absence seizures and/or rhythmic activity characteristic of the standard, non-epileptic, laboratory rat. We also observed examples of relatively brief seizures, but they occurred after MID near the end of otherwise typical electrographic seizures. As generally appreciated in the classical literature, both nonconvulsive and convulsive seizures undergo an evolution as they progress, and we have provided an objective and quantitative framework for this subjective phenomenon. This feature, as much or possibly more than seizure duration, provides a practical method to identify the electrographic seizures of acquired epilepsy and to distinguish them from events not characteristic of acquired epilepsy. Taken together, our results indicate that nonconvulsive seizures appear electrographically similar to convulsive seizures and are a prevalent component of epileptogenesis in animal models of acquired epilepsy, including models based on SE.

Chapter 4:

Immunization with heat-killed *Mycobacterium vaccae* in pregnant rats and offspring prevents autistic-like behavior in the stress-terbutaline model of comorbid autism spectrum disorder (ASD) and epilepsy

Abstract

Autism Spectrum Disorders (ASD) and epilepsy are often comorbid. The basis for this cooccurrence remains unknown, however inflammatory stressors during development are a shared risk factor. To explore this association, we used repeated immunizations of a heat-killed preparation of the stress-protective immunoregulatory microbe *Mycobacterium vaccae (M. vaccae;* NCTC 11659*)* on the behavioral and epileptogenic consequences of the combined stress-terbutaline (ST) rat model of ASD/epilepsy*.* Repeated immunization with *M. vaccae* prevented the expression of ASD-like behavior but did not protect against the spontaneous epileptogenic effects of stress-terbutaline. Additionally, epileptogenesis did not influence ASD-like behavior in this model. Maternal *M. vaccae* injections transferred an anti-inflammatory immunophenotype to offspring, and repeated injections across development prevented ST-induced increases in microglial density at early developmental time points in a region-specific manner. *M. vaccae* did not prevent ST-induced extrahypothalamic CRH expression changes, and stress coping behavior within this model was predictive of seizure development. Despite extensive epidemiological comorbidity between ASD and epileptic conditions and shared environmental risk factors, these results suggest that the contributing factors toward the development of seizures and the expression of ASD-like behavior remain entirely separable. Additionally, these data provide support for the exploration immunoregulatory strategies to prevent the negative effects of stressors during early critical periods.

Introduction

Autism spectrum disorders (ASD) are a group of disorders identified by two core behaviors; deficits social communication and restricted, repetitive behaviors or interests (American Psychological Association, 2013).These hallmark characteristics are often coupled with secondary diagnostic criterion including GI distress (Chaidez et al., 2014), immune abnormalities (Edmiston et al., 2017), anxiety (White et al., 2009), and improper stress regulation (Mazefsky et al., 2013). Additionally, epidemiological data suggest that 20-30% of children with ASD will

develop spontaneous recurrent seizures (SRS) reflective of epilepsy (Besag, 2017) and up to 70% will have epileptiform abnormalities (Ghacibeh & Fields, 2015). The ASD population represents a significant portion (~30%) of people diagnosed with epilepsy, but an underrepresented population for the development of combined treatment strategies. Despite the high rate of comorbidity between epilepsy and ASD, common pathological mechanisms remain theoretical (Gao & Penzes, 2015). While both disorders have some amount of heritability, they also share significant environmental risk factors that could guide research toward successful therapeutic interventions.

Prenatal stress is a predominant linking environmental risk factor in the development of both ASD and epilepsy (Kinney, Munir, Crowley, & Miller, 2008; van Campen, Jansen, de Graan, Braun, & Joels, 2014). However, stress is a multifactorial phenomenon, encompassing the activation of several interacting neuronal, hormonal, and immunological systems (McEwen, 1998). Stressors during development cause the release of inflammatory mediators (Gumusoglu, Fine, Murray, Bittle, & Stevens, 2017) and elevate several stress-associated hormones (Harris & Seckl, 2011), which can independently cause long-term changes in the composition and function of brain structures associated with stress reactivity, ASD, and epilepsy. Previous work from our lab using a two-hit early developmental teratogen approach (stress + the tocolytic B2 receptor agonist terbutaline; ST) in rats resulted in long-term ASD-like behavioral consequences, accompanying epileptogenesis, and heightened markers of chronic neuroinflammation (Bercum et al., 2015). However, the contributing role of stress-terbutaline induced inflammation to the comorbid consequences within this model have yet to be explored.

The hygiene, or “Old Friends” hypothesis, suggests that rapid increases in the prevalence of chronic inflammatory disorders observed in developed nations is the direct result of a diminished exposure to microbial diversity in “clean” urban environments (Rook, 2013). The loss of coevolved commensal microbe interactions, especially during early developmental critical periods, leads to improper immunoregulatory maturation, resulting in deleterious and prolonged

immune reactivity. While this hypothesis is rooted in the pervasiveness of allergies and overt autoimmune disorders in modern society, it has recently been extended to encompass the observed increase in susceptibility to neurodevelopmental and stress-related disorders, of which inflammatory mediators are believed to play a significant role (reviewed in; Lowry et al., 2016). This hypothesis is further supported by recent work highlighting the effectiveness of immunomodulatory microbe treatments in preventing stress-induced pathology. One such treatment, heat-killed preparations of *Mycobacterium vaccae,* has recently been demonstrated to be a successful immunoregulatory agent capable of immunizing against the negative inflammatory effects of psychosocial stressors (Reber et al., 2016). Additionally, *M. vaccae* acts as a peripheral anti-inflammatory agent through regulatory T-cell expansion (Reber et al., 2016), and centrally through the prevention of stress-induced microglial priming (Fonken et al., 2018; Frank et al., 2018), without modulating of stress-induced glucocorticoid release or stress-induced changes in the composition of the microbiome (Frank et al., 2018; Reber et al., 2016).

Within ASD, which has had a substantial increase in prevalence within the past few decades (Rice et al., 2012), several lines of work utilizing animal models have implicated microbial dysbiosis and the subsequent loss of immunoregulatory mechanisms in the development of the disorder (Agüero et al., 2016; Desbonnet et al., 2015; Rook, Lowry, & Raison, 2015). Additionally, microbial based interventions within animal models of ASD that target this mechanism have proven successful in reducing the expression of ASD-like behaviors (Hsiao et al., 2013; Sgritta et al., 2018). However, despite the proposed role for developmental stressors in ASD (Varcin, Alvares, Uljarević, & Whitehouse, 2017), and long-term immunoregulatory deficits (Jašarević, Rodgers, & Bale, 2014) studies directly targeting stress-induced inflammation with respect to ASD during development are lacking.

Because stress-terbutaline results in a comorbid ASD/epilepsy phenotype with prolonged neuroinflammation and *M. vaccae* has been shown to immunize against the inflammatory but not hormonal consequences of chronic stress, we hypothesized that treatment with this

immunoregulatory microbe may mitigate the early inflammatory contributors within this model. To explore this, we utilized repeated immunizations of heat-killed *M. vaccae* across development within rats undergoing a stress-terbutaline procedure and leveraged behavioral measures across time with 24/7 video EEG analysis to explore the dissociation between the inflammatory and neuroendocrine consequences of stress-terbutaline with respect to ASD and epilepsy.

Materials & Methods

Animals

Female Sprague-Dawley rats (*N* = 24; ENVIGO, Indianapolis, IN, USA) weighing 200-220 grams at embryonic day (E) 2 were used and given one day to acclimate to the animal facility before experimental manipulations were performed. Pregnant dams were individually housed in 26.67 cm x 48.26 cm x 20.32 cm sealed and ventilated static cages (Allentown Inc., Allentown, NJ, USA). Animals were housed under standard conditions in a temperature-controlled environment (20 °C ± 1, relative humidity 22%), with a 12h light/dark cycle (lights on from 7:00 A.M. – 7:00 P.M.), and *ad libitum* food and water. All procedures were performed in accordance with University of Colorado Boulder Institutional Animal Care and Use Committee guidelines for humane use of laboratory rats in biological research.

Developmental stressors and immunization

To mimic chronic stress exposure during pregnancy in humans, we combined several established stress paradigms to create a singular “developmental stress + terbutaline” rat model starting on Embryonic Day 3 (E3) and continuing until post-natal day 7 (P7). Rats are an altricial species, meaning that many developmental events occur postnatally, with P1-10 considered roughly equivalent to the third trimester in humans (Sengupta, 2013). To account for this, environmental stressors were continued during the first post-natal week as a slight modification to the previously published stress+ terbutaline method used (Bercum et al., 2015).

In total, 18 dams were randomly assigned to one of two experimental groups (developmental stress + terbutaline + *M. vaccae*; ST+ *M. vaccae*, *n* = 9) or developmental stress + terbutaline + vehicle (ST+ veh, *n* = 9). Due to the complexity of this chronic stress model, the potential confounding stressors of injection, and previous results demonstrating that behavioral and peripheral anti-inflammatory effects of *M. vaccae* are only present during periods of stress, a completely undisturbed no-stress control group was chosen for comparison in this study (NSC, *n* = 6).

Chronic Maternal Stress. Experimental dams were exposed to a repeated mild stress paradigm from E3-E20 (**Figure 4.1**). On E3, dams were habituated to the novel context in a sound-attenuated chamber (44.5 cm X 45.7 cm X 67.3 cm) containing a plexiglass apparatus (31.8 cm X 22.9 cm X 45.7 cm) with a shock grid floor (27.3 cm x 35.6 cm x 3.38 cm, Model E10-30SR, Coulbourn Instruments, Holliston, MA, USA) for 5 minutes (Bercum et al., 2015). From E4-E9, animals underwent a 7 day context re-exposure stress paradigm. On E4, contextual fear was established by returning the pregnant dams to the same context. After an initial 60 s exposure, two 1 s 1 mA foot shocks were delivered (at 60 s intervals) followed by an additional 5-minute exposure to the context post-shock. The following 2 days the dams were returned to the context for 5 min each day. To avoid complete fear extinction, the shock paradigm was repeated on E7, followed by 2 days of contextual environment exposure. On E10, the pregnant dams were left undisturbed, before repeating the 7-day context re-exposure paradigm. This paradigm was repeated until E20. During each trial, freezing time was recorded via a blind observer using a stopwatch. Dams were weighed every day to ensure pregnancy was not terminated.

Maternal immunization. On E2, E9, and E16 the experimental pregnant dams received either subcutaneous immunization with 0.1 mg whole heat-killed *M. vaccae* suspension (10 mg/mL solution; strain NCTC 11659, batch ENG 1, provided by Bio Elpida) diluted to 1 mg/mL in 100 µL sterile borate-buffered saline (BBS) using 21-gauge needles or injections of 100 µL of the vehicle, BBS, at 10:00 am. The control group was left completely unmanipulated.

Cross Fostering. On post-natal day (P2), females were culled and pups from all litters were cross fostered within treatment group. Pups were counterbalanced across dams so that no dam had greater than 6 pups.

Terbutaline Injections. Terbutaline injections were administered once daily on P2-5 to the ST+ *M. vaccae* and ST+ vehicle groups using terbutaline sulfate (Sigma-Aldrich, St. Louis, MO, USA) in doses of 10 mg/kg dissolved in saline (Bercum et al., 2015; Slotkin & Seidler, 2013; Zerrate et al., 2007),

Limited Bedding. On P2-7 the dams and pups were exposed to a limited bedding paradigm, mimicking procedures in previous experiments (Ivy, Brunson, Sandman, & Baram, 2008; Molet, Maras, Avishai-Eliner, & Baram, 2014; C. J. Rice, Sandman, Lenjavi, & Baram, 2008). The animals were placed in a chronic video recording cage (Axis M3104-L network Camera) and were given 6 pieces of food daily (26 grams, Tekland, ENVIGO) and *ad libitum* water. At P8, animals were returned to their home cage with normal amount of bedding and *ad libitum* access to food and water (Ivy et al., 2008; Molet et al., 2014). Maternal behavior (nursing, pup grooming, self-grooming, and eating/drinking) was observed at three time points on P7, 11:00 A.M, 1:30 P.M., an 6:30 P.M. for an hour and a half (Ivy et al., 2008) to observe any disturbances in maternal care.

Maternal Separation. On P2-7, pups were removed from their mother and litter mates. Dams were returned to their home cage. The pups were placed in individual cages (28.79 cm x 19.96 cm x 11.43 cm) with one paper towel, without any temperature regulating mechanisms in a separate room from the dams for 3 hours each day (Molet et al., 2014).

Post-natal immunization. *M. vaccae* and vehicle solutions were prepared as stated above and administered intraperitoneally on P7, P13, and P20 at 10:00 A.M. to pups according to their maternal treatment group.

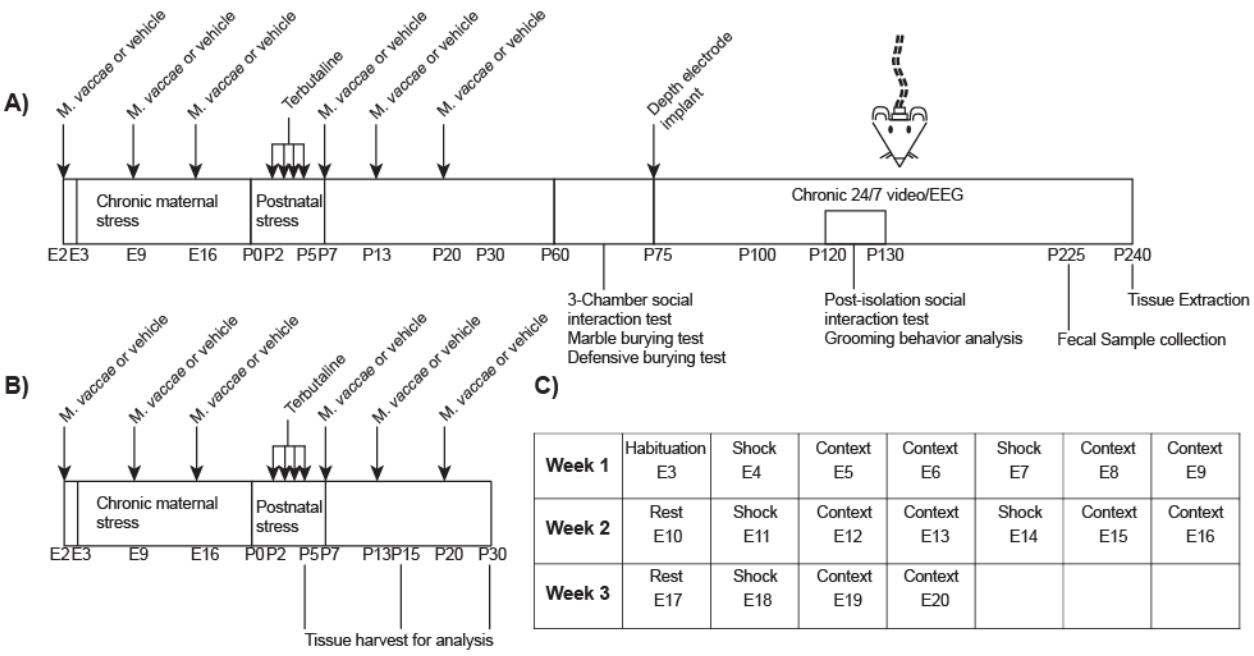

Week 1	Habituation E3	Shock E4	Context E5	Context E6	Shock E7	Context E8	Context E9
Week 2	Rest E10	Shock E11	Context E12	Context E13	Shock E14	Context E15	Context E16
Week 3	Rest E17	Shock E18	Context E19	Context E20			

Figure 4.1: Illustration of experimental timeline. (*A*) Illustration of the stress + terbutaline protocol. From E3-P0, pregnant dams undergo a chronic mild stress procedure. Male pups are selected and cross-fostered within treatment group at P2 so that each mother has no more than 6 pups. From P2-5, pups receive injections once-daily with terbutaline sulfate in doses of 10 mg/kg dissolved in saline. Concurrent early life stress exposure consists of limited bedding and 1-hr maternal separation from P2-P7. Pregnant dams undergoing the developmental stress + terbutaline procedure receive injections on days E2, E9, and E16 with 0.1 mg whole heat-killed *M. vaccae* suspension or injections of 100 µL of vehicle, sterile borate-buffered saline (BBS), at 10:00 A.M. Rat pups subsequently receive intraperitoneal injections on postnatal days P7, P13, and P20 at 10:00 A.M. with the same solutions. Behavioral tests were performed beginning on P60 and beginning on P120. On P75, all animals received electrode implants and were moved into static cages permitting free movement while tethered to an electrode harness. Subsequent EEG was continuously recorded until the end of the experiment. Control animals were cross-fostered and culled to select for males at P2, but otherwise remained undisturbed in their home cages. (*B*) A second group of animals underwent the stress + terbutaline procedure, but tissue was harvested at P5, P15 and P30 for analysis. (*C*) 3-day repeating contextual fear exposure and reinstatement paradigm schedule for chronic maternal stress. Abbreviations: E, embryonic day; EEG; electroencephalography; *M. vaccae*, *Mycobacterium vaccae*; P, postnatal day.

Behavioral Tests

Social Interaction

3 Chamber Social Interaction Test. At 2 months, social interaction and social novelty preference were assessed using a 3-chamber test consisting of two trials. The apparatus (91.4 cm x 41.9 cm x 41.9 cm) was divided into 3 (30.5 cm x 41.9 cm x 41.9 cm) chambers with doorways to allow free movement between chambers when doors were removed. The test rat was placed in the center chamber for a 5-minute habituation period without access to the other 2 chambers before the first trial of the test had begun. The first trial consisted of an age- and weight-matched novel rat placed into a 6-inch diameter cylindrical apparatus in one of the chambers and an identical empty cylindrical apparatus placed in the other. The doors were then removed at the beginning of the trial, allowing the rat 10 minutes to explore all three chambers. For the second trial, the same rat from the first trial was placed back in the cylindrical apparatus in the same chamber with a new age- and weight-matched novel rat placed into the previously empty cylindrical apparatus. The test rat was then placed in the center chamber and the doors were removed at the start of the 10-minute trial (Banerjee et al., 2014; Wöhr & Scattoni, 2013). Interaction and latency to interact with the novel rat, object, familiar rat, time spent in each chamber, total overall social interaction behavior, and number of entries in each chamber were measured using Anymaze (version 4.99z, Stoelting Co., Wood Dale, IL, USA).

Post-isolation Social Interaction. At 4 months, single-housed rats were habituated to the testing room for 1 hour in their home cage the day before the experiment began. The test was conducted in a low-lit room (10 lux) in a 43 cm × 28 cm × 15 cm testing box. On days 1 and 2 of the testing paradigm, the rat was placed into the testing chamber for 5 minutes to habituate to the testing environment. On the third testing day the rat was placed in the testing environment with an age-

and weight-matched novel animal. The socialization behavior defined as active contact (sniffing, grooming, nipping, wrestling, mounting, and crawling on or under partner) was observed and recorded (File & Hyde, 1978).

Repetitive Behavior

Marble Burying Test. At 2 months, animals underwent a 2-day habituation period in static cages (26.67 cm x 48.26 cm x 20.32 cm, Allentown Inc.) with 5 cm of bedding for a half an hour each day in the testing room. On the day of the test the rat was placed in a cage, identical to the habituation cage, with 5 cm of bedding and 18 clear glass marbles lined up in a 3x6 grid for 10 minutes. At the end of each trial the number of marbles buried, defined by 2/3 of the marble embedded in the bedding, number of marbles placed in a pile, and number of marbles undisturbed were recorded (De Boer & Koolhaas, 2003; Wöhr & Scattoni, 2013).

Home Cage Repetitive Grooming. At 4 months, animals were chronically recorded in their home cage using an overhead camera (Axis M3104-L Network Camera, Axis communications, Lund, Sweden). A single hour epoch of time (22:30-23:30 h) was used to score grooming behavior. The time interval 22:30-23:30 was chosen to score due to a lack of handling and manipulation, as well as, a time point that was in the median range of locomotor activity within the diurnal cycle (Gorka, Moryl, & Papp, 1996).

Stress reactivity

Defensive Burying Task. At 2 months of age, rats were habituated for 1-hour over 2 consecutive days in a cage identical to their home cage (26.67 cm x 48.26 cm x 20.32 cm, Allentown Inc.) with 5 cm of bedding. The 3rd day of the experiment the rat was placed in a cage for 15 minutes with a probe that was wired to deliver a shock (1mV) when the rat contacted it. At the end of each trial the height of bedding was recorded, and the video scored for the number of shocks and latency to bury the probe (Anderson, McWaters, McFadden, & Matuszewich, 2018).

Epileptogenesis

Chronic video/EEG recording. At P75, after early behavioral data were collected and ASD-like behaviors were assessed, 12 rats from each treatment group and 8 rats from the control group were instrumented for chronic video/EEG recording. Aseptic surgical procedures were used for all chronic preparations. Under isoflurane anesthesia (2.5%), rat pups (2 months of age; 275–300 g) were implanted with a Teflon-coated hippocampal wire electrode (AP, -4.0, ML, 2.0, DV 3.4 mm bregma), a ground screw (AP,-1, ML, 1 mm bregma), somatosensory screw (AP, 2, ML, 2 mm bregma) and a reference screw (AP, 4.0, ML, 2.0) mm bregma (Cat. no. E363-20 Elect W – 3.2 mm screw, 20 mm length; Plastics One) over the occipital bone. Two self-tapping anchor screws were implanted contralateral to the reference and ground screws (Small Parts, B000FN89DM, Logansport, Indiana, USA). Buprenorphine hydrochloride (Par Pharmaceuticals Companies, Inc.) (0.1 mg/kg, subcutaneously) was administered immediately after the surgical procedure and again every 12 h for a 72-h period. Following a 2-week recovery period, animals were tethered to an electrode harness (Cat. no. 363, Plastics One) and a slip-ring commutator (Cat. no. SL6C, Plastics One) permitted free movement for 24/7 video/EEG monitoring throughout the duration of the experiment. EEG signals were amplified and digitized at 500 Hz and stored in 30-min segments with time-locked video records for subsequent seizure and interictal spike analysis. EEG was continuously and entirely monitored, seizures were identified by the appearance of large-amplitude high frequency activity, with progression of the spike frequency that lasted for a minimum of 10 seconds. Behavioral video data were used to determine seizure intensity on the Racine scale (Racine, 1972) and to confirm EEG seizure activity versus potential animal-generated noise such as eating and grooming.

Manual EEG analysis. High-resolution monitors were used to display 30-min blocks of EEG divided into 10-s segments in raster-plot format. Both cortical and hippocampal channels could be observed simultaneously with on-demand time-locked video. Observers (ZZS and RAK) were trained to identify epileptiform EEG activity, monitor the behavioral correlates while ignoring

obvious noise from normal behaviors (chewing, head scratching, etc.), and identify possible ictal patterns for further analysis. Electroencephalographic seizures were differentiated from background noise by the appearance of large-amplitude, high-frequency (minimum 5 Hz) activity, with an evolution of EEG spike frequency lasting at least 5 s. However, to prevent missed seizures, all suspected seizure discharges with no minimum time limit were observed with concurrent video. Seizure flags were time-locked to the EEG and scored via the Racine scale (Racine, 1972) through video observation. Animals demonstrating electrical seizure activity, with a behavioral Racine scale of 2 or below (head bobbing, staring, lack of forelimb clonus) were identified as having a nonconvulsive seizure, while animals demonstrating a behavioral Racine scale of 3 or above (forelimb clonus, rearing, rearing and falling) were identified as having a convulsive seizure. Video monitoring was performed during the entire seizure as well as 40 s before and after an event. To prevent possible misidentifications, all seizures were behaviorally scored twice by independent observers (ZZS and RAK) for racine verification.

Epileptiform Spikes (ES): We used supervised pattern recognition to detect ES. Of the 10 rats with detectable ES, 9 had sufficiently robust ES for successful automatic detection. 1 SRS rat from the ST+ vehicle group was not used for spike rate quantification. For each rat, 20-30 ES were visually identified, temporally aligned according to the negative peak of the spike and averaged to create a template (± 200 msec window surrounding the peak). The spike template was then shifted point by point through the same data from which the spikes were visually identified and the covariance between data and template were computed as a function of time. The covariance time-series was visually thresholded to separate noise from correct detections. The time-shifted covariance between the spike template and 5 h baseline data (EEG data free from ES, but potentially containing high frequency noise) was computed and the threshold applied to examine false detections. False detections from the baseline were averaged to create a non-spike template. All subsequent detections compared the covariance between the data and both the spike and non-spike templates. While the two-template approach improved correct detections,

many spikes were still falsely detected in the baseline. To reduce false detections further, we added a second level of analysis relying on a Support Vector Machine (SVM) for pattern recognition (Orrù et al., 2012). For each rat individually, the SVM kernel was trained to discriminate the 20-30 initially identified spikes from approximately 1000 miss-identified spikes in the baseline. The combination of templates and SVM were then used to detect ES for all subsequent data for a given rat.

Histology

Fecal Corticosterone Assessment. Rats were placed in a clean cage overnight and fecal pellets were collected in the morning and stored at -80 °C until assay was ran. Corticosterone was extracted from 0.2 g of dried fecal solid vortexed in 2 mL of 200 proof ethanol (Decon Laboratories, Inc., King of Prussia, PA, USA). Samples were then centrifuged at 5,000 rpm for 15 minutes. Supernatant (1 mL) was transferred into clean centrifuge tubes and liquid evaporated off using a Speedvac. A corticosterone ELISA (Corticosterone ELISA kit, Enzo Life Sciences, Farmingdale, NY, USA) was ran according to manufacturer's recommendations. Intra-assay %CV: Low, 8.0; Medium. 8.4; High; 6.6. Inter-assay %CV: Low, 13.1; Medium, 8.2; High, 7.8. Lower limit: 26.99pg/ml; Upper limit: 20,000 pg/ml).

Euthanasia and tissue collection. Implanted animals were sacrificed at 9 months of age between 7 A.M. and 2 P.M. The animals were randomized to account for time of day and weighed before rapid decapitation. The brains, adrenals, and thymus were removed and weighed. Brains were immediately frozen on dry ice and stored at -80 °C. Trunk blood was collected, centrifuged (10,000 x g, 4°C, 20 min), and serum was extracted then stored at −80 °C. Aushon Biosystems (Catalog number: 114-D45-1-AB, Billerica, MA, USA) rat 6-plex arrays were used to measure the concentration of IL-1β, IL-2, IL-6, IL-10, IFNγ, and TNF-α according to manufacturer's instructions.

In situ hybridization histochemistry

Previously published methods were used for *in situ* hybridization histochemistry (Day & Akil, 1996; Fox et al., 2017; Loupy et al., 2019). Brains were sectioned into 12-µm thick sections on a cryostat

(Leica CM 1950, Leica Biosystems, Buffalo Grove, IL, USA), in a series of 20 alternate sections from +0.20 mm to –.71 mm from bregma and –1.4 mm to –2.83 mm according to a stereotaxic atlas of the rat brain (Paxinos and Watson, 1998), thaw-mounted on Histobond® slides (Cat. No. 16,004-406; VWR, West Chester, PA, USA), and stored at −80 °C. Sample sizes for *in situ* hybridization histochemistry for CRH were 1) home cage control (*n* = 8), 2) ST+ vehicle (*n* = 12) and 3) ST+ *M. vaccae* (*n* = 12).

Riboprobe preparation

Riboprobes targeting *Crh* mRNA were generated using standard transcription methods, as described previously (Day & Akil, 1996).

Crh mRNA was detected using a 770 base antisense riboprobe (from Dr. Robert Thompson) complementary to the rat cDNA encoding *Crh* (i.e., *crh*, NCBI Reference Sequence: NC_005101.4).

Riboprobes were radiolabeled via in vitro transcription, incorporating [35S]-UTP. Briefly, a nucleotide mix of ATP, CTP, GTP (1 µl of 10 mM each) was added to 5 µl 5× transcription buffer (Promega, Madison, WI, USA, cat. no. FP021), 2.5 µl 0.1 M dithiothreitol (DTT), and 4 µl sterile MilliQ water. Added to this solution was 1 µl (1 µg) cut DNA (antisense or sense), 1 µl RNase inhibitor (Invitrogen, RNaseOUT, cat. no. 100000840), 7.5 µl [35S]-UTP (1250 Ci/mmol; New England Nuclear-Perkin Elmer, Boston, MA, USA, cat. no. NEG039H001MC), and 1 µl of the appropriate RNA polymerase (T3 for antisense (cat. no. P208C) and T7 for sense (cat. no. P207B), Promega). The mixture was incubated at 37 °C for 2 h. The template DNA was then removed by digestion with 1 µl RNase-free DNase I (Promega, RQ1 DNase Stop Solution, cat. no. M199A) for 15 min at 20 °C. The probe was purified on G50/50 sephadex columns. Probe activity (1 µl) was counted in 7 ml scintillation fluid (Beckman Coulter, Ready Safe, Fullerton, CA, USA, cat. no. p/n484013-ae) with a beta counter (Beckman LS 3801, ser. no. 7013835).

In situ hybridization histochemistry

Tissue sections were fixed in 4% paraformaldehyde for 1 h, acetylated in 0.1 M triethanolamine hydrochloride with 0.25% acetic anhydride for 10 min, and dehydrated through graded alcohols. Sections were hybridized overnight at 55 °C with a [^{35}S]-UTP-labeled riboprobe diluted in hybridization buffer containing 50% formamide, 10% dextran sulfate, 2× saline sodium citrate (SSC), 50 mM PBS, pH 7.4, 1× Denhardt's solution, and 0.1 mg/ml yeast tRNA. The following day, sections were treated with RNase A, 200 µg/ml at 37 °C for 1 h, and washed to a final stringency of 0.1× SSC at 65 °C (1 h). Dehydrated sections were exposed to x-ray film (BioMax MR; Eastman Kodak, Rochester, NY, USA) for region- and probe-appropriate times (*Crh*, 20 days; *Crhr2*, 25 days) prior to film development.

Imaging and densitometry of in situ hybridization histochemistry autoradiograms

Autoradiographic images of the probe bound to *Crh* mRNA, encoding corticotropin-releasing hormone, together with ^{14}C-labeled standards, were measured using a computer-assisted image analysis system.

Analysis was performed on a PC using the publicly available NIH-developed image analysis software ImageJ (https://imagej.nih.gov/ij/). All measurements were taken while blinded to the treatment groups. Virtual matrices in the shape of respective bed nucleus of the stria terminalis (BNST) subregions, paraventricular nucleus of the hypothalamus (PVN), and central nucleus of the amygdala (CeA), and dorsal hippocampus were created (**Fig. 4.6**), overlaid with the image and the "mean gray value x area" within each matrix was measured, taking into account only the area of the above-threshold signal. During the entire analysis, a constant threshold function was applied, which determined the area that was actually measured within each matrix. Thus, all pixels

with a gray density below threshold were automatically excluded. The individual background of each image was measured and subtracted from the mean gray value.

Rostrocaudal analysis atlases for *Crh* and *Crhr2* expression in the BNST, PVN, hippocampus, and CeA subdivisions were created by comparing the image of the tissue sections with a stereotaxic atlas of the rat brain (George Paxinos and Charles Watson, 1998) and with *Crh* mRNA expression from this experiment. In other words, all rostrocaudal levels for each gene were assigned based on the rostrocaudal levels defined using *Crh in situ* hybridization histochemistry. According to Paxinos and Watson (George Paxinos and Charles Watson, 1998), each rostrocaudal level of the BNST was further divided into two subregions, the bed nucleus of the stria terminalis, lateral dorsal part (BNSTLD) and bed nucleus of the stria terminalis, lateral ventral part (BNSTLV). The dorsal hippocampus subregions were subdivided into the dentate gyrus (DG), *cornu ammonis 1* (CA1) *and cornu ammonis 3* (CA3). The PVN and CeA were not further divided. At each rostrocaudal level, the mean gray value x area values for the left and right sides of each subdivision were averaged. Overall mRNA expression within the two subregions of the BNST, the PVN, the hippocampus, and the CeA were displayed by averaging mean gray value x area values across all rostrocaudal levels per treatment group. A total of 8 rostrocaudal levels were studied throughout the forebrain (**Fig. 4.6**). The subdivisions studied were summarized into the following functional subregions and regions: BNSTLD, –0.10 mm to –0.34 mm from bregma; BNSTLV, –0.10 mm to –0.34 mm from bregma; PVN, –1.66 mm to –1.78 mm from bregma; CeA, –2.38 mm to –2.62 mm from bregma; and dorsal hippocampus -2.62mm to -2.83mm from bregma.

Immunofluorescence

Immunohistochemistry: At P15 and P30, select rats were anesthetized with isoflurane and transcardially perfused with ice-cold saline, followed by 4% paraformaldehyde. Brains were removed and post-fixed for 24 h in 4% paraformaldehyde. Brains were cryoprotected in 30% sucrose and then frozen using dry ice and isopentane. Brains were sectioned onto Histobond®

slides (Cat. No. 16,004-406; VWR, West Chester, PA, USA) at 20 µm using a cryostat (Leica CM 1950, Leica Biosystems, Buffalo Grove, IL, USA) and stored at -80 °C. Slides were removed from refrigeration and allowed to reach room temperature before being washed in 1X PBS for 5 min. Slides were blocked with 10% NGS in 1X PBS with 0.2% Triton X (PBS + Tx) for 1 h at room temperature. Slides were incubated at room temperature overnight in 1X PBS + Tx with the following primary antibodies: rabbit anti-Iba1 (Cat. no. 019-19741, rabbit, 1:1000, Wako, Richmond, VA, USA) and mouse anti-GFAP (mouse; MP691102, 1:100, MP Biomedicals, Santa Ana, CA, USA). Slides were washed in 1X PBS 3 times for 5 minutes, then incubated for 2 hours in the dark in 1X PBS + Tx with the following secondary antibodies: 488 goat anti-rabbit (1:500) and 594 goat anti-mouse (1:500). Slides were washed with 1X PBS, then coverslipped using Vectashield with DAPI (Vectashield). Images were taken using a Nikon Eclipse 90 with a Lumen Dynamics X-Cite 120 Fluorescence Light Source and analyzed using an automated FIJI cell counting protocol.

Results

Effects of *M. vaccae* immunization on ASD-like behaviors

Social communicative function. ST animals have been previously shown to demonstrate deficits in social communicative function and increases in repetitive behaviors (Bercum et al., 2015), both hallmarks for the clinical diagnosis of autism (American Psychiatric Association, 2013; Happé, 2011) and for modeling ASD-like behavior in rodents (Patterson, 2011; Silverman, Yang, Lord, & Crawley, 2010). To explore possible effects of immunization with *M. vaccae* on preventing these behaviors in the ST model, we examined deficits in social interaction and repetitive behavior during adulthood at P60 and P120 (Sengupta, 2013) (**Fig. 4.2A**). For the 3-chamber social interaction task performed at P60, ANOVA revealed differences in the level of total social interaction among treatment groups ($F_{(2,27)} = 3.506$, $p < 0.05$), with vehicle treated ST animals engaging in less overall social interaction behavior (137.7 ± 16.7 s) compared to controls (186.4 ± 27.8 s; $p < 0.05$; **Fig. 4.2A**). However, this effect was not seen in ST animals treated with *M.*

vaccae, who engaged in higher (202.0 ± 13.1 s) social interaction behavior than the vehicle-treated ST group ($p < 0.05$) and were no different than controls. The same pattern was observed when a post-isolation reciprocal social interaction task was performed 60 days later (**Fig. 4.2A**; P120). Differences in social behavior at P120 between treatment groups were observed ($F_{(2,28)} = 6.508$, $P < 0.01$), with vehicle-treated ST animals engaging in less social interaction behavior (109.9 ± 11.0 s) compared to controls (166.5 ± 15.8 s; $P < 0.05$). Again, this effect was not seen in ST animals treated with *M. vaccae*, who demonstrated higher (147.8 ± 8.6 s) overall social interaction behavior than vehicle-treated ST animals ($P < 0.05$) and did not differ from control unstressed animals.

Marble burying (P60) and home-cage grooming (P120) were both assessed as markers for repetitive behavior. At P60, ANOVA revealed differences in marbles buried across groups ($F_{(2,29)} = 8.0321$, $P < 0.01$), while pairwise comparisons demonstrated that vehicle-treated animals buried more marbles (3.1 ± 0.5) than controls (1.4 ± 0.5; $p < 0.01$). This increase was not seen in ST animals treated with *M. vaccae* (1.2 ± 0.3), who buried fewer marbles than vehicle treated ST animals ($P < 0.05$; **Fig. 4.2B**). At P120, group differences in grooming behavior were identified ($F_{(2,28)} = 4.953$, $P < 0.05$), mirroring P60, with vehicle-treated ST animals (439.6 ± 84.4 s) engaging in more grooming behavior than controls (139.4 ± 57.3 s; $P < 0.05$). As observed with marble burying at P60, ST animals treated with *M. vaccae* had less grooming behavior (188.6 ± 58.9 s) than vehicle-treated ST animals ($P < 0.05$). Performance of *M. vaccae*-treated rats in both the marble burying and grooming tests were the same as control rats that did not experience developmental stress-terbutaline.

Composite Spectrum Score. By combining behavioral tasks into a single composite score, we were able to assign each animal on a spectrum of ASD-like behavior (**Fig. 4.2C**). Repetitive behavior scores were inverted so that negative Z-scores reflected increases in repetitive behavior. If animals performed consistently across behavioral measures, then combining the scores should reflect overall behavioral severity. ANOVA of the combined scores (Z-scores) revealed significant

differences among groups ($F_{(2,26)}$ = 13.004, P < 0.001). As in the individual behavioral tests, vehicle-treated ST animals had consistently lower Z-scores (-0.16 ± 0.19) than control animals (0.79 ± 0.33; P < 0.05) and ST animals treated with *M. vaccae* (1.28 ± 0.16; P < 0.001), who showed no signs of ASD-associated behavioral deficits like the controls. Across the lifetime of the rat, *M. vaccae* treated ST animals showed no evidence of core ASD-like behaviors found in vehicle-treated stress-terbutaline animals.

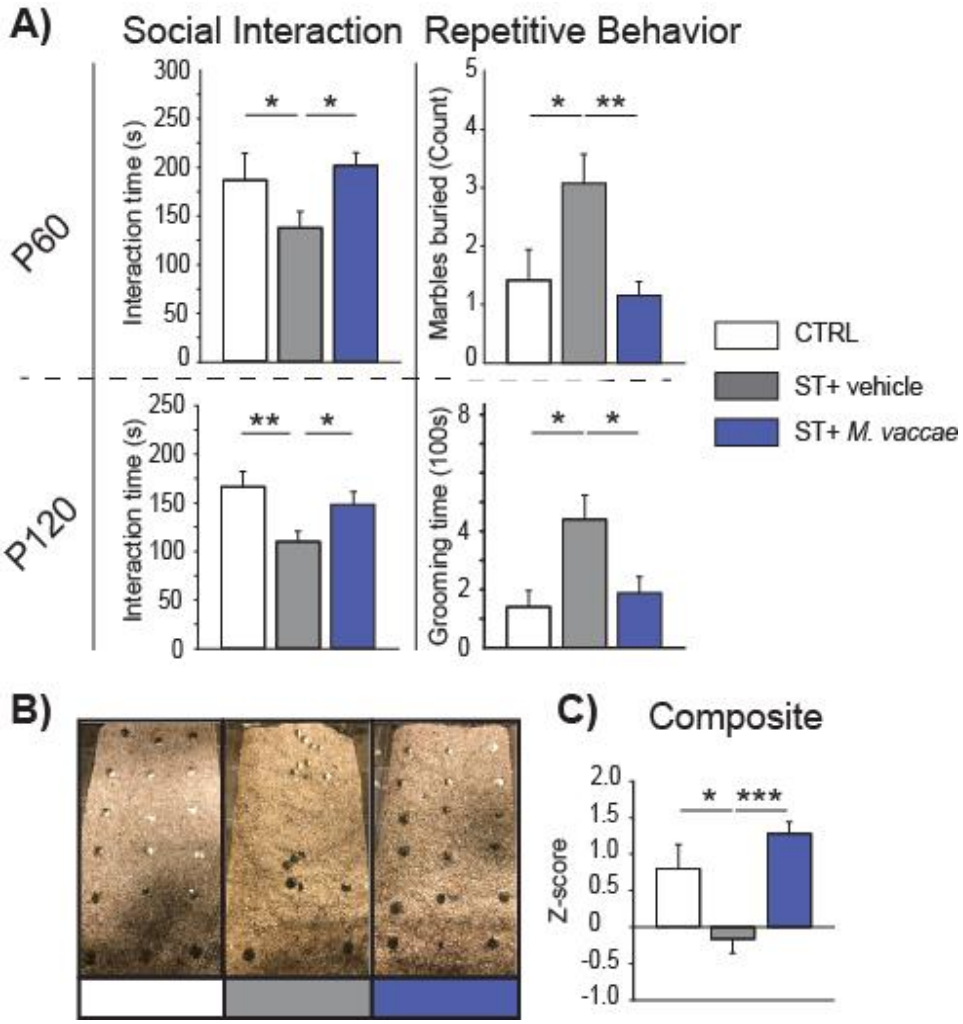

Figure 4.2: Immunization with *M. vaccae* prevents effects of stress-terbutaline on autism spectrum disorder (ASD)-like core behavioral symptoms. (*A*) Behavioral tests performed at postnatal day 60 (P60) and P120 to test social interaction deficits and repetitive behavior. P60: Social interaction behavior was assessed via total social interaction behavior in seconds during the 3-chamber task, while repetitive behavior was assessed by measuring the number of marbles buried during the marble-burying task. P120: Social interaction was assessed by measuring active contact time in seconds during a post-isolation social interaction task, while repetitive behavior was identified through home-cage grooming time between 22:30 and 23:30. (*B*) Representative images from each group following the marble burying task. (*C*) A composite ASD score was computed by combining normalized values within behavioral tasks. Repetitive behavior z-scores were inverted to account for their positive association with ASD. Bars represent means of each group, error bars represent + SEM. Comparisons were made between untreated control (CTRL; $n = 8$, white), vehicle-treated stress-terbutaline (ST+ vehicle; $n = 12$, grey), and *M. vaccae*-treated stress-terbutaline (ST+ *M. vaccae; n* = 12, blue) groups. **P* < .05, ***P* < .01, ****P* < .001. Abbreviations: CTRL, control; *M. vaccae*, *Mycobacterium vaccae*; P60, postnatal day 60; P120, postnatal day 120; SEM, standard error of the mean; ST, stress-terbutaline.

Effects of *M. vaccae* immunization on epileptogenesis. To capture the time-course of epileptogenesis (the transition from normal to epileptic brain excitability) following stress-terbutaline, animals were implanted with chronic electrodes in the somatosensory cortex and hippocampal dentate gyrus (**Fig. 4.3A**). Chronic video/EEG recording began at P75 and continued until rats were 8 months of age. Electrographic seizures were visually identified based on characteristics defined in previous studies (Smith, Benison, Bercum, Dudek, & Barth, 2018). Seizures ranged from 10 to 170 s (mean = 97.6 ± .8 s) and had a classic complex-partial profile characterized by large amplitude spiking with a typical progression of frequency (**Fig. 4.3B**; i-v), followed by post-ictal (post-seizure) suppression (**Fig. 4.3B**; vi). The number of rats developing spontaneous recurrent seizures (SRS) was 7 out of 24 across treatment groups. None of the control animals developed SRSs. The number of SRSs during the recording period varied between animals, ranging from 2 to 16 and averaging 9.8 ± 1.9 per animal. SRSs in both *M. vaccae* and vehicle-treated rats began to emerge at approximately 3 months of age (**Fig. 4.3C**). By the end of the experiment, 25% of the vehicle-treated rats had experienced at least one seizure. This seizure prevalence, however, did not differ from the *M. vaccae*-treated rats (33%), nor were there significant differences in seizure rates between the vehicle-treated (10.3 ± 4.3) or *M. vaccae*-treated (9.5 ± 1.9) rats.

As an additional measure of possible differences in epileptic excitability between treatment groups, we examined “epileptiform spikes” (ESs) which may or may not occur with SRSs and are thought to be associated with epileptogenesis in animal models of acquired epilepsy (Staley & Dudek, 2006). As in previous studies, ESs were automatically detected and quantified using pattern recognition based on a support vector machine (Nandan et al., 2010; Orrù et al., 2012). Figure 4.3D (upper and lower traces) shows an example of ES rates recorded over approximately 100 days (following electrode implant at 3 mo of age) in a vehicle-treated and an *M. vaccae*-treated ST rat. ES rates in both groups had similar profiles, with a continuous progression across epileptogenesis (**Fig. 4.3D**; grey and blue). Measurable ESs (**Fig.4.3**) were detected in 33% of

ST+ vehicle (4 of 12), 50% of ST+ *M. vaccae* (6 of 12) and were not detected in control animals (*n* = 8). Average ES morphologies (waveforms; **Fig. 4.3D**: upper and lower) were similar between groups. Finally, no differences in hourly spike rates between ST+ vehicle (3 ± 1.1/h and ST+ *M. vaccae* (4.3 ± 0.7/h) animals were found via automatic spike detection (**Fig. 4.3E**; *p* = 0.35).

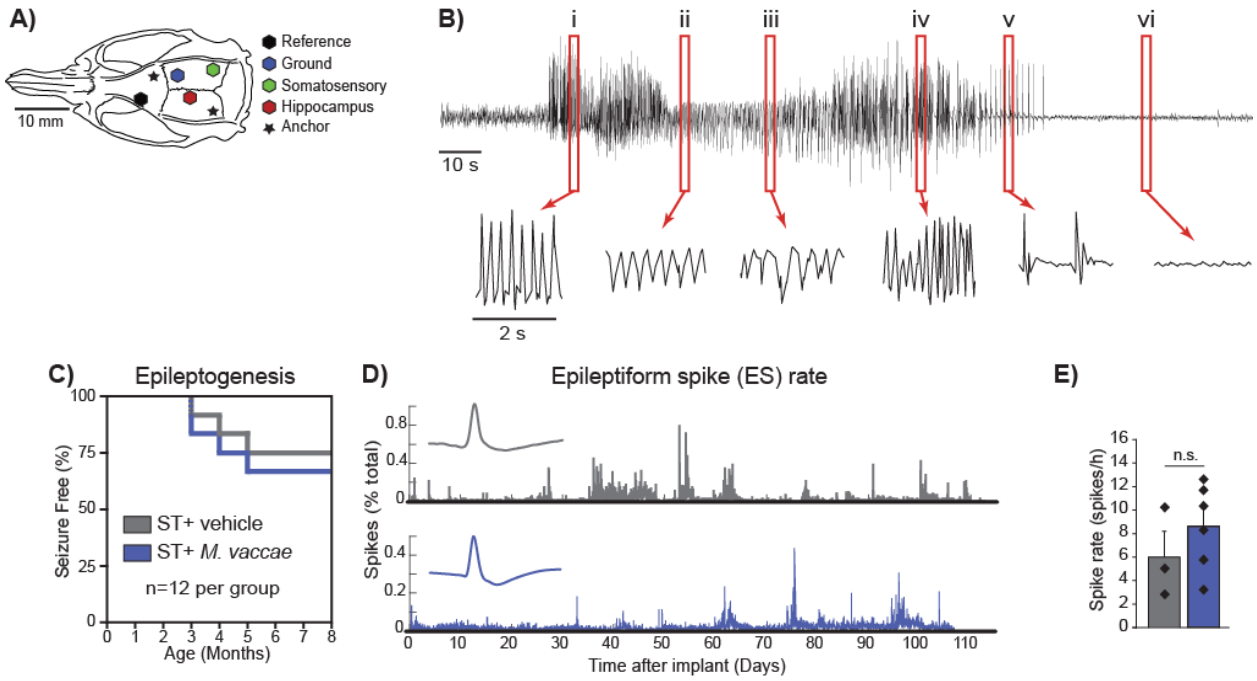

Figure 4.3: Progressive epileptogenesis within stress-terbutaline animals is not affected by treatment with *M. vaccae* during development. (*A*) Location of electrodes and anchors used for chronic implantation surgery. Left to right represent the rostro-caudal axis. Hippocampal depth electrodes were placed at -3.8 mm bregma stereotaxically and lowered until dentate granule cell responses were recorded. (*B*) Time series of ictal activity from a representative seizure recorded in the hippocampus. Isolated 2-second segments are enlarged to show variable fundamental frequencies throughout the seizure (*i-v*) and characteristic post-ictal suppression (*vi*). (*C*) Survival curve representing the number of seizure-free animals across the course of the experiment reveals similar rates of spontaneous seizure development for vehicle- (grey) and *M. vaccae*-treated (blue) stress-terbutaline animals. (*D*) Representative time course data of detected epileptiform spikes (ES) across the chronic recording period with individual spike templates (average 20-30 spikes) used for automatic detection for vehicle- (grey) and *M. vaccae*-treated (blue) stress-terbutaline animals. (*E*) Averaged rate comparison for animals with automatically detected ES (ST+ vehicle; n = 3, grey ST+ *M. vaccae; n* = 6, blue). Bars represent means; error bars represent +SEM, individual data points are plotted as diamonds. $^{n.s.}$ $P > .05$. Abbreviations: ES, epileptiform spikes; *M. vaccae*, *Mycobacterium vaccae*; SEM, standard error of the mean; ST, stress-terbutaline.

Relationship of ASD-like behavior to epileptogenesis. The fact that *M. vaccae* treatment prevented the expression of ASD-like behavioral impairments but had no apparent effect on epileptogenesis, raised the question of whether any potential interactions between core ASD-like behavioral features and epileptogenesis exist. Are ASD-like behaviors in rats that eventually develop seizures differentially affected by *M. vaccae* compared to rats that remain seizure free? To explore this question, we reanalyzed the behavioral data after the identification of SRS by separating animals into 4 groups, dependent on two factors. Rats were organized first by treatment and then by whether they eventually developed SRSs. Two-way ANOVA, corrected for uneven groups, was performed to analyze main effects and interactions. Pilot data from ST animals implanted (n = 24) on P7 and recorded intermittently until chronic implants and 24/7 video EEG became sustainable had demonstrated that epileptiform activity begins to appear around 3 months of age. Because ST animals begin to show epileptiform activity at around 3 months of age, but not before (**Fig. 4.3C&D**), differences in behavior before P90 between animals that would eventually develop seizures and those that would remain seizure-free could be considered as predictive or linked to epileptogenesis, without being driven by seizures themselves. As expected, main effects of treatment remained consistent across ASD measures at P60 for social interaction ($F_{(1,18)}$ = 8.552; p < 0.01) and marble burying ($F_{(1,20)}$ = 10.832; p < 0.01) and at P120 for social interaction ($F_{(1,20)}$ = 5.449; p < 0.05) and grooming ($F_{(1,20)}$ = 6.338, p < 0.05), but no interactions or main effects of epileptogenesis (SRS vs Non-SRS) were found (**Fig. 4.4A**). With the combined ASD score, two-way ANOVA revealed a significant effect of treatment ($F_{(1,18)}$ = 32.629, p <.001) but no interaction between treatment and SRS development ($F_{(1,18)}$ = 1.286, p =.272) (**Fig. 4.4B**). Taken together, these data demonstrate that immunization with *M. vaccae* during development prevents the appearance of core behavioral features of ASD within the stress-terbutaline model at every time-point measured but fails to affect the progression of epileptogenesis. Additionally, core behavioral features of ASD measured here do not appear to be related to, predictive of, or enhanced by epileptogenesis.

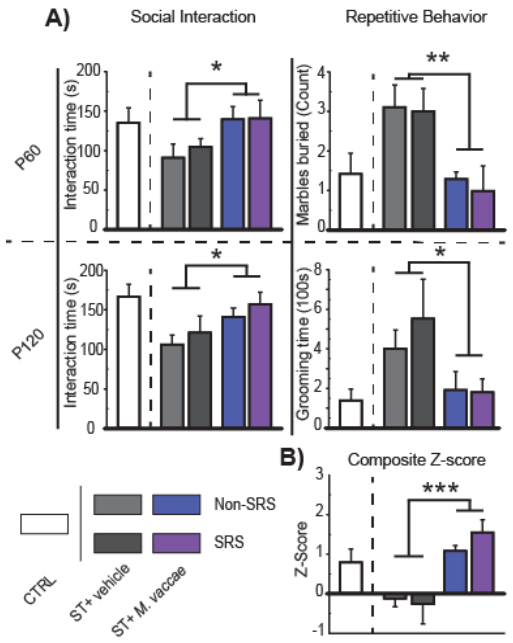

Figure 4.4: Epileptogenesis is unrelated to core behavioral features of ASD. (*A*) Behavioral tests performed at P60 and P120 to test social interaction deficits and repetitive behavior. P60: Social interaction behavior was assessed by measurement of total social interaction behavior in seconds during the 3-chamber task, while repetitive behavior was assessed by measurement of the number of marbles buried during the marble-burying task. P120: Social interaction was assessed via active contact time in seconds during a post-isolation social interaction task, while repetitive behavior was identified through home-cage grooming time between 22:30 and 23:30. (*B*) A composite ASD score was computed by combining normalized values within behavioral tasks. Repetitive behavior z-scores were inverted to account for their positive association with ASD. Bars represent means of each group, error bars represent + SEM. Dotted lines on each graph separate control animals from stress-terbutaline animals included in the 2 x 2 analysis. Stress-terbutaline groups are subdivided by treatment (vehicle or *M. vaccae*) and whether animals were undergoing epileptogenesis (non-SRS or SRS). Comparisons were made between vehicle-treated stress-terbutaline animals that remained seizure-free (ST + vehicle + Non-SRS; $n = 9$, light grey), vehicle-treated stress-terbutaline animals undergoing epileptogenesis (ST + vehicle + SRS; $n = 3$, dark grey), *M. vaccae*-treated stress-terbutaline animals that remained seizure-free (ST+ *M. vaccae* + Non-SRS*;* $n = 8$, blue), and *M. vaccae*-treated stress-terbutaline animals undergoing epileptogenesis (ST + *M. vaccae* + SRS*;* $n = 4$, purple). *$P < .05$, **$P < .01$, ***$P < .001$. Abbreviations: CTRL, control; *M. vaccae*, *Mycobacterium vaccae*; P60, postnatal day 60; P120, postnatal day 120; SEM, standard error of the mean; SRS; spontaneous recurrent seizures; ST, stress-terbutaline.

Early developmental CNS cytokine profile is anti-inflammatory in stress-terbutaline animals treated with *M. vaccae*. We have previously shown that ST rats express increased hippocampal gliosis compared to controls (Bercum et al., 2015), suggesting a prolonged neuroinflammatory trajectory in this model that could be altered by *M. vaccae* (Frank et al., 2018) and explain its effect on attenuating ASD-like behavior. In other studies, *M. vaccae* has been shown to increase peripheral levels of the anti-inflammatory cytokine, IL10, in adult animals (Reber et al., 2016) and hippocampal levels of the CNS anti-inflammatory cytokine IL4 (Frank et al., 2018, 2018). Additionally, IL4 injections have been shown to recapitulate the effects of *M. vaccae* on hippocampal gene expression (Frank et al., 2018). We therefore measured whole-brain levels of several cytokines. To separate possible anti-inflammatory effects of *M. vaccae* immunization of the dams from subsequent treatment of the pups, we measured cytokines at P6, after the final terbutaline injection, but prior to the first offspring injection of *M. vaccae* to see if this stress-protective anti-inflammatory phenotype was present during post-natal stress-terbutaline. Significant group differences existed in whole brain mRNA levels of IL4 ($F_{(2,9)}$ = 12.644, p <.01) and IL10 ($F_{(2,9)}$ = 5.584, p <.05) at this time point. As shown in figure 4.5A, P6 pups from S + vehicle-treated dams demonstrated significantly lower levels of IL10 compared to control (p < .05), while P6 pups from S + *M. vaccae*- treated dams displayed significantly higher levels of IL4 than both controls (p < .05) and P6 pups from S + vehicle-treated dams (p < .01). This anti-inflammatory phenotype exists prior to the first offspring injection with *M. vaccae*, suggesting that the maternal neuroinflammatory protection conferred by *M. vaccae* is incorporated into offspring through a maternal transfer mechanism.

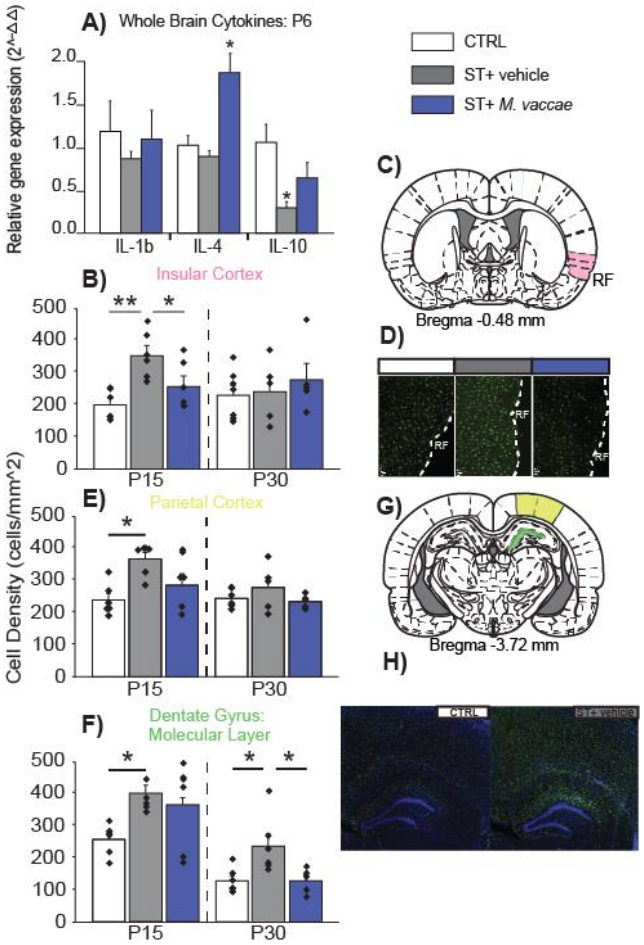

Figure 4.5: *M. vaccae* treatment mitigates region-specific developmental alterations in microglial number in stress-terbutaline animals. *(A)* Relative expression of whole brain cytokine levels measured at P6. (*B,E,F*) cell density measures, expressed in terms of ionized calcium-binding adapter molecule 1- (Iba-1-) positive cells/mm^2, for each region of interest at P15 and P30. (*C&G*) Illustrations of brain regions that were sampled for measurement of Iba1 immunostaining with the rhinal fissure for reference (pink, insular cortex; yellow, parietal cortex; red, dentate hilus; green, dentate gyrus molecular layer). Equivalent adult rostrocaudal location, expressed in millimeters from bregma are listed below each image, according to a stereotaxic atlas of the adult rat brain (Paxinos & Watson, 2007). (*D*) Representative images at 100X of Iba-1-positive cells in the insular cortex at P15 with the rhinal fissure (RF) for reference for each group. (*H*) Representative images at 40X of Iba-1-positive staining within the hippocampus and cortex, co-stained with DAPI for subregion localization at P15 in control and ST + vehicle animals. Bars represent means of each group, error bars represent + SEM, individual data points are plotted as diamonds. Comparisons were made between CTRL (white; *n* = 6), ST + vehicle (grey; *n* = 6), and ST + *M. vaccae* (blue; *n* = 6) groups. **P* < .05, ***P* < .01, ****P* < .001. Abbreviations: CTRL, control; *M. vaccae*, *Mycobacterium vaccae*; P15, postnatal day 15; P30, postnatal day 30; RF, rhinal fissure; SEM, standard error of the mean; ST, stress-terbutaline.

Developmental trajectory of microglial density is altered by stress + terbutaline and mitigated by *M. vaccae* in a subregion-specific manner. Microglia are the principle innate immune cells of the CNS, not only responsible for release of both pro- and anti-inflammatory cytokines, but also instrumental for early developmental processes such as synaptogenesis (Paolicelli et al., 2011). Terbutaline and developmental stress can induce pathological changes in microglial function during developmental critical periods (Delpech et al., 2016; Zerrate et al., 2007). These alterations have been implicated in improper neurodevelopment and suggested as a mechanism contributing to the development of excitatory/inhibitory imbalances seen in both ASD and epilepsy (Koyama & Ikegaya, 2015). Thus, neuroinflammatory protection conferred by *M. vaccae* could be reflected in changes in microglial function. This possibility is supported by recent studies demonstrating the ability of *M. vaccae* to bias microglia toward an anti-inflammatory and stress-protective immunophenotype (Fonken et al., 2018; Frank et al., 2018). We therefore examined changes in CNS microglial density at two critical periods of neurodevelopment; at P15 (when microglial density is at a developmental peak and actively guiding synapse development (Kim et al., 2015; Nikodemova et al., 2015) and at P30, where many neurodevelopmental processes should be close to reaching adult levels (Wei et al., 2015).

At P15, significant between-group differences in microglial density were observed in the insular cortex (**Fig. 4.5, B&D**; $F_{(2,15)} = 8.17381$, $p < .01$), parietal cortex (**Fig. 4.5E**; $F_{(2,14)} = 6.93149$, $p < .01$), and the molecular layer of the dentate gyrus (**Fig. 4.5**, F&H; $F_{(2,15)} = 4.127$, $p < .05$). No differences were observed in other brain regions, including the dentate hilus ($F_{(2,14)} = .565$, $p = .581$) and primary somatosensory cortex ($F_{(2,14)} = .6887$, $p = .518$). Post-hoc analysis demonstrated that ST+ vehicle animals had significantly higher cell density counts than controls in insular cortex (**Fig. 4.5B**; $n = 6$; 353.97 ± 25.34 cells/mm^2; $p < .01$), parietal cortex (**Fig. 4.5E**; $n = 6$; 350.290 ± 19.14344 cells/mm^2; $p < .01$), and in the dentate molecular layer (**Fig. 3F&H**; $n = 6$; 401.582 ± 25.442 cells/mm^2; $p < .01$). In the insula, microglia density in *M. vaccae*-treated ST rats was significantly reduced (258.48 ± 30.631 cells/mm^2; $p < .05$) compared to vehicle-

treated ST rats and could not be distinguished from control animals (201.04 ± 19.879 cells/mm^2; p = .142) (**Fig. 4.5B**). However, microglia density in *M. vaccae*-treated ST rats was more variable in both the parietal cortex (**Fig. 4.5E**; n = 5; 271.866 ± 34.519 cells/mm^2) and the dentate molecular layer (**Fig. 4.5F**; n = 6; 366.262 ± 55.542 cells/mm^2) and did not significantly differ from controls or vehicle-treated ST animals. By P30, there were no significant group differences in microglial density in the insular or parietal cortices, or dentate hilus. However, significant group differences where still present in the molecular layer of the dentate gyrus (**Fig. 4.5F**; P30; $F_{(2,14)}$ = 5.7438, p < .05), with ST+ vehicle-treated animals maintaining significantly elevated levels (n = 6; 238.53 ± 37.675 cells/mm^2) when compared to controls (n = 6; 129.93 ±15.834 cells/mm^2; p < .05). Unlike P15, ST+ *M. vaccae*-treated animals also had reduced density counts (n = 5; 129.24 ± 17.427 cells/mm^2) when compared to vehicle-treated ST animals (p < .05).

Neuroendocrine disruption and stress-terbutaline

The neuroinflammatory effects of stress-terbutaline, and their attenuation by *M. vaccae*, suggested that neuroinflammation, especially during early critical developmental periods, may play a significant role in the development of ASD-like behavior in our model, as proposed in other models of ASD-like behavior (Choi et al., 2016). However, other physiological mediators of psychosocial stressors during development could also influence ASD-like behavior. Prenatal and early postnatal exposures to excess glucocorticoids have been shown to permanently alter the function of the hypothalamic-pituitary-adrenal (HPA) axis in rodent offspring by inducing epigenetic changes in the expression of corticotropin-releasing hormone (CRH) (Glover, O'Connor, & O'Donnell, 2010; van Bodegom, Homberg, & Henckens, 2017). We used *in situ* hybridization histochemistry to determine if long-term changes in basal CRH mRNA expression were evident in the ST model and, if so, whether they were affected by *M. vaccae* immunization (**Fig. 4.6A,B**). No differences were seen in the expression of CRH in the PVN or dorsal hippocampus in any group (**Fig. 4.6B**), signifying that stress-terbutaline does not cause long-term changes in CRH expression within the major output node of the HPA-axis. Surprisingly, CRH

expression was consistently decreased in the BNST and CeA of all stress-terbutaline animals (i.e., both vehicle- and M. vaccae-treated ST animals) compared to control animals (**Fig. 4.6B**), an effect that was unchanged by *M. vaccae* treatment (BNST ($F_{(1,38)}$ = 6.928, p < .012); CeA ($F_{(1,19)}$ = 9.515, p < .006). While functional changes in these brain regions have the potential to influence ASD-like behavior, *M. vaccae* immunization did not influence stress-terbutaline-induced changes in CRH expression within extrahypothalamic brain regions, suggesting that restoration of extrahypothalamic CRH was not necessary for the ability for *M. vaccae* to prevent ASD-like behavior within these animals.

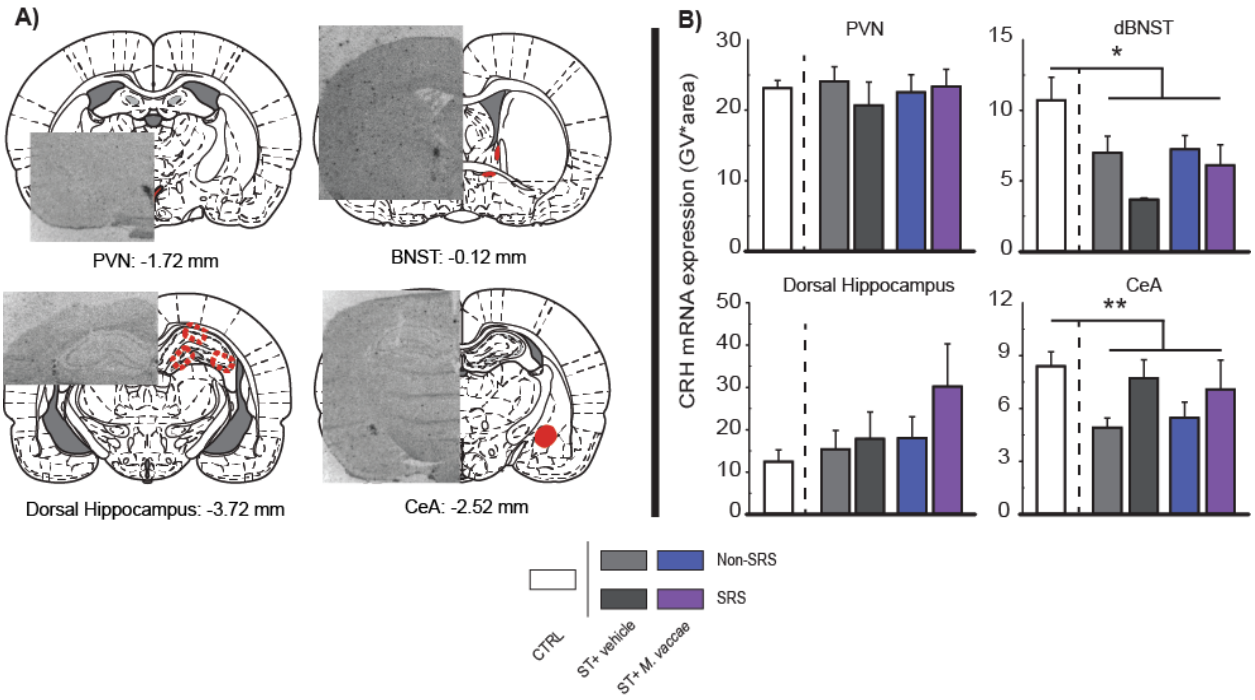

Figure 4.6: Immunization with *M. vaccae* does not prevent stress-terbutaline-induced changes in extrahypothalamic CRH expression. (*A*) Illustrations of brain regions used for semiquantitative analysis of the expression of corticotropin-releasing hormone (CRH) mRNA with regions used for analysis highlighted in red. Ipsilateral to the illustration region are overlaid example images from *in situ* hybridization histochemistry of CRH mRNA. Rostrocaudal locations, expressed in millimeters from bregma are listed below each image, according to a stereotaxic atlas of the rat brain (Paxinos & Watson, 2007). (*B*) CRH mRNA expression in each region as measured by mean grey value x area within the area of each specified brain region. Bars represent means of each group, error bars represent + SEM. Comparisons were first made between control animals and all stress-terbutaline animals regardless of treatment. Dotted lines on each graph separate control animals from stress-terbutaline animals included in the 2 x 2 analysis. Stress-terbutaline groups are subdivided by treatment (vehicle or *M. vaccae*) and whether animals were undergoing epileptogenesis (non-SRS or SRS). 2 x 2 comparisons were made between vehicle-treated stress-terbutaline animals that remained seizure-free (ST + vehicle + Non-SRS; $n = 9$, light grey), vehicle-treated stress-terbutaline animals undergoing epileptogenesis (ST + vehicle + SRS; $n = 3$, dark grey), *M. vaccae*-treated stress-terbutaline animals that remained seizure free (ST+ *M. vaccae* + Non-SRS*;* $n = 8$, blue), and *M. vaccae*-treated stress-terbutaline animals undergoing epileptogenesis (ST+ *M. vaccae* + SRS*;* $n = 4$, purple). $^{*}P < .05$, $^{n.s.}P > .05$. Abbreviations: CeA, central nucleus of the amygdala; CRH, corticotropin-releasing hormone; CTRL, control; dBNST, dorsal bed nucleus of the stria terminals; PVN, paraventricular nucleus of the hypothalamus; *M. vaccae*, *Mycobacterium vaccae*; SEM, standard error of the mean; SRS; spontaneous recurrent seizures; ST, stress-terbutaline.

The effectiveness of *M. vaccae* in reducing ASD-like behavior without affecting epileptogenesis raised the question as to whether any behavior would be comorbid with epilepsy within this model. Because *M. vaccae* immunization did not influence epileptogenesis within ST animals or ST-induced changes in BNST and CeA CRH expression, and these brain regions are integral for fear and anxiety behavior, we tested whether a behavioral task involving these regions would be closely associated with epileptogenesis within this model. To explore the potential association with epileptogenesis, animals were tested using a defensive burying task (De Boer & Koolhaas, 2003) in conjunction with ASD core symptoms at P60, prior to the development of spontaneous seizures. This allowed us to assess ST animals without the potential confounding effect of seizures on anxiety-related defensive behavioral responses (Chen, Wang, Liang, & Shaw, 2016). We were not able to identify any statistically significant group difference in defensive burying behavior ($F_{(2,28)}$ = 1.137, p = .335) when comparing vehicle- and *M. vaccae*-treated ST rats to control animals (**Fig. 4.7A**). However, there appeared to be a bimodal distribution in task performance within ST animals contributing to significant variability in our data (**Fig. 4.7A**: red box). Later analysis after the development of seizures, separating animals by vehicle/*M. vaccae* treatment and epileptogenesis, revealed a significant main effect of epileptogenesis on burying behavior ($F_{(1,20)}$ = 11.227, p < .01) (**Fig. 4.8A**). 6/7 animals undergoing epileptogenesis, ***prior to the development of spontaneous seizures***, failed to engage in any defensive burying behavior at all. Post hoc tests revealed that *M. vaccae*-treated animals that would remain seizure-free engaged in significantly more proactive burying behavior than *M. vaccae*-treated animals destined to develop spontaneous seizures or other animals exposed to developmental stress + terbutaline (**Fig 4.8A**; blue). This suggested that stress-reactivity, and not core features of ASD, represents the major behavioral risk factor comorbid with epilepsy within this model.

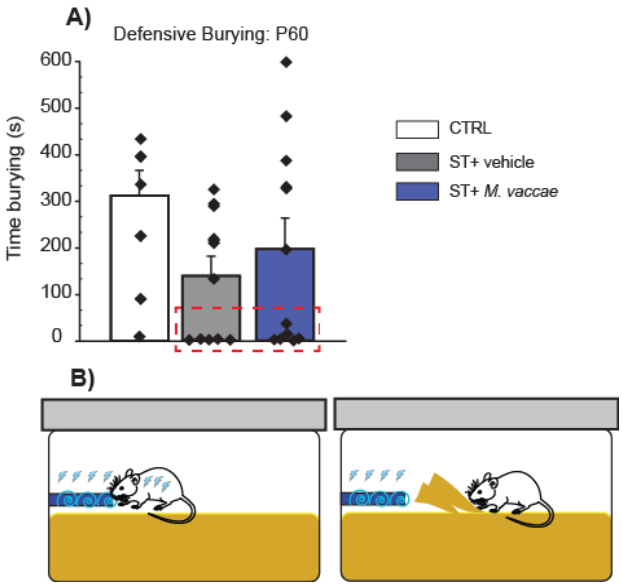

Figure 4.7: Stress terbutaline animals have variable stress-coping styles regardless of *M. vaccae* immunization. (*A*) Proactive coping behavior, measured by time spent burying during the defensive burying task at P60, prior to the development of spontaneous seizures. Animals within the red box failed to engage in any burying behavior. (*B*) illustration of the defensive burying procedure demonstrating proactive coping behavior to an electrified probe. Bars represent means of each group, error bars represent + SEM, individual data points are plotted as diamonds. Comparisons were made between untreated control (CTRL; $n = 8$, white), vehicle-treated stress-terbutaline (ST + vehicle; $n = 12$, grey), and *M. vaccae*-treated stress-terbutaline (ST + *M. vaccae;* $n = 12$, blue) groups. $^{n.s.}$ $P > .05$. Abbreviations: CTRL, control; *M. vaccae*, *Mycobacterium vaccae*; P60, postnatal day 60; SEM, standard error of the mean; ST, stress-terbutaline.

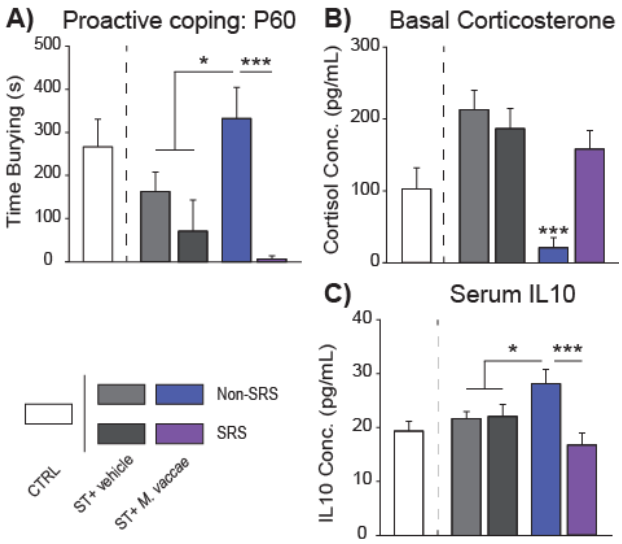

Figure 4.8: *M. vaccae*-immunized, stress-terbutaline animals without behavioral and epileptic comorbidities display a stress-protected phenotype. (*A*) Proactive coping behavior, measured by time spent burying during the defensive burying task at P60, prior to the development of spontaneous seizures. 1/7 (14.3%) rats that would develop epilepsy engaged in proactive burying behavior while 13/17 (76.5%) rats that would not develop epilepsy engaged in proactive burying behavior. (*B*) Basal fecal corticosterone concentrations assessed at P225. (*C*) Serum IL-10 concentrations assessed at P240. Dotted lines on each graph separate control animals from stress-terbutaline animals included in the 2 x 2 analysis. Stress-terbutaline groups are subdivided by treatment (vehicle or *M. vaccae*) and whether animals were undergoing epileptogenesis (non-SRS or SRS). Bars represent means of each group, error bars represent + SEM. Comparisons were made between vehicle-treated stress-terbutaline animals that remained seizure-free (ST + vehicle + Non-SRS; n = 9, light grey), vehicle-treated stress-terbutaline animals undergoing epileptogenesis (ST + vehicle + SRS; n = 3, dark grey), *M. vaccae*-treated stress-terbutaline animals that remained seizure-free (ST + *M. vaccae* + Non-SRS*; n* = 8, blue), and *M. vaccae*-treated stress-terbutaline animals undergoing epileptogenesis (ST+ *M. vaccae* + SRS*; n* = 4, purple). *P < .05, ***P < .001. Abbreviations: CTRL, control; IL-10; interleukin-10; *M. vaccae*, *Mycobacterium vaccae*; P60, postnatal day 60; SEM, standard error of the mean; SRS, spontaneous recurrent seizures; ST, stress-terbutaline.

Despite the lack of evidence for PVN CRH expression mediated changes in HPA axis reactivity, this did not rule out the possibility of chronic HPA-axis dysfunction within ST animals. Previous research has demonstrated long-term changes in basal levels of the stress hormone cortisol in people with epilepsy and autistic children (Mehta, Dham, Lazar, Narayanswamy, & Prasad, 1994; Nir et al., 1995). To test basal glucocorticoid levels (i.e., corticosterone in mice), we measured a peripheral snapshot via fecal concentration. Significant group differences were observed in the level of basal corticosterone ($F_{(2,28)} = 8.552$, $p < .01$). Analysis revealed that vehicle-treated ST animals had elevated levels (208.88 ± 22.91 pg/mL) compared to controls (103.20 ±29.23 pg/mL; $p < .05$) or *M. vaccae*-treated ST animals (78.46 ± 24.06 pg/mL; $p < .001$). No differences were observed between controls and *M. vaccae*-treated ST animals. However, because seizures may influence basal corticosterone secretion, even during the inter-ictal period (Maguire & Salpekar, 2013), we further subdivided animals based on epileptogenesis, revealing a significant interaction between treatment and spontaneous seizures within ST animals ($F_{(1,20)} = 6.322$, $p < .05$). ST animals treated with *M. vaccae* that did not develop seizures had lower circulating corticosterone levels compared to other animals within the stress-terbutaline group (**Fig. 4.8B**; blue; $p < .001$). Basal corticosterone levels were significantly correlated with burying behavior in all animals ($n = 31$; $r = -.386$; $p < .05$) suggesting that lower basal corticosterone is reflective of a stress-protected phenotype.

Serum Cytokine Profile

Because chronic peripheral inflammation has been identified in people with ASD and is associated with spontaneous seizures and could lead to dysregulation of the HPA axis (Aronica & Crino, 2011; Depino, 2013; Dinan et al., 2006), we tested the circulating inflammatory profile of ST animals. No differences were observed in the levels of cytokines IL1b, IL-2, or IL-6 (**Fig. 4.9**). However, 2-way ANOVA revealed a significant main effect of epileptogenesis ($F_{(1,21)} = 5.744$, $p < .05$) and an interaction between treatment and epileptogenesis on serum levels of the anti-inflammatory cytokine IL-10 ($F_{(1,21)} = 6.592$, $p < .05$) (**Fig. 4.8C**). Post hoc tests revealed that serum

IL10 concentration was significantly lower in ST+ *M. vaccae* animals that develop spontaneous seizures (Mean difference= -11.4203, SE = 3.058, $p < .001$) and seizure-free ST+ vehicle animals (MD = 6.467, SE = 2.574, $p < .05$) compared to ST+ *M. vaccae* animals without an epileptic phenotype. Surprisingly, peripheral inflammatory cytokine differences were not apparent between seizing and non-seizing animals (**Fig. 4.9**). These data suggest a role for the peripheral anti-inflammatory cytokine IL-10 in the long-term protection of ST animals from an epileptic and behavioral phenotype consistent with stress-responsive and epilepsy comorbidity.

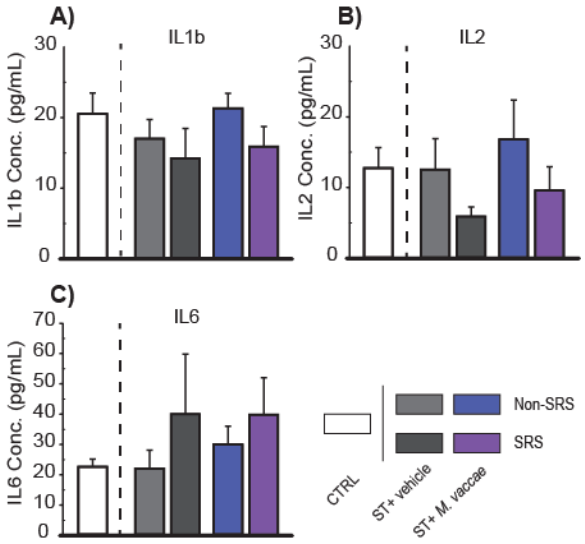

Figure 4.9: Long-term circulating cytokine profiles are not affected by stress-terbutaline, epileptogenesis, or influenced by *M. vaccae* immunization**.** At PN180, at least >24hrs after seizure, animals were euthanized and blood was collected for analysis of circulating inflammatory markers. (*A*-*C*) serum levels of cytokines IL-1b (*A*), IL-2 (*B*), and IL-6 (*C*) expressed in picograms per milliliter (pg/mL). Dotted lines on each graph separate control animals from stress-terbutaline animals included in the 2 x 2 analysis. Stress-terbutaline groups are subdivided by treatment (vehicle or *M. vaccae*) and whether animals were undergoing epileptogenesis (non-SRS or SRS). Bars represent means of each group, error bars represent + SEM. 2 x 2 comparisons were made between vehicle-treated stress-terbutaline animals that remained seizure free (ST + vehicle + Non-SRS; *n* = 9, light grey), vehicle-treated stress-terbutaline animals undergoing epileptogenesis (ST + vehicle + SRS; *n* = 3, dark grey), *M. vaccae*-treated stress-terbutaline animals that remained seizure free (ST+ *M. vaccae* + Non-SRS*; n* = 8, blue), and *M. vaccae*-treated stress-terbutaline animals undergoing epileptogenesis (ST + *M. vaccae* + SRS*; n* = 4, purple). Abbreviations: CTRL, control; IL1b, interleukin 1 beta; IL2, interleukin 2; IL6, interleukin 6; SEM, standard error of the mean; SRS; spontaneous recurrent seizures; ST, stress-terbutaline.

Discussion

Divergence of core-symptoms and epileptogenesis

Repeated immunizations with heat-killed *M. vaccae* prevented the expression of core ASD-like behavior in ST rats. However, ASD-like behaviors within ST rats are entirely separable from epileptogenesis. Vehicle-treated ST rats displayed a consistent ASD-like severity across time, regardless of EEG abnormalities (**Fig. 4.4**). Within *M. vaccae*-treated animals, SRS emerged despite the alleviation of ASD-like behavior (**Fig. 4.4**). In a previous ST study, combining stress and terbutaline was necessary for epileptogenesis, but this mixture did not enhance ASD-like behavioral severity (Bercum et al., 2015). This reflects research using idiopathic ASD-like (BTBR) mice exposed to post-natal lipopolysaccharide (LPS), where mice develop SRS, but LPS did not enhance ASD behaviors (Lewis, Kesler, Candy, Rho, & Pittman, 2018). With the exception of rare conditions (Deonna, 1991), there is minimal evidence that epilepsy is a causative factor in ASD development (Deonna & Roulet, 2006). Within ASD animal models, seizure induction can increase social behavior (Washington et al., 2015) and anti-epileptic drugs rarely improve ASD symptoms (Hirota, Veenstra-VanderWeele, Hollander, & Kishi, 2014). Seizures may influence the development of ASD by driving pathological synaptic plasticity (Brooks-Kayal, 2010), as rats with early-life seizures show long-term changes in brain-connectivity, sociability, and seizure thresholds (Holmes et al., 2015). However, we found no evidence that the expression of ASD-like behaviors resulted from seizure-induced pathology. Therefore, we propose that despite shared environmental risk factors, the expression of ASD-like behavior and the development of SRS are not bidirectionally causative.

Stress-Terbutaline as a model of allostatic overload

Critical to our understanding of stress is the repeated “wear and tear” of multiple adaptive responses causing “allostatic overload” (McEwen, 1998). This process is believed to be instrumental in the development and expression of ASD (McEwen, 2016; Picci & Scherf, 2015; Singletary, 2015). A unique feature of the ST model is the presence of multiple prolonged

environmental insults. While this adds difficulty in isolating specific causative factors, we propose that this approach is a more etiologically relevant method for understanding developmental disorders with multiple interacting mechanisms, such as ASD and epilepsy. In practice, terbutaline is combined with the synthetic glucocorticoid dexamethasone during tocolysis (Haas, Benjamin, Sawyer, & Quinney, 2014), a combination that is synergistically neurotoxic and glial modulatory in-vitro (Slotkin et al., 2018). Glucocorticoids alone can "prime" microglia to respond to subsequent inflammatory responses (Frank, Hershman, Weber, Watkins, & Maier, 2014), an effect that might influence susceptibility to a "second hit" like terbutaline. Within this framework, multiple stressors and terbutaline reflect the additive allostatic inducers facilitating ASD and epileptogenesis.

ST-induced microglial expansion during critical developmental periods

These data support a critical role for the dysregulation of microglia during development in ST-induced pathology. Converging evidence implicates inflammatory processes as contributing factor toward ASD (Meltzer & Van de Water, 2017) and epilepsy (Vezzani, Friedman, & Dingledine, 2013). Microglia sit at a communicative junction between the periphery and CNS (Riazi et al., 2008) and facilitate the deleterious effects of environmental stressors throughout development (Bilbo, Block, Bolton, Hanamsagar, & Tran, 2018; Hanamsagar & Bilbo, 2017; Paolicelli & Ferretti, 2017). In addition to directly effecting excitability through the release of inflammatory mediators (Devinsky, Vezzani, Najjar, De Lanerolle, & Rogawski, 2013; Ferrini & De Koninck, 2013), microglia also play a diverse role in neurodevelopment by effecting synaptogenesis, myelination, and synaptic pruning (Paolicelli et al., 2011; Schafer & Stevens, 2015; Sominsky, De Luca, & Spencer, 2018). Genetic modifications in microglial mediated synaptic pruning can cause ASD-behavior (Kim et al., 2017) and several microglia-targeted interventions have proven successful in rodents and humans at ameliorating social deficits (Kim, Hong, & Bae, 2018). In line with this study, previous reports have observed terbutaline-induced microglial density increases consistent with a neuroinflammatory phenotype (Zerrate et al., 2007),

believed to be the mechanism driving synaptic and structural changes observed after terbutaline treatment (Rhodes et al., 2004; Slotkin et al., 1989; Zerrate et al., 2007) and arising due to noradrenergic signaling disruption (Sanders, Happe, Bylund, & Murrin, 2011; Slotkin et al., 2001; Slotkin & Seidler, 2006, 2013) influencing microglial control mechanisms (Fujita, Tanaka, Maeda, & Sakanaka, 1998; Gyoneva & Traynelis, 2013). Within developmental stress models, acute expansion in density within the first two postnatal weeks (Delpech et al., 2016), or prolonged functional changes have repeatedly been observed (reviewed in; Johnson & Kaffman, 2018; Roque, Ochoa-Zarzosa, & Torner, 2016). Previous reports have demonstrated that *M. vaccae* acts in part by preventing stress-induced microglial priming via an IL-4 dependent mechanism (Frank et al., 2018). Our data demonstrated that pups of *M. vaccae*-treated mothers had increased expression of whole-brain IL-4 during exposure to a "second hit", which may be contributing to a protective mechanism. If dysfunctional microglia are involved in the effects of stress-terbutaline (Zerrate et al., 2007), it is necessary to address the actual function of microglia in future studies using in-vitro stimulation paradigms that may identify a primed or activated state (Frank, Wieseler-Frank, Watkins, & Maier, 2006). However, due to the necessity for functional microglia in neurodevelopmental processes (Paolicelli et al., 2011; Paolicelli & Ferretti, 2017; Wu, Dissing-Olesen, MacVicar, & Stevens, 2015) and prior work demonstrating a stress protected microglial phenotype following *M. vaccae* (Fonken et al., 2018; Frank et al., 2018), our data supports that targeting microglia-associated neuroinflammation may be a beneficial ASD prevention strategy.

Region specific alterations in microglial density

The regional specificity of ST-induced microglial increases and the protective effects of *M. vaccae* (**Fig. 4.5**) highlight candidate brain structures involved in the behavioral and epileptogenic effects observed in this study. Specifically, *M. vaccae* treated rats do not show density increases in the insular cortex but do in the molecular layer of the dentate gyrus. The insular cortex, fundamental for salience processing (Uddin, 2015) and the integration of sensory (Rodgers, Benison, Klein, &

Barth, 2008) and interoceptive information (Craig, 2002), is heavily implicated in ASD (Uddin & Menon, 2009). Multiple animal models of ASD demonstrate inhibitory network maturation deficits during critical periods and improper sensory integration within the insula (Gogolla, Takesian, Feng, Fagiolini, & Hensch, 2014). Alternatively, the dentate gyrus is a critical node within epileptic circuitry (Buckmaster & Dudek, 1997; Lothman et al., 1992). The cytoarchitecture of this region contains multiple interacting inhibitory systems (Amaral, Scharfman, & Lavenex, 2007; Scharfman, 2007, 2016) that have disrupted synaptic efficacy in rodent seizure models (Calcagnotto, Paredes, Tihan, Barbaro, & Baraban, 2005; W. Zhang & Buckmaster, 2009). Further exploration of the functional consequences of increased microglial proliferation within these regions are necessary. However, the early expansion within ST animals, and subsequent mitigation with *M. vaccae* suggests that the insular cortex is involved in the expression of ASD-like behaviors within this model. Additionally, elevated levels during development may contribute to epilepsy promoting inhibitory synaptic dysfunction in the dentate gyrus.

Cytokine separation of ASD and epilepsy

Our data supports that shared environmental risk factors for ASD/epilepsy might be operating under differential mechanisms. This concept has previously been shown using other inflammatory driven models of ASD. Maternal immune activation (MIA) can enhance epileptogenesis triggered via hippocampal kindling (Pineda et al., 2013). However, it appears that this is reliant on the combination of maternal cytokines IL-6 and IL-1b, as neither alone is sufficient to enhance epileptogenesis (Washington et al., 2015). Alternatively, the ASD-assosciated effects of MIA is dependent solely on maternal IL6 (Hsiao & Patterson, 2011; Smith, Li, Garbett, Mirnics, & Patterson, 2007), sitmulating RORγt-expressing T cells (including Th17) to release IL-17a (Choi et al., 2016). Blocking Th17 cells prevents MIA-induced ASD-like behavior in offspring (Choi et al., 2016). Due to *M. vaccae's* ability to enhance IL-10 producing regulatory T cells (Reber et al., 2016), this could balance the expansion of IL-17a producing cells without directly preventing

maternal stress induced elevations in IL-6 and IL-1b levels, limiting the ASD-promoting effects of developmental stress while failing to regulate epilepsy enhancing inflammatory components.

CRH expression

Stress is a multimodal phenomenon, encompassing several reciprocally interacting factors (McEwen, 1998). Developmental stressors can alter the function of the HPA axis, reflected by long-term increases in the expression of CRH (Charil, Laplante, Vaillancourt, & King, 2010; Entringer, Kumsta, Hellhammer, Wadhwa, & Wüst, 2009; van Bodegom et al., 2017). Our data demonstrate that *M. vaccae*-induced modulation of centrally mediated changes in CRH expression is not required to avoid an ASD-like phenotype. Previous work using *M. vaccae* has demonstrated that repeated treatment does not prevent stress-induced glucocorticoid release (Frank et al., 2018; Reber et al., 2016). Additionally, an alternative regulatory microbe treatment, *Bifidobacterium infantis,* can rescue behavioral and cytokine profiles, but not CRH expression in the amygdala following maternal-separation stress (Desbonnet et al., 2010). Additionally, a recent study successfully reducing ASD-like behavior within multiple animal models using *Lactobacillus reuteri*, has shown that this microbial intervention acts directly via vagal nerve afferents targeting the PVN (Sgritta et al., 2018). While this illustrates the limitations of microbial based therapies during development, it also demonstrates the lack of necessity for CRH normalization in the prevention of ASD-like behavior in animal models.

An unexpected result of this experiment was the observation that ST decreases CRH expression in extrahypothalamic brain regions. CRH is an excitatory neuropeptide able to directly promote seizures (Gunn et al., 2017; Hollrigel et al., 1998). Previous work utilizing maternal-separation stress resulted in long-term epilepsy-promoting increases in CRH expression levels within the CeA (Dubé et al., 2015). Despite the observed average levels of CRH expression in the CeA among seizing animals (7.3 ± 1.1) and seizure free animals (5.2 ± .5) within the ST group (**Fig. 4.6B**), this difference was not statistically significant ($F_{(1,12)}$ = 4.16, p =.064). Additionally, it appears that combining stress and terbutaline results in a unique CRH expression profile. This

may be a result of interacting factors between endocrine and autonomic systems, such as alterations in GR receptor function (Schmidt, Holsboer, & Spengler, 2001; Ulrich-Lai & Herman, 2009). While we found no evidence of increases in CRH expression in the PVN, ST decreased CRH expression in extrahypothalamic regions and increased basal corticosterone circulation, indicative of neuroendocrine disruption. Significant analysis of stress-induced corticosterone release, adrenal hypertrophy, or measurements of GR or MR expression might highlight additional endocrine disruptions that occur due to ST.

Stress coping in ST and epileptogenesis

Stress-coping behavior is inherently linked to epileptogenesis, prior to the development of seizures, within ST rats. Reactive vs active stress coping strategies have been identified as a risk factor for vulnerability to the development of affective disorders like anxiety and depression (Wood, Walker, Valentino, & Bhatnagar, 2010). This is of particular interest due to the presence of atypical emotional regulation in human ASD (Mazefsky et al., 2013), the disproportionate rates of affective disorders within epilepsy (Beyenburg, Mitchell, Schmidt, Elger, & Reuber, 2005; Ekinci, Titus, Rodopman, Berkem, & Trevathan, 2009; Kanner, 2008), and the presence of anxiety–like behavior in animal models of both ASD (Banerjee et al., 2014; Crawley, 2012; Kazdoba, Leach, & Crawley, 2016) and epilepsy (Chen et al., 2016; Kalynchuk, 2000; Umpierre et al., 2014). However, within epilepsy, it is unknown whether affective disorders are a direct result of seizures. Our data suggests stress-coping should be explored as a potential behavioral biomarker indicative of underlying epileptogenic mechanisms.

Previous reports utilizing repeated immunizations of *M. vaccae* have used proactive coping behavior as an indication of stress resilience and effective treatment (Reber et al., 2016). Unlike the anxiolytic effects of *M. vaccae*, this effect occurs independent of the peripheral actions of *M. vaccae* (Reber et al., 2016). Because a subset of ST animals treated with *M. vaccae* failed to engage in proactive coping behavior, it is possible that CNS mediated actions of immunization were less effective in these animals, and further treatment may be required to ameliorate SRS.

This is apparent in the variability of microglial density within the dentate gyrus at P15 in ST+ *M. vaccae* rats (**Fig. 4.5F**) and the bimodal distribution of defensive burying behavior (**Fig. 4.7A**), reflecting the development of SRS (**Fig. 4.8**) Protective effects of heat-killed *M. vaccae* on allergic airway inflammation have been demonstrated for up to 12 weeks (Zuany-Amorim et al., 2002), however this extended anti-inflammatory phenotype may not be adequately translated into a CNS mediated immunophenotype, where *M. vaccae* effects have been shown for 7 days (Frank et al., 2018). Seizures within this model do not begin to appear until after 3 months, and epileptogenesis is a continuous process, extending past the first spontaneous seizure (Maguire, 2016; Pitkänen et al., 2015; Smith et al., 2018; Williams et al., 2009). If underlying CNS inflammatory epileptogenic processes triggered by ST require maturation, extended administrations of *M. vaccae* might be necessary to prevent SRS. Neuroinflammation has an established role in epileptogenesis (Vezzani et al., 2013), providing support for the development of anti-inflammatory interventions (Vezzani, 2015) that may need to be administered long-term. This research highlights the ineffectiveness of acute anti-inflammatory microbe interventions given during epileptogenic insults, providing a rationale for prolonged treatment strategies that encompass the entire duration of epileptogenesis.

Anti-inflammatory microbe intervention and ASD

The propensity for microbial-based therapies to alleviate ASD-like behavior has been demonstrated in several animal models (Buffington et al., 2016; Hsiao et al., 2013; Sgritta et al., 2018). These data support the emerging role for microbe-immune interactions in neurodevelopmental disorders like ASD and also inspire therapeutic possibilities. *M. vaccae* has proven successful in immunizing against the inflammatory effects of chronic stress both peripherally (Reber et al., 2016) and centrally (Frank et al., 2018), a prospect made more promising by recent results indicating the safety of heat-killed *M. vaccae* immunotherapy in human trials (Gröschel, Prabowo, Cardona, Stanford, & Werf, 2014). However, like previous microbial-based ASD interventions, the exploration of multi-model studies must be pursued to demonstrate

translatability throughout multiple ASD-promoting factors (genetic, environmental, idiopathic) (Sgritta et al., 2018). Additionally, while this experiment demonstrated the efficacy of repeated immunizations across development, determining the necessity for both pre- and post-natal injections is paramount for deconstructing the time course of ASD-promoting factors within this rat model, possibly reducing the need for repeated intervention. However, the current data suggests it may be possible to immunize against ASD when stress and inflammatory components are a precipitating factor.

Chapter 5:

General Discussion and future experiments

The experiments presented within this dissertation began with a desire to transform epileptogenesis away from an all-or-nothing seizure phenomenon and towards a continuous variable. To this end, the initial work presented in chapter 2 focused on active measures of a silent epileptogenesis within the latent period. Our inclination was that a probable biomarker would surpass 24/7 video/EEG in predictive validity, unlocking hidden aspects of epileptogenesis. By combining a continuous measure with advanced pattern recognition techniques, we predicted the development of epilepsy days before the first spontaneous seizure in pilocarpine rats. An integral finding within this study was that hAEP waveforms adopt an “epileptic” characteristic prior to the development of SRS. This raises the question about the nature of defining epilepsy that requires further discussion. If epileptogenesis is the process by which a brain becomes “epileptic”, then is there a unifying transition point that can be diagnosed without the presentation of spontaneous seizures? Clinical diagnosis requires 2 or more discrete seizure events, but our results suggest that a brain can be considered epileptic long before then. Our hAEP data suggests that a time point exists after an insult, measured by hippocampal responsiveness, where epileptogenesis has progressed sufficiently to classify an animal as epileptic before spontaneous seizures emerge. In some animals, this classification occurred weeks before the first SRS (**Fig. 2.6**). If the process of epileptogenesis increases the propensity to develop spontaneous seizures, but the presentation of a seizure requires multiple interacting factors, then these results suggest that a brain can be “epileptic” before a clinical manifestation of the defining characteristic of epilepsy; the spontaneous seizure.

Perhaps more valuable from the hAEP was the identification of a “normal” response via a return to baseline in animals that failed to develop spontaneous seizures. Animals experienced a prolonged “early” period, with a multi-day modification of hippocampal responsiveness induced via SE followed by a transitional period of responsiveness during the first week. All animals experienced similar SE durations and had resurgences in SE with early seizures. Within our results, there were no predictive early indicators in animals recovering from SE that somehow the

“insult” was less severe. Then why did these animals not develop SRS? Our focus, reflecting the priorities of epilepsy research, had been on predicting epileptogenesis and seizure risk. However, the animal model is designed to produce rapid epileptogenesis. The surprising result is not when it is successful, but when animals spontaneously recover. Perhaps it would be a better to determine when epileptogenesis is not occurring, utilizing a return to baseline following injury as a “safety” signal, in future studies. Predicting the lack of epileptogenesis and the removal of seizure risk may be a more parsimonious observation, serving both as a predictive and treatment outcome measure. Rarely do studies involving epileptogenesis focus on animals where epilepsy did not progress, and with a tool that can delineate between animals who are at risk for seizure from those that definitively will not could serve to facilitate the discovery of underlying processes surrounding epileptogenesis prior to the development of spontaneous seizures. While this tool needs further validation, long-term SE-induced non-seizure changes within pilocarpine rats appear to be measurable and have predictive value.

In chapter 3, we outlined fundamental characteristics of epileptogenesis within the pilocarpine model. The main result was the identification of bona-fide nonconvulsive seizures, manifesting after a latent period, that were in no way related to the presence of SWDs/EEEs. These seizures reflected electrographic characteristics clinically associated with partial seizures seen in humans. It is our hope that with foundational objective characteristics of seizures: duration, acute shifts in frequency components, and the presence of post-ictal suppression that further research may be able to focus on the identification and prevention of actual seizures. Despite research demonstrating the presence of SWDs/EEEs in control animals and various genetic lines of animals, the characteristics of partial seizures within animal models is a highly debated topic within the field of epilepsy (D’Ambrosio & Miller, 2010; Dudek & Bertram, 2010).

Despite the success of the hAEP experiment, our attempts to relegate 24/7 video/EEG to a realm of tools necessary only for the validation of better measures was premature. It became apparent that continuous monitoring of animals could provide tremendous value, especially within

a field wrought with uncertainty about fundamental properties of seizures and epileptogenesis. First, on average, the hAEP was slightly better at predicting epileptogenesis compared to the passive measure of epileptiform spikes. Upon further examination in chapter 3, epileptiform spikes began to appear exactly at the halfway point between the end of the injury and SRS within pilocarpine animals suggesting that the presence of ES has significant predictive value. Upon reaching a stable dysfunctional hAEP signal during the latent period, hippocampal responsiveness did not radically adjust in a manner reflective of the increased seizure frequency during progressive epileptogenesis. Meanwhile, ES appeared to peak around the presentation of seizures and increased as epileptogenesis progressed. These studies highlight the value of 24/7 Video EEG for seizures and epilepsy-associated activity identification, supporting the implementation of chronic monitoring techniques in patients at risk for the development of spontaneous seizures. With the use of automatic detection techniques derived during these studies, reducing the time demand for signal analysis, 24/7 ambulatory EEG could be a viable option for a larger population of people with epilepsy.

A surprising, and until recently unpublished, finding was the recurrence of acute seizures and SE following anticonvulsant termination within pilocarpine animals (**Fig 2.1; Fig 3.1**). Various methodological reports outlining chemoconvulsant procedures hailed the rapid termination of SE using anti-convulsants at specified time-points as a strength of experimental controllability and replicability (Curia et al., 2008). Many studies still use an established 60-minute post-SE anti-convulsant procedure as the proposed “end of insult” timepoint (Kim & Cho, 2018; Lemos & Cavalheiro, 1995; Reddy & Kuruba, 2013; Zhang, Todorovic, Williamson, & Kapur, 2017). A singular study identified this recurrence as a possible bias in identifying the duration of SE associated insults and targeted effective polypharmacy termination to prevent recurrence (Brandt, Töllner, Klee, Bröer, & Löscher, 2015). However, even within this study, acute recording procedures limited to the first 24hrs following pilocarpine were used to determine complete suppression of seizures. However, this may be inadequate to identify complete remission leading

into the latent period, as our results suggest that SE recurrence can continue for multiple days (**Fig 2.1**). While this may lead to false interpretations of the duration of the initial insult and the start of a latent period, this is of significant concern when applied to the notion of “immediate epileptogenesis”. Within the kainaite model, research identifying the presence of spontaneous seizures within the first 72 hours have described these seizures in the framework of “immediate epileptogenesis” (Puttachary et al., 2015), when these events may still be part of the initial SE. Stringent identification of the duration of “insult” needs to be addressed within future studies attempting to delineate between acute insult related seizure and spontaneous seizures indicative of epileptogenesis.

In chapter 4, we applied passive EEG monitoring tools in conjunction with behavioral measures to assess epileptogenesis in the stress-terbutaline model of comorbid ASD and epilepsy. A major question driving this experiment was the assessment of the relationship between ASD-like behavior and epileptogenesis. Utilizing comorbid animal models can provide insight into where these disorders converge, but more importantly, highlight where they do not. The significant comorbidity between the two disorders have led some research to hypothesize that the risk of developing seizures is an integral part of ASD pathology and both are manifestations of the same pathological condition (Jeste & Tuchman, 2015). Our results suggest that epilepsy and ASD have shared risk factors, but their expression is not succinctly linked. If ASD and epilepsy were part of the same disorder, one would expect anti-epileptic drugs to be an effective intervention strategy to mitigate the behavioral symptoms of ASD. However, traditional AEDs targeting neuronal excitability to control seizures have shown minimal success in preventing ASD behavioral symptoms (Hirota et al., 2014).

Our results found that it is possible to separate the expression of these disorders but does not rule out that they can be targeted together. Some evidence suggests that surgical interventions aimed at removing the seizure focus can be positively beneficial in the treatment of ASD associated social deficits in children (Neville et al., 1997). Additionally, early surgical

intervention is associated with better neurocognitive outcomes in children with temporal lobe epilepsy (Lee et al., 2015). Alternative treatment options such as the adoption of a ketogenic diet (Ni et al., 2016) and vagal nerve stimulation (Engineer, Hays, & Kilgard, 2017) have been shown to be effective at treating both ASD and seizures in children with combined symptoms. Additionally, the anti-epileptic and anti-ASD effects of the ketogenic diet require a functional microbiome (Newell et al., 2016; Olson et al., 2018), suggesting that peripheral to brain communicative mechanisms can have a valuable role in epilepsy and ASD. It is possible, the separation of ASD like behaviors and epileptogenesis could be a result of our treatment masking the expression of ASD-like behavior and that underlying mechanisms the would contribute to an observed comorbidity are still present and not behaviorally expressed. However, the nature of ASD/Epilepsy comorbidity remains complicated and future studies using novel inflammation-based ASD/epilepsy comorbidity could serve to further disentangle the two disorders.

Microglia expansion in ST

A critical correlational finding within chapter 4, was the presence of microglial expansion within early periods within ST animals and subsequent mitigation by *M. vaccae* immunization. It is likely that stress and terbutaline both contribute to this increase. Maternal and early life stress (ELS) can lead to the dysregulation of microglia during development. Recent research has shown that ELS induced in a manner similar this study resulted in increases in microglial density in the hippocampus of 14-day old mice (Delpech et al., 2016). Previous studies have demonstrated the dysregulation of microglia via early administration of terbutaline (Zerrate et al., 2007). Like this current study, increases in microglial density were no longer seen in 28-day old mice. However, transcriptome analysis revealed long-term changes indicative of immune sensitization. While increases in microglial density are not always observed in maternal or ELS animal models, morphological changes and proinflammatory phenotypes have been demonstrated in several studies reviewed in (Roque et al., 2016). Within the MIA model of ASD, contradictory findings in microglial density changes are rampant, highlighting the need for model-specific assessments

and rigorous analysis of environmentally induced microglial disfunction with respect to ASD (Smolders, Notter, Smolders, Rigo, & Brône, 2018). This does challenge the necessity for microglial expansion for detriments in neurodevelopment. Because microglia are necessary for synapse development (Wu et al., 2015) and actively involved in the sculpting of inhibitory networks (Um, 2017), dysfunctional microglia could disrupt the excitation inhibition (E/I) balance in ST rats, promoting behavioral and epileptic outcomes. However, It is difficult to conclude a specific pathological effect of microglial density changes, and due to the limitations of this study, address whether a lack of density increase is reflective of a normal immunophenotype. However, further studies using in-vitro stimulation paradigms with isolated microglia are warranted with respect to stress terbutaline. Analyzing whether microglia exist in a chronic primed state in future studies should be addressed.

The existence of a latent period

Concern has been raised recently over the existence of a latent period (Löscher, Hirsch, & Schmidt, 2015), combining evidence from immediate changes in network excitability (Sloviter, Bumanglag, Schwarcz, & Frotscher, 2012), with the presence of EEEs seen in TBI models (D'Ambrosio et al., 2009). Some researchers argue that the notion of delayed epileptogenesis does not exist (Sloviter & Bumanglag, 2013). This line of research has pushed for the targeting of excitability prevention for anti-epileptogenesis, using kindling a primary mechanism for "epileptic maturation", instead of secondary mechanisms such as neuroinflammation or circuit remodeling for progressive epileptogenesis. In line with the concept of immediate epileptogenesis, these data demonstrated instant and lasting changes in the hAEP response, even using a conservative estimate of 72hrs for the initial injury (**Fig 2.6**). Additionally, most animals demonstrated a recurrence of SE, or the presence of acute seizures during the first 72 hours. However not all animals demonstrating acute seizures, or this acute shift in response went on the develop progressive increases in SRS. Additionally, in chapter 4, we demonstrated that ST animals

develop spontaneous seizures after a significant delay, suggesting that slow processes contributing to the development of SRS are occurring within these animals. A recent study using interneuron abalation in the hippocampal CA1 region demonstrated acute spontaneous seizures for multiple days, but not the development of SRS, arguing the necessity for underlying secondary mechanisms (Spampanato & Dudek, 2017). The definitive identification of a latent period with delayed secondary mechanisms is crucial for determining the possibility of “anti-epileptogenic” treatments. Our results suggest that a latent period, where epileptogenesis has not yet occurred and disease modifying interventions are possible, does exist.

Direct hAEP

A benefit of utilizing auditory signals for tracking hippocampal responses is the ability for non-invasive stimulation that may be adequately translated for clinical effectiveness. However, the hippocampus is not usually associated with auditory responses. Auditory signals enter the hippocampus through the perforant path, via the entorhinal cortex. This pathway, through the “dentate gate” is heavily implemented in the expression of spontaneous seizures (Heinemann et al., 1992; Sloviter et al., 2012). While this would be an ideal measure of epileptic excitability, directly targeting hippocampal inputs might provide a better tool for exploring hippocampal responsiveness.

One technique would be to use a targeted circuit approach to explore hippocampal responses in-vivo during epileptogenesis. Excitatory fibers originating from the entorhinal cortex terminate onto granule and inhibitory basket cell dendrites within the molecular layer (Amaral et al., 2007). Additionally, CA3 back projections (Scharfman, 2007) and a diverse population of localized interneuron subtypes synapse in this area (Scharfman, 2016). Dysfunctional synapses within this region have been demonstrated in both genetic and induced rodent seizure models (Calcagnotto et al., 2005; Zhang & Buckmaster, 2009). Targeted approaches could utilize a retrogradely transported AAV vector expressing Cre-recombinase or HVS-FLP injected into the

dentate gyrus, coupled with an entorhinal injected Cre or FLP dependent ChR2 vector, allowing for specific manipulations of DG projecting excitatory signaling (Kim, Adhikari, & Deisseroth, 2017). Measuring direct responses could add another level of information to long-term changes in hippocampal excitability. However, this approach may present with some challenges within the pilocarpine model. Pilocarpine induces significant cell loss in layer 2/3 of the entorhinal cortex, altering performant path stimulation strength (De Guzman et al., 2008). Therefore, immediate cell death following SE, might indicate sudden changes in hippocampal responsiveness unrelated to the development of spontaneous seizures. However, this issue may be resolved using the stress-terbutaline model. Applying a hAEP procedure in this model should validate the predictive nature of long-term hippocampal responsiveness in epileptogenesis.

Diurnal seizure risk and the hAEP

One finding that remains to be explored using the hAEP was a significant repeatable pattern of diurnal fluctuations in hippocampal responsiveness. Exploring this observation may add to the predictive validity of this tool within epilepsy. While predicting seizures before they occur is currently an insurmountable task, an observation conserved across patients and animal models is the propensity for spontaneous seizures to arise in specific patterns relating to the circadian cycle (Cho, 2012). Specifically, among patients with mTLE and animal models reflecting this disorder, seizures peak during the late afternoon and early evening (Matzen, Buchheim, & Holtkamp, 2012; Pavlova, Shea, & Bromfield, 2004; Pitsch et al., 2017; Quigg, Straume, Menaker, & Bertram, 1998). Additionally, it is a common occurrence for external factors to serve as a mitigating seizure trigger. The most commonly identified factor contributing to the aggravation of epilepsy is stress, however there is no consensus on the mechanism by which stress increases seizure risk (McKee & Privitera, 2017). Despite stress and time of day representing the two most consistent exogenous factors when predicting seizures, there is currently insufficient evidence exploring the potential link between stress and the circadian cycle with respect to epilepsy.

Circadian rhythms are the daily cycles in behavior and bodily function, controlled by light input to the master regulatory clock, the Suprachiasmatic Nucleus of the Hypothalamus (SCN) (Reppert & Weaver, 2002). On a molecular level, there is an oscillating expression of gene activity that operates on a self-sustaining 24 hr feedback cycle in tissues throughout the body and the central nervous system. Proteins CLOCK and BMAL1 form a heterodimer that acts as a transcription factor that drives the expression of the cryptochrome and period genes. The protein products from this expression then translocate to the nucleus to act as a negative regulator by interacting with CLOCK/BMAL1 (Reppert & Weaver, 2002). While clock gene expression profiles may exhibit different peaks, troughs, and amplitudes in different brain regions (Chun, Woodruff, Morton, Hinds, & Spencer, 2015) glucocorticoid hormone (i.e., cortisol in humans, corticosterone in rodents), which is secreted into the bloodstream on a 24-hr cycle and during stress, appears necessary for entraining and sufficient for modulating these expression profiles in the central nervous system (Woodruff, Chun, Hinds, & Spencer, 2016).

However, despite usually clustering around the late afternoon in seizures originating from the temporal lobe, seizure circadian occurrence varies depending on what brain region the seizure is arising (Durazzo et al., 2008). The near 24 hour oscillatory cycle of seizure occurrence has been challenged by some studies (Bajorat, Wilde, Sellmann, Kirschstein, & Köhling, 2011), is maintained in the absence of light (Quigg et al., 1998) and others have reported that seizures from the Kainate model of epilepsy are more likely to occur during periods of inactivity rather than as a direct result of time of day or the light cycle (Hellier & Dudek, 1999). This evidence suggests that circadian mechanisms besides light, such as glucocorticoid hormone, may play a major role in the observation of circadian seizures, but studies have yet to disentangle the contribution of hormones from the direct actions of light or time of day. Afferent stimulation of hippocampal input demonstrates a 24 hr rhythmic change in excitability (Barnes, McNaughton, Goddard, Douglas, & Adamec, 1977) and hippocampal LTP (Chaudhury, Wang, & Colwell, 2005), as well shifts in responsiveness during peak seizure times (Matzen et al., 2012), but the mechanisms for this shift

are not well understood. Emerging evidence have suggested a role for clock gene expression in epilepsy with the identification that BMAL1 KO mice have an increased risk of seizures and lose the normal circadian variability in seizure threshold (Gerstner et al., 2014). Just recently, it was demonstrated that reduced Clock expression is a common feature in two focal epilepsies and that targeted deletion of Clock in pyramidal cells was sufficient to cause spontaneous seizures in mice (Li et al., 2017).

Since light cycles alone cannot adequately explain the circadian clustering of seizures, Clock genes shifts can result in epileptic phenotypes, and circulating stress hormone corticosterone modulates Clock gene expression, it would stand to reason that glucocorticoid mediated changes in clock gene expression are a contributor to both the time of day and stress reactive aspects of seizure risk. Therefore, a future study, exploring whether the diurnal stress hormone cortisol acts via entrainment of clock gene signaling to modulate neuronal excitability and seizures is warranted. To this end it would be necessary to address whether spontaneous seizures in the pilocarpine model of epilepsy and seizure threshold in normal animals oscillate on a 24-hour cycle, congruent with hAEP measured excitability changes. In addition, demonstrate that hAEP activity and seizure threshold rely on self-sustaining oscillatory mechanisms, but entrain to the light cycle via a CORT dependent mechanism. Finally, demonstrate that a CORT dependent modulation of Clock gene activity results in a shift in hAEP measured hippocampal excitability and acute seizure threshold. Then it would be possible to conclude that the stress and time of day influences on seizure risk may be adequately explained by CORT mediated alterations in oscillatory Clock gene activity that result in shifts in hippocampal excitability.

CL shifts and GABAergic inhibition

Epilepsy is a disorder of excitation inhibition imbalance. Inhibitory interneurons are preferentially lost in animal models of epilepsy and in human post-traumatic epilepsy (Swartz et al., 2006). With this evidence, it would be expected that chronic GABAergic deficits are rampant in PWE and that progressive losses in GABAergic signaling leading to E/I imbalance are a key

feature of epileptogenesis. Surprisingly GABA release is enhanced and reuptake diminished in epileptogenic tissue (During, Ryder, & Spencer, 1995). In general, despite the initial interneuron loss, GABAergic synapses increase in the epileptic hippocampus (Thind et al., 2010). In animal models, while SE induces acute decreases in inhibition in the days following SE due to the loss of inhibitory neurons, this loss of inhibition is resolved quickly by several compensatory mechanisms, so that tonic inhibition recovers, or is even enhanced within the hippocampus prior to the development of SRS (Sperk et al., 2011.; Zhan & Nadler, 2009; Zhang, Wei, Mody, & Houser, 2007). The conservation or enhancement of tonic inhibition is also present in animal models of epilepsy using fluid percussion (FPI) induced traumatic brain injury (TBI), and controlled cortical impact (CCI) (Kharlamov et al., 2011; Mtchedlishvili et al., 2010; Santhakumar, Ratzliff, Jeng, Toth, & Soltesz, 2001). Chemoconvulsant treated rats display extensive interneuron loss correlated with shifts in dentate excitability, but animals with the more extensive loss do not have the most seizures (Buckmaster & Dudek, 1997). Mimicking their preferential loss, via selective ablation of inhibitory interneurons in isolated hippocampal regions, is sufficient to induce acute spontaneous seizures, but fails to generate progressive epileptogenesis (Drexel et al., 2017; Spampanato & Dudek, 2017). While there has been a general assumption that interneuron loss is a major contributing factor to epileptogenesis, with some evidence supporting this claim (Gorter, Vliet, Aronica, & Silva, 2004; Sayin, Osting, Hagen, Rutecki, & Sutula, 2003), extensive analysis of interneuron subtype loss in both SE and TBI models seems to imply that greater interneuron loss could be correlated with decreased seizure risk (Huusko, Römer, Ndode-Ekane, Lukasiuk, & Pitkänen, 2015). Whether epileptogenesis can occur without acute neuron loss is a heavily debated topic (Dudek, Ekstrand, & Staley, 2010). But there is strong evidence for the role of functioning inhibitory microcircuits in the propagation of non-seizure epileptiform activity (Muldoon et al., 2015). Taken together, evidence suggest that loss of inhibitory neurons or loss of GABA signaling is not the primary factor contributing to chronic epilepsy.

Recent research suggests a role for dysfunctional inhibition reliant on the improper chloride homeostatic mechanisms within epilepsy and ASD. Researchers demonstrated that offspring of mice exposed to maternal immune activation (MIA) via a single injection of poli I:C lacked chronic neuroinflammation and had functional inhibitory and excitatory synapses, but mice maintained long-lasting increases in seizure risk and delayed shifts in the NKCC1/KCC2 balance (Corradini et al., 2018). IL-1r KO embryos, transplanted into WT mothers are resistant to the MIA induced KCC2 downregulation, indicating that embryonic response to maternal inflammatory processes are necessary for this defective transporter development in this model. Importantly, reducing maternal circulating cytokine levels using MgSO4 prevented deficits in KCC2 channel expression and reduced the increased seizure susceptibility, which may be a therapeutic strategy (Corradini et al., 2018). A recent study utilizing time-dependent calcium imaging showing muscimol-induced pyramidal cell activity shows that maternal separation delays the developmental switch toward inhibitory GABA and decreases membrane-localized KCC2, which persists after the cessation of MS (Furukawa et al., 2017). Early life stress alters the long-term expression of CCCs within peripheral organs like the lungs and bladder (Everington, Gibbard, Swinny, & Seifi, 2018). Non-genetic factors such as early life stress and neuroinflammation are implicated in the risk for ASD/epilepsy and directly affect the mechanisms responsible for the GABA switch during development leading to long-lasting inhibitory defects. This emerging avenue of research represent a promising target for a shared mechanism approach to understanding the effect of environmental risk factors on epilepsy-associated neurodevelopment. A future study involving the expression of chloride extrusion proteins in ST animals might shed light on inhibitory mechanisms contributing to epileptogenesis within this model.

NE signaling

Previous works have discussed the importance of disrupted adrenergic signaling in the pathological effects of early administration of terbutaline. Receptor sensitization levels and

improper norepinephrine neurotrophic signaling are routinely observed within terbutaline exposed animals (Sanders et al., 2011; Slotkin et al., 2001; Slotkin & Seidler, 2006, 2013). Innate lymphoid cells are largely controlled by β_2 signaling, which when taken offline can result in enhanced inflammatory responses (Moriyama et al., 2018). Microglial proliferation is controlled in part via β_2 adrenergic receptor signaling and can be acutely suppressed by terbutaline (Fujita et al., 1998). Additionally, adrenergic signaling through β_2 receptors can also decrease the motility of microglia (Gyoneva & Traynelis, 2013). Our current studies did not assess dysfunctional adrenergic signaling within the stress terbutaline model. Dysregulated control mechanisms in animals exposed to terbutaline early in development could play a role in the increased microglial densities and behavioral features of ST. Future studies should address the level of adrenergic signaling disruption and autonomic nervous system (ANS) function in relation to the development of spontaneous seizures. ANS function is commonly assessed via an electrocardiogram, measuring acute and prolonged changes in the electrical signature produced during cardiac contractions (Zygmunt & Stanczyk, 2010). One method would be to chronically implant an EKG monitoring system into ST rats in conjunction implanted depth electrodes. Because our current data analysis techniques asses acute wave characteristics, similar assessments of electrographic characteristics in EKG can be adequately applied with little change to analysis paradigms. Additionally, EKG data time locked to EEG could provide predictive validity toward seizures or epileptogenesis with extreme temporal precision. Pilot data from our lab has demonstrated that this is especially useful in animals at risk for sudden unexpected death from epilepsy (SUDEP), where cardiac dysfunction is a risk factor and EKG has predictive value. Applying this technique to ST animals, where ANS disruption is believed to have a causative role, could a beneficial and translatable peripheral biomarker (Euteneuer, Mills, Rief, Ziegler, & Dimsdale, 2012; Osuala et al., 2012).

Multisensory integration in ASD models

Our current work suggests that the insular cortex may play a role in the behavioral comorbidities seen following exposure to stress-terbutaline. In a seminal paper, Nadine Gogolla and colleagues demonstrated multi-sensory integration deficits associated with multiple animal models of ASD, contingent on improper inhibitory network maturation within the sensory insula during developmental critical periods (Gogolla et al., 2014). Work from chapter 4 demonstrated that a potential CNS mediated mechanism by which *M. vaccae* prevented ST-induced ASD like behavior was by the reduction in microglial expansion within the insula during early critical periods. Because microglia are heavily involved in the sculpting of inhibitory networks, assessing the functional role of this expansion in the electrophysiological properties within this region are warranted. Previous work from our lab discovered and functionally mapped the sensory insula (Rodgers et al., 2008). By applying a multi-sensory integration paradigm to ST rats using a 256-channel surface array to record insula sensory fields, it would be possible to identify long-term changes in E/I imbalance within ST rats. If present, as has been demonstrated within several animal models of ASD, exploring the effect of *M. vaccae* immunization on multi-sensory integration within ST rats could identify a CNS mediated mitigation linked to our behavioral findings.

Conclusion

Epilepsy is universal neurological disorder, pervasive throughout history within people of all ages, genders, and nationalities. However, epilepsy has not always been understood as a treatable condition. History is wrought with stigma promoting consequences for people with epilepsy. Even the earliest complete set of fundamental laws governing civilization, the code of hamurabi (1754BCE), contains a section specifically devoted to discriminatory laws regarding people epilepsy. Our understanding of the underlying neuropathological factors contributing to epilepsy remains limited and fundamental questions regarding seizures remain unanswered. However, recent advances in long-term recording capabilities, and novel animal models that explore etiologically relevant epilepsy comorbidities can guide future research toward effective treatment options and an understanding of how seizures occur. The history of epilepsy has been described as “4000 years of ignorance, superstition and stigma, followed by 100 years of knowledge, superstition, and stigma” (Kale, 1997). While society has come a long way from pulling a child through a hole in a tree to ground convulsions, or outcasting “lunatics” for their moon-induced seizures, epilepsy treatments remain woefully inadequate. Predictive biomarkers, the accurate identification of partial seizures, and exploring behavioral comorbidities with novel animal models represent the first step in a long road to understanding spontaneous seizures. Perhaps the next hundred years of epilepsy will be its last.

References

Afra, P., Jouny, C. C., & Bergey, G. K. (2008). Duration of complex partial seizures: An intracranial EEG study. *Epilepsia*, *49*(4), 677–684. https://doi.org/10.1111/j.1528-1167.2007.01420.x

Agrawal, A., Timothy, J., Pandit, L., & Manju, M. (2006). Post-traumatic epilepsy: An overview. *Clinical Neurology and Neurosurgery*, *108*(5), 433–439. https://doi.org/10.1016/j.clineuro.2005.09.001

Agster, K. L., & Burwell, R. D. (2009). Cortical efferents of the perirhinal, postrhinal, and entorhinal cortoces or the rat. *Hippocampus*, *19*(12), 1159–1186. https://doi.org/10.1002/hipo.20578

Agüero, M. G. de, Ganal-Vonarburg, S. C., Fuhrer, T., Rupp, S., Uchimura, Y., Li, H., … Macpherson, A. J. (2016). The maternal microbiota drives early postnatal innate immune development. *Science*, *351*(6279), 1296–1302. https://doi.org/10.1126/science.aad2571

Al Khalili, Y., & Murphy, P. B. (2019). Carbamazepine Toxicity. In *StatPearls*. Retrieved from http://www.ncbi.nlm.nih.gov/books/NBK507852/

Alarcon, G. (1996). Electrophysiological aspects of interictal and ictal activity in human partial epilepsy. *Seizure*, *5*(1), 7–33. https://doi.org/10.1016/S1059-1311(96)80014-8

Amaral, D. G., Scharfman, H. E., & Lavenex, P. (2007). The dentate gyrus: fundamental neuroanatomical organization (dentate gyrus for dummies). *Progress in Brain Research*, *163*, 3–22. https://doi.org/10.1016/S0079-6123(07)63001-5

American-Psychiatric-Association. (2013). *Diagnostic and Statistical Manual of Mental Disorders:: DSM-5* (5th ed.). APA, Washington DC.

Anderson, E. M., McWaters, M. L., McFadden, L. M., & Matuszewich, L. (2018). Defensive burying as an ethological approach to studying anxiety: Influence of juvenile methamphetamine on adult defensive burying behavior in rats. *Learning and Motivation*, *61*, 97–106. https://doi.org/10.1016/j.lmot.2017.02.001

Annegers, J. F., Hauser, W. A., Coan, S. P., & Rocca, W. A. (1998). A population-based study of seizures after traumatic brain injuries. *The New England Journal of Medicine*, *338*(1), 20–24. https://doi.org/10.1056/NEJM199801013380104

Aronica, E., & Crino, P. B. (2011). Inflammation in epilepsy: Clinical observations. *Epilepsia*, *52*(s3), 26–32. https://doi.org/10.1111/j.1528-1167.2011.03033.x

Asikainen, I., Kaste, M., & Sarna, S. (1999). Early and Late Posttraumatic Seizures in Traumatic Brain Injury Rehabilitation Patients: Brain Injury Factors Causing Late Seizures and

Influence of Seizures on Long-Term Outcome. *Epilepsia*, *40*(5), 584–589. https://doi.org/10.1111/j.1528-1157.1999.tb05560.x

Avoli, M., Biagini, G., & de Curtis, M. (2006). Do Interictal Spikes Sustain Seizures and Epileptogenesis? *Epilepsy Currents*, *6*(6), 203–207. https://doi.org/10.1111/j.1535-7511.2006.00146.x

Avoli, M., de Curtis, M., & Köhling, R. (2013). Does interictal synchronization influence ictogenesis? *Neuropharmacology*, *69*(Supplement C), 37–44. https://doi.org/10.1016/j.neuropharm.2012.06.044

Bajorat, R., Wilde, M., Sellmann, T., Kirschstein, T., & Köhling, R. (2011). Seizure frequency in pilocarpine-treated rats is independent of circadian rhythm. *Epilepsia*, *52*(9), e118-122. https://doi.org/10.1111/j.1528-1167.2011.03200.x

Banerjee, A., Engineer, C. T., Sauls, B. L., Morales, A. A., Kilgard, M. P., & Ploski, J. E. (2014). Abnormal emotional learning in a rat model of autism exposed to valproic acid in utero. *Frontiers in Behavioral Neuroscience*, *8*. https://doi.org/10.3389/fnbeh.2014.00387

Barnes, C. A., McNaughton, B. L., Goddard, G. V., Douglas, R. M., & Adamec, R. (1977). Circadian rhythm of synaptic excitability in rat and monkey central nervous system. *Science*, *197*(4298), 91–92. https://doi.org/10.1126/science.194313

Barth, D. S., Di, S., & Baumgartner, C. (1989). Laminar cortical interactions during epileptic spikes studied with principal component analysis and physiological modeling. *Brain Research*, *484*(1–2), 13–35. https://doi.org/10.1016/0006-8993(89)90344-2

Bateup, H. S., Takasaki, K. T., Saulnier, J. L., Denefrio, C. L., & Sabatini, B. L. (2011). Loss of Tsc1 in vivo impairs hippocampal mGluR-LTD and increases excitatory synaptic function. *The Journal of Neuroscience: The Official Journal of the Society for Neuroscience*, *31*(24), 8862–8869. https://doi.org/10.1523/JNEUROSCI.1617-11.2011

Baulac, M., de Boer, H., Elger, C., Glynn, M., Kälviäinen, R., Little, A., … Ryvlin, P. (2015). Epilepsy priorities in Europe: A report of the ILAE-IBE Epilepsy Advocacy Europe Task Force. *Epilepsia*, *56*(11), 1687–1695. https://doi.org/10.1111/epi.13201

Bedner, P., Dupper, A., Hüttmann, K., Müller, J., Herde, M. K., Dublin, P., … Steinhäuser, C. (2015). Astrocyte uncoupling as a cause of human temporal lobe epilepsy. *Brain*, *138*(5), 1208–1222. https://doi.org/10.1093/brain/awv067

Bengio, Y., Delalleau, O., Le Roux, N., & Paiement, J. F. (2006). *Spectral dimensionality reduction*. Retrieved from http://link.springer.com/chapter/10.1007/978-3-540-35488-8_28

Benjamini, Y., & Hochberg, Y. (1995). Controlling the False Discovery Rate: A Practical and Powerful Approach to Multiple Testing on JSTOR. *Journal of the Royal Statistical Society Series B …*. Retrieved from http://www.jstor.org/stable/2346101

Bercum, F. M., Rodgers, K. M., Benison, A. M., Smith, Z. Z., Taylor, J., Kornreich, E., … Barth, D. S. (2015). Maternal Stress Combined with Terbutaline Leads to Comorbid Autistic-Like Behavior and Epilepsy in a Rat Model. *Journal of Neuroscience*, *35*(48), 15894–15902. https://doi.org/10.1523/JNEUROSCI.2803-15.2015

Bertram, E. H., & Cornett, J. F. (1994). The evolution of a rat model of chronic spontaneous limbic seizures. *Brain Research*, *661*(1–2), 157–162.

Besag, F. M. (2017). Epilepsy in patients with autism: links, risks and treatment challenges. *Neuropsychiatric Disease and Treatment*, *14*, 1–10. https://doi.org/10.2147/NDT.S120509

Beyenburg, S., Mitchell, A. J., Schmidt, D., Elger, C. E., & Reuber, M. (2005). Anxiety in patients with epilepsy: Systematic review and suggestions for clinical management. *Epilepsy & Behavior*, *7*(2), 161–171. https://doi.org/10.1016/j.yebeh.2005.05.014

Biagini, G., Baldelli, E., Longo, D., Pradelli, L., Zini, I., Rogawski, M. A., & Avoli, M. (2006). Endogenous neurosteroids modulate epileptogenesis in a model of temporal lobe epilepsy. *Experimental Neurology*, *201*(2), 519–524. https://doi.org/10.1016/j.expneurol.2006.04.029

Bilbo, S. D., Block, C. L., Bolton, J. L., Hanamsagar, R., & Tran, P. K. (2018). Beyond infection - Maternal immune activation by environmental factors, microglial development, and relevance for autism spectrum disorders. *Experimental Neurology*, *299*, 241–251. https://doi.org/10.1016/j.expneurol.2017.07.002

Bin, N.-R., Song, H., Wu, C., Lau, M., Sugita, S., Eubanks, J. H., & Zhang, L. (2017). Continuous Monitoring via Tethered Electroencephalography of Spontaneous Recurrent Seizures in Mice. *Frontiers in Behavioral Neuroscience*, *11*. https://doi.org/10.3389/fnbeh.2017.00172

Binnie, C. D., & Prior, P. F. (1994). Electroencephalography. *Journal of Neurology, Neurosurgery, and Psychiatry*, *57*(11), 1308–1319.

Bower, M. R., Kucewicz, M. T., St. Louis, E. K., Meyer, F. B., Marsh, W. R., Stead, M., & Worrell, G. A. (2017). Reactivation of seizure-related changes to interictal spike shape and synchrony during postseizure sleep in patients. *Epilepsia*, *58*(1), 94–104. https://doi.org/10.1111/epi.13614

Bozzi, Y., Provenzano, G., & Casarosa, S. (2018). Neurobiological bases of autism–epilepsy comorbidity: a focus on excitation/inhibition imbalance. *European Journal of Neuroscience*, *47*(6), 534–548. https://doi.org/10.1111/ejn.13595

Bradley, A. P., & Wilson, W. J. (2004). On wavelet analysis of auditory evoked potentials. *Clinical Neurophysiology : Official Journal of the International Federation of Clinical Neurophysiology*, *115*(5), 1114–1128. https://doi.org/10.1016/j.clinph.2003.11.016

Bragin, A., Wilson, C. L., Almajano, J., Mody, I., & Engel, J. (2004). High-frequency oscillations after status epilepticus: epileptogenesis and seizure genesis. *Epilepsia*, *45*(9), 1017–1023. https://doi.org/10.1111/j.0013-9580.2004.17004.x

Brandt, C., Töllner, K., Klee, R., Bröer, S., & Löscher, W. (2015). Effective termination of status epilepticus by rational polypharmacy in the lithium-pilocarpine model in rats: Window of opportunity to prevent epilepsy and prediction of epilepsy by biomarkers. *Neurobiology of Disease*, *75*, 78–90. https://doi.org/10.1016/j.nbd.2014.12.015

Brankack, J., & Buzsaki, G. (1986). Hippocampal responses evoked by tooth pulp and acoustic stimulation: depth profiles and effect of behavior. *Brain Research*, *378*(2), 303–314.

Brigo, F., Trinka, E., Lattanzi, S., Bragazzi, N. L., Nardone, R., & Martini, M. (2018). A brief history of typical absence seizures — Petit mal revisited. *Epilepsy & Behavior*, *80*, 346–353. https://doi.org/10.1016/j.yebeh.2018.01.007

Bromfield, E. B., Cavazos, J. E., & Sirven, J. I. (2006). *Basic Mechanisms Underlying Seizures and Epilepsy*. Retrieved from https://www.ncbi.nlm.nih.gov/books/NBK2510/

Brooks-Kayal, A. (2010). Epilepsy and autism spectrum disorders: Are there common developmental mechanisms? *Brain and Development*, *32*(9), 731–738. https://doi.org/10.1016/j.braindev.2010.04.010

Buckley, A. W., & Holmes, G. L. (2016). Epilepsy and Autism. *Cold Spring Harbor Perspectives in Medicine*, *6*(4), a022749. https://doi.org/10.1101/cshperspect.a022749

Buckmaster, P S, & Dudek, F. E. (1997a). Network properties of the dentate gyrus in epileptic rate with hilar neuron loss and granule cell axon reorganization. *Journal of Neurophysiology*, *77*, 2685–2696.

Buckmaster, P. S., & Dudek, F. E. (1997b). Neuron loss, granule cell axon reorganization, and functional changes in the dentate gyrus of epileptic kainate-treated rats. *The Journal of Comparative Neurology*, *385*(3), 385–404.

Buffington, S. A., Viana Di Prisco, G., Auchtung, T. A., Ajami, N. J., Petrosino, J. F., & Costa-Mattioli, M. (2016). Microbial reconstitution reverses maternal diet-induced social and synaptic deficits in offspring. *Cell*, *165*(7), 1762–1775. https://doi.org/10.1016/j.cell.2016.06.001

Burkholder, D. B., Britton, J. W., Rajasekaran, V., Fabris, R. R., Cherian, P. J., Kelly-Williams, K. M., … Wirrell, E. C. (2016). Routine vs extended outpatient EEG for the detection of interictal epileptiform discharges. *Neurology*, *86*(16), 1524–1530. https://doi.org/10.1212/WNL.0000000000002592

Calabrese, M., De Stefano, N., Atzori, M., Bernardi, V., Mattisi, I., Barachino, L., … Gallo, P. (2008). Extensive cortical inflammation is associated with epilepsy in multiple sclerosis. *Journal of Neurology*, *255*(4), 581–586. https://doi.org/10.1007/s00415-008-0752-7

Calcagnotto, M. E., Paredes, M. F., Tihan, T., Barbaro, N. M., & Baraban, S. C. (2005). Dysfunction of Synaptic Inhibition in Epilepsy Associated with Focal Cortical Dysplasia. *Journal of Neuroscience*, *25*(42), 9649–9657. https://doi.org/10.1523/JNEUROSCI.2687-05.2005

Cappé, O., Moulines, E., & Rydén, T. (2005). *Inference in hidden Markov models*. New York ; London: Springer.

Cascino, G. D. (1992). Complex partial seizures. Clinical features and differential diagnosis. *The Psychiatric Clinics of North America*, *15*(2), 373–382.

Chaidez, V., Hansen, R. L., & Hertz-Picciotto, I. (2014). Gastrointestinal problems in children with autism, developmental delays or typical development. *Journal of Autism and Developmental Disorders*, *44*(5), 1117–1127. https://doi.org/10.1007/s10803-013-1973-x

Charil, A., Laplante, D. P., Vaillancourt, C., & King, S. (2010). Prenatal stress and brain development. *Brain Research Reviews*, *65*(1), 56–79. https://doi.org/10.1016/j.brainresrev.2010.06.002

Chaudhury, D., Wang, L. M., & Colwell, C. S. (2005). Circadian Regulation of Hippocampal Long-Term Potentiation. *Journal of Biological Rhythms*, *20*(3), 225–236. https://doi.org/10.1177/0748730405276352

Chauvière, L., Doublet, T., Ghestem, A., Siyoucef, S. S., Wendling, F., Huys, R., … Bernard, C. (2012). Changes in interictal spike features precede the onset of temporal lobe epilepsy. *Annals of Neurology*, *71*(6), 805–814. https://doi.org/10.1002/ana.23549

Chen, S.-D., Wang, Y.-L., Liang, S.-F., & Shaw, F.-Z. (2016). Rapid Amygdala Kindling Causes Motor Seizure and Comorbidity of Anxiety- and Depression-Like Behaviors in Rats. *Frontiers in Behavioral Neuroscience*, *10*. https://doi.org/10.3389/fnbeh.2016.00129

Cho, C.-H. (2012). Molecular mechanism of circadian rhythmicity of seizures in temporal lobe epilepsy. *Frontiers in Cellular Neuroscience*, *6*. https://doi.org/10.3389/fncel.2012.00055

Choi, G. B., Yim, Y. S., Wong, H., Kim, S., Kim, H., Kim, S. V., … Huh, J. R. (2016). The maternal interleukin-17a pathway in mice promotes autism-like phenotypes in offspring. *Science*, *351*(6276), 933–939. https://doi.org/10.1126/science.aad0314

Chou, I.-C., Wang, C.-H., Lin, W.-D., Tsai, F.-J., Lin, C.-C., & Kao, C.-H. (2016). Risk of epilepsy in type 1 diabetes mellitus: a population-based cohort study. *Diabetologia*, *59*(6), 1196–1203. https://doi.org/10.1007/s00125-016-3929-0

Chun, L. E., Woodruff, E. R., Morton, S., Hinds, L. R., & Spencer, R. L. (2015). Variations in phase and amplitude of rhythmic clock gene expression across prefrontal cortex, hippocampus, amygdala, and hypothalamic paraventricular and suprachiasmatic nuclei of male and female rats. *Journal of Biological Rhythms*, *30*(5), 417–436.

Coan, A. C., & Cendes, F. (2013). Epilepsy as progressive disorders: What is the evidence that can guide our clinical decisions and how can neuroimaging help? *Epilepsy & Behavior*, *26*(3), 313–321. https://doi.org/10.1016/j.yebeh.2012.09.027

Connors, S. L., Crowell, D. E., Eberhart, C. G., Copeland, J., Newschaffer, C. J., Spence, S. J., & Zimmerman, A. W. (2005). β 2-Adrenergic Receptor Activation and Genetic Polymorphisms in Autism: Data from Dizygotic Twins. *Journal of Child Neurology*, *20*(11), 876–884. https://doi.org/10.1177/08830738050200110401

Cook, M. J., Karoly, P. J., Freestone, D. R., Himes, D., Leyde, K., Berkovic, S., … Boston, R. (2016). Human focal seizures are characterized by populations of fixed duration and interval. *Epilepsia*, *57*(3), 359–368. https://doi.org/10.1111/epi.13291

Corradini, I., Focchi, E., Rasile, M., Morini, R., Desiato, G., Tomasoni, R., … Matteoli, M. (2018). Maternal Immune Activation Delays Excitatory-to-Inhibitory Gamma-Aminobutyric Acid Switch in Offspring. *Biological Psychiatry*, *83*(8), 680–691. https://doi.org/10.1016/j.biopsych.2017.09.030

Craig, A. D. (2002). How do you feel? Interoception: the sense of the physiological condition of the body. *Nature Reviews Neuroscience*, *3*(8), 655–666. https://doi.org/10.1038/nrn894

Crawley, J. N. (2012). Translational animal models of autism and neurodevelopmental disorders. *Dialogues in Clinical Neuroscience*, *14*(3), 293–305.

Croen, L. A., Connors, S. L., Matevia, M., Qian, Y., Newschaffer, C., & Zimmerman, A. W. (2011). Prenatal exposure to β2-adrenergic receptor agonists and risk of autism spectrum disorders. *Journal of Neurodevelopmental Disorders*, *3*(4), 307–315. https://doi.org/10.1007/s11689-011-9093-4

Cunningham, J. P., & Byron, M. Y. (2014). Dimensionality reduction for large-scale neural recordings. *Nature Neuroscience*. Retrieved from http://www.nature.com/neuro/journal/vaop/ncurrent/full/nn.3776.html

Curia, G., Longo, D., Biagini, G., Jones, R. S. G., & Avoli, M. (2008). The pilocarpine model of temporal lobe epilepsy. *Journal of Neuroscience Methods*, *172*(2), 143–157. https://doi.org/10.1016/j.jneumeth.2008.04.019

Dalby, N. O., & Mody, I. (2001). The process of epileptogenesis: a pathophysiological approach. *Current Opinion in Neurology*, *14*(2), 187–192.

D'Ambrosio, R., Fairbanks, J. P., Fender, J. S., Born, D. E., Doyle, D. L., & Miller, J. W. (2004). Post-traumatic epilepsy following fluid percussion injury in the rat. *Brain*, *127*(Pt 2), 304–314. https://doi.org/10.1093/brain/awh038

D'Ambrosio, R., Fender, J. S., Fairbanks, J. P., Simon, E. A., Born, D. E., Doyle, D. L., & Miller, J. W. (2005). Progression From Frontal-Parietal To Mesial-Temporal Epilepsy After Fluid Percussion Injury In The Rat. *Brain : A Journal of Neurology*, *128*(Pt 1), 174–188. https://doi.org/10.1093/brain/awh337

D'Ambrosio, R., Hakimian, S., Stewart, T., Verley, D. R., Fender, J. S., Eastman, C. L., … Miller, J. W. (2009). Functional definition of seizure provides new insight into post-traumatic epileptogenesis. *Brain*, *132*(Pt 10), 2805–2821. https://doi.org/10.1093/brain/awp217

D'Ambrosio, R., & Miller, J. W. (2010). What is an epileptic seizure? Unifying definitions in clinical practice and animal research to develop novel treatments. *Epilepsy Currents*, *10*(3), 61–66. https://doi.org/10.1111/j.1535-7511.2010.01358.x

Day, H. E. W., & Akil, H. (1996). Differential Pattern of c-fos mRNA in Rat Brain following Central and Systemic Administration of Interleukin-1-Beta: Implications for Mechanism of Action. *Neuroendocrinology*, *63*(3), 207–218. https://doi.org/10.1159/000126959

De Boer, S. F., & Koolhaas, J. M. (2003). Defensive burying in rodents: ethology, neurobiology and psychopharmacology. *European Journal of Pharmacology*, *463*(1), 145–161. https://doi.org/10.1016/S0014-2999(03)01278-0

De Guzman, P., Inaba, Y., Baldelli, E., De Curtis, M., Biagini, G., & Avoli, M. (2008). Network hyperexcitability within the deep layers of the pilocarpine-treated rat entorhinal cortex. *The Journal of Physiology*, *586*(7), 1867–1883. https://doi.org/10.1113/jphysiol.2007.146159

Delpech, J.-C., Wei, L., Hao, J., Yu, X., Madore, C., Butovsky, O., & Kaffman, A. (2016). Early life stress perturbs the maturation of microglia in the developing hippocampus. *Brain, Behavior, and Immunity*, *57*, 79–93. https://doi.org/10.1016/j.bbi.2016.06.006

Deonna, T., & Roulet, E. (2006). Autistic Spectrum Disorder: Evaluating a Possible Contributing or Causal Role of Epilepsy. *Epilepsia*, *47*(s2), 79–82. https://doi.org/10.1111/j.1528-1167.2006.00697.x

Deonna, T. W. (1991). Acquired epileptiform aphasia in children (Landau-Kleffner syndrome). *Journal of Clinical Neurophysiology: Official Publication of the American Electroencephalographic Society*, *8*(3), 288–298.

Depino, A. M. (2013). Peripheral and central inflammation in autism spectrum disorders. *Molecular and Cellular Neurosciences*, *53*, 69–76. https://doi.org/10.1016/j.mcn.2012.10.003

Desbonnet, L., Garrett, L., Clarke, G., Kiely, B., Cryan, J. F., & Dinan, T. G. (2010). Effects of the probiotic Bifidobacterium infantis in the maternal separation model of depression. *Neuroscience*, *170*(4), 1179–1188. https://doi.org/10.1016/j.neuroscience.2010.08.005

Desbonnet, Lieve, Clarke, G., Traplin, A., O'Sullivan, O., Crispie, F., Moloney, R. D., … Cryan, J. F. (2015). Gut microbiota depletion from early adolescence in mice: Implications for brain and behaviour. *Brain, Behavior, and Immunity*, *48*, 165–173. https://doi.org/10.1016/j.bbi.2015.04.004

Deshpande, L. S., & DeLorenzo, R. J. (2014). Mechanisms of Levetiracetam in the Control of Status Epilepticus and Epilepsy. *Frontiers in Neurology*, *5*. https://doi.org/10.3389/fneur.2014.00011

Devinsky, O., Sato, S., Kufta, C. V., Ito, B., Rose, D. F., Theodore, W. H., & Porter, R. J. (1989). Electroencephalographic studies of simple partial seizures with subdural electrode recordings. *Neurology*, *39*(4), 527–533.

Devinsky, Orrin. (2008). Postictal Psychosis: Common, Dangerous, and Treatable. *Epilepsy Currents*, *8*(2), 31–34. https://doi.org/10.1111/j.1535-7511.2008.00227.x

Devinsky, Orrin, Schein, A., & Najjar, S. (2013). Epilepsy Associated with Systemic Autoimmune Disorders. *Epilepsy Currents*, *13*(2), 62–68. https://doi.org/10.5698/1535-7597-13.2.62

Devinsky, Orrin, Vezzani, A., Najjar, S., De Lanerolle, N. C., & Rogawski, M. A. (2013). Glia and epilepsy: excitability and inflammation. *Trends in Neurosciences*, *36*(3), 174–184. https://doi.org/10.1016/j.tins.2012.11.008

Dey, A., Kang, X., Qiu, J., Du, Y., & Jiang, J. (2016). Anti-Inflammatory Small Molecules To Treat Seizures and Epilepsy: From Bench to Bedside. *Trends in Pharmacological Sciences*, *37*(6), 463–484. https://doi.org/10.1016/j.tips.2016.03.001

Dichter, M. A., & Ayala, G. F. (1987). Cellular mechanisms of epilepsy: a status report. *Science*, *237*(4811), 157–164. https://doi.org/10.1126/science.3037700

Dinan, T. G., Quigley, E. M. M., Ahmed, S. M. M., Scully, P., O'Brien, S., O'Mahony, L., … Keeling, P. W. N. (2006). Hypothalamic-Pituitary-Gut Axis Dysregulation in Irritable Bowel Syndrome: Plasma Cytokines as a Potential Biomarker? *Gastroenterology*, *130*(2), 304–311. https://doi.org/10.1053/j.gastro.2005.11.033

Ding, K., Gupta, P. K., & Diaz-Arrastia, R. (2016). Epilepsy after Traumatic Brain Injury. In D. Laskowitz & G. Grant (Eds.), *Translational Research in Traumatic Brain Injury*. Retrieved from http://www.ncbi.nlm.nih.gov/books/NBK326716/

Dissing-Olesen, L., LeDue, J. M., Rungta, R. L., Hefendehl, J. K., Choi, H. B., & MacVicar, B. A. (2014). Activation of Neuronal NMDA Receptors Triggers Transient ATP-Mediated Microglial Process Outgrowth. *The Journal of Neuroscience*, *34*(32), 10511–10527. https://doi.org/10.1523/JNEUROSCI.0405-14.2014

Dölen, G., & Bear, M. F. (2008). Role for metabotropic glutamate receptor 5 (mGluR5) in the pathogenesis of fragile X syndrome. *The Journal of Physiology*, *586*(6), 1503–1508. https://doi.org/10.1113/jphysiol.2008.150722

Drexel, M., Romanov, R. A., Wood, J., Weger, S., Heilbronn, R., Wulff, P., … Sperk, G. (2017). Selective Silencing of Hippocampal Parvalbumin Interneurons Induces Development of Recurrent Spontaneous Limbic Seizures in Mice. *The Journal of Neuroscience: The Official Journal of the Society for Neuroscience*, *37*(34), 8166–8179. https://doi.org/10.1523/JNEUROSCI.3456-16.2017

Dubé, C. M., Molet, J., Singh-Taylor, A., Ivy, A., Maras, P. M., & Baram, T. Z. (2015). Hyper-excitability and epilepsy generated by chronic early-life stress. *Neurobiology of Stress*, *2*, 10–19. https://doi.org/10.1016/j.ynstr.2015.03.001

Dubé, C., Richichi, C., Bender, R. A., Chung, G., Litt, B., & Baram, T. Z. (2006). Temporal lobe epilepsy after experimental prolonged febrile seizures: prospective analysis. *Brain*, *129*(Pt 4), 911–922. https://doi.org/10.1093/brain/awl018

Dudek, F. E., & Bertram, E. H. (2010). Counterpoint to "What Is an Epileptic Seizure?" By D'Ambrosio and Miller. *Epilepsy Currents*, *10*(4), 91–94. https://doi.org/10.1111/j.1535-7511.2010.01368.x

Dudek, F. E., Ekstrand, J. J., & Staley, K. J. (2010). Is Neuronal Death Necessary for Acquired Epileptogenesis in the Immature Brain? *Epilepsy Currents*, *10*(4), 95–99. https://doi.org/10.1111/j.1535-7511.2010.01369.x

Durazzo, T. S., Spencer, S. S., Duckrow, R. B., Novotny, E. J., Spencer, D. D., & Zaveri, H. P. (2008). Temporal distributions of seizure occurrence from various epileptogenic regions. *Neurology*, *70*(15), 1265–1271. https://doi.org/10.1212/01.wnl.0000308938.84918.3f

During, M. J., Ryder, K. M., & Spencer, D. D. (1995). Hippocampal GABA transporter function in temporal-lobe epilepsy. *Nature*, *376*(6536), 174–177. https://doi.org/10.1038/376174a0

Eastman, C. L., Fender, J. S., Temkin, N. R., & D'Ambrosio, R. (2015). Optimized methods for epilepsy therapy development using an etiologically realistic model of focal epilepsy in the rat. *Experimental Neurology*, *264*, 150–162. https://doi.org/10.1016/j.expneurol.2014.12.010

Edmiston, E., Ashwood, P., & Van de Water, J. (2017). Autoimmunity, Autoantibodies, and Autism Spectrum Disorder. *Biological Psychiatry*, *81*(5), 383–390. https://doi.org/10.1016/j.biopsych.2016.08.031

Ekinci, O., Titus, J. B., Rodopman, A. A., Berkem, M., & Trevathan, E. (2009). Depression and anxiety in children and adolescents with epilepsy: Prevalence, risk factors, and treatment. *Epilepsy & Behavior*, *14*(1), 8–18. https://doi.org/10.1016/j.yebeh.2008.08.015

Engel, J. (2001). A proposed diagnostic scheme for people with epileptic seizures and with epilepsy: report of the ILAE Task Force on Classification and Terminology. *Epilepsia*, *42*(6), 796–803. https://doi.org/10.1046/j.1528-1157.2001.10401.x

Engel, J., Pitkanen, A., Loeb, J. A., Edward Dudek, F., Bertram, E. H., Cole, A. J., … Vezzani, A. (2013). Epilepsy biomarkers. *Epilepsia*, *54 Suppl 4*, 61–69. https://doi.org/10.1111/epi.12299

Engineer, C. T., Hays, S. A., & Kilgard, M. P. (2017). Vagus nerve stimulation as a potential adjuvant to behavioral therapy for autism and other neurodevelopmental disorders. *Journal of Neurodevelopmental Disorders*, *9*. https://doi.org/10.1186/s11689-017-9203-z

Entringer, S., Kumsta, R., Hellhammer, D. H., Wadhwa, P. D., & Wüst, S. (2009). Prenatal exposure to maternal psychosocial stress and HPA axis regulation in young adults. *Hormones and Behavior*, *55*(2), 292–298. https://doi.org/10.1016/j.yhbeh.2008.11.006

Euteneuer, F., Mills, P. J., Rief, W., Ziegler, M. G., & Dimsdale, J. E. (2012). Association of In Vivo Beta-Adrenergic Receptor Sensitivity with Inflammatory Markers in Healthy Subjects. *Psychosomatic Medicine*, *74*(3), 271–277. https://doi.org/10.1097/PSY.0b013e318245d762

Everington, E. A., Gibbard, A. G., Swinny, J. D., & Seifi, M. (2018). Molecular Characterization of GABA-A Receptor Subunit Diversity within Major Peripheral Organs and Their Plasticity

in Response to Early Life Psychosocial Stress. *Frontiers in Molecular Neuroscience*, *11*. https://doi.org/10.3389/fnmol.2018.00018

Falco-Walter, J. J., & Bleck, T. (2016). Treatment of Established Status Epilepticus. *Journal of Clinical Medicine*, *5*(5). https://doi.org/10.3390/jcm5050049

Ferrini, F., & De Koninck, Y. (2013). Microglia Control Neuronal Network Excitability via BDNF Signalling. *Neural Plasticity*, *2013*. https://doi.org/10.1155/2013/429815

Fiest, K. M., Sauro, K. M., Wiebe, S., Patten, S. B., Kwon, C.-S., Dykeman, J., … Jetté, N. (2017). Prevalence and incidence of epilepsy. *Neurology*, *88*(3), 296–303. https://doi.org/10.1212/WNL.0000000000003509

File, S. E., & Hyde, J. r. g. (1978). Can Social Interaction Be Used to Measure Anxiety? *British Journal of Pharmacology*, *62*(1), 19–24. https://doi.org/10.1111/j.1476-5381.1978.tb07001.x

Fisher, R. S., Boas, W. van E., Blume, W., Elger, C., Genton, P., Lee, P., & Engel, J. (2005). Epileptic Seizures and Epilepsy: Definitions Proposed by the International League Against Epilepsy (ILAE) and the International Bureau for Epilepsy (IBE). *Epilepsia*, *46*(4), 470–472. https://doi.org/10.1111/j.0013-9580.2005.66104.x

Fisher, R. S., Cross, J. H., French, J. A., Higurashi, N., Hirsch, E., Jansen, F. E., … Zuberi, S. M. (2017). Operational classification of seizure types by the International League Against Epilepsy: Position Paper of the ILAE Commission for Classification and Terminology. *Epilepsia*, *58*(4), 522–530. https://doi.org/10.1111/epi.13670

Fonken, L. K., Frank, M. G., D'Angelo, H. M., Heinze, J. D., Watkins, L. R., Lowry, C. A., & Maier, S. F. (2018). Mycobacterium vaccae immunization protects aged rats from surgery-elicited neuroinflammation and cognitive dysfunction. *Neurobiology of Aging*, *71*, 105–114. https://doi.org/10.1016/j.neurobiolaging.2018.07.012

Fox, J. H., Hassell, J. E., Siebler, P. H., Arnold, M. R., Lamb, A. K., Smith, D. G., … Lowry, C. A. (2017). Preimmunization with a heat-killed preparation of Mycobacterium vaccae enhances fear extinction in the fear-potentiated startle paradigm. *Brain, Behavior, and Immunity*, *66*, 70–84. https://doi.org/10.1016/j.bbi.2017.08.014

Frank, M. G., Fonken, L. K., Dolzani, S. D., Annis, J. L., Siebler, P. H., Schmidt, D., … Lowry, C. A. (2018). Immunization with Mycobacterium vaccae induces an anti-inflammatory milieu in the CNS: Attenuation of stress-induced microglial priming, alarmins and anxiety-like behavior. *Brain, Behavior, and Immunity*, *73*, 352–363. https://doi.org/10.1016/j.bbi.2018.05.020

Frank, M. G., Hershman, S. A., Weber, M. D., Watkins, L. R., & Maier, S. F. (2014). Chronic exposure to exogenous glucocorticoids primes microglia to pro-inflammatory stimuli and induces NLRP3 mRNA in the hippocampus. *Psychoneuroendocrinology*, *40*, 191–200. https://doi.org/10.1016/j.psyneuen.2013.11.006

Frank, M. G., Wieseler-Frank, J. L., Watkins, L. R., & Maier, S. F. (2006). Rapid isolation of highly enriched and quiescent microglia from adult rat hippocampus: immunophenotypic and functional characteristics. *Journal of Neuroscience Methods*, *151*(2), 121–130. https://doi.org/10.1016/j.jneumeth.2005.06.026

French, J. A., Williamson, P. D., Thadani, V. M., Darcey, T. M., Mattson, R. H., Spencer, S. S., & Spencer, D. D. (1993). Characteristics of medial temporal lobe epilepsy: I. Results of history and physical examination. *Annals of Neurology*, *34*(6), 774–780. https://doi.org/10.1002/ana.410340604

French, Jacqueline A. (2005). Seizure Exacerbation by Antiepileptic Drugs. *Epilepsy Currents*, *5*(5), 192–193. https://doi.org/10.1111/j.1535-7511.2005.00061.x

French, Jacqueline A. (2007). Refractory Epilepsy: Clinical Overview. *Epilepsia*, *48*(s1), 3–7. https://doi.org/10.1111/j.1528-1167.2007.00992.x

Frey, L. C. (2003). Epidemiology of posttraumatic epilepsy: a critical review. *Epilepsia*, *44 Suppl 10*, 11–17.

Fritschy, J.-M. (2008). Epilepsy, E/I balance and GABAA receptor plasticity. *Frontiers in Molecular Neuroscience*, *1*. https://doi.org/10.3389/neuro.02.005.2008

Frye, R. E., Casanova, M. F., Fatemi, S. H., Folsom, T. D., Reutiman, T. J., Brown, G. L., … Adams, J. B. (2016). Neuropathological Mechanisms of Seizures in Autism Spectrum Disorder. *Frontiers in Neuroscience*, *10*. https://doi.org/10.3389/fnins.2016.00192

Fujita, H., Tanaka, J., Maeda, N., & Sakanaka, M. (1998). Adrenergic agonists suppress the proliferation of microglia through β2-adrenergic receptor. *Neuroscience Letters*, *242*(1), 37–40. https://doi.org/10.1016/S0304-3940(98)00003-2

Furukawa, M., Tsukahara, T., Tomita, K., Iwai, H., Sonomura, T., Miyawaki, S., & Sato, T. (2017). Neonatal maternal separation delays the GABA excitatory-to-inhibitory functional switch by inhibiting KCC2 expression. *Biochemical and Biophysical Research Communications*, *493*(3), 1243–1249. https://doi.org/10.1016/j.bbrc.2017.09.143

Gao, R., & Penzes, P. (2015). Common Mechanisms of Excitatory and Inhibitory Imbalance in Schizophrenia and Autism Spectrum Disorders. *Current Molecular Medicine*, *15*(2), 146–167.

Gaudet, L. M., Singh, K., Weeks, L., Skidmore, B., Tsertsvadze, A., & Ansari, M. T. (2012). Effectiveness of Terbutaline Pump for the Prevention of Preterm Birth. A Systematic Review and Meta-Analysis. *PLoS ONE*, *7*(2). https://doi.org/10.1371/journal.pone.0031679

Genton, P. (2000). When antiepileptic drugs aggravate epilepsy. *Brain and Development*, *22*(2), 75–80. https://doi.org/10.1016/S0387-7604(99)00113-8

George Paxinos and Charles Watson. (1998). *The Rat Brain in Stereotaxic Coordinates*. San Diego: Academic Press.

Gerstner, J. R., Smith, G. G., Lenz, O., Perron, I. J., Buono, R. J., & Ferraro, T. N. (2014). BMAL1 controls the diurnal rhythm and set point for electrical seizure threshold in mice. *Frontiers in Systems Neuroscience*, *8*. https://doi.org/10.3389/fnsys.2014.00121

Ghacibeh, G. A., & Fields, C. (2015). Interictal epileptiform activity and autism. *Epilepsy & Behavior*, *47*, 158–162. https://doi.org/10.1016/j.yebeh.2015.02.025

Gidaya, N. B., Lee, B. K., Burstyn, I., Michael, Y., Newschaffer, C. J., & Mortensen, E. L. (2016). In utero Exposure to β-2-Adrenergic Receptor Agonist Drugs and Risk for Autism Spectrum Disorders. *Pediatrics*, *137*(2), e20151316. https://doi.org/10.1542/peds.2015-1316

Gillberg, C., & Billstedt, E. (2000). Autism and Asperger syndrome: coexistence with other clinical disorders. *Acta Psychiatrica Scandinavica*, *102*(5), 321–330.

Glover, V., O'Connor, T. G., & O'Donnell, K. (2010). Prenatal stress and the programming of the HPA axis. *Neuroscience & Biobehavioral Reviews*, *35*(1), 17–22. https://doi.org/10.1016/j.neubiorev.2009.11.008

Gogolla, N., Takesian, A. E., Feng, G., Fagiolini, M., & Hensch, T. K. (2014). Sensory Integration in Mouse Insular Cortex Reflects GABA Circuit Maturation. *Neuron*, *83*(4), 894–905. https://doi.org/10.1016/j.neuron.2014.06.033

Gorka, Z., Moryl, E., & Papp, M. (1996). Effect of chronic mild stress on circadian rhythms in the locomotor activity in rats. *Pharmacology Biochemistry and Behavior*, *54*(1), 229–234. https://doi.org/10.1016/0091-3057(95)02173-6

Gorter, J. A., Vliet, E. A. V., Aronica, E., & Silva, F. H. L. D. (2001). Progression of spontaneous seizures after status epilepticus is associated with mossy fibre sprouting and extensive bilateral loss of hilar parvalbumin and somatostatin-immunoreactive neurons. *European Journal of Neuroscience*, *13*(4), 657–669. https://doi.org/10.1046/j.1460-9568.2001.01428.x

Greenfield, L. J. (2013). Molecular mechanisms of antiseizure drug activity at GABAA receptors. *Seizure*, *22*(8), 589–600. https://doi.org/10.1016/j.seizure.2013.04.015

Gröschel, M. I., Prabowo, S. A., Cardona, P.-J., Stanford, J. L., & Werf, T. S. van der. (2014). Therapeutic vaccines for tuberculosis—A systematic review. *Vaccine*, *32*(26), 3162–3168. https://doi.org/10.1016/j.vaccine.2014.03.047

Gumusoglu, S. B., Fine, R. S., Murray, S. J., Bittle, J. L., & Stevens, H. E. (2017). The role of IL-6 in neurodevelopment after prenatal stress. *Brain, Behavior, and Immunity*, *65*, 274–283. https://doi.org/10.1016/j.bbi.2017.05.015

Gunn, B. G., Cox, C. D., Chen, Y., Frotscher, M., Gall, C. M., Baram, T. Z., & Lynch, G. (2017). The Endogenous Stress Hormone CRH Modulates Excitatory Transmission and Network Physiology in Hippocampus. *Cerebral Cortex*, *27*(8), 4182–4198. https://doi.org/10.1093/cercor/bhx103

Gyoneva, S., & Traynelis, S. F. (2013). Norepinephrine Modulates the Motility of Resting and Activated Microglia via Different Adrenergic Receptors. *Journal of Biological Chemistry*, *288*(21), 15291–15302. https://doi.org/10.1074/jbc.M113.458901

Haas, D. M., Benjamin, T., Sawyer, R., & Quinney, S. K. (2014). Short-term tocolytics for preterm delivery – current perspectives. *International Journal of Women's Health*, *6*, 343–349. https://doi.org/10.2147/IJWH.S44048

Hamer, H. M., Lüders, H. O., Knake, S., Fritsch, B., Oertel, W. H., & Rosenow, F. (2003). Electrophysiology of focal clonic seizures in humans: a study using subdural and depth electrodes. *Brain*, *126*(3), 547–555. https://doi.org/10.1093/brain/awg051

Hanamsagar, R., & Bilbo, S. D. (2017). Environment matters: microglia function and dysfunction in a changing world. *Current Opinion in Neurobiology*, *47*, 146–155. https://doi.org/10.1016/j.conb.2017.10.007

Happé, F. (2011). Criteria, categories, and continua: autism and related disorders in DSM-5. *Journal of the American Academy of Child & Adolescent Psychiatry*, *50*(6), 540–542.

Harris, A., & Seckl, J. (2011). Glucocorticoids, prenatal stress and the programming of disease. *Hormones and Behavior*, *59*(3), 279–289. https://doi.org/10.1016/j.yhbeh.2010.06.007

Hart, Y. M., Sander, J. W. A. S., Shorvon, S. D., & Johnson, A. L. (1990). National General Practice Study of Epilepsy: recurrence after a first seizure. *The Lancet*, *336*(8726), 1271–1274. https://doi.org/10.1016/0140-6736(90)92960-P

Haut, S. R., Bigal, M. E., & Lipton, R. B. (2006). Chronic disorders with episodic manifestations: focus on epilepsy and migraine. *Lancet Neurology*, *5*(2), 148–157. https://doi.org/10.1016/S1474-4422(06)70348-9

Heinemann, U., Beck, H., Dreier, J. P., Ficker, E., Stabel, J., & Zhang, C. L. (1992). The dentate gyrus as a regulated gate for the propagation of epileptiform activity. In C. E. Ribak, C. M. Gall, & I. Mody (Eds.), *The Dentate Gyrus and Its Role in Seizures* (pp. 273–280). Elsevier Science Publishers B.V.

Hellier, J. L., & Dudek, F. E. (1999). Spontaneous motor seizures of rats with kainate-induced epilepsy: effect of time of day and activity state. *Epilepsy Research*, *35*(1), 47–57. https://doi.org/10.1016/S0920-1211(98)00127-2

Hirota, T., Veenstra-VanderWeele, J., Hollander, E., & Kishi, T. (2014). Antiepileptic Medications in Autism Spectrum Disorder: A Systematic Review and Meta-Analysis. *Journal of Autism and Developmental Disorders*, *44*(4), 948–957. https://doi.org/10.1007/s10803-013-1952-2

HOLLRIGEL, G. S., CHEN, K., BARAM, T. Z., & SOLTESZ, I. (1998). THE PRO-CONVULSANT ACTIONS OF CORTICOTROPIN-RELEASING HORMONE IN THE HIPPOCAMPUS OF INFANT RATS. *Neuroscience*, *84*(1), 71–79.

Holmes, G. L., Tian, C., Hernan, A. E., Flynn, S., Camp, D., & Barry, J. (2015). Alterations in sociability and functional brain connectivity caused by early-life seizures are prevented by bumetanide. *Neurobiology of Disease*, *77*, 204–219. https://doi.org/10.1016/j.nbd.2015.02.015

Hoppe, C., Poepel, A., & Elger, C. E. (2007). Epilepsy: accuracy of patient seizure counts. *Archives of Neurology*, *64*(11), 1595–1599. https://doi.org/10.1001/archneur.64.11.1595

Hsiao, E. Y., McBride, S. W., Hsien, S., Sharon, G., Hyde, E. R., McCue, T., … Mazmanian, S. K. (2013). Microbiota Modulate Behavioral and Physiological Abnormalities Associated with Neurodevelopmental Disorders. *Cell*, *155*(7), 1451–1463. https://doi.org/10.1016/j.cell.2013.11.024

Hsiao, E. Y., & Patterson, P. H. (2011). Activation of the Maternal Immune System Induces Endocrine Changes in the Placenta via IL-6. *Brain, Behavior, and Immunity*, *25*(4), 604–615. https://doi.org/10.1016/j.bbi.2010.12.017

Huneau, C., Benquet, P., Dieuset, G., Biraben, A., Martin, B., & Wendling, F. (2013). Shape features of epileptic spikes are a marker of epileptogenesis in mice. *Epilepsia*, *54*(12), 2219–2227. https://doi.org/10.1111/epi.12406

Huusko, N., Römer, C., Ndode-Ekane, X. E., Lukasiuk, K., & Pitkänen, A. (2015). Loss of hippocampal interneurons and epileptogenesis: a comparison of two animal models of acquired epilepsy. *Brain Structure and Function*, *220*(1), 153–191. https://doi.org/10.1007/s00429-013-0644-1

Ingemarsson, I., Westgren, M., Lindberg, C., Ahrén, B., Lundquist, I., & Carlsson, C. (1981). Single injection of terbutaline in term labor: Placental transfer and effects on maternal and fetal carbohydrate metabolism. *American Journal of Obstetrics and Gynecology*, *139*(6), 697–701. https://doi.org/10.1016/0002-9378(81)90489-0

Irmen, F., Wehner, T., & Lemieux, L. (2015). Do reflex seizures and spontaneous seizures form a continuum? – Triggering factors and possible common mechanisms. *Seizure - European Journal of Epilepsy*, *25*, 72–79. https://doi.org/10.1016/j.seizure.2014.12.006

Ivy, A. S., Brunson, K. L., Sandman, C., & Baram, T. Z. (2008). Dysfunctional nurturing behavior in rat dams with limited access to nesting material: a clinically relevant model for early-life stress. *Neuroscience*, *154*(3), 1132–1142. https://doi.org/10.1016/j.neuroscience.2008.04.019

Jaffard, S. (2001). Wavelet expansions, function spaces and multifractal analysis. In *Twentieth Century Harmonic Analysis—A Celebration* (Vols. 1–Chapter 6, pp. 127–144). Retrieved from http://www.springerlink.com/index/10.1007/978-94-010-0662-0_6

Jain, K. K. (2000). An assessment of levetiracetam as an anti-epileptic drug. *Expert Opinion on Investigational Drugs*, *9*(7), 1611–1624. https://doi.org/10.1517/13543784.9.7.1611

Jašarević, E., Rodgers, A. B., & Bale, T. L. (2014). A novel role for maternal stress and microbial transmission in early life programming and neurodevelopment. *Neurobiology of Stress*, *1*, 81–88. https://doi.org/10.1016/j.ynstr.2014.10.005

Jenssen, S., Gracely, E. J., & Sperling, M. R. (2006). How Long Do Most Seizures Last? A Systematic Comparison of Seizures Recorded in the Epilepsy Monitoring Unit. *Epilepsia*, *47*(9), 1499–1503. https://doi.org/10.1111/j.1528-1167.2006.00622.x

Jeste, S. S., & Tuchman, R. (2015). Autism Spectrum Disorder and Epilepsy: Two Sides of the Same Coin? *Journal of Child Neurology*, *30*(14), 1963–1971. https://doi.org/10.1177/0883073815601501

Jin, B., Wang, S., Yang, L., Shen, C., Ding, Y., Guo, Y., … Ding, M. (2016). Prevalence and predictors of subclinical seizures during scalp video-EEG monitoring in patients with epilepsy. *International Journal of Neuroscience*, 1–8. https://doi.org/10.1080/00207454.2016.1220946

Johnson, F. K., & Kaffman, A. (2018). Early life stress perturbs the function of microglia in the developing rodent brain: New insights and future challenges. *Brain, Behavior, and Immunity*, *69*, 18–27. https://doi.org/10.1016/j.bbi.2017.06.008

Jung, S., Jones, T. D., Lugo, J. N., Sheerin, A. H., Miller, J. W., D'Ambrosio, R., … Poolos, N. P. (2007). Progressive dendritic HCN channelopathy during epileptogenesis in the rat pilocarpine model of epilepsy. *The Journal of Neuroscience : The Official Journal of the Society for Neuroscience*, *27*(47), 13012–13021. https://doi.org/10.1523/JNEUROSCI.3605-07.2007

Kadam, S. D., White, A. M., Staley, K. J., & Dudek, F. E. (2010). Continuous Electroencephalographic Monitoring with Radio-Telemetry in a Rat Model of Perinatal Hypoxia–Ischemia Reveals Progressive Post-Stroke Epilepsy. *The Journal of Neuroscience*, *30*(1), 404–415. https://doi.org/10.1523/JNEUROSCI.4093-09.2010

Kale, R. (1997). Bringing epilepsy out of the shadows. *BMJ : British Medical Journal*, *315*(7099), 2–3.

Kalynchuk, L. E. (2000). Long-term amygdala kindling in rats as a model for the study of interictal emotionality in temporal lobe epilepsy. *Neuroscience & Biobehavioral Reviews*, *24*(7), 691–704. https://doi.org/10.1016/S0149-7634(00)00031-2

Kammerman, S., & Wasserman, L. (2001). Seizure disorders: Part 1. Classification and diagnosis. *The Western Journal of Medicine*, *175*(2), 99–103.

Kandratavicius, L., Balista, P. A., Lopes-Aguiar, C., Ruggiero, R. N., Umeoka, E. H., Garcia-Cairasco, N., … Leite, J. P. (2014). Animal models of epilepsy: use and limitations. *Neuropsychiatric Disease and Treatment*, *10*, 1693–1705. https://doi.org/10.2147/NDT.S50371

Kanner, A. M. (2008). Mood disorder and epilepsy: a neurobiologic perspective of their relationship. *Dialogues in Clinical Neuroscience*, *10*(1), 39–45.

Karoly, P. J., Freestone, D. R., Boston, R., Grayden, D. B., Himes, D., Leyde, K., … Cook, M. J. (2016). Interictal spikes and epileptic seizures: their relationship and underlying rhythmicity. *Brain*, *139*(4), 1066–1078. https://doi.org/10.1093/brain/aww019

Kazdoba, T. M., Leach, P. T., & Crawley, J. N. (2016). Behavioral phenotypes of genetic mouse models of autism. *Genes, Brain, and Behavior*, *15*(1), 7–26. https://doi.org/10.1111/gbb.12256

Kelemen, A., Barsi, P., Erőss, L., Vajda, J., Czirják, S., Borbély, C., … Halász, P. (2006). Long-term outcome after temporal lobe surgery—Prediction of late worsening of seizure control. *Seizure*, *15*(1), 49–55. https://doi.org/10.1016/j.seizure.2005.10.007

Kellinghaus, C. (2009). Lacosamide as treatment for partial epilepsy: mechanisms of action, pharmacology, effects, and safety. *Therapeutics and Clinical Risk Management*, *5*, 757–766.

Kelly, K., Jukkola, P., Kharlamov, E., Downey, K., Mcbride, J., Strong, R., & Aronowski, J. (2006). Long-term video-EEG recordings following transient unilateral middle cerebral and common carotid artery occlusion in Long–Evans rats. *Experimental Neurology*, *201*(2), 495–506. https://doi.org/10.1016/j.expneurol.2006.05.006

Kelly, K. M. (2004). Spike-wave Discharges: Absence or Not, a Common Finding in Common Laboratory Rats. *Epilepsy Currents*, *4*(5), 176–177. https://doi.org/10.1111/j.1535-7597.2004.04503.x

Kelly, K. M., Miller, E. R., Lepsveridze, E., Kharlamov, E. A., & Mchedlishvili, Z. (2015). Posttraumatic seizures and epilepsy in adult rats after controlled cortical impact. *Epilepsy Research*, *117*, 104–116. https://doi.org/10.1016/j.eplepsyres.2015.09.009

Kharatishvili, I., Nissinen, J., Immonen, R., Grohn, O., & Pitkanen, A. (2006). Persistent susceptibility to seizures after traumatic brain injury. *Epilepsia*, *47*, 81–81.

Kharatishvili, I., Nissinen, J. P., McIntosh, T. K., & Pitkänen, A. (2006). A model of posttraumatic epilepsy induced by lateral fluid-percussion brain injury in rats. *Neuroscience*, *140*(2), 685–697. https://doi.org/10.1016/j.neuroscience.2006.03.012

Kharlamov, E. A., Lepsveridze, E., Meparishvili, M., Solomonia, R. O., Lu, B., Miller, E. R., … Mtchedlishvili, Z. (2011). Alterations of GABAA and glutamate receptor subunits and heat shock protein in rat hippocampus following traumatic brain injury and in posttraumatic epilepsy. *Epilepsy Research*, *95*(1), 20–34. https://doi.org/10.1016/j.eplepsyres.2011.02.008

Kikuyama, H., Hanaoka, T., Kanazawa, T., Yoshida, Y., Mizuno, T., Toyoda, H., & Yoneda, H. (2017). The Mechanism of Anti-Epileptogenesis by Levetiracetam Treatment is Similar to the Spontaneous Recovery of Idiopathic Generalized Epilepsy during Adolescence. *Psychiatry Investigation*, *14*(6), 844–850. https://doi.org/10.4306/pi.2017.14.6.844

Kim, C. K., Adhikari, A., & Deisseroth, K. (2017). Integration of optogenetics with complementary methodologies in systems neuroscience. *Nature Reviews. Neuroscience*, *18*(4), 222–235. https://doi.org/10.1038/nrn.2017.15

Kim, D., Cho, J.-W., Lee, J., Joo, E. Y., Hong, S. C., Hong, S. B., & Seo, D.-W. (2011). Seizure Duration Determined by Subdural Electrode Recordings in Adult Patients with Intractable Focal Epilepsy. *Journal of Epilepsy Research*, *1*(2), 57–64. https://doi.org/10.14581/jer.11011

Kim, H.-J., Cho, M.-H., Shim, W. H., Kim, J. K., Jeon, E.-Y., Kim, D.-H., & Yoon, S.-Y. (2017). Deficient autophagy in microglia impairs synaptic pruning and causes social behavioral defects. *Molecular Psychiatry*, *22*(11), 1576–1584. https://doi.org/10.1038/mp.2016.103

Kim, I., Mlsna, L. M., Yoon, S., Le, B., Yu, S., Xu, D., & Koh, S. (2015). A postnatal peak in microglial development in the mouse hippocampus is correlated with heightened sensitivity to seizure triggers. *Brain and Behavior*, *5*(12). https://doi.org/10.1002/brb3.403

Kim, J. W., Hong, J. Y., & Bae, S. M. (2018). Microglia and Autism Spectrum Disorder: Overview of Current Evidence and Novel Immunomodulatory Treatment Options. *Clinical Psychopharmacology and Neuroscience*, *16*(3), 246–252. https://doi.org/10.9758/cpn.2018.16.3.246

Kim, J.-E., & Cho, K.-O. (2018). The Pilocarpine Model of Temporal Lobe Epilepsy and EEG Monitoring Using Radiotelemetry System in Mice. *JoVE (Journal of Visualized Experiments)*, (132), e56831. https://doi.org/10.3791/56831

Kinney, D. K., Munir, K. M., Crowley, D. J., & Miller, A. M. (2008). Prenatal stress and risk for autism. *Neuroscience & Biobehavioral Reviews*, *32*(8), 1519–1532. https://doi.org/10.1016/j.neubiorev.2008.06.004

Klitgaard, H., Matagne, A., Vanneste-Goemaere, J., & Margineanu, D.-G. (2002). Pilocarpine-induced epileptogenesis in the rat: Impact of initial duration of status epilepticus on electrophysiological and neuropathological alterations. *Epilepsy Research*, *51*(1–2), 93–107. https://doi.org/10.1016/S0920-1211(02)00099-2

Koyama, R., & Ikegaya, Y. (2015). Microglia in the pathogenesis of autism spectrum disorders. *Neuroscience Research*, *100*, 1–5. https://doi.org/10.1016/j.neures.2015.06.005

Kwan, P., Cabral-Lim, L., D'Souza, W., Jain, S., Lee, B.-I., Liao, W., … CAOA Research Task Force. (2015). Research priorities in epilepsy for the Asia-Oceanian region. *Epilepsia*, *56*(5), 667–673. https://doi.org/10.1111/epi.12957

Kwan, P., Schachter, S. C., & Brodie, M. J. (2011). Drug-Resistant Epilepsy. *New England Journal of Medicine*, *365*(10), 919–926. https://doi.org/10.1056/NEJMra1004418

Lee, Y.-J., Kang, H.-C., Kim, H. D., Kim, D.-S., Shim, K.-W., Eom, S., & Lee, J. S. (2015). Neurocognitive Function in Children After Anterior Temporal Lobectomy With Amygdalohippocampectomy. *Pediatric Neurology*, *52*(1), 88–93. https://doi.org/10.1016/j.pediatrneurol.2014.09.006

Lemos, T., & Cavalheiro, E. A. (1995). Suppression of pilocarpine-induced status epilepticus and the late development of epilepsy in rats. *Experimental Brain Research*, *102*(3), 423–428.

Lévesque, M., Behr, C., & Avoli, M. (2015). The anti-ictogenic effects of levetiracetam are mirrored by interictal spiking and high-frequency oscillation changes in a model of temporal lobe epilepsy. *Seizure*, *25*, 18–25. https://doi.org/10.1016/j.seizure.2014.11.008

Lewis, M. L., Kesler, M., Candy, S. A., Rho, J. M., & Pittman, Q. J. (2018). Comorbid epilepsy in autism spectrum disorder: Implications of postnatal inflammation for brain excitability. *Epilepsia*, *59*(7), 1316–1326. https://doi.org/10.1111/epi.14440

Li, P., Fu, X., Smith, N. A., Ziobro, J., Curiel, J., Tenga, M. J., … Liu, J. S. (2017). Loss of CLOCK Results in Dysfunction of Brain Circuits Underlying Focal Epilepsy. *Neuron*, *96*(2), 387-401.e6. https://doi.org/10.1016/j.neuron.2017.09.044

Liu, L., Zheng, T., Morris, M. J., Wallengren, C., Clarke, A. L., Reid, C. A., … O'Brien, T. J. (2006). The Mechanism of Carbamazepine Aggravation of Absence Seizures. *Journal of Pharmacology and Experimental Therapeutics*, *319*(2), 790–798. https://doi.org/10.1124/jpet.106.104968

Löscher, W. (2005). How to Explain Multidrug Resistance in Epilepsy? *Epilepsy Currents*, *5*(3), 107–112. https://doi.org/10.1111/j.1535-7511.2005.05311.x

Löscher, W. (2007). The pharmacokinetics of antiepileptic drugs in rats: consequences for maintaining effective drug levels during prolonged drug administration in rat models of epilepsy. *Epilepsia*, *48*(7), 1245–1258. https://doi.org/10.1111/j.1528-1167.2007.01093.x

Löscher, W. (2011). Critical review of current animal models of seizures and epilepsy used in the discovery and development of new antiepileptic drugs. *Seizure*, *20*(5), 359–368. https://doi.org/10.1016/j.seizure.2011.01.003

Löscher, W., & Brandt, C. (2010). Prevention or modification of epileptogenesis after brain insults: experimental approaches and translational research. *Pharmacological Reviews*, *62*(4), 668–700. https://doi.org/10.1124/pr.110.003046

Löscher, W., Hirsch, L. J., & Schmidt, D. (2015). The enigma of the latent period in the development of symptomatic acquired epilepsy — Traditional view versus new concepts. *Epilepsy & Behavior*, *52, Part A*, 78–92. https://doi.org/10.1016/j.yebeh.2015.08.037

Lothman, E. W., Stringer, J. L., & Bertram, E. H. (1992). The dentate gyrus as a control point for seizures in the hippocampus and beyond. In C. E. Ribak, C. M. Gall, & I. Mody (Eds.), *The Dentate Gyrus and Its Role in Seizures* (pp. 301–313). Elsevier Science Publishers B.V.

Loupy, K. M., Arnold, M. R., Hassell, J. E., Lieb, M. W., Milton, L. N., Cler, K. E., … Lowry, C. A. (2019). Evidence that preimmunization with a heat-killed preparation of Mycobacterium vaccae reduces corticotropin-releasing hormone mRNA expression in the extended

amygdala in a fear-potentiated startle paradigm. *Brain, Behavior, and Immunity*, *77*, 127–140. https://doi.org/10.1016/j.bbi.2018.12.015

Lowenstein, D. H. (2006). The Management of Refractory Status Epilepticus: An Update. *Epilepsia*, *47*, 35–40. https://doi.org/10.1111/j.1528-1167.2006.00658.x

Lowenstein, D. H. (2011). Interview: The National Institute of Neurological Diseases and Stroke/American Epilepsy Society benchmarks and research priorities for epilepsy research. *Biomarkers in Medicine*, *5*(5), 531–535. https://doi.org/10.2217/bmm.11.69

Lowry, C. A., Smith, D. G., Siebler, P. H., Schmidt, D., Stamper, C. E., Hassell, J. E., … Rook, G. A. W. (2016). The Microbiota, Immunoregulation, and Mental Health: Implications for Public Health. *Current Environmental Health Reports*, *3*(3), 270–286. https://doi.org/10.1007/s40572-016-0100-5

Maguire, J. (2016). Epileptogenesis: More Than Just the Latent Period. *Epilepsy Currents*, *16*(1), 31–33. https://doi.org/10.5698/1535-7597-16.1.31

Maguire, J., & Salpekar, J. A. (2013). Stress, Seizures, and Hypothalamic-Pituitary-Adrenal Axis Targets for the Treatment of Epilepsy. *Epilepsy & Behavior : E&B*, *26*(3). https://doi.org/10.1016/j.yebeh.2012.09.040

Matagne, A., Margineanu, D.-G., Kenda, B., Michel, P., & Klitgaard, H. (2008). Anti-convulsive and anti-epileptic properties of brivaracetam (ucb 34714), a high-affinity ligand for the synaptic vesicle protein, SV2A. *British Journal of Pharmacology*, *154*(8), 1662–1671. https://doi.org/10.1038/bjp.2008.198

Matzen, J., Buchheim, K., & Holtkamp, M. (2012). Circadian dentate gyrus excitability in a rat model of temporal lobe epilepsy. *Experimental Neurology*, *234*(1), 105–111. https://doi.org/10.1016/j.expneurol.2011.12.029

Mazefsky, C. A., Herrington, J., Siegel, M., Scarpa, A., Maddox, B. B., Scahill, L., & White, S. W. (2013). The Role of Emotion Regulation in Autism Spectrum Disorder RH: Emotion Regulation in ASD. *Journal of the American Academy of Child and Adolescent Psychiatry*, *52*(7), 679–688. https://doi.org/10.1016/j.jaac.2013.05.006

Mazzuferi, M., Kumar, G., Rospo, C., & Kaminski, R. M. (2012). Rapid epileptogenesis in the mouse pilocarpine model: video-EEG, pharmacokinetic and histopathological characterization. *Experimental Neurology*, *238*(2), 156–167. https://doi.org/10.1016/j.expneurol.2012.08.022

McEwen, B. S. (1998). Stress, adaptation, and disease. Allostasis and allostatic load. *Annals of the New York Academy of Sciences*, *840*, 33–44.

McEwen, Bruce S. (2016). A key role for allostatic overload in ASD and other disorders. Commentary on “An integrative model of autism spectrum disorder: ASD as a neurobiological disorder of experienced environmental deprivation, early life stress, and allostatic overload” by William M. Singletary, MD. *Neuropsychoanalysis*, *18*(1), 9–14. https://doi.org/10.1080/15294145.2016.1149686

McKee, H. R., & Privitera, M. D. (2017). Stress as a seizure precipitant: Identification, associated factors, and treatment options. *Seizure*, *44*(Supplement C), 21–26. https://doi.org/10.1016/j.seizure.2016.12.009

Mehta, S. R., Dham, S. K., Lazar, A. I., Narayanswamy, A. S., & Prasad, G. S. (1994). Prolactin and cortisol levels in seizure disorders. *The Journal of the Association of Physicians of India*, *42*(9), 709–712.

Meltzer, A., & Van de Water, J. (2017). The Role of the Immune System in Autism Spectrum Disorder. *Neuropsychopharmacology*, *42*(1), 284–298. https://doi.org/10.1038/npp.2016.158

Molet, J., Maras, P. M., Avishai-Eliner, S., & Baram, T. Z. (2014). Naturalistic rodent models of chronic early-life stress. *Developmental Psychobiology*, *56*(8), 1675–1688. https://doi.org/10.1002/dev.21230

Molokwu, O. A., Ezeala-Adikaibe, B. A., & Onwuekwe, I. O. (2015). Levetiracetam-induced rage and suicidality: Two case reports and review of literature. *Epilepsy & Behavior Case Reports*, *4*, 79–81. https://doi.org/10.1016/j.ebcr.2015.07.004

Moran, N. F., Poole, K., Bell, G., Solomon, J., Kendall, S., McCarthy, M., … Shorvon, S. D. (2004). Epilepsy in the United Kingdom: seizure frequency and severity, anti-epileptic drug utilization and impact on life in 1652 people with epilepsy. *Seizure*, *13*(6), 425–433. https://doi.org/10.1016/j.seizure.2003.10.002

Moriyama, S., Brestoff, J. R., Flamar, A.-L., Moeller, J. B., Klose, C. S. N., Rankin, L. C., … Artis, D. (2018). β2-adrenergic receptor–mediated negative regulation of group 2 innate lymphoid cell responses. *Science*, *359*(6379), 1056–1061. https://doi.org/10.1126/science.aan4829

Mtchedlishvili, Z., Lepsveridze, E., Xu, H., Kharlamov, E. A., Lu, B., & Kelly, K. M. (2010). Increase of GABAA receptor-mediated tonic inhibition in dentate granule cells after traumatic brain injury. *Neurobiology of Disease*, *38*(3), 464–475. https://doi.org/10.1016/j.nbd.2010.03.012

Muldoon, S. F., Villette, V., Tressard, T., Malvache, A., Reichinnek, S., Bartolomei, F., & Cossart, R. (2015). GABAergic inhibition shapes interictal dynamics in awake epileptic mice. *Brain*, *138*(10), 2875–2890. https://doi.org/10.1093/brain/awv227

Nandan, M., Talathi, S. S., Myers, S., Ditto, W. L., Khargonekar, P. P., & Carney, P. R. (2010). Support vector machines for seizure detection in an animal model of chronic epilepsy. *Journal of Neural Engineering*, *7*(3), 036001. https://doi.org/10.1088/1741-2560/7/3/036001

Neville, B. G. R., Harkness, W. F. J., Cross, J. H., Cass, H. C., Burch, V. C., Lees, J. A., & Taylor, D. C. (1997). Surgical treatment of severe autistic regression in childhood epilepsy. *Pediatric Neurology*, *16*(2), 137–140. https://doi.org/10.1016/S0887-8994(96)00297-4

Newell, C., Bomhof, M. R., Reimer, R. A., Hittel, D. S., Rho, J. M., & Shearer, J. (2016). Ketogenic diet modifies the gut microbiota in a murine model of autism spectrum disorder. *Molecular Autism*, *7*(1), 37. https://doi.org/10.1186/s13229-016-0099-3

Ni, F.-F., Li, C.-R., Liao, J.-X., Wang, G.-B., Lin, S.-F., Xia, Y., & Wen, J.-L. (2016). The effects of ketogenic diet on the Th17/Treg cells imbalance in patients with intractable childhood epilepsy. *Seizure - European Journal of Epilepsy*, *38*, 17–22. https://doi.org/10.1016/j.seizure.2016.03.006

Nickels, K. C. (2016). Routine Versus Extended Outpatient EEG: Too Short, Too Long, or Just Right? *Epilepsy Currents*, *16*(6), 382–383. https://doi.org/10.5698/1535-7511-16.6.382

Nikodemova, M., Kimyon, R. S., De, I., Small, A. L., Collier, L. S., & Watters, J. J. (2015). Microglial numbers attain adult levels after undergoing a rapid decrease in cell number in the third postnatal week. *Journal of Neuroimmunology*, *278*, 280–288. https://doi.org/10.1016/j.jneuroim.2014.11.018

Nir, I., Meir, D., Zilber, N., Knobler, H., Hadjez, J., & Lerner, Y. (1995). Brief report: Circadian melatonin, thyroid-stimulating hormone, prolactin, and cortisol levels in serum of young adults with autism. *Journal of Autism and Developmental Disorders*, *25*(6), 641–654. https://doi.org/10.1007/BF02178193

Olson, C. A., Vuong, H. E., Yano, J. M., Liang, Q. Y., Nusbaum, D. J., & Hsiao, E. Y. (2018). The Gut Microbiota Mediates the Anti-Seizure Effects of the Ketogenic Diet. *Cell*, *173*(7), 1728-1741.e13. https://doi.org/10.1016/j.cell.2018.04.027

Ong, M.-S., Kohane, I., Cai, T., Gorman, M. P., & Mandl, K. (2014). Population-Level Evidence for an Autoimmune Etiology of Epilepsy. *JAMA Neurology*, *71*(5), 569–574. https://doi.org/10.1001/jamaneurol.2014.188

Orrù, G., Pettersson-Yeo, W., Marquand, A. F., Sartori, G., & Mechelli, A. (2012). Using Support Vector Machine to identify imaging biomarkers of neurological and psychiatric disease: A critical review. *Neuroscience & Biobehavioral Reviews*, *36*(4), 1140–1152. https://doi.org/10.1016/j.neubiorev.2012.01.004

Osuala, K., Baker, C. N., Nguyen, H.-L., Martinez, C., Weinshenker, D., & Ebert, S. N. (2012). Physiological and genomic consequences of adrenergic deficiency during embryonic/fetal development in mice: impact on retinoic acid metabolism. *Physiological Genomics*, *44*(19), 934–947. https://doi.org/10.1152/physiolgenomics.00180.2011

Panayiotopoulos, C. P. (2005). *Optimal Use of the EEG in the Diagnosis and Management of Epilepsies*. Retrieved from https://www.ncbi.nlm.nih.gov/books/NBK2601/

Paolicelli, R. C., Bolasco, G., Pagani, F., Maggi, L., Scianni, M., Panzanelli, P., … Gross, C. T. (2011). Synaptic Pruning by Microglia Is Necessary for Normal Brain Development. *Science*, *333*(6048), 1456–1458. https://doi.org/10.1126/science.1202529

Paolicelli, R. C., & Ferretti, M. T. (2017). Function and Dysfunction of Microglia during Brain Development: Consequences for Synapses and Neural Circuits. *Frontiers in Synaptic Neuroscience*, *9*. https://doi.org/10.3389/fnsyn.2017.00009

Patterson, P. H. (2011). Modeling autistic features in animals. *Pediatric Research*, *69*(5 Pt 2), 34R-40R. https://doi.org/10.1203/PDR.0b013e318212b80f

Pavlova, M. K., Shea, S. A., & Bromfield, E. B. (2004). Day/night patterns of focal seizures. *Epilepsy & Behavior*, *5*(1), 44–49. https://doi.org/10.1016/j.yebeh.2003.10.013

Paxinos, G., & Watson, C. (2007). *The Rat Brain in Stereotaxic Coordinates - 6th Edition* (6th ed.). Retrieved from https://www.elsevier.com/books/the-rat-brain-in-stereotaxic-coordinates/paxinos/978-0-12-374121-9

Pearce, P. S., Friedman, D., LaFrancois, J. J., Iyengar, S. S., Fenton, A. A., MacLusky, N. J., & Scharfman, H. E. (2014). Spike–wave discharges in adult Sprague–Dawley rats and their implications for animal models of temporal lobe epilepsy. *Epilepsy & Behavior*, *32*, 121–131. https://doi.org/10.1016/j.yebeh.2014.01.004

Peñagarikano, O., Abrahams, B. S., Herman, E. I., Winden, K. D., Gdalyahu, A., Dong, H., … Geschwind, D. H. (2011). Absence of CNTNAP2 leads to epilepsy, neuronal migration abnormalities, and core autism-related deficits. *Cell*, *147*(1), 235–246. https://doi.org/10.1016/j.cell.2011.08.040

Penfield, W. (1961). Introduction to Symposium on Post-traumatic Epilepsy. *Epilepsia*, *2*, 109–110.

Perucca, E., Gram, L., Avanzini, G., & Dulac, O. (1998). Antiepileptic Drugs as a Cause of Worsening Seizures. *Epilepsia*, *39*(1), 5–17. https://doi.org/10.1111/j.1528-1157.1998.tb01268.x

Picci, G., & Scherf, K. S. (2015). A Two-Hit Model of Autism: Adolescence as the Second Hit. *Clinical Psychological Science : A Journal of the Association for Psychological Science*, *3*(3), 349–371. https://doi.org/10.1177/2167702614540646

Pineda, E., Shin, D., You, S. J., Auvin, S., Sankar, R., & Mazarati, A. (2013). Maternal immune activation promotes hippocampal kindling epileptogenesis in mice. *Annals of Neurology*, *74*(1), 11–19. https://doi.org/10.1002/ana.23898

Pitkänen, A. (2010). Therapeutic Approaches to Epileptogenesis – Hope on the Horizon. *Epilepsia*, *51*(Suppl 3), 2–17. https://doi.org/10.1111/j.1528-1167.2010.02602.x

Pitkänen, A., & Immonen, R. (2014). Epilepsy Related to Traumatic Brain Injury. *Neurotherapeutics*, *11*(2), 286–296. https://doi.org/10.1007/s13311-014-0260-7

Pitkänen, A., Lukasiuk, K., Dudek, F. E., & Staley, K. J. (2015). Epileptogenesis. *Cold Spring Harbor Perspectives in Medicine*, *5*(10), a022822. https://doi.org/10.1101/cshperspect.a022822

Pitkanen, A., & Sutula, T. P. (2002). Is epilepsy a progressive disorder? Prospects for new therapeutic approaches in temporal-lobe epilepsy. *Lancet Neurology*, *1*(3), 173–181.

Pitsch, J., Becker, A. J., Schoch, S., Müller, J. A., de Curtis, M., & Gnatkovsky, V. (2017). Circadian clustering of spontaneous epileptic seizures emerges after pilocarpine-induced status epilepticus. *Epilepsia*, *58*(7), 1159–1171. https://doi.org/10.1111/epi.13795

Potter, J. M. (1978). The personal factor in the maturation of epileptogenic brain scars: review and hypothesis. *Journal of Neurology, Neurosurgery & Psychiatry*, *41*(3), 265–271. https://doi.org/10.1136/jnnp.41.3.265

Putnam, T. B., & Merritt, H. H. (1937). Experimental determination of the anticonvulsant properties of some phenyl derivatives. *Science*, *85*, 525–526. https://doi.org/10.1126/science.85.2213.525

Puttachary, S., Sharma, S., Tse, K., Beamer, E., Sexton, A., Crutison, J., & Thippeswamy, T. (2015). Immediate Epileptogenesis after Kainate-Induced Status Epilepticus in C57BL/6J Mice: Evidence from Long Term Continuous Video-EEG Telemetry. *PLOS ONE*, *10*(7), e0131705. https://doi.org/10.1371/journal.pone.0131705

Quigg, M., Straume, M., Menaker, M., & Bertram, E. H. (1998). Temporal distribution of partial seizures: comparison of an animal model with human partial epilepsy. *Annals of Neurology*, *43*(6), 748–755. https://doi.org/10.1002/ana.410430609

Racine, R J. (1972). Modification of seizure activity by electrical stimulation. II. Motor seizure. *Electroencephalography and Clinical Neurophysiology*, *32*(3), 281–294.

Racine, Ronald J. (1972). Modification of seizure activity by electrical stimulation: II. Motor seizure. *Electroencephalography and Clinical Neurophysiology*, *32*(3), 281–294. https://doi.org/10.1016/0013-4694(72)90177-0

Rakhade, S. N., Klein, P., Huynh, T., Hilario-Gomez, C., Kosaras, B., Rotenberg, A., & Jensen, F. E. (2011). Development of later life spontaneous seizures in a rodent model of hypoxia induced neonatal seizures. *Epilepsia*, *52*(4), 753–765. https://doi.org/10.1111/j.1528-1167.2011.02992.x

Rana, A., & Musto, A. E. (2018). The role of inflammation in the development of epilepsy. *Journal of Neuroinflammation*, *15*. https://doi.org/10.1186/s12974-018-1192-7

Rattka, M., Brandt, C., Bankstahl, M., Bröer, S., & Löscher, W. (2011). Enhanced susceptibility to the GABA antagonist pentylenetetrazole during the latent period following a pilocarpine-induced status epilepticus in rats. *Neuropharmacology*, *60*(2–3), 505–512. https://doi.org/10.1016/j.neuropharm.2010.11.005

Reber, S. O., Siebler, P. H., Donner, N. C., Morton, J. T., Smith, D. G., Kopelman, J. M., … Lowry, C. A. (2016). Immunization with a heat-killed preparation of the environmental bacterium Mycobacterium vaccae promotes stress resilience in mice. *Proceedings of the National Academy of Sciences*, *113*(22), E3130–E3139. https://doi.org/10.1073/pnas.1600324113

Reddy, D. S., & Kuruba, R. (2013). Experimental models of status epilepticus and neuronal injury for evaluation of therapeutic interventions. *International Journal of Molecular Sciences*, *14*(9), 18284–18318. https://doi.org/10.3390/ijms140918284

Reppert, S. M., & Weaver, D. R. (2002). Coordination of circadian timing in mammals. *Nature*, *418*(6901), 935–941. https://doi.org/10.1038/nature00965

Rhodes, M. C., Seidler, F. J., Abdel-Rahman, A., Tate, C. A., Nyska, A., Rincavage, H. L., & Slotkin, T. A. (2004). Terbutaline is a developmental neurotoxicant: effects on neuroproteins and morphology in cerebellum, hippocampus, and somatosensory cortex. *The Journal of Pharmacology and Experimental Therapeutics*, *308*(2), 529–537. https://doi.org/10.1124/jpet.103.060095

Riazi, K., Galic, M. A., Kuzmiski, J. B., Ho, W., Sharkey, K. A., & Pittman, Q. J. (2008). Microglial activation and TNFα production mediate altered CNS excitability following peripheral inflammation. *Proceedings of the National Academy of Sciences*, *105*(44), 17151–17156. https://doi.org/10.1073/pnas.0806682105

Rice, C. E., Rosanoff, M., Dawson, G., Durkin, M. S., Croen, L. A., Singer, A., & Yeargin-Allsopp, M. (2012). Evaluating Changes in the Prevalence of the Autism Spectrum Disorders (ASDs). *Public Health Reviews*, *34*(2), 1–22.

Rice, C. J., Sandman, C. A., Lenjavi, M. R., & Baram, T. Z. (2008). A Novel Mouse Model for Acute and Long-Lasting Consequences of Early Life Stress. *Endocrinology*, *149*(10), 4892–4900. https://doi.org/10.1210/en.2008-0633

Rodgers, K. M., Dudek, F. E., & Barth, D. S. (2015). Progressive, Seizure-Like, Spike-Wave Discharges Are Common in Both Injured and Uninjured Sprague-Dawley Rats: Implications for the Fluid Percussion Injury Model of Post-Traumatic Epilepsy. *Journal of Neuroscience*, *35*(24), 9194–9204. https://doi.org/10.1523/JNEUROSCI.0919-15.2015

Rodgers, Krista M., Benison, A. M., Klein, A., & Barth, D. S. (2008). Auditory, Somatosensory, and Multisensory Insular Cortex in the Rat. *Cerebral Cortex (New York, NY)*, *18*(12), 2941–2951. https://doi.org/10.1093/cercor/bhn054

Rodgers, Krista M., Hutchinson, M. R., Northcutt, A., Maier, S. F., Watkins, L. R., & Barth, D. S. (2009). The cortical innate immune response increases local neuronal excitability leading to seizures. *Brain*, *132*(9), 2478–2486. https://doi.org/10.1093/brain/awp177

Roffman, J. L., & Stern, T. A. (2006). A Complex Presentation of Complex Partial Seizures. *Primary Care Companion to The Journal of Clinical Psychiatry*, *8*(2), 98–100.

Rook, G. A. (2013). Regulation of the immune system by biodiversity from the natural environment: An ecosystem service essential to health. *Proceedings of the National Academy of Sciences*, *110*(46), 18360–18367. https://doi.org/10.1073/pnas.1313731110

Rook, G. A. W., Lowry, C. A., & Raison, C. L. (2015). Hygiene and other early childhood influences on the subsequent function of the immune system. *Brain Research*, *1617*, 47–62. https://doi.org/10.1016/j.brainres.2014.04.004

Roque, A., Ochoa-Zarzosa, A., & Torner, L. (2016). Maternal separation activates microglial cells and induces an inflammatory response in the hippocampus of male rat pups, independently of hypothalamic and peripheral cytokine levels. *Brain, Behavior, and Immunity*, *55*, 39–48. https://doi.org/10.1016/j.bbi.2015.09.017

Salami, P., Lévesque, M., Benini, R., Behr, C., Gotman, J., & Avoli, M. (2014). Dynamics of interictal spikes and high-frequency oscillations during epileptogenesis in temporal lobe epilepsy. *Neurobiology of Disease*, *67*, 97–106. https://doi.org/10.1016/j.nbd.2014.03.012

Salinsky, M., Kanter, R., & Dasheiff, R. M. (1987). Effectiveness of Multiple EEGs in Supporting the Diagnosis of Epilepsy: An Operational Curve. *Epilepsia*, *28*(4), 331–334. https://doi.org/10.1111/j.1528-1157.1987.tb03652.x

Sanders, J. D., Happe, H. K., Bylund, D. B., & Murrin, L. C. (2011). Changes in postnatal norepinephrine alter alpha-2 adrenergic receptor development. *Neuroscience*, *192*, 761–772. https://doi.org/10.1016/j.neuroscience.2011.06.045

Santhakumar, V., Ratzliff, A. D. H., Jeng, J., Toth, Z., & Soltesz, I. (2001). Long-term hyperexcitability in the hippocampus after experimental head trauma. *Annals of Neurology*, *50*(6), 708–717. https://doi.org/10.1002/ana.1230

Sayin, U., Osting, S., Hagen, J., Rutecki, P., & Sutula, T. (2003). *Spontaneous Seizures and Loss of Axo-Axonic and Axo- Somatic Inhibition Induced by Repeated Brief Seizures in Kindled Rats*. 10.

Sazgar, M., & Bourgeois, B. F. D. (2005). Aggravation of Epilepsy By Antiepileptic Drugs. *Pediatric Neurology*, *33*(4), 227–234. https://doi.org/10.1016/j.pediatrneurol.2005.03.001

Schafer, D. P., & Stevens, B. (2015). Microglia Function in Central Nervous System Development and Plasticity. *Cold Spring Harbor Perspectives in Biology*, *7*(10), a020545. https://doi.org/10.1101/cshperspect.a020545

Scharfman, H. E. (2007). The CA3 "Backprojection" to the Dentate Gyrus. *Progress in Brain Research*, *163*, 627–637. https://doi.org/10.1016/S0079-6123(07)63034-9

Scharfman, H. E. (2016). The enigmatic mossy cell of the dentate gyrus. *Nature Reviews Neuroscience*, *17*(9), 562–575. https://doi.org/10.1038/nrn.2016.87

Schmidt, D. (2012). Is antiepileptogenesis a realistic goal in clinical trials? Concerns and new horizons. *Epileptic Disorders*, *14*(2), 105–113. https://doi.org/10.1684/epd.2012.0512

Schmidt, P., Holsboer, F., & Spengler, D. (2001). Beta(2)-adrenergic receptors potentiate glucocorticoid receptor transactivation via G protein beta gamma-subunits and the phosphoinositide 3-kinase pathway. *Molecular Endocrinology (Baltimore, Md.)*, *15*(4), 553–564. https://doi.org/10.1210/mend.15.4.0613

Scholl, E. A., Dudek, F. E., & Ekstrand, J. J. (2013). Neuronal degeneration is observed in multiple regions outside the hippocampus after lithium pilocarpine-induced status epilepticus in the immature rat. *Neuroscience*, *252*, 45–59. https://doi.org/10.1016/j.neuroscience.2013.07.045

Sengupta, P. (2013). The Laboratory Rat: Relating Its Age With Human's. *International Journal of Preventive Medicine*, *4*(6), 624–630.

Serafini, A., Gigli, G. L., Gregoraci, G., Janes, F., Cancelli, I., Novello, S., & Valente, M. (2015). Are Early Seizures Predictive of Epilepsy after a Stroke? Results of a Population-Based Study. *Neuroepidemiology*, *45*(1), 50–58. https://doi.org/10.1159/000382078

Sgritta, M., Dooling, S. W., Buffington, S. A., Momin, E. N., Francis, M. B., Britton, R. A., & Costa-Mattioli, M. (2018). Mechanisms Underlying Microbial-Mediated Changes in Social Behavior in Mouse Models of Autism Spectrum Disorder. *Neuron*, *0*(0). https://doi.org/10.1016/j.neuron.2018.11.018

Shih, J. J., Fountain, N. B., Herman, S. T., Bagic, A., Lado, F., Arnold, S., … Labiner, D. M. (2018). Indications and methodology for video-electroencephalographic studies in the epilepsy monitoring unit. *Epilepsia*, *59*(1), 27–36. https://doi.org/10.1111/epi.13938

Shultz, S. R., Cardamone, L., Liu, Y. R., Hogan, R. E., Maccotta, L., Wright, D. K., … Bouilleret, V. (2013). Can structural or functional changes following traumatic brain injury in the rat predict epileptic outcome? *Epilepsia*, *54*(7), 1240–1250. https://doi.org/10.1111/epi.12223

Silverman, J. L., Yang, M., Lord, C., & Crawley, J. N. (2010). Behavioural phenotyping assays for mouse models of autism. *Nature Reviews Neuroscience*, *11*(7), 490–502. https://doi.org/10.1038/nrn2851

Singletary, W. M. (2015). An integrative model of autism spectrum disorder: ASD as a neurobiological disorder of experienced environmental deprivation, early life stress and allostatic overload. *Neuropsychoanalysis*, *17*(2), 81–119. https://doi.org/10.1080/15294145.2015.1092334

Sirven, J. I. (2009). Not All First Seizures Are Created Equally. *Epilepsy Currents*, *9*(6), 164–165. https://doi.org/10.1111/j.1535-7511.2009.01330.x

Slotkin, T. A., Baker, F. E., Dobbins, S. S., Eylers, J. P., Lappi, S. E., & Seidler, F. J. (1989). Prenatal terbutaline exposure in the rat: selective effects on development of noradrenergic projections to cerebellum. *Brain Research Bulletin*, *23*(4–5), 263–265.

Slotkin, T. A, Tate, C. A., Cousins, M. M., & Seidler, F. J. (2001). β-Adrenoceptor signaling in the developing brain: sensitization or desensitization in response to terbutaline. *Developmental Brain Research*, *131*(1), 113–125. https://doi.org/10.1016/S0165-3806(01)00282-6

Slotkin, Theodore A., & Seidler, F. J. (2006). Anomalous regulation of β-adrenoceptor signaling in brain regions of the newborn rat. *Brain Research*, *1077*(1), 54–58. https://doi.org/10.1016/j.brainres.2006.01.047

Slotkin, Theodore A., & Seidler, F. J. (2013). Terbutaline impairs the development of peripheral noradrenergic projections: Potential implications for autism spectrum disorders and pharmacotherapy of preterm labor. *Neurotoxicology and Teratology*, *36*, 91–96. https://doi.org/10.1016/j.ntt.2012.07.003

Slotkin, Theodore A., Skavicus, S., & Seidler, F. J. (2018). Developmental neurotoxicity resulting from pharmacotherapy of preterm labor, modeled in vitro: Terbutaline and dexamethasone, separately and together. *Toxicology*, *400–401*, 57–64. https://doi.org/10.1016/j.tox.2018.03.001

Sloviter, R. S., & Bumanglag, A. V. (2013). Defining “epileptogenesis” and identifying “antiepileptogenic targets” in animal models of acquired temporal lobe epilepsy is not as simple as it might seem. *Neuropharmacology*, *69*, 3–15. https://doi.org/10.1016/j.neuropharm.2012.01.022

Sloviter, R. S., Bumanglag, A. V., Schwarcz, R., & Frotscher, M. (2012). Abnormal dentate gyrus network circuitry in temporal lobe epilepsy. In J. L. Noebels, M. Avoli, M. A. Rogawski, R. W. Olsen, & A. V. Delgado-Escueta (Eds.), *Jasper’s Basic Mechanisms of the Epilepsies* (4th ed.). Retrieved from http://www.ncbi.nlm.nih.gov/books/NBK98207/

Smith, S. E. P., Li, J., Garbett, K., Mirnics, K., & Patterson, P. H. (2007). Maternal Immune Activation Alters Fetal Brain Development through Interleukin-6. *Journal of Neuroscience*, *27*(40), 10695–10702. https://doi.org/10.1523/JNEUROSCI.2178-07.2007

Smith, Z. Z., Benison, A. M., Bercum, F. M., Dudek, F. E., & Barth, D. S. (2018). Progression of convulsive and nonconvulsive seizures during epileptogenesis after pilocarpine-induced status epilepticus. *Journal of Neurophysiology*, *119*(5), 1818–1835. https://doi.org/10.1152/jn.00721.2017

Smolders, S., Notter, T., Smolders, S. M. T., Rigo, J.-M., & Brône, B. (2018). Controversies and prospects about microglia in maternal immune activation models for neurodevelopmental disorders. *Brain, Behavior, and Immunity*, *73*, 51–65. https://doi.org/10.1016/j.bbi.2018.06.001

Sominsky, L., De Luca, S., & Spencer, S. J. (2018). Microglia: Key players in neurodevelopment and neuronal plasticity. *The International Journal of Biochemistry & Cell Biology*, *94*, 56–60. https://doi.org/10.1016/j.biocel.2017.11.012

Spampanato, J., & Dudek, F. E. (2017). Targeted Interneuron Ablation in the Mouse Hippocampus Can Cause Spontaneous Recurrent Seizures. *ENeuro*, *4*(4). https://doi.org/10.1523/ENEURO.0130-17.2017

Sperk, G., Schwarzer, C., Heilman, J., Furtinger, S., Reimer, R. J., Edwards, R. H., & Nelson, N. (n.d.). Expression of plasma membrane GABA transporters but not of the vesicular GABA transporter in dentate granule cells after kainic acid seizures. *Hippocampus*, *13*(7), 806–815. https://doi.org/10.1002/hipo.10133

St. Louis, E. K., Rosenfeld, W. E., & Bramley, T. (2009). Antiepileptic Drug Monotherapy: The Initial Approach in Epilepsy Management. *Current Neuropharmacology*, *7*(2), 77–82. https://doi.org/10.2174/157015909788848866

Staley, K., Hellier, J. L., & Dudek, F. E. (2005). Do interictal spikes drive epileptogenesis? *The Neuroscientist : A Review Journal Bringing Neurobiology, Neurology and Psychiatry*, *11*(4), 272–276. https://doi.org/10.1177/1073858405278239

Staley, K. J., & Dudek, F. E. (2006). Interictal Spikes and Epileptogenesis. *Epilepsy Currents*, *6*(6), 199–202. https://doi.org/10.1111/j.1535-7511.2006.00145.x

Staley, K. J., White, A., & Dudek, F. E. (2011). Interictal spikes: harbingers or causes of epilepsy? *Neuroscience Letters*, *497*(3), 247–250. https://doi.org/10.1016/j.neulet.2011.03.070

Stead, M., Bower, M., Brinkmann, B. H., Lee, K., Marsh, W. R., Meyer, F. B., … Worrell, G. A. (2010). Microseizures and the spatiotemporal scales of human partial epilepsy. *Brain*, *133*(9), 2789–2797. https://doi.org/10.1093/brain/awq190

Steinhäuser, C., Grunnet, M., & Carmignoto, G. (2016). Crucial role of astrocytes in temporal lobe epilepsy. *Neuroscience*. https://doi.org/10.1016/j.neuroscience.2014.12.047

Swartz, B. E., Houser, C. R., Tomiyasu, U., Walsh, G. O., DeSalles, A., Rich, J. R., & Delgado-Escueta, A. (2006). Hippocampal Cell Loss in Posttraumatic Human Epilepsy. *Epilepsia*, *47*(8), 1373–1382. https://doi.org/10.1111/j.1528-1167.2006.00602.x

Taylor, J. A., Reuter, J. D., Kubiak, R. A., Mufford, T. T., Booth, C. J., Dudek, F. E., & Barth, D. S. (2019). Spontaneous Recurrent Absence Seizure-like Events in Wild-Caught Rats. *Journal of Neuroscience*, 1167–18. https://doi.org/10.1523/JNEUROSCI.1167-18.2019

Taylor, J. A., Rodgers, K. M., Bercum, F. M., Booth, C. J., Dudek, F. E., & Barth, D. S. (2017). Voluntary Control of Epileptiform Spike?Wave Discharges in Awake Rats. *The Journal of Neuroscience*, *37*(24), 5861–5869. https://doi.org/10.1523/JNEUROSCI.3235-16.2017

Theodore, W. H., Porter, R. J., Albert, P., Kelley, K., Bromfield, E., Devinsky, O., & Sato, S. (1994). The secondarily generalized tonic-clonic seizure A videotape analysis. *Neurology*, *44*(8), 1403–1403.

Theodore, William H., Porter, R. J., & Penry, J. K. (1983). Complex partial seizures Clinical characteristics and differential diagnosis. *Neurology*, *33*(9), 11515–11515.

Thind, K. K., Yamawaki, R., Phanwar, I., Zhang, G., Wen, X., & Buckmaster, P. S. (2010). Initial loss but later excess of GABAergic synapses with dentate granule cells in a rat model of temporal lobe epilepsy. *Journal of Comparative Neurology*, *518*(5), 647–667. https://doi.org/10.1002/cne.22235

Tipping, M. E., & Bishop, C. M. (1999). Mixtures of probabilistic principal component analyzers. *Neural Comput.*, *11*(2), 443–482.

Trinka, E., & Brigo, F. (2014). Antiepileptogenesis in humans. *Current Opinion in Neurology*, *27*(2), 227–235. https://doi.org/10.1097/WCO.0000000000000067

Tsai, J.-D., Lin, C.-L., Lin, C.-C., Sung, F.-C., & Lue, K.-H. (2014). Risk of epilepsy in patients with systemic lupus erythematosus – a retrospective cohort study. *Neuropsychiatric Disease and Treatment*, *10*, 1635–1643. https://doi.org/10.2147/NDT.S64323

Uddin, L. Q. (2015). Salience processing and insular cortical function and dysfunction. *Nature Reviews Neuroscience*, *16*(1), 55–61. https://doi.org/10.1038/nrn3857

Uddin, L. Q., & Menon, V. (2009). The anterior insula in autism: Under-connected and under-examined. *Neuroscience and Biobehavioral Reviews*, *33*(8), 1198–1203. https://doi.org/10.1016/j.neubiorev.2009.06.002

Ulrich-Lai, Y. M., & Herman, J. P. (2009). Neural Regulation of Endocrine and Autonomic Stress Responses. *Nature Reviews. Neuroscience*, *10*(6), 397–409. https://doi.org/10.1038/nrn2647

Um, J. W. (2017). Roles of Glial Cells in Sculpting Inhibitory Synapses and Neural Circuits. *Frontiers in Molecular Neuroscience*, *10*. https://doi.org/10.3389/fnmol.2017.00381

Umpierre, A. D., Remigio, G. J., Dahle, E. J., Bradford, K., Alex, A. B., Smith, M. D., … Wilcox, K. S. (2014). Impaired cognitive ability and anxiety-like behavior following acute seizures in the Theiler's virus model of temporal lobe epilepsy. *Neurobiology of Disease*, *64*, 98–106. https://doi.org/10.1016/j.nbd.2013.12.015

Uzunova, G., Pallanti, S., & Hollander, E. (2016). Excitatory/inhibitory imbalance in autism spectrum disorders: Implications for interventions and therapeutics. *The World Journal of Biological Psychiatry*, *17*(3), 174–186. https://doi.org/10.3109/15622975.2015.1085597

van Bodegom, M., Homberg, J. R., & Henckens, M. J. A. G. (2017). Modulation of the Hypothalamic-Pituitary-Adrenal Axis by Early Life Stress Exposure. *Frontiers in Cellular Neuroscience*, *11*. https://doi.org/10.3389/fncel.2017.00087

van Campen, J. S., Jansen, F. E., de Graan, P. N. E., Braun, K. P. J., & Joels, M. (2014). Early life stress in epilepsy: A seizure precipitant and risk factor for epileptogenesis. *Epilepsy & Behavior*, *38*, 160–171. https://doi.org/10.1016/j.yebeh.2013.09.029

Varcin, K. J., Alvares, G. A., Uljarević, M., & Whitehouse, A. J. O. (2017). Prenatal maternal stress events and phenotypic outcomes in Autism Spectrum Disorder. *Autism Research: Official*

Journal of the International Society for Autism Research, *10*(11), 1866–1877. https://doi.org/10.1002/aur.1830

Velioğlu, S. K., Ozmenoğlu, M., & Komsuoğlu, S. S. (1997). EEG investigation of temporal lobe epilepsy. *Clinical EEG (Electroencephalography)*, *28*(2), 121–126.

Velíšková, J., Silverman, J. L., Benson, M., & Lenck-Santini, P.-P. (2018). Autistic traits in epilepsy models: Why, when and how? *Epilepsy Research*, *144*, 62–70. https://doi.org/10.1016/j.eplepsyres.2018.05.009

Ventola, C. L. (2014). Epilepsy Management: Newer Agents, Unmet Needs, and Future Treatment Strategies. *Pharmacy and Therapeutics*, *39*(11), 776–792.

Vezzani, A. (2015). Anti-inflammatory drugs in epilepsy: does it impact epileptogenesis? *Expert Opinion on Drug Safety*, *14*(4), 583–592. https://doi.org/10.1517/14740338.2015.1010508

Vezzani, A., Friedman, A., & Dingledine, R. J. (2013). The role of inflammation in epileptogenesis. *Neuropharmacology*, *69*, 16–24. https://doi.org/10.1016/j.neuropharm.2012.04.004

Vezzani, A., Fujinami, R. S., White, H. S., Preux, P.-M., Blümcke, I., Sander, J. W., & Löscher, W. (2015). Infections, inflammation and epilepsy. *Acta Neuropathologica*, 1–24. https://doi.org/10.1007/s00401-015-1481-5

Viteva, E. (2014). Basic cellular and molecular mechanisms of refractory epilepsy: a review of current hypotheses. *Molecular & Cellular Epilepsy*, *1*(0). Retrieved from http://www.smartscitech.com/index.php/MCE/article/view/17

Walker, M. C., White, H. S., & Sander, J. W. a. S. (2002). Disease modification in partial epilepsy. *Brain: A Journal of Neurology*, *125*(Pt 9), 1937–1950.

Washington, J., Kumar, U., Medel-Matus, J.-S., Shin, D., Sankar, R., & Mazarati, A. (2015). Cytokine-dependent bidirectional connection between impaired social behavior and susceptibility to seizures associated with maternal immune activation in mice. *Epilepsy & Behavior : E&B*, *50*, 40–45. https://doi.org/10.1016/j.yebeh.2015.05.040

Webster, K. M., Sun, M., Crack, P., O'Brien, T. J., Shultz, S. R., & Semple, B. D. (2017). Inflammation in epileptogenesis after traumatic brain injury. *Journal of Neuroinflammation*, *14*(1), 10. https://doi.org/10.1186/s12974-016-0786-1

Wei, L., Hao, J., Lacher, R. K., Abbott, T., Chung, L., Colangelo, C. M., & Kaffman, A. (2015). Early-Life Stress Perturbs Key Cellular Programs in the Developing Mouse Hippocampus. *Developmental Neuroscience*, *37*(6), 476–488. https://doi.org/10.1159/000430861

White, A., Williams, P. A., Hellier, J. L., Clark, S., Dudek, F. E., & Staley, K. J. (2010). EEG spike activity precedes epilepsy after kainate-induced status epilepticus. *Epilepsia*, *51*(3), 371–383. https://doi.org/10.1111/j.1528-1167.2009.02339.x

White, S. W., Oswald, D., Ollendick, T., & Scahill, L. (2009). Anxiety in Children and Adolescents with Autism Spectrum Disorders. *Clinical Psychology Review*, *29*(3), 216–229. https://doi.org/10.1016/j.cpr.2009.01.003

Wilcox, K. S., Dixon-Salazar, T., Sills, G. J., Ben-Menachem, E., White, H. S., Porter, R. J., … Rogawski, M. A. (2013). Issues related to development of new anti-seizure treatments. *Epilepsia*, *54*(0 4), 24–34. https://doi.org/10.1111/epi.12296

Williams, P. A., White, A. M., Clark, S., Ferraro, D. J., Swiercz, W., Staley, K. J., & Dudek, F. E. (2009). Development of spontaneous recurrent seizures after kainate-induced status epilepticus. *Journal of Neuroscience*, *29*(7), 2103–2112. https://doi.org/10.1523/JNEUROSCI.0980-08.2009

Williamson, P. D., Thadani, V. M., French, J. A., Darcey, T. M., Mattson, R. H., Spencer, S. S., & others. (1998). Medial Temporal Objective Lobe Epilepsy: Videotape Analysis of Clinical Seizure Characteristics. *Epilepsia*, *39*(11), 1182–1188.

Wöhr, M., & Scattoni, M. L. (2013). Behavioural methods used in rodent models of autism spectrum disorders: Current standards and new developments. *Behavioural Brain Research*, *251*, 5–17. https://doi.org/10.1016/j.bbr.2013.05.047

Wong, S., Gardner, A. B., Krieger, A. M., & Litt, B. (2007). A stochastic framework for evaluating seizure prediction algorithms using hidden Markov models. *Journal of Neurophysiology*, *97*(3), 2525–2532. https://doi.org/10.1152/jn.00190.2006

Wood, S. K., Walker, H. E., Valentino, R. J., & Bhatnagar, S. (2010). Individual differences in reactivity to social stress predict susceptibility and resilience to a depressive phenotype: role of corticotropin-releasing factor. *Endocrinology*, *151*(4), 1795–1805. https://doi.org/10.1210/en.2009-1026

Woodruff, E. R., Chun, L. E., Hinds, L. R., & Spencer, R. L. (2016). Diurnal Corticosterone Presence and Phase Modulate Clock Gene Expression in the Male Rat Prefrontal Cortex. *Endocrinology*, *157*(4), 1522–1534. https://doi.org/10.1210/en.2015-1884

Wu, Y., Dissing-Olesen, L., MacVicar, B. A., & Stevens, B. (2015). Microglia: Dynamic Mediators of Synapse Development and Plasticity. *Trends in Immunology*, *36*(10), 605–613. https://doi.org/10.1016/j.it.2015.08.008

Yizhar, O., Fenno, L. E., Prigge, M., Schneider, F., Davidson, T. J., O'Shea, D. J., … Deisseroth, K. (2011). Neocortical excitation/inhibition balance in information processing and social dysfunction. *Nature*, *477*(7363), 171–178. https://doi.org/10.1038/nature10360

Zangaladze, A., Nei, M., Liporace, J. D., & Sperling, M. R. (2008). Characteristics and clinical significance of subclinical seizures. *Epilepsia*, *49*(12), 2016–2021. https://doi.org/10.1111/j.1528-1167.2008.01672.x

Zerrate, M. C., Pletnikov, M., Connors, S. L., Vargas, D. L., Seidler, F. J., Zimmerman, A. W., … Pardo, C. A. (2007). Neuroinflammation and Behavioral Abnormalities after Neonatal Terbutaline Treatment in Rats: Implications for Autism. *Journal of Pharmacology and Experimental Therapeutics*, *322*(1), 16–22. https://doi.org/10.1124/jpet.107.121483

Zhan, R.-Z., & Nadler, J. V. (2009). Enhanced Tonic GABA Current in Normotopic and Hilar Ectopic Dentate Granule Cells After Pilocarpine-Induced Status Epilepticus. *Journal of Neurophysiology*, *102*(2), 670–681. https://doi.org/10.1152/jn.00147.2009

Zhang, N., Wei, W., Mody, I., & Houser, C. R. (2007). Altered Localization of GABAA Receptor Subunits on Dentate Granule Cell Dendrites Influences Tonic and Phasic Inhibition in a Mouse Model of Epilepsy. *Journal of Neuroscience*, *27*(28), 7520–7531. https://doi.org/10.1523/JNEUROSCI.1555-07.2007

Zhang, T., Todorovic, M. S., Williamson, J., & Kapur, J. (2017). Flupirtine and diazepam combination terminates established status epilepticus: results in three rodent models. *Annals of Clinical and Translational Neurology*, *4*(12), 888–896. https://doi.org/10.1002/acn3.497

Zhang, W., & Buckmaster, P. S. (2009). Dysfunction of the dentate basket cell circuit in a rat model of temporal lobe epilepsy. *The Journal of Neuroscience : The Official Journal of the Society for Neuroscience*, *29*(24), 7846–7856. https://doi.org/10.1523/JNEUROSCI.6199-08.2009

Zhao, X., Liao, Y., Morgan, S., Mathur, R., Feustel, P., Mazurkiewicz, J., … Huang, Y. (2018). Noninflammatory Changes of Microglia Are Sufficient to Cause Epilepsy. *Cell Reports*, *22*(8), 2080–2093. https://doi.org/10.1016/j.celrep.2018.02.004

Zuany-Amorim, C., Sawicka, E., Manlius, C., Moine, A. L., Brunet, L. R., Kemeny, D. M., … Walker, C. (2002). Suppression of airway eosinophilia by killed *Mycobacterium vaccae*-induced allergen-specific regulatory T-cells. *Nature Medicine*, *8*(6), 625–629. https://doi.org/10.1038/nm0602-625

Zygmunt, A., & Stanczyk, J. (2010). Methods of evaluation of autonomic nervous system function. *Archives of Medical Science : AMS*, *6*(1), 11–18. https://doi.org/10.5114/aoms.2010.13500